



**FEDERAL UNIVERSITY OF SANTA CATARINA  
CAMPUS REITOR JOÃO DAVID FERREIRA LIMA  
GRADUATE PROGRAM IN MECHANICAL ENGINEERING**

Julian Esteban Barrera Torres

**THE IMPACT OF THERMAL ENERGY STORAGE ON COMBINED  
COOLING, HEATING, AND POWER STRUCTURES UNDERSIZED DUE TO  
THE ADOPTION OF LARGE TIMESCALES ON THEIR SYNTHESIS**

Florianópolis

2020

Julian Esteban Barrera Torres

**THE IMPACT OF THERMAL ENERGY STORAGE ON COMBINED  
COOLING, HEATING, AND POWER STRUCTURES UNDERSIZED DUE TO  
THE ADOPTION OF LARGE TIMESCALES ON THEIR SYNTHESIS**

Thesis submitted to the Graduate Program in Mechanical Engineering of the Federal University of Santa Catarina for the obtention of the title of Doctor of Mechanical Engineering.

Advisor: Prof. Edson Bazzo, Dr.Eng.

Florianópolis

2020

Ficha de identificação da obra elaborada pelo autor,  
através do Programa de Geração Automática da Biblioteca Universitária da UFSC.

Barrera, Julian Esteban

The impact of thermal energy storage on combined cooling, heating, and power structures undersized due to the adoption of large timescales on their synthesis / Julian Esteban Barrera ; orientador, Edson Bazzo, 2020.

196 p.

Tese (doutorado) - Universidade Federal de Santa Catarina, Centro Tecnológico, Programa de Pós-Graduação em Engenharia Mecânica, Florianópolis, 2020.

Inclui referências.

1. Engenharia Mecânica. 2. Cogeração. 3. Programação linear inteira mista. 4. Armazenamento térmico. 5. Eficiência energética em prédios. I. Bazzo, Edson. II. Universidade Federal de Santa Catarina. Programa de Pós Graduação em Engenharia Mecânica. III. Título.

Julian Esteban Barrera Torres

**The Impact of Thermal Energy Storage on Combined Cooling, Heating, and  
Power Structures Undersized Due to the Adoption of Large Timescales on  
Their Synthesis**

O presente trabalho em nível de doutorado foi avaliado e aprovado por banca  
examinadora composta pelos seguintes membros:

Prof. Jose Alexandre Matelli, Dr.Eng.

Universidade Estadual Paulista—UNESP

Prof. José Antônio Perrella Balestieri, Dr.Eng.

Universidade Estadual Paulista—UNESP

Prof. Alexandre Kupka da Silva, PhD.

Universidade Federal de Santa Catarina—UFSC

Certificamos que esta é a **versão original e final** do trabalho de conclusão que foi  
julgado adequado para obtenção do título de Doutor em Engenharia Mecânica.

---

Jonny Carlos da Silva, Dr.Eng.

Coordenador do Programa

---

Edson Bazzo, Dr.Eng.

Orientador

Florianópolis, 2020.

to my parents, Julio and Lucrecia.

## ACKNOWLEDGMENTS

I want to express my gratitude to everybody that have contributed—directly or indirectly—to my research activities and the preparation of this manuscript. Firstly, to the Brazilian government that through the foundation *Coordenação de Aperfeiçoamento de Pessoal de Nível Superior (CAPES)* has granted my scholarship and to the Federal University of Santa Catarina, where I received a public, free and high-standard education. In particular to my advisor, Professor Edson Bazzo, his supportive attitude and disposition were fundamental for facing the multiple challenges inherent to the research labor. Thanks to his advice and example, I have recognized the importance of the rational energy use and put it as the cornerstone of my present and future research. Additionally, I am thankful for the reception and invaluable support of Professors Luis Maria Serra and Miguel Angel Lozano, from the University of Zaragoza, who taught me how to formulate mathematical programming models for optimizing energy production systems.

Undoubtedly, during the doctorate period I have thrived personally and professionally, through the learning in diverse knowledge areas. In that respect I want to express my appreciation to Professors Jonny Carlos da Silva and José Alexandre Matelli, who have introduced the AI potential in designing thermal systems to me. In addition, I am grateful to the professionals who shared their knowledge and expertise with me, in particular to Newton Moura from Petrobras, Celestino Boente from Bahia Gas, Celso Bertinotti from Gas Brasileiro, and Ivan Rocha from SCGAS. Finally, I want to express my gratitude to my laboratory colleagues, specially to Nury Nieto, who supports me in the data acquisition from the university hospital.

All my gratitude and affection to my family and friends, who support me all this time.

## RESUMO

O projeto de sistemas de fornecimento de utilidades energéticas implementando a produção combinada de frio, calor e potência elétrica (CCHP) em prédios comerciais exhibe um alto nível de complexidade, dado o grande número de variáveis de decisão a serem consideradas e a incerteza em vários parâmetros de projeto. Usualmente, a seleção de tecnologias que formam a estrutura<sup>1</sup> CCHP—ou seja, a síntese da estrutura CCHP—é baseada na experiência profissional de especialistas e, para estudos mais avançados, é suportada por modelos de simulação e/ou otimização. Um assunto recorrente na síntese de estruturas CCHP em prédios existentes é a ausência de informação acerca do consumo de utilidades térmicas, sobretudo onde medições regulares de parâmetros energéticos não estão disponíveis, o que encoraja a adoção de hipóteses e aproximações que impactam diretamente na seleção das tecnologias. Na maioria das vezes, a falta de dados é causada por uma baixa frequência de medição (quando ela existe), o que omite as flutuações das demandas de utilidades térmicas, levando a estruturas subdimensionadas. Por outro lado, é bem conhecido que a implementação de armazenamento térmico (TES) permite um melhor gerenciamento para lidar com ditas flutuações. Assim, reconhecendo que escalas de tempo longas (ou seja, menores frequências de medição) na coleta de dados mascara as flutuações nos perfis de demanda, esta tese pretende identificar como a incorporação de TES em estruturas CCHP mitiga o subdimensionamento causado pela falta de dados. A estrutura metodológica adotada nessa tese é formada por várias etapas, atendendo às tarefas usualmente encontradas em qualquer projeto desse tipo, mas focada num hospital localizado na cidade de Florianópolis, Brasil, embora outros perfis de consumo sob diferentes condições climáticas foram também avaliados. A síntese é conduzida através da combinação de um modelo de programação linear para determinar a melhor distribuição de utilidades de calor, baseado na integração térmica de utilidades, e um outro modelo de programação linear inteira mista (MILP) para reduzir uma superestrutura contendo um conjunto de tecnologias candidatas na síntese. Finalmente, o impacto da implementação de TES nas estruturas ótimas obtidas usando diferentes escalas de tempo é analisada através de uma análise de sensibilidade que adota perfis aleatórios gerados a partir da informação coletada. A principal contribuição desta tese é a identificação da máxima escala de tempo de projeto que pode ser ajustada pela implementação de TES, junto com várias melhorias introduzidas na formulação dos modelos.

**Palavras-chave:** Cogeração. Produção combinada de frio, calor e potência. Programação linear inteira mista, Eficiência energética.

---

<sup>1</sup> A estrutura corresponde ao conjunto de tecnologias interligadas que compõem o sistema de abastecimento.

# RESUMO EXPANDIDO

## Introdução

Apesar de ser amplamente documentada, a produção combinada de frio, calor e potência elétrica (CCHP) caracteriza-se por ser um problema complexo de engenharia, dado o grande número de alternativas que podem-se adotar, junto a incerteza inerente a vários parâmetros de projeto. Assim, diversas abordagens tem sido usadas, como a simulação e posterior análise de múltiplas alternativas de projeto para orientar a sua seleção, ou uso de algoritmos de otimização capazes de indicar a melhor alternativa (para um conjunto de parâmetros adotados). Atualmente a pesquisa está focada no desenvolvimento de modelos de otimização robustos, que consideram a incerteza dos parâmetros de projeto através do computo de grandes volumes de dados. Isto é contrastado pelos projetos fora do âmbito acadêmico, onde a falta de dados associados à demanda energética é muito comum, o que resulta num mascaramento das flutuações presentes nos perfis de demanda. Por outro lado, é bem sabido que sistemas de armazenamento térmico (TES) permitem lidar com ditas flutuações. Assim, a presente tese mostra resultados relativos à forma como esses sistemas mitigam o subdimensionamento causado pela falta de dados, visando a possibilidade de evitar a necessidade de uma coleta exaustiva de dados nesse tipo de projetos.

## Objetivos

O objetivo dessa tese é demonstrar que a implementação de TES permitiu obter sistemas de produção capazes de atender satisfatoriamente as demandas energéticas de um prédio comercial, inclusive com uma quantidade limitada de dados. Para atingir este objetivo, uma serie de objetivos específicos é proposta:

1. Realizar um diagnóstico das práticas adotadas atualmente no projeto de sistemas de abastecimento no âmbito não acadêmico.
2. Caracterizar e definir adequadamente os perfis de demanda energética para diferentes aplicações, baseado em dados disponíveis, considerando possível correlação entre a temperatura ambiente e a demanda de utilidades térmicas.
3. Desenvolver um modelo de síntese de sistemas de abastecimento baseado em técnicas de otimização vigentes, incluindo tecnologias disponíveis no mercado. Considerando o impacto da temperatura ambiente no desempenho de turbinas e microturbinas.
4. Realizar análises de sensibilidade para verificar a resposta do modelo de síntese e o impacto do armazenamento térmico nas estruturas subdimensionadas.

## Metodologia

A metodologia proposta foi constituída por várias etapas, conforme os objetivos apresentados previamente. Primeiro, a forma mais convencional para abordar o projeto de



sistemas de abastecimento no âmbito não acadêmico foi apresentada. Esta consiste na simulação de várias alternativas contempladas, com posterior análise do seu desempenho para orientar a tomada de decisões. O potencial e as limitações desta abordagem foram apontadas e a oportunidade de aplicação de algoritmos de otimização mais sofisticados foi evidenciada. Posteriormente se apresentou, através de um estudo de caso, a construção dos perfis de demanda elétrica e de água fria para climatização, considerando a correlação existente entre o consumo elétrico e a temperatura ambiente. Adicionalmente, um algoritmo de classificação (*k-means clustering*) foi implementado na construção dos perfis das utilidades térmicas (vapor e água quente), partindo de uma quantidade limitada de medições.

Uma vez os perfis foram definidos, se apresentou o modelo de síntese de sistemas de abastecimento, que combinou dois modelos de programação linear. O primeiro foi usado para definir a rede de troca de calor necessária para maximizar o aproveitamento do calor oriundo dos acionadores primários considerados (moto-geradores e microturbinas). O segundo modelo, que corresponde a um modelo de programação linear mista, foi usado para a seleção das tecnologias que formam a estrutura ótima, que neste trabalho corresponde aquela que minimiza o custo anual de operação do sistema. Finalmente, os resultados do modelo de síntese foram considerados em duas análises de sensibilidade. A primeira levou em conta uma variação de  $\pm 30\%$  no preço do gás natural e no fator anual de amortização, tidos como os parâmetros econômicos mais relevantes. A segunda análise de sensibilidade contemplou a variação dos perfis de demanda de acordo com a escala temporal usada para descrevê-los, junto com o nível de armazenamento térmico da estrutura. Particularmente, esta análise de sensibilidade foi suportada por uma simulação Montecarlo, útil para estudar o efeito do armazenamento térmico na magnitude e na probabilidade de falência para estruturas de abastecimento subdimensionadas.

## Resultados e Discussão

Através do desenvolvimento de uma ferramenta computacional e posterior análise de um estudo de caso particular, foi possível identificar que a simulação de processos aplicada no projeto de sistemas de abastecimento é útil para a tomada de decisões quando a estrutura já é definida, ou quando o número de alternativas é reduzido. Se a quantidade de variáveis de decisão é considerável, o uso dessa abordagem torna-se uma tarefa bastante dispendiosa, dado o caráter combinatório do problema de seleção de tecnologias. Adicionalmente, foi evidenciado que na prática, a falta de dados obriga aos especialistas a tomar decisões baseadas no próprio conhecimento e experiência, muitas vezes sem sequer contar com uma simulação das alternativas.

Com a adaptação do método conhecido como *Princeton scorekeeping method* para escalas de tempo menores de um dia, foi possível construir os perfis horários de demanda elétrica

e de água gelada para climatização para um hospital localizado na cidade de Florianópolis. Adicionalmente, foi reconhecido que nem sempre seria possível obter perfis satisfatórios para essa escala, mas para escalas maiores (e.g. cada três horas, diário ou semanal). Por outro lado, perfis de demanda térmica (vapor e água quente) foram construídos a partir de uma série de medições no sistema de abastecimento atual. O processamento desses dados por meio de um algoritmo de classificação permitiu a definição de uma série de seis dias típicos para caracterizar o perfil anual. Finalmente, o método foi corroborado com os perfis de demanda de outras aplicações.

O modelo de síntese para o caso do hospital indicou que a estrutura ótima inclui dois tipos de microturbinas, o primeiro produzindo gases quentes para ativar um chiller de absorção e outro produzindo vapor. Para outras aplicações, motores de combustão interna e microturbinas foram também considerados. A análise de sensibilidade baseada nos parâmetros econômicos indicou que as estruturas obtidas permanecem ótimas na maior parte dos cenários. Mudanças foram evidenciadas só para valores extremos. Por outro lado, conforme esperado, maiores escalas de tempo na definição dos perfis de demanda resultaram em estruturas com menor número de equipamentos (i.e. estruturas subdimensionadas). A análise de sensibilidade baseada no nível de armazenamento térmico indicou que a inclusão desses sistemas ajuda as estruturas subdimensionadas a diminuir o *deficit* no abastecimento de utilidades. No entanto, a sua omissão aumenta a chance da estrutura apresentar *deficit*, inclusive para aquelas que superaram a análise de sensibilidade prévia. De acordo com os resultados, estruturas obtidas a partir de escalas de tempo maiores de um dia não conseguem suprir satisfatoriamente a demanda de utilidades, mesmo tendo um alto nível de armazenamento. Finalmente, os principais motivos para uma estrutura apresentar *deficit* foram a limitação no fornecimento de vapor—que não é acumulado—e a limitação na capacidade das torres de arrefecimento usadas para dissipar o calor residual do sistema.

### **Considerações Finais**

O procedimento apresentado atende, em muitos aspectos, os requerimentos comuns ao projeto de sistemas de abastecimento em um âmbito não acadêmico, sobretudo se relacionado à falta de informações para descrever a demanda de utilidades. A partir dos resultados obtidos, pode-se identificar claramente a limitação das soluções obtidas a partir de uma abordagem suportada apenas por simulação de processos e a recomendação para adotar algoritmos de otimização.

Por outro lado, os resultados do modelo de síntese e posterior análise de sensibilidade, indicam que a implementação de sistemas de armazenamento térmico tem o potencial de aumentar a capacidade de uma estrutura subdimensionada para atender completamente os requerimentos de uma aplicação. Esta característica pode implicar que a adoção do

armazenamento térmico—de antemão—pode poupar a aquisição de dados nas primeiras etapas do projeto. Adicionalmente, a não implementação desses sistemas pode acarretar *deficit* em estruturas, inclusive aquelas consideradas não subdimensionadas.

Futuros trabalhos são sugeridos contemplando novas aplicações e visando o tamanho do armazenamento térmico necessário para garantir cobertura total das demandas energéticas, de acordo com a escala de tempo usada para descrevê-las.

**Palavras-chave:** Cogeração. Produção combinada de frio, calor e potência. Programação linear inteira mista. Eficiência energética.

## ABSTRACT

The design of utilities' supply systems implementing combined cooling, heating, and power (CCHP) for commercial buildings exhibits a high level of complexity, given the great number of decision variables to be considered and the uncertainty on various design parameters. Usually, the selection of technologies forming the CCHP structure—namely the CCHP synthesis—is based on the judgment of experienced professionals and, for more detailed studies, it is supported by simulation and/or optimization models. One recurrent issue present in the CCHP synthesis for existing buildings is the lack of information about the thermal utilities' consumption, specially where regular measurement of energy-related parameters is not provided, which encourages the adoption of assumptions and approximations impacting directly on the selection of technologies. Most of time, the data insufficiency is due to a low measurement frequency (if it exists), which overlook the fluctuations present on thermal utilities' demands, leading to undersized structures. On the other hand, it is well known that the implementation of thermal energy storage (TES) enables a better supply management for dealing with these fluctuations. Thus, recognizing that larger timescales (i.e. lower measurement frequency) used for collecting the energy-use data mask fluctuations on the demand profiles, this thesis aims to identify how the TES incorporated into CCHP structures mitigates this undersizing effect caused by the lack of data. The methodology adopted in this thesis is formed by several stages, addressing the tasks normally involved in any CCHP project, but focused on an existing hospital located in Florianópolis, Brazil although various consumption patterns under different climate conditions were also checked. The synthesis is conducted through the combination of a linear programming model for determining the best apportioning of heat utilities based on a pinch analysis and other mixed-integer linear programming (MILP) model for reducing a superstructure containing a set of candidate technologies involved in the CCHP synthesis. Finally, the impact of the TES implementation on optimal structures obtained using different timescales is analyzed through a sensitivity analysis adopting random profiles generated from the information gathered. The main contribution of this thesis is the identification of a maximum design timescale that can be corrected by implementing TES, along with several improvements introduced into the formulation of the model.

**Keywords:** Cogeneration. Combined cooling, heating and power. Mixed integer linear programming. Energy efficiency.

## LIST OF FIGURES

Figure 1 – Topic areas approached by the research. . . . .	34
Figure 2 – Methodology structure of the research. . . . .	38
Figure 3 – Conceptual scheme of the production chain of utilities. . . . .	40
Figure 4 – Scheme of the conventional supply system. . . . .	41
Figure 5 – Scheme of a supply system applying CCHP. . . . .	42
Figure 6 – Demand profiles and simple CCHP production in a small hotel: (a) electric base load; CASE A: (b) heat demand, (d) cold demand; CASE B (separated production): (c) heat demand, (e) cold demand. . . . .	43
Figure 7 – CCHP layouts for supplying : (a) using ICE-based generator sets and hot water-activated chillers, (b) using turbine-based generator sets and steam-activated chillers. . . . .	49
Figure 8 – Sizing of CCHP devices: (a) Maximum area without heat wasting, (b) Larger size with heat wasting enabled, (c) Multiple sizes, (d) Larger size with modulation enabled. . . . .	50
Figure 9 – Tasks forming the CCHP design (specification) problem. . . . .	52
Figure 10 – Example of a CCHP layout for production of electricity, steam, hot water, and cold water. . . . .	63
Figure 11 – Solution space of the simulation model of the proposed layout, limited at maximum production of utilities by CCHP. . . . .	67
Figure 12 – Scheme of the current hospital supply facilities. . . . .	70
Figure 13 – Energy signature of the hospital: (a) Data records, (b) Distinction between business and non-business days. . . . .	72
Figure 14 – Energy performance lines of the hospital. . . . .	74
Figure 15 – Selected energy signatures of the hospital using different timescales: (a) 12 hours, (b) three hours, and (c) one hour. . . . .	75
Figure 16 – Base temperatures for different timescales: (a) Business days, (b) Non-business days. . . . .	76

Figure 17 – Selected performance lines for different timescales: a) one hour (9h-10h), b) three hours (9h-12h), c) one week. . . . .	77
Figure 18 – One-year demand profiles for the hospital case using the greatest times- cales: (a) Cooling load profile, (b) Base load profile. . . . .	78
Figure 19 – Duration curves for hospital base load and cooling demand: (a) Base load demand, (b) Cooling load demand. . . . .	79
Figure 20 – Hot water demand calculated using collected data. . . . .	80
Figure 21 – Steam production calculated using collected data. . . . .	81
Figure 22 – Duration curves of utilities required at a large office building, modeled using meteorological data of Los Angeles California. Data extracted from OPENEI (2018). . . . .	82
Figure 23 – Daily profiles for the hospital: (a) steam, (b) hot water. . . . .	87
Figure 24 – Heat-supplying streams of natural gas engine Caterpillar model G3516 LE: A. Exhaust gases, B. Compressed air, and C. Engine block water. . . . .	94
Figure 25 – Sankey diagram for cogeneration module based on natural gas engines. EE: Electricity, EG: Exhaust gases, EW: Engine block water, HA: Hot air, HG: Hot gases, HW: Hot water, ST: Steam. . . . .	96
Figure 26 – Thermal integration: (a) Temperature scale, (b) Energy balance on in- terval $j$ . . . . .	98
Figure 27 – Supply regions for cogeneration modules based on selected natural gas engine: (a) HW vs HG, (b) HW vs ST, (c) ST vs HG, and (d) Supply surface. . . . .	102
Figure 28 – Typical schemes for natural gas turbines and microturbines. . . . .	103
Figure 29 – Typical Sankey diagram for gas turbines and microturbines-based mo- dules. . . . .	104
Figure 30 – Performance parameters of gas turbines and microturbines as function of the ambient temperature: (a) electricity, (b) exhaust mass flow, (c) efficiency, and (d) exhaust gas temperature. Data from (CAPSTONE, 2005; SOLAR, 2014). . . . .	105
Figure 31 – Heat supply of devices to the production of thermal utilities: (a) tur- bine/HW and HG, (b) microturbine/HG and HW, (c) turbine/ST, (d) microturbine/ST. . . . .	107

Figure 32 – Technical factors of turbine and microturbine-based modules: (a) TCM01 and TCM03, (b) MCM01 and MCM03, (c) TCM02, and (d) MCM02. . . . .	107
Figure 33 – Procedure for matching heat-supplying and heat-demanding streams into the heat exchange network: (a) design above the pinch point, (b) design below the pinch point. Figure adapted from Kemp (2007). . . . .	109
Figure 34 – Matching of heat-supplying and heat-demanding streams in the heat exchange network of the cogeneration module EMC01. . . . .	110
Figure 35 – Superstructure considered for the MILP model. . . . .	113
Figure 36 – Installed capacity required for each technology category. . . . .	127
Figure 37 – Optimal structure for the hospital building. . . . .	130
Figure 38 – Results of the sensitivity analysis for the synthesis of the hospital case. . . . .	136
Figure 39 – Supply of utilities for two typical days in the hospital building case. . . . .	140
Figure 40 – Flowchart for the generation of random profiles, per utility. . . . .	145
Figure 41 – Flowchart for the Monte Carlo Simulations. . . . .	147
Figure 42 – Deficit in the thermal utilities supply and heat rejection deficit: (a) steam supply, (b) warm water supply, (c) cold water supply, (d) cooling tower capacity. . . . .	149
Figure 43 – Number of failed (deficit) scenarios: (a) CW deficit, (b) Heat rejection deficit. . . . .	151
Figure 44 – Configurations of heat exchanger networks for engine-based cogeneration sets. . . . .	169
Figure 45 – Configuration of microturbine bundle. Taken from (CAPSTONE, 2005) . . . . .	171
Figure 46 – Investment for steam boilers and heaters, installation included. . . . .	176
Figure 47 – Investment for electric chillers, installation included. . . . .	177
Figure 48 – Investment for absorption chillers, installation included. . . . .	178
Figure 49 – Investment for heat exchangers, installation included. . . . .	179
Figure 50 – Investment for cooling towers, installation included. . . . .	179
Figure 51 – First screen of <i>CogeCalc 2 (in portuguese)</i> : technical inputs. . . . .	184
Figure 52 – Second screen of <i>CogeCalc 2 (in portuguese)</i> : economic inputs. . . . .	186
Figure 53 – Third screen of <i>CogeCalc 2 (in portuguese)</i> : Economic inputs (2). . . . .	188
Figure 54 – Technical results reported by <i>CogeCalc 2 (in portuguese)</i> . . . . .	189
Figure 55 – Economic results reported by <i>CogeCalc 2</i> . . . . .	190

Figure 56 – Example of explanatory messages presented by *CogeCalc 2*. . . . . 191



## LIST OF TABLES

Table 1 – Examples of utilities commonly supplied in buildings. . . . .	39
Table 2 – Electricity price structure. . . . .	56
Table 3 – Components of the natural gas tariff (ARESC, 2019). . . . .	58
Table 4 – Equipment unitary costs for CCHP layout of Fig. 10, installation included. . . . .	65
Table 5 – Maximum supply of thermal utilities by CCHP layout. . . . .	66
Table 6 – Features of the current supply system of the hospital. . . . .	71
Table 7 – Electric base loads for the periods of each timescale. . . . .	78
Table 8 – Results for the thermal efficiency of the boiler. . . . .	81
Table 9 – Peak, annual consumption and duration time of utilities for various applications. . . . .	83
Table 10 – Features of utilities’ demand profiles for three building applications . . . . .	84
Table 11 – Ambient temperature tertiles and number of base-load levels for classification. . . . .	85
Table 12 – Typical days classification for aggregating data. . . . .	86
Table 13 – Typical days profiles for the hospital building . . . . .	88
Table 14 – Heat-demanding streams included in heat recovery exchange network. . . . .	93
Table 15 – Heat-supplying streams considered for cogeneration modules based on generator set Caterpillar model G3516LE. . . . .	97
Table 16 – Supply of utilities per unitary mass flow of streams. . . . .	100
Table 17 – Values of the remaining inputs of the thermal integration LP model. . . . .	101
Table 18 – Supply of utilities by cogeneration modules based on a 1035 kW generator set. . . . .	101
Table 19 – Formulation of technical factors (TF) as function of $T_0$ for turbine and microturbine-based modules. . . . .	108
Table 20 – Number of units and total area for the heat exchange networks of modules. . . . .	112
Table 21 – List of technologies considered in the synthesis model. . . . .	114

Table 22 – Technical factors correlating the technologies with the production/consumption of utilities. . . . .	115
Table 23 – Unitary capacity of each technology, for each application. . . . .	128
Table 24 – Technology selection for the hospital case . . . . .	129
Table 25 – Parameters of interest for the scenarios analyzed in the hospital building application. . . . .	132
Table 26 – Technology selection for simulated buildings applications. . . . .	138
Table 27 – Synthesis results using timescales longer than one hour for hospital case. . . . .	143
Table 28 – Effect of TES incorporation on the total operation costs. . . . .	148
Table 29 – Technical features of the generator sets considered . . . . .	168
Table 30 – Technical features of the turbine considered . . . . .	170
Table 31 – Technical features of the microturbine considered . . . . .	170
Table 32 – Technical features of the steam boilers considered . . . . .	171
Table 33 – Technical features of the hot-water boilers considered . . . . .	172
Table 34 – Technical information of electric chillers. . . . .	172
Table 35 – Technical features of absorption chillers. . . . .	173
Table 36 – Plant cost index (PCI) for the last 10 years (CEP, 2019). . . . .	174
Table 37 – Investment costs breakdown for cogeneration modules. . . . .	175
Table 38 – Fitting of linear regressions for performance lines. . . . .	194

## NOMENCLATURE

### Acronyms

ANEEL	Agência Nacional de Energia Elétrica
ANP	Agência Nacional do Petróleo
ARESC	Agência Nacional de Regulação de Santa Catarina
BFM	Bare module factor
CCHP	Combined Cooling, Heating and Power
CEPCI	Chemical engineering plant cost index
DOE	U.S. Department of Energy
EES	Engineering Equation Solver
EPA	U.S. Environmental Protection Agency
FEL	Following electric load
FTL	Following thermal load
HEX	Heat exchange
HRSG	Heat recovery steam generator
HT	High temperature
ICE	Internal combustion engine
INPI	Instituto Nacional da Propriedade Intelectual
LP	Linear programming
LT	Low temperature
MILP	Mixed-integer linear programming

NTU	Number of transfer units
PER	Primary energy rate
PBP	Payback period
PP	Pinch point
TES	Thermal energy storage
TK	Total costs, k\$

### **Greek**

$\alpha$	Intercept of linear regression
$\alpha'$	Significance level.
$\beta$	Slope of linear regression
$\Delta h$	Specific enthalpy difference, kJ/kg
$\Delta T_{min}$	Minimum temperature difference, K
$\Delta h_v$	Specific heat of vaporization, kJ/kg
$\epsilon$	Effectiveness
$\eta_I$	First-law efficiency
$\nu$	Degrees of freedom.
$\overline{\rho}$	Average density, kg/m <sup>3</sup>
$\tau$	Base temperature, °C
$\eta$	Efficiency

### **Roman**

AA	Ambient air
ACC	Accumulation of utility, kWh
af	Annuity factor
BK	Base cost, k\$

$\overline{cdd}$	Average cooling degree-days per day, $\Delta^{\circ}\text{C}$
$\overline{cdi}$	Average cooling degree interval, $\Delta^{\circ}\text{C}$
$\overline{C}_P$	Average specific heat capacity, kJ/kg-K
CAP	Capacity, kW or kWh
CDD	Cooling degree-days, $\Delta^{\circ}\text{C-day}$
CDI	Cooling degree interval, $\Delta^{\circ}\text{C-interval}$
CP	Heat capacity rate, kW/K
CWABS	Annual cold water production by absorption chillers, MWh
CWCNV	Annual cold water production by conventional devices, MWh
COP	Coefficient of performance
DEM	Demand, kW
E	Energy, kWh
EC	Electric consumption, kWh
EE	Electricity
EEK	Annual electricity purchase costs, k\$
EEMAX	Maximum electricity sale allowed, kWh
EG	Exhaust gases
EPRD	Electricity production, MWh
EUF	Energy utilization factor
EW	Engine block (cooling) water
FCON	Fuel consumption, MWh
FES	Fuel energy savings
H	Number of hours
h	Specific enthalpy, kJ/kg

HA	Hot air
HD	Heat demand, kW
HE	Heat excess, kW
HG	Hot gases
HPRD	Heat production, MWh
HS	Heat supply, kW
HTCHP	Heat produced and used by CCHP (annual), MWh
HW	Hot water
HWCNV	Annual hot water production by conventional devices, MWh
Q	Heat, kWh
EK	Equipment purchase costs, k\$
IK	Investment costs, k\$
INV	Investment, k\$
$k_p$	Coverage factor.
LF	Loss factor, $h^{-1}$
LHV	Low heating value, kJ/kg
LOS	Losses
LT	Lower temperature limit, °C
$\dot{m}$	Mass flow, kg/s
MAX	Maximum
MF	Mass flow, kg/s
MIN	Minimum
MOK	Maintenance and operation costs, \$
NI	Number of intervals

N	Number
n	Sample size.
ND	Number of days
NE	Number of equipment
NG	Natural gas
NGCHP	Natural gas used by CCHP, MWh
NGK	Annual natural gas purchase costs, k\$
NH	Number of hours per interval
NMAX	Maximum number of units (components)
NOREC	Heat produced but not used (annual), MWh
NU	Number of utilities
OK	Operating costs, \$
OPK	Annual O&M costs, k\$
OPR	Operating level, kW
OPR	Operating level
PCI	Plant cost index
PES	Primary energy savings
PESR	Primary energy savings ratio
PRDEE	Annual production of electricity, MWh
PRDHT	Annual production of thermal utilities, MWh
PUR	Purchase of utility, kWh
PUREE	Annual purchase of electricity, MWh
PURNG	Annual purchase of natural gas, MWh
$\dot{Q}$	Heat transfer rate or heat exchange duty, kW

QTY	Quantity
$R^2$	Coefficient of determination
T	Temperature, °C
SAL	Sales of utility, kWh
SALEE	Annual sale of electricity, MWh
SIN	Storage input rate, kW
SOUT	Storage output rate, kW
SP	Sales price, \$/kWh
ST	Steam
STCNV	Annual steam production by conventional devices, MWh
SUP	Supply of utility, kW
TF	Technical factor
TF0	Technical factor (constant)
TF1	Technical factor (variable addend)
TOK	Total operation costs, k\$
$u_c$	Standard uncertainty.
$U_p$	Expanded uncertainty.
U	Overall heat transfer coefficient, kW/m <sup>2</sup> -K
UCAP	Unitary capacity
UF	Utilization factor
UHD	Unitary heat demand, kJ/kg
UHS	Unitary heat supply, kJ/kg
UK	Unitary cost, k\$ or \$
UP	Unitary production, kJ/kg



USE	Demand of utility (by technologies), kW
UT	Upper temperature limit, °C
UTLCW	Heat used for activating absorption chillers (annual), MWh
UVKl	Unitary variable cost, k\$/kW
V	Volume, m <sup>3</sup>
W	Work, kWh
WPRD	Wasted (heat) production, MWh
WW	Warm water
X	Ratio
Y	Binary variable
y	Output estimative.
YSAL	Binary for enabling/disabling electricity sales
<b>Subscript</b>	
0	Ambient conditions
bol	Boiler.
c	Cooling, cold, counter for heat-supplying streams
cchp	Combined cooling heat and power
conv	Conventional
d	daily
e	counter for equipment.
eff	effective.
el	Electric
f	Fuel
h	Heating, hot, hourly, counter for hours and heat-demanding streams

hw	Hot water.
i	Counter
in	Inlet
in	Input
j	Temperature interval
l	Lower
max	Maximum
min	Minimum
mkp	makeup
op	operation, operating
out	Outlet
p	Corresponding to a probability $p$ .
ret	return
sp	Steam production.
st	Steam demand.
sup	supply
t	Counter for technologies
th	Thermal
tk	tank
u	Counter for utilities
up	Upper
y	year

### **Superscript**

h	corresponding to a hour $h$ .
---	-------------------------------

# CONTENTS

<b>1</b>	<b>INTRODUCTION . . . . .</b>	<b>30</b>
1.1	Problem Statement . . . . .	32
1.2	Motivation . . . . .	35
1.3	Objectives . . . . .	35
1.4	Scope . . . . .	36
1.5	Organization of the Manuscript . . . . .	36
1.6	Methodology Structure . . . . .	37
<b>2</b>	<b>ENERGY USE AND CCHP IN BUILDINGS . . . . .</b>	<b>39</b>
2.1	Features of the CCHP Implementation . . . . .	43
2.1.1	Selection of components . . . . .	45
2.1.2	Definition of capacity and number of components . . . . .	48
2.1.3	Definition of operation strategy . . . . .	51
2.2	Metrics . . . . .	52
2.3	Price Structure . . . . .	54
2.4	Regulations . . . . .	58
2.5	Premises Commonly Considered in CCHP design . . . . .	59
2.6	Preliminary Assessment of CCHP Projects . . . . .	61
<b>3</b>	<b>MODELING OF UTILITIES LOAD PROFILES . . . . .</b>	<b>69</b>
3.1	Data-driven Modeling . . . . .	69
3.1.1	Electric Base Load and Cold Water Demand Profile . . . . .	71
3.1.2	Hot Water Demand Profile . . . . .	79
3.1.3	Steam Production Profile . . . . .	80
3.2	Forward Modeling . . . . .	82
3.3	Typical Days Profiles . . . . .	83
3.4	Closing Remarks . . . . .	89

<b>4</b>	<b>THE CCHP SYNTHESIS</b>	<b>91</b>
<b>4.1</b>	<b>Characterization of Cogeneration Modules</b>	<b>92</b>
4.1.1	Turbocharged natural gas engines	94
4.1.2	Natural Gas Turbines and Microturbines	103
4.1.3	Heat Recovery Network of Cogeneration Modules	108
<b>4.2</b>	<b>Technology Selection</b>	<b>112</b>
4.2.1	The Superstructure	112
4.2.2	Mixed Integer Linear Programming	116
<b>4.3</b>	<b>Closing Remarks</b>	<b>123</b>
<b>5</b>	<b>RESULTS AND SENSITIVITY ANALYSES</b>	<b>125</b>
<b>5.1</b>	<b>Estimation of the Installed Capacity of Technologies</b>	<b>126</b>
<b>5.2</b>	<b>Synthesis Results</b>	<b>128</b>
5.2.1	Selection of Technologies	129
5.2.2	Supply System Balances and Performance	131
<b>5.3</b>	<b>Sensitivity Analysis</b>	<b>135</b>
<b>5.4</b>	<b>Operation Strategy</b>	<b>139</b>
<b>5.5</b>	<b>Optimal Structures for Timescales Longer than One Hour</b>	<b>142</b>
<b>5.6</b>	<b>Effect of TES on Undersized Optimal Structures</b>	<b>144</b>
5.6.1	Impact on Annual Total Costs	147
5.6.2	Deficit in the Thermal Utilities Supply	149
<b>5.7</b>	<b>Closing Remarks</b>	<b>152</b>
<b>6</b>	<b>CONCLUSION</b>	<b>154</b>
<b>6.1</b>	<b>Further Works</b>	<b>156</b>
	<b>BIBLIOGRAPHY</b>	<b>157</b>
<b>A</b>	<b>CHARACTERIZATION OF TECHNOLOGIES</b>	<b>168</b>
<b>A.1</b>	<b>Technical Information</b>	<b>168</b>
A.1.1	Engine-based Cogeneration Modules	168
A.1.2	Turbine-based Cogeneration Modules	170
A.1.3	Microturbine-based Cogeneration Modules	170

A.1.4	Steam Boilers and Heaters . . . . .	171
A.1.5	Electric Chillers . . . . .	172
A.1.6	Absorption Chillers . . . . .	173
A.1.7	Cooling Towers . . . . .	173
<b>A.2</b>	<b>Economic Information . . . . .</b>	<b>174</b>
A.2.1	Cogeneration Modules . . . . .	174
A.2.2	Boilers and Heaters . . . . .	176
A.2.3	Electric Chillers . . . . .	177
A.2.4	Absorption chillers . . . . .	177
A.2.5	Heat Exchangers . . . . .	177
A.2.6	Cooling Towers . . . . .	178
A.2.7	Thermal Storage . . . . .	180
<b>B</b>	<b>DEVELOPMENT OF A PROGRAM FOR THE FEASIBILITY ASSESSMENT OF CCHP ALTERNATIVES . . . . .</b>	<b>181</b>
<b>C</b>	<b>UNCERTAINTY ON THE UTILITIES' LOAD PROFILES . . .</b>	<b>193</b>
C.1	Base temperatures for cooling degree-intervals . . . . .	193
C.2	performance lines of cooling degree-intervals . . . . .	193
C.3	Steam production . . . . .	194
C.4	Steam Demand . . . . .	195

## Chapter 1

---

# INTRODUCTION

Over the last three decades, Combined Cooling, Heating and Power (CCHP<sup>1</sup>) have caught much attention among building owners and managers, mainly because of its potential economic benefits and the high level of maturity of the technologies involved in its application. Furthermore, CCHP technical and academic literature is quite extensive, given that—from the author’s point of view—the design of these systems configures an interesting engineering problem that permits multiple solution approaches, involving several knowledge areas. Despite of the fact of being a well-known area, the design of utilities’ supply systems adopting CCHP is yet a complex task, specially because of the great number of decision variables involved in the selection of technologies and the uncertainty on some key parameters such as the utilities’ demand profiles, and the equipment and fuels’ purchase prices. In this way, the research in this field has been focused on the development and improvement of methods capable of returning satisfactory CCHP designs meeting a series of requirements. The academic production about CCHP has been extensively and continuously reviewed, and through some selected reviews, it is possible to show the state-of-the-art concerning the design of utilities’ supply systems implementing CCHP. Starting with the review done by Cho, Smith and Mago (2014), it still highlights studies in which the decision-making is based on the comparison of energy, exergy, economic, and environmental performances of a set of predefined CCHP alternatives, varying aspects as the operation strategy and the selection of technologies. Later, in the review made by Al-Moussawi, Fardoun and Louahlia (2016), some works implementing these analysis-based approaches are presented, but CCHP design methods based on optimization routines and sensitivity analyses receive more attention. More recently, the review of Rong and Su (2017) focuses only on optimization methods applied on CCHP design, revealing

---

<sup>1</sup> Diverse terms as have been adopted in the literature to refer CCHP in diverse contexts: *Cogeneration*, *Trigeneration*, *Polygeneration*, *Combined Heat and Power* (CHP), *Building Cooling, Heating and Power* (BCHP), among others. In this work the term CCHP is adopted because it refers precisely to the concept referred in this thesis and appears more frequently in recent literature.

the growing interest in this approach. Particularly this review, besides describing briefly the most used optimization methods in the literature, introduces some works focused on modeling the uncertainty inherent to CCHP parameters for further incorporation into optimization models and sensitivity analyses. Finally, reviews of Mavromatidis, Orehounig and Carmeliet (2018a) and Yue et al. (2018) gather information from works focused on characterizing and modeling the uncertainty inherent to the design and optimization of distributed energy systems. The former is focused on works considering one or more energy resources including wind and solar in buildings and microgrids, while the latter is focused on reviewing the characterization methods used in larger scales, and is directed mainly to policy makers. It is important to mention that, although these reviews are useful to get a general picture of a great part of this research field, there are publications—devoted to CCHP—that were not scoped, e.g. the work of Matelli and Goebel (2018) regarding the application of resilient design concept in CCHP implementation, or publications based on detailed simulation and thermoeconomic analyses of specific cases such as (CALISE et al., 2017) or (JIANG et al., 2018).

In general, it is evinced a trend favoring the adoption of optimization routines considering the effect of uncertainty of CCHP parameters on its design. Works of Rong and Su (2017) and Yue et al. (2018) have identified three specific approaches for incorporating the uncertainty in CCHP optimization. First, the stochastic programming, where the uncertain parameters are modeled as continuous random variables with an assumed probability distribution (e.g. (MAVROMATIDIS; OREHOUNIG; CARMELIET, 2018b)) and a number of random scenarios are solved in order to optimize the expected value of the objective function. Additionally, there is the robust optimization, that contemplates uncertainty through intervals, overcoming the need of defining probability distributions, and ensures the feasibility of each possible scenario while optimizing the value of the objective function for the worst-case scenario (GABRIELLI et al., 2019). Finally, there are the deterministic optimization routines accomplished with risk analyses based on Monte Carlo simulations, e.g. (URBANUCCI; TESTI, 2018). Particularly, the last approach is considered in the present work. This choice enables a better examination of the optimization outputs for decision-making, and implies the least computational burden compared with the other alternatives.

In regard of the computational burden, one aspect frequently mentioned by authors adopting optimization routines is the existing compromise between the level of detailing used in the formulation of optimization models and their runtime. While the advances on computational capacity have enabled the development of elaborated algorithms dealing with great amount of data, the combinatorial nature of the CCHP optimization problems (synthesis) can still cause what is known as a *dimension disaster* (LI et al., 2010). More specifically, when there is one or more flag variables<sup>2</sup> into the formulation, the number of intervals forming the time horizon of the problem is one of, if not the most critical parameter increasing the computational effort for solving it. This feature also has been subject of works focused on preprocessing time-dependent data (e.g. utilities demands, ambient temperature, electricity prices, etc.) in order to reduce the size of CCHP optimization problems. For example, the paper of Pinto, Serra and Lázaro (2019), which assesses and compares different classification methods for defining a set of typical days from hourly data, the work of Bahl et al. (2018) that proposes a two-stage procedure for verifying the typical-periods reduction through energy balances performed along the entire time horizon, or the work of (CARPANETO et al., 2011), which groups hourly data using a clustering algorithm according to their similarity.

## 1.1 PROBLEM STATEMENT

Improved optimization models considering uncertainty in their inputs are being developed accomplished with data preprocessing algorithms for reducing the size of the optimization problem. However, in practice, the implementation of CCHP in existing building applications—done for decades—is far from being optimal. While preprocessing algorithms aid to reduce a greater set of data gathered for research purposes, in actual applications is not usual to find historical records that enable the inference of time-dependent data for performing an optimal CCHP implementation. Because of this, and since measurements of energy-related parameters during long periods (months to years) are rarely allowed, the decision-making involved in CCHP design lies on the criteria of experienced specialists supported by a limited amount of data. Thus, there is a gap between the CCHP

---

<sup>2</sup> Flag variables have a default value until some condition is true, in which case, it adopts a different one. For example, a variable adopting the unity value whenever a technology is on and a zero-value when it is off.



design based on optimization routines dealing with a great amount of data and the CCHP design based on the specialist judgment of a limited amount of data.

This gap was evidenced thanks to the experience shared with various engineers involved in the implementation of CCHP projects, and that participated—together with the author—in the development of a computational tool for the quick appraisal of CCHP alternatives. Particularly, one aspect that is usually overlooked is the level of detail used for describing the thermal utilities' demand profiles. Commonly it is approximated by monthly, seasonal, even annual averages, which of course, can result in misleading CCHP designs.

In that direction, the present thesis explores the possibility of designing utilities supply systems capable of addressing completely the requirements of a building, adopting an optimization approach, but starting with profiles whose best estimation corresponds to large timescales. It will be demonstrated that initial CCHP designs derived from large timescales are undersized but similar to that obtained from hourly profiles, and that the inclusion of thermal energy storage (TES) reduces their supply requirements. Thus, the hypothesis checked is that *an undersized optimal structure, derived from profiles whose best estimation corresponds to a large timescale, could address the energy requirements of an existing building, as long as it is complemented with TES.*

Similar topics have been approached recently, e.g. Gabrielli et al. (2019) proposed a method for determining the required time resolution and getting the optimal design of distributed energy systems, using a limited amount of information through a robust optimization. However, here the time resolution refers only to the number of typical days (timescale remains equal to one hour) and, despite TES is contemplated, its impact on optimal design is not analyzed. On the other hand, Kotzur et al. (2018b) has proposed a method for modeling TES on consideration of interstitial periods linking typical periods, and the work of Marquant et al. (2017) compares the design of distributed energy systems obtained using full hourly profiles, typical (clustered) days, and rolling-horizon profiles. Finally, the work of Poncelet et al. (2016) analyzes the temporal detail in energy-planning models (i.e. only operation schedule). However, to the best of the author knowledge, studies with similar purpose, focused on the compromise between the timescale of the utilities' demand profiles and the incorporation of TES in CCHP designs have not been

conducted so far. Figure 1 shows the topic areas approached by this research, which correspond to the inclusion of TES, the selection of technologies (synthesis), and the amount of data used for describing the energy demands. This last related to the timescale of their profiles.

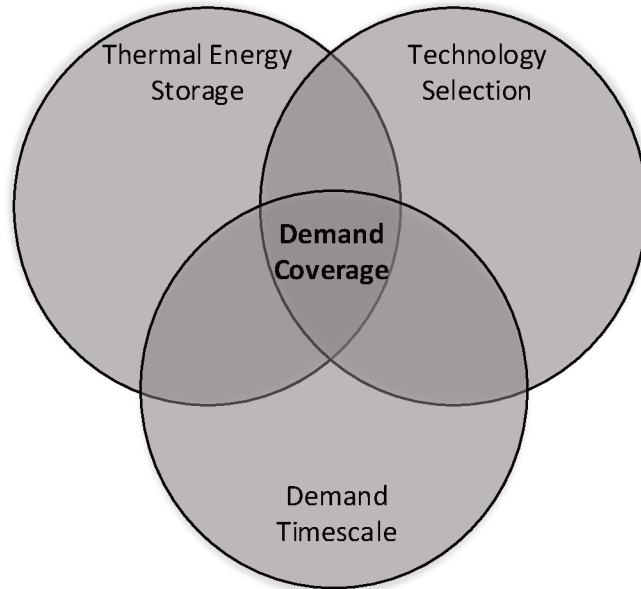


Figure 1 – Topic areas approached by the research.

This research demonstrates that the implementation of TES allows the design of fully capable CCHP systems through optimization routines, even with a limited amount of data (caused by long timescales). In other words, a detailed characterization of thermal utilities demands would not be strictly necessary for getting a close-to-optimal CCHP implementation, as long as TES is included. Other relevant contributions are listed as follows:

- Construction of consistent sub-daily profiles through the correlation of electricity consumption and ambient temperature (Princeton score-keeping method).
- Application of a clustering (classification) routine based on electricity consumption and average ambient temperature for obtaining consistent utilities' profiles with a limited amount of measurements.
- Inclusion of a thermal integration routine for determining the maximum heat exportation of cogeneration modules with small-to-medium capacity  $\sim 200$  to  $1000$  kW.

The heat transfer area is taken into account for the economic appraisal of these cogeneration modules.

- Development of a technology selection algorithm including internal combustion engines and microturbines considering the influence of the ambient temperature on the latter's performance.
- Elaboration of a sensitivity analysis through the generation of Monte Carlo simulation scenarios, taking into account the correlation between the thermal utilities demands and the prevailing ambient temperature.

## 1.2 MOTIVATION

Besides the well-known economic, reliability, and environmental benefits of CCHP implementation (see e.g. the publication of IEA (2014) or the guide by ASHRAE (2015b)), the report made by the IEA (2017), concerning the technology perspectives for decarbonizing the energy sector, states that research and development efforts should focus on bringing to market very high-performance natural gas technologies, including cogeneration systems<sup>3</sup>. Furthermore, the current liberalization of the Brazilian natural gas market (LIS, 2019) can favor the implementation of CCHP based on natural gas, as long as its price decreases with respect to the electricity. Thus, this research can bring insights regarding the CCHP design in a moment that they may be particularly useful.

Additionally, the development of the present research involves interesting areas, such as the modeling, optimization, and analysis of processes, involving applied thermodynamics' concepts.

## 1.3 OBJECTIVES

The main objective of this thesis is to assess the effect of TES on CCHP structures undersized due to the adoption of large timescales on their synthesis, and check whether the TES implementation can make these structures to completely address the utilities' demand profiles of a building. Taking into account also the tasks commonly involved in non-academic CCHP projects, the following specific objectives are proposed for this study:

---

<sup>3</sup> In the context of this publication, the term 'cogeneration' includes CCHP.

1. Make a diagnosis of the current practices adopted in the development of non-academic CCHP projects.
2. Characterize and set adequately the cooling, heating, and electric demand profiles of different building applications, based on data commonly available and taking advantage from the possible correlation between the thermal utilities' demand and the prevailing ambient temperature.
3. Develop a CCHP synthesis model based on state-of-the-art optimization techniques, including currently-available technologies. The effect of ambient temperature should be considered for turbines and microturbines performance.
4. Perform sensitivity analyses for verifying the synthesis model outputs and the impact of TES on undersized CCHP structures.

#### 1.4 SCOPE

The stages of the methodology adopted in this thesis address the circumstances normally found in CCHP projects and are focused on the university hospital Polydoro Ernani de São Thiago, located in the city of Florianópolis, Brazil. However, as it will be shown, this methodology is suitable for applications where historical records of ambient temperature and electricity consumption exist, showing certain correlation, and the regularity on their thermal utilities' consumption enables the replication of one-day profiles several times a year. Additionally, the synthesis model was checked for various building applications with different climatic conditions and consumption patterns, in order to verify that it is capable of returning different sets of technologies.

#### 1.5 ORGANIZATION OF THE MANUSCRIPT

Firstly, Ch. 2, which is the introductory chapter, briefly describes the CCHP design problem and, through a basic simulation approach, introduces common premises adopted in non-academic CCHP projects. The price structure of electricity and natural gas are presented. Some usual metrics for assessing the economic and energy performance of these projects are also introduced. Finally, the limitations of this approach are discussed through an example.

Ch. 3 presents the procedure adopted for constructing the utilities' demand profiles from available data and measurements of energy-related parameters. The application of this procedure is focused on the hospital building; nevertheless, profiles from three additional applications with different consumption patterns are also presented. On the one hand, the electricity base load and the cold water demands are estimated through a method known as the Princeton score-keeping, while the thermal utilities demands, steam and hot water, are estimated through the processing of measurements' data by a classification algorithm (k-means clustering).

Chapter 4 explains the formulation of the synthesis problem. The first part is focused on the characterization of cogeneration modules according to its prime mover; natural gas internal combustion engines, gas turbines and microturbines are considered. The heat production of each module is determined by a thermal integration algorithm, which enables the determination of the maximum recoverable heat and its corresponding exchange area. Next, the second part of this chapter is focused on the formulation of the technologies' selection problem as a mixed-integer linear programming (MILP) model. This approach is based on the construction of a reducible superstructure formed by all the candidate technologies; hot-gases-driven and direct-fired absorption chillers are included, which is not found in previous literature. Additionally, the effect of the ambient temperature on the supply of turbines and microturbines also was considered.

In Ch. 5 the outputs of the synthesis model are presented for each building application considered, and a series of sensitivity analyses were conducted in order to check them. Firstly, the impact of natural gas tariffs and the annuity factor on the selection of technologies is verified through a scenarios-based sensitivity analysis. Next, the effect of the timescale used and the TES share into the CCHP structure is analyzed through a series of Monte Carlo scenarios, involving the generation of random demand profiles using the information gathered for the hospital building. Finally, Ch. 6 presents the conclusions of this thesis.

## 1.6 METHODOLOGY STRUCTURE

The methodology proposal is formed by a sequence of stages, whose partial results are presented in each chapter. For this reason, there is not a chapter devoted entirely

for the methodology structure. In this way, in order to expose more clearly it to the reader, Fig. 2 shows the methodology structure of the present thesis. Note that Chapters 3 through 5 have a set of procedures (surrounded by a square), fed with information derived from previous stages.

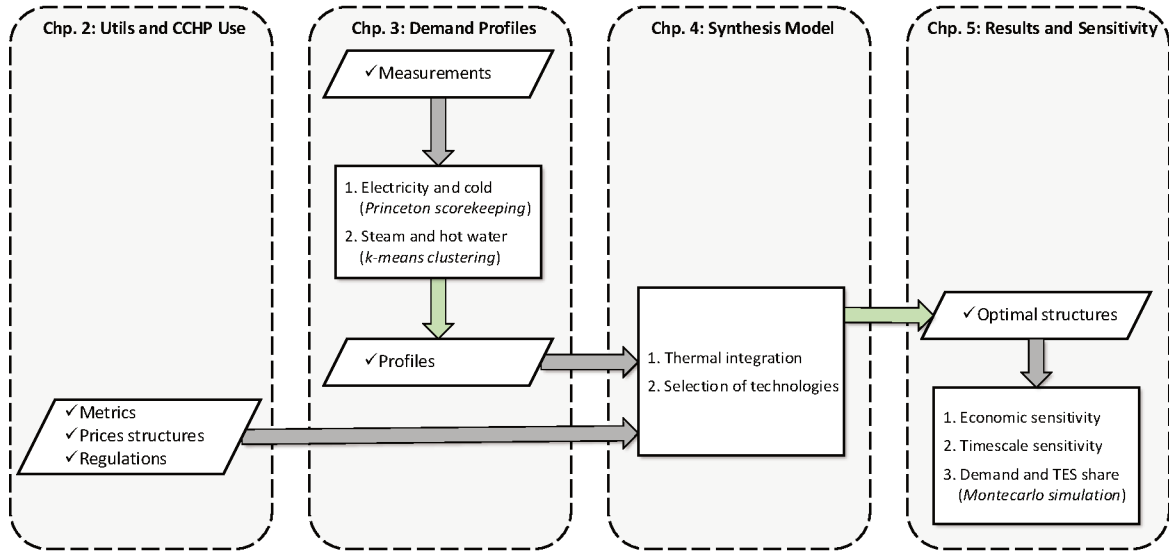


Figure 2 – Methodology structure of the research.

## Chapter 2

### ENERGY USE AND CCHP IN BUILDINGS

The proper operation of any building requires the use of energy provided in different forms, referred as *utilities* or *services*; although there are many possible building applications (*e.g.* schools, hotels, hospitals, malls, gyms, etc.), there are some utilities that are very common. For illustration, Table 1 presents some examples of utilities commonly supplied in buildings (excluding electricity).

Table 1 – Examples of utilities commonly supplied in buildings.

Utility / Function	Terminals	Conditions*		Usual to
<i>Saturated Steam</i>		Supply pressure, bar		
Laundry, drying	Dryers	5.5 - 6.9		Hotels
Sterilization	Sterilizers	3.5 - 5.6		Hospital
Laundry, washing	Washers	2.1 - 5.9		Hospitals
Kitchen, cooking	Jacketed vessels	2.0 - 3.9		Hotels
Space heating	Radiators	2.0 - 3.0		Any
Humidification	Disperser	1.2 - 2.0		Any
<i>Hot water</i>		Temperature, °C		
		<i>Supply</i>	<i>Return</i>	
Laundry, washing	Washers	75 - 80	–	Hospitals
Space heating	Radiators	60 - 80	40 - 60	Any
	Fan coils	60 - 65	50 - 55	Any
	Radiant floor	45 - 50	40 - 45	Any
Kitchen, cleaning	water taps	60 - 70	–	Hotels
Pool heating	Heat exchanger	60 - 65	55 - 60	Hotels
Sanitary	Sinks, showers	40 - 60	–	Hotels
<i>Cold water</i>				
Air conditioning	Fan coils	5 - 9	12 - 14	Any
	Chilled beams	13 - 15	18 - 20	Any
	Radiant panels	15 -17	18 -20	Any

\*Most values reported in (ASHRAE, 2016; ASHRAE, 2015a), other were obtained from specific catalogs.

Independently of the building activity, the production and distribution of utilities can be conceptualized as a transformation process of energy resources into energy utilities. Adapting the conception of Lozano (2017), Fig. 3 shows this process starting with a stage named *production*, which involves technologies that directly use energy resources in order to produce energy utilities, some of which pass right to the distribution stage. Note that the electricity (imported) can be seen as an external resource, for example for producing cold water with electric chillers, or as an external utility whenever it is used directly, for example, for lightning. Afterward it can be (in dashed lines) a second stage named *transformation*, which comprises heat-recovery and thermal-activated technologies destined to transform intermediate utilities into utilities suitable for distribution. Examples of these technologies are the heat recovery steam generators (HRSG), that transform the intermediate utility *hot gases*<sup>1</sup> into the utility *steam*, and the absorption chillers used for producing *cold water*.

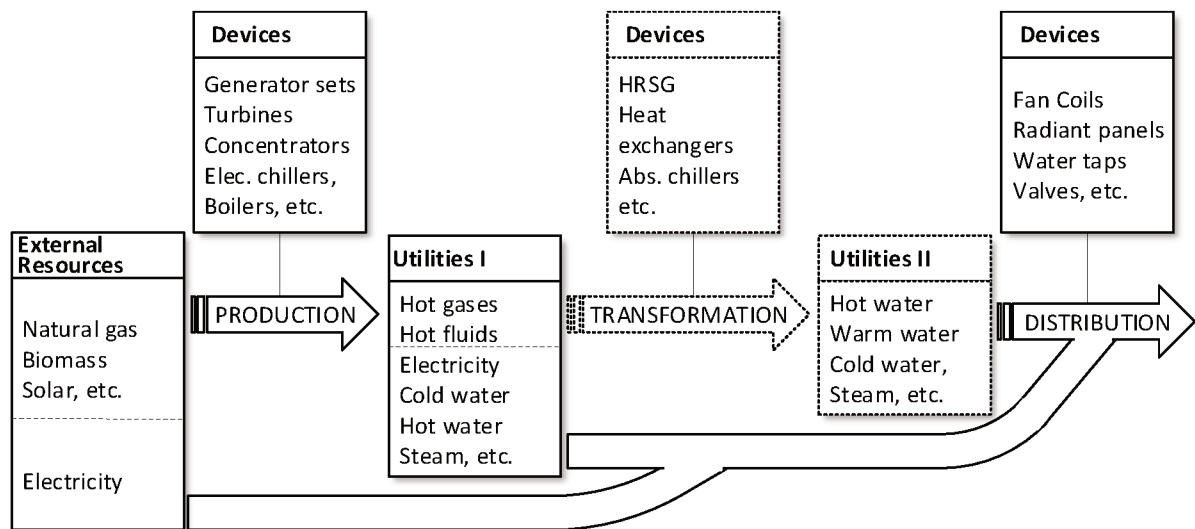


Figure 3 – Conceptual scheme of the production chain of utilities.

One key aspect of the demand of utilities in buildings is that—different from the industrial segment—it exhibits a remarked fluctuation and randomness due to the effect of multiple features such as:

<sup>1</sup> Note that in contexts different from the buildings segment, hot gases can be used directly, for example for wood drying.



- Building location and predominant weather conditions.
- Features related to the building use (*e.g.* equipment used, operation schedules, etc.).
- Building occupancy.
- Physical characteristics of the building structure (*e.g.* size, orientation, materials of construction, space distribution, fenestration, etc.).

Consequently, supply systems should operate according to the fluctuations on the utilities' demands. Usually, the simplest way to supply—for instance—cold (water), heat (in the form of steam or hot water), and electricity, is by importing the latter directly from the grid including for cooling devices, and feed a boiler with a fuel for addressing the heat demands. This supply system, illustrated in Fig. 4, is commonly referred in the literature as the conventional system, many times used as the reference for demonstrating the impacts of CCHP application.

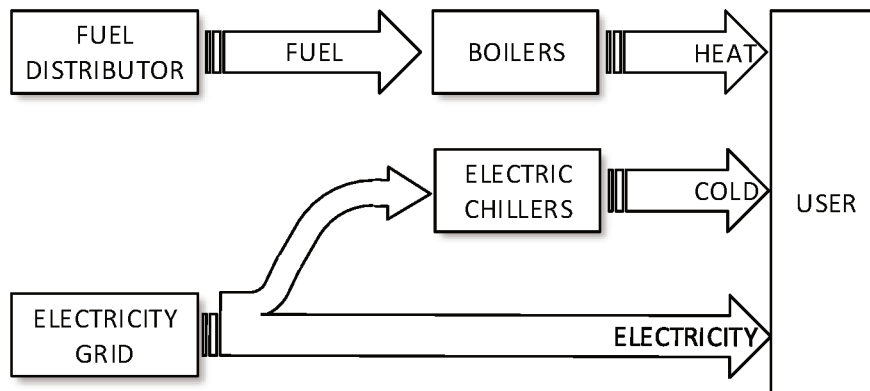


Figure 4 – Scheme of the conventional supply system.

By contrast, CCHP is characterized for producing simultaneously cold, heat and power (electricity) using a unique fuel, addressing totally or partially the required demands. Since the CCHP applied in commercial buildings commonly corresponds to *topping cycles*, where the electricity production drives the production of the rest of utilities<sup>2</sup>, the inclusion of conventional boilers and electric chillers into the supply system is very usual for supporting production and addressing completely the demands of heat and cold. As it

<sup>2</sup> further information in this regard can be consulted in (BALESTIERI, 2002).

can be seen in the Fig. 5, the adoption of CCHP—in this case based on generator sets<sup>3</sup>—enables the importation/exportation of electricity from/to the grid (dashed lines), as well as the operation in isolated mode (neither importation nor exportation of electricity). On the other hand, the frontier indicated in dashed lines depicts the cases where each generator set is mounted together with the heat recovery devices into a single structure; these assemblies are commonly referred as *cogeneration modules*.

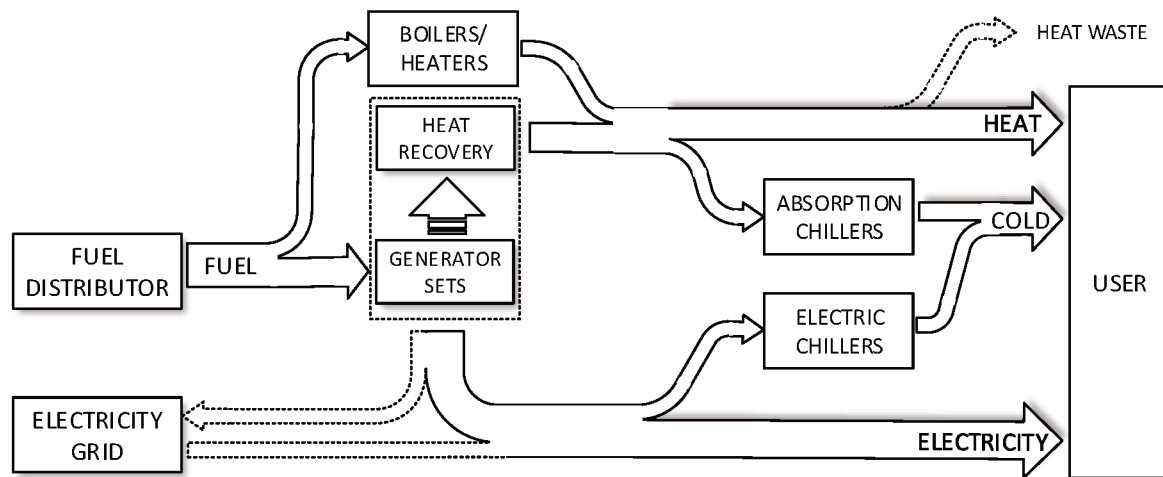


Figure 5 – Scheme of a supply system applying CCHP.

Evidently, the implementation of CCHP adds complexity into the supply system, which has to be justified by the attainment of a set of benefits; among them, a reduced operating costs and a higher reliability in the power supply are the most relevant for typical applications. Moreover, the deployment of CCHP on a large scale enables further social benefits as the reduction of potential emissions<sup>4</sup>, or the increase of the grid reliability due to a better load distribution during peaks. This later benefit distinguishes CCHP from renewables such as eolic energy, concentrated solar power or biomass, since it promotes the decentralization of the electricity supply; further discussion about these and other CCHP advantages can be found in the design guide published by ASHRAE (2015b).

<sup>3</sup> The term *generator set* denotes an internal combustion engine (or microturbine) coupled to an electrical generator in a single piece of equipment for producing electrical power.

<sup>4</sup> It corresponds to the emissions avoided due to the selection of supply systems incorporating CCHP over higher emissions alternatives.

## 2.1 FEATURES OF THE CCHP IMPLEMENTATION

Recognizing that operation costs are lower when implementing CCHP as long as the price of the chosen fuel is lower than the imported electricity, it follows that the annual avoided costs (or savings) along the lifetime of the system should offset the initial investment caused by the CCHP implementation, for demonstrating—at least—an economic advantage. Consequently, since higher avoided costs promote the CCHP implementation, it becomes convenient, at first, to operate the CCHP devices as much as possible, producing as much as they can. However, the fluctuations on the utilities demands imply, beforehand, a mismatch with their (CCHP) production. For illustration, consider the demands depicted in Fig. 6 for a small hotel (OPENEI, 2018) and suppose that a 50 kW generator set is installed for supplying the electric base load (see Fig. 6a).

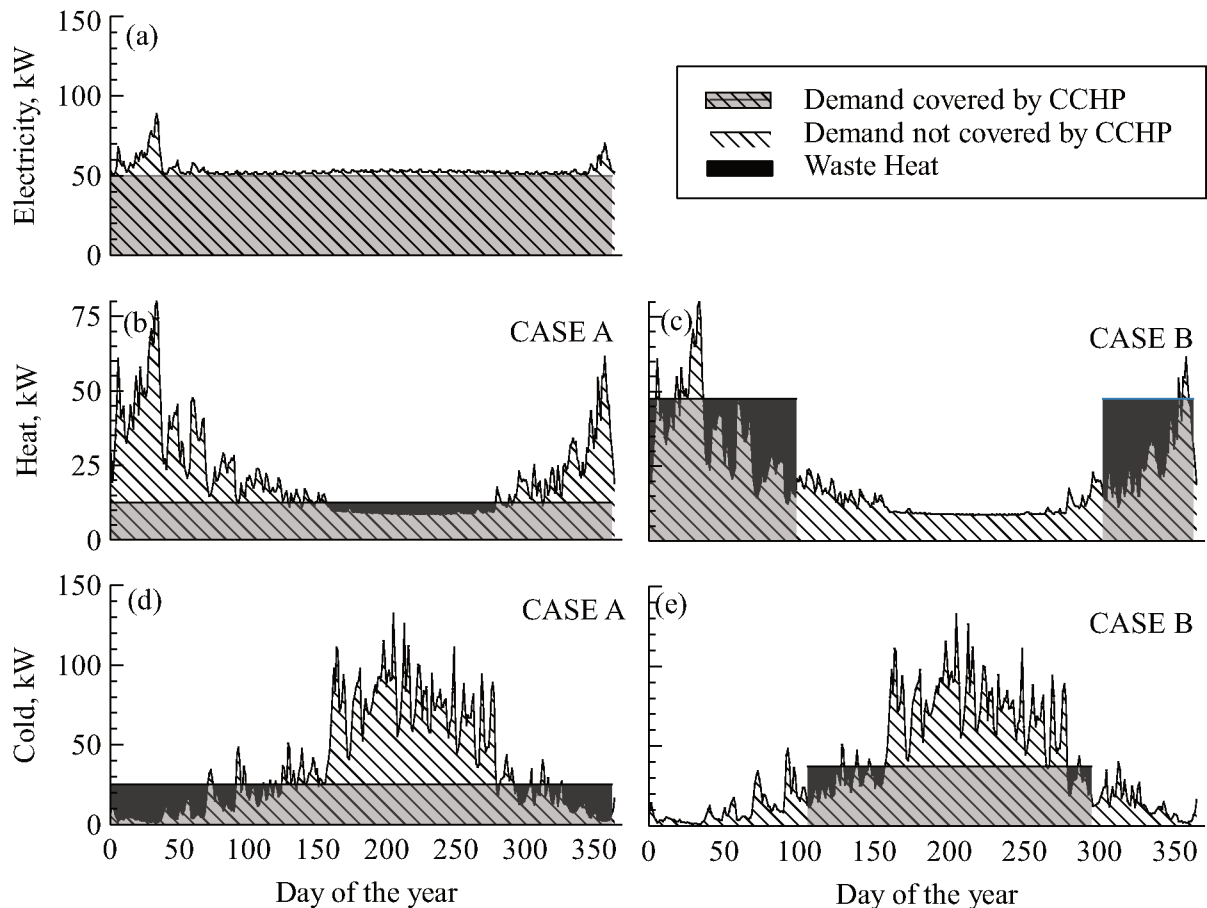


Figure 6 – Demand profiles and simple CCHP production in a small hotel: (a) electric base load; CASE A: (b) heat demand, (d) cold demand; CASE B (separated production): (c) heat demand, (e) cold demand.

In this case, the daily electric base load, not associated with air conditioning nor space-heating devices is very regular, which enables the continuous operation of the generator set at its full capacity and seems to favor the CCHP adoption. However, the heating and cooling demands present remarked fluctuations and have a clear seasonal pattern, which introduce some difficulties in the CCHP specification. For simplicity, let consider that 0.25 kW of heat and 0.5 kW of cold can be simultaneously produced per each kW of electricity produced by the generator set without modulation (see 'CASE A' depicted in Figs. 6b and 6d); it becomes evident that heat and cold demands cannot be addressed totally by CCHP and even that there are periods reporting wasted heat because there is not enough demand to address. Another option without modulating the electricity production consist in producing only one thermal utility at once, in order to increase its production per kW of electricity produced; as depicted in 'CASE B' (Figs. 6c and 6e), despite the improvement on these parameters—now 0.95 for heat and 0.75 for cold—results are not very different from the 'CASE A'.

This simple example introduces one important aspect of implementing CCHP, related to the interdependence among the amount of utilities produced. It means that their production can be redistributed just within certain limits. Since the supply system usually deals with non-coincident production and demand of utilities, this aspect can cause some mismatch between the CCHP production and the demand of utilities. Moreover, it explains the necessity of boilers and electric chillers for addressing completely the building demands when there is a production deficit, as well as the necessity of wasting (rejecting) heat when there is a surplus. Particularly, when this waste of energy is excessive due to a great mismatch (e.g. due to demand intermittencies over long periods), it can be an indication of the inconvenience of CCHP due the low utilization of its devices. Another evident feature is the existence of multiple choices in the CCHP specification for addressing a given set of utilities (e.g. the size of generator set and operation strategy in this example); in that regard, some key features involved in CCHP implementation are briefly described in the following sub sections.

### 2.1.1 Selection of components

There are various technology options<sup>5</sup> involved in the production of utilities (see Fig. 3), whose selection should be done according to adequate cost, technical or environmental premises. CCHP and conventional technologies can be grouped according to their function:

- *Prime movers*: these devices transform the chemical energy of a fuel into mechanical energy and are the core of the generator sets, since they provide this mechanical energy to a coupled electrical generator in order to be transformed into electricity. The most common choices for this equipment are internal combustion engines (ICE) and gas microturbines, although small gas turbines (capacity of about 2 MW or above) can be considered for large building applications. According to the review of Al-Moussawi, Fardoun and Louahlia (2017), steam turbines and combined cycles in commercial and residential applications is rarely used. Typically, these devices transform only around 30—38% of the energy input into mechanical energy and the rest is transformed into heat that is ultimately wasted if no heat recovery is done through the flue gas, one or more cooling loops (commonly hydronic), and by radiation. Particularly, the recovery of the first two heat waste sources through heat-recovery devices is the basis of CCHP (see Fig. 5). Parameters commonly taken into account for selecting a prime mover include the fuel used (natural gas and diesel are the most common), the electric efficiency at full capacity and at partial load, the response to load fluctuations, noise level, etc. Further technical information can be found in Orlando (1996) and other cogeneration design manuals.
- *Boilers/heaters*: depending on the utilities required in the building, boilers produce saturated steam, from 1 to 7 bar, while heaters produce hot water supplied at 80°C or less, conventionally using a fuel input. Fuels commonly used include natural gas, propane, diesel, and fuel oil, although electrical boilers and heaters also are available. When both services are demanded, it is very common to use part of the steam produced for producing hot water. The choice of these devices is based mainly on

---

<sup>5</sup> In this document, the term *technology* refers to a set of devices that performs the same energy transformations, using the same sources, producing the same outputs, and with the same principles of operation.

the fuel used, their emissions levels and their thermal efficiency; typical values for the latter are around 80-95%. Further information about the features and operation of these equipment can be found in the literature (BAZZO, 1995; Babcock and Wilcox, 2005).

- *Heat exchangers*: Their purpose is enabling the heat transfer between fluid streams in order to transform or produce utilities (see Fig 3). Particularly, equipment referred as *heat-recovery devices* transform the heat carried by the hot streams coming from prime movers into utilities; the HRSG for steam production and the heat exchangers used for hot water production are the most usual, even assisted by supplementary firing—see the review of Al-Moussawi, Fardoun and Louahlia (2016). The selection of these devices in CCHP applications stands for the definition of the heat exchanges necessary for the transformation/production of utilities. Common choices are:
  - *Exhaust gases* → *water*: It is proper to the HRSGs used for steam production, economizers, and heat exchangers gas/liquid used for hot water production.
  - *Hot air* → *water*: Most of turbocharged ICEs already has one or two cooling circuits whose heat exchangers are commonly referred as high-temperature (HT) and low-temperature (LT) intercoolers, which recover heat from the compressed air at a temperature of 150-200°C and produce hot streams at around 90°C and 50°, respectively (HIERETH, 2003). However, it is also possible, under certain conditions, to modify the heat recovery from the hot air stream in order to improve the production of CCHP utilities (RAMOS, 2012).
  - *Steam* → *water*: This is the case of exchangers and coils that use part of the steam produced in a boiler to produce hot water.
  - *Water* → *water*: It is very common in ICE-based CCHP to produce hot water using the heat dissipated through the engine block coolant circuit (commonly use water), which is available usually at 85-90°C, although some special designs use pressurized water at temperatures over 100°C. Another case is when a utility is produced from a hotter one, for example, when the supply system of a hotel produce hot water at 80°C for laundry and part of that is used in a heat exchanger for supplying heat to the pools.

- *Oil* → *water*: heat from engine lubricant oil, commonly available at around 75°C can also be recovered through a heat exchanger oil/water.
- *Water* → *air*: Includes the air-cooled heat exchangers (indirect) and cooling towers (direct) destined to dissipate heat to the atmosphere; in this case no utility is produced. On the other hand, radiant panels are used as terminals for the hot water utility (acclimatization).

Once the heat exchanges are defined for a given CCHP application, the specification for the construction or selection of each device is done according to the features of the hot/cold streams pairs, as well as their operation conditions.

- *Chillers*: These devices use heat or electricity for producing cold water through a thermodynamic refrigeration cycle. For electricity-driven chillers, this cycle corresponds to a vapor-compression cycle, while for heat-driven chillers, it corresponds to a vapor-absorption cycle. Independently of the type, their operation requires the rejection of heat to a temperature sink; for compression cycles, this is equal to the sum of the compression work and the heat removed from the cold water return (usually at 12°C) to produce the cold water stream (usually at 7°C), while for absorption cycles is that heat plus the heat absorbed from the heat source for activating the cycle. Fundamentals, features, and operation principles of this type of equipment is extensively reviewed in technical literature; particularly, Herold, Rademacher and Sanford (2016) is a good reference about heat-driven chillers (a.k.a. absorption chillers). Among the CCHP-related technologies, chillers are the most diverse since there are many technology options, although the most determining feature for selection is their coefficient of performance (COP). For electric chillers, other selection parameters include: type of compressor (reciprocating or centrifugal), rotation speed control enabled/disabled, and type of bearings, among others. On the other hand, the selection of an absorption chiller is mainly based on the heat source used for its activation; it can be hot gases, steam, hot water, or even combinations among them.

Moreover, there are two types of chillers that were omitted in Fig. 5 for simplicity, both using the energy from a fuel (commonly natural gas or diesel) for producing cold water; the first is a vapor-compression cycle whose compressor is moved by an ICE

instead of an electric motor and the second corresponds to a vapor-absorption cycle activated from the hot gases produced by direct combustion of the fuel in burners.

- *Energy storage devices:* the function of these devices is to accumulate energy from the utilities produced during a certain period, in order to be used later, either to final distribution or to further production of utilities. This accumulation can be done in diverse forms, of which the simplest is to storage utilities to be dispatched later; apparent examples are the batteries for electricity storage, and the tanks used for hot and cold water storage. Particularly, thermal energy storage (TES) refers to any device used for storing cold and heat utilities. The main advantage of energy storage devices in CCHP is that they enable to overcome the mismatch between energy generation and energy use, together with other derived benefits as the decrease of the required size of other CCHP devices, the increase of their operation time, and the improvement of the waste heat recovery. In practice, the adoption of TES is determined mainly by the availability of the space necessary for their accommodation. The selection of these devices are commonly based on parameters as the type of storage (active or passive, direct or indirect), the energy density, thermal losses during the storage period, and respond time between charging→storing→discharging cycles. Fundamentals of TES can be found in dedicated references as the works of Kalaiselvam and Parameshwaran (2014) and Li and Chan (2017).

Process flow diagrams depicted in Fig. 7 illustrate the issue of selecting the components forming a supply plant based on CCHP; both configurations are capable of supplying the same utilities (electricity, steam, hot water and cold water), but the structure on the left side uses engine-based generator set(s) and hot water-activated absorption chiller(s), while the structure on the right side uses gas turbine-based generator set(s) and steam-activated absorption chiller(s). Note that conventional boilers and electric chillers are not included for simplicity and that each symbol on diagram represents one or more pieces of equipment; in this type of diagrams, connectors represent mass and energy streams.

### 2.1.2 Definition of capacity and number of components

Another key feature proper to the design of any supply system incorporating CCHP is the necessity of defining the number and the size of its components. For illustration,





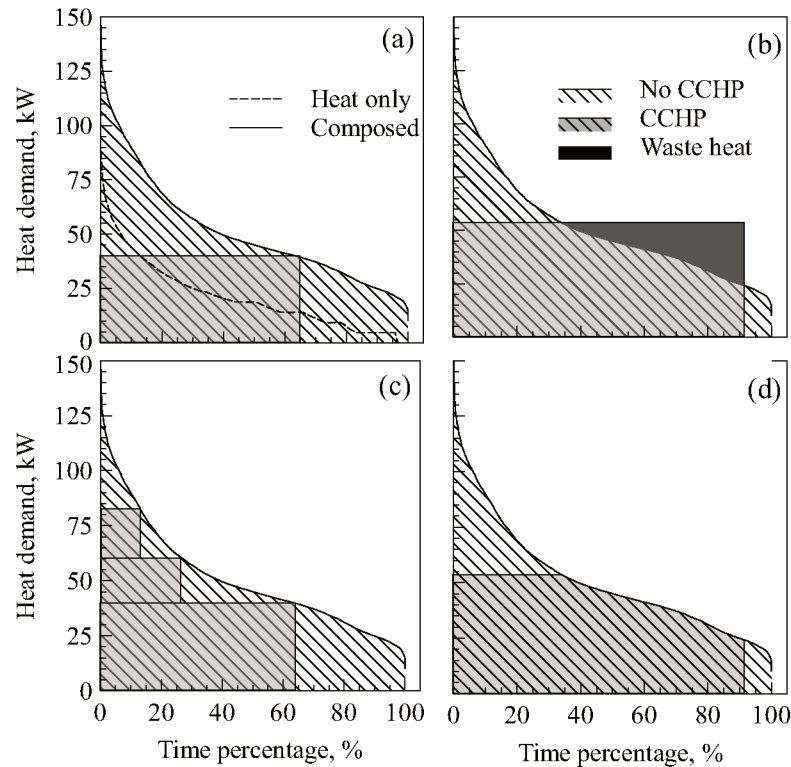


Figure 8 – Sizing of CCHP devices: (a) Maximum area without heat wasting, (b) Larger size with heat wasting enabled, (c) Multiple sizes, (d) Larger size with modulation enabled.

can be extended—see Fig. 8b—by letting some waste of heat until certain limit is reached<sup>6</sup>. Evidently, for both cases, there is a considerable portion of the demand not covered by CCHP, but this can be improved by the sizing strategy of Fig. 8c, where various generator sets are considered. However, the greater the number of equipment the lesser the quantity of individual operating hours, which impair the economic performance of CCHP. Finally, a larger generator set with modulation can be considered, as seen in Fig. 8d.

It is important to note that these basic sizing approaches are based on various premises beforehand, especially—as mentioned by Voorspools and Haeseleer (2006)—that CCHP electricity is produced only when enough heat is required, fact that not always is true. Additionally, some key features are omitted, for example backup and redundancy strategies, minimum and partial-load operation, cost analysis, available sizes in the market, etc. However, they serve for illustrating the multiple choices when deciding the size and the number of CCHP devices.

<sup>6</sup> This limit can correspond to a restriction on atmospheric emissions or until the primary energy savings are null (CARDONA; PIACENTINO, 2003)

### 2.1.3 Definition of operation strategy

Other CCHP implementation aspect that must be defined is the operation strategy of the supply system, which embraces all the decisions on how it will produce the utilities for addressing the building load demands. Important issues of this concern includes, but are not limited to:

- Enabling (or not) the importation/exportation of electricity from/to the grid.
- The use (or not) of energy storage devices, and their charging → storing → discharging schedule.
- The CCHP scheduling premise, i.e. defining whether the CCHP production would address preferably base loads over prolonged periods, or peak loads over shorter—possibly intermittent—periods.
- Enabling or limiting (or not) the waste of heat during certain number of periods.
- Modulation of CCHP devices within their proper operating range.
- Priority for addressing the load demands, e.g. CCHP production following electricity demand (heat/cold production as consequence), or CCHP production following the cold/hot demand with the electricity production as consequence (implies enabling the importation/exportation from/to the grid)—see Fig. 8d. In this regard, these options are known as *following energy load* (FEL) strategy and *following thermal load* (FTL) strategy, respectively; other operation (or switching) strategies are also found in the literature (SHI; MINGXI; FANG, 2017).

These basic issues are commonly analyzed and set during the plant design, and are apparently formed by simple choices; however, the CCHP operation schedule itself is the subject of various works focused on its improvement—as reviewed by Cho, Smith and Mago (2014)—frequently adopting optimization routines for obtaining the maximum benefit from it. Finally, note that these and other operational issues affect the selection of technologies (section 2.1.1), as well as the definition of the size and number of components (section 2.1.2), which conforms the CCHP design problem as the set of three interrelated tasks, as represented in the diagram of the Fig. 9; between parentheses appear the terms commonly used in the literature for referring to them.

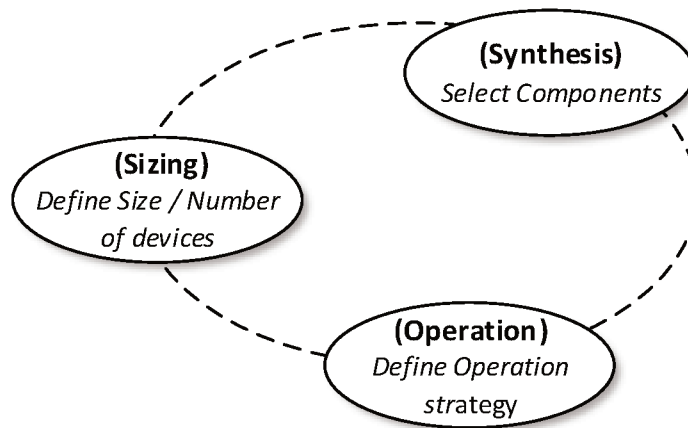


Figure 9 – Tasks forming the CCHP design (specification) problem.

## 2.2 METRICS

The use of metrics enables the comparison of diverse performance aspects of CCHP for supporting the decision-making involved in its design, even for determining the convenience of its implementation. These metrics are classified by Al-Moussawi, Fardoun and Louahlia (2016) according to the aspects they refer into energy, environmental, economic and exergy metrics. It is important to remark that there is not a 'universal' metric capable of allowing a clear distinction of the most convenient design, thus the selection process involves the judgment of various of these parameters simultaneously. Some metrics are widely used, while some authors (e.g. Smith, Luck and Mago (2010)) have proposed their own modifications according to their scope; in the following paragraphs, some usual energy metrics are briefly described:

- *First-law Efficiency ( $\eta_I$ )*: The portion of the energy input transformed into electric and heat power. It is presented in Eqn. 2.1, and counts all the heat flows  $Q_i$  used by CCHP, including the heat used for activating chillers. The higher the  $\eta_I$ , the lesser the fuel energy input required for a given set of electric and heat power outputs, thus it is suitable for express the energy input savings of a given supply system. However, it does not differentiate the relative values of each output and is not directly comparable to any metric of separate power and thermal production.

$$\eta_I = \frac{W_{el} + \sum Q_i}{E_{in}} = \eta_{el} + \eta_{th} \quad (2.1)$$

- *Primary Energy Rate (PER)*: It is the ratio between the system outputs (utilities) and its energy inputs. Note that the cold and heat produced are added directly, which implies that, depending on the chillers' COP, this parameter can be greater than the unity. Despite it is not a general efficiency parameter, since its value is not bounded between zero and the unity, its formulation is mathematically consistent. As evidenced by Matelli and Bazzo (2013), for a given output, it is proportional to the fuel savings due to CCHP and reflects the duality of CCHP systems, which behave as a thermal engine and as a refrigerator.

$$PER = \frac{\sum W_{el} + \sum Q_h + \sum Q_c}{\sum E_{in}} \quad (2.2)$$

note that this formulation is general for production systems and considers multiple fuel sources, multiple heat and cold utilities, and multiple forms of electricity production; in the particular case when there is a unique fuel, this parameter is equivalent to that referred as *Energy Utilization Factor (EUF)*.

- *Primary Energy Savings (PES)*: it is the energy input avoided by implementing CCHP, compared to a conventional system with the same outputs, sometimes expressed as a ratio (PESR). Some authors use the term *Fuel Energy Savings (FES)*.

$$PES = E_{in,conv} - E_{in,cchp} = \frac{W}{\eta_{el,conv}} + \frac{Q}{\eta_{th,conv}} - E_{in,cchp} \quad (2.3)$$

$$PESR = \frac{PES}{E_{in,conv}} = 1 - \frac{E_{in,cchp}}{\frac{W}{\eta_{el,conv}} + \frac{Q}{\eta_{th,conv}}} \quad (2.4)$$

values of  $\eta_{el,conv}$  and  $\eta_{th,conv}$  take into account the way how the electricity and the heat are originally produced; for example, they can adopt the values of 0.55 and 0.90 if a combined cycle and a natural gas boiler are considered, respectively.

These parameters are calculated in terms of energy transferred (kWh) over a given period, but for steady-state operation it is more convenient to calculate them in terms of energy transfer rates (HORLOCK, 1987).

## 2.3 PRICE STRUCTURE

The price structure of the energy resources is a key aspect for the economic performance of any CCHP project, since a great part of the operation costs come from their purchase, as well as the most of the CCHP incomes is derived from the sale of electricity (when enabled). This structure, namely the cost rates forming the price, can vary according to the purchase and sales options present in the market, specific to the CCHP project; however, specifically for electricity prices, there are some rates that are commonly present (ORLANDO, 1996):

- A. *Customer charge*: It is a fixed charge, generally applicable regardless whether any power is used or not. It is based on the fixed costs of the utility and is charged in monetary units<sup>7</sup>.
- B. *Demand charge*: It is based on a maximum demand that can refer to the peak occurring during the rate period, to a certain contracted value, or may be restricted to the peak occurring only during on-peak periods. It is intended to recover electricity production costs and is commonly charged in monetary units per kW supplied.
- C. *Distribution charge*: It is based on the peak occurring during the rate period and intends to recover transmission and distribution costs; it is commonly charged in monetary units per kW delivered.
- D. *Energy charge*: It refers to the amount of energy actually used on-site. It may be billed in different blocks, which can be specified in energy baselines terms, in use-of-demand terms, or based on the time at which energy is used; in that case, time-defined blocks include on-peak, off-peak and intermediate periods. It is commonly charged in monetary units per kWh used.
- E. *Taxes*: Are imposed on behalf of a government body, typically the state and the local municipality. They are commonly charged as a percentage of the energy charges.
- F. *Surcharges*: They are destined for recovering specific costs and can vary from period to period. They commonly are referred to as cost adjustments and are commonly applied on monetary units per kWh used.

---

<sup>7</sup> In this thesis, unless otherwise specified, the unit adopted for monetary quantities is the U.S. dollar, expressed with the symbol \$.

G. *Supplemental power charge*: It applies to CCHP and other cogeneration facilities, since they continue to purchase some electricity from the electric utility. This charge corresponds to the difference between cogeneration output and the site requirements and has differentiated rates for the demand and the energy used on-site.

The structure for natural gas usually is simpler than for electricity and is based on the amount of gas delivered to consumer, normally charged in monetary units per normal cubic meter of gas ( $\text{Nm}^3$ ). Distribution charge and taxes also apply. Current Brazilian structures, valid for the state of Santa Catarina are adopted in the present work, which are described in the following paragraphs.

Firstly, in the country there are two electricity commercialization markets: the regulated market and the free market; in the first—wherein the residential customers are included—the rates are established or limited by the Brazilian energy regulatory agency (ANEEL) and are charged by the local electric concessionaire to the customers. In this case, the concessionaires hold long-term contracts directly with power suppliers through public auctions. Conversely, costumers in the free market have the option of negotiating the price (excluding taxes and distribution rates) as well as the term of the contract directly with power suppliers or through electricity retailers. Taking into account that, under the current regulation, only customers with a power demand greater than 500 kW can apply to participate in the free market, large commercial buildings have the option to choose the price structure for purchasing electricity, while smaller applications have to accept the regulated prices. Details about the current legislation, conditions and terms of the electricity commercialization can be consulted in (ANEEL, 2019); specifically, the normative resolution 414 (ANEEL, 2010) establish the general conditions for the electricity supply. Table 2 summarizes the electric price structure adopted in this work, which is currently used by the local electric concessionaire, whose rates can be accessed at CELESC (2019) and explained in PROCEL (2011). Note that values reported correspond to the category where most of the commercial building applications could be classified: They are from group B3, where the required supply voltage is lesser than 2.3 kV and the building application does not correspond to rural, residential, nor public lightning. Values reported were valid by July/2019.

Table 2 – Electricity price structure.

Rate	Features	Value*
<b>A</b>	It is embedded in the energy charge (rate D). However, the availability rate applies when the monthly electricity consumption is lesser than a certain value, depending on the type of power supply (single-phase, two-phase, or three-phase).	<i>Embedded in D</i>
<b>B</b>	Applies on a demand contracted with the concessionaire that is charged even if the consumer does not use it. Whenever a demand exceeding by more than 5% of this value is measured for at least 15 min, surcharges apply on the extra demand with a greater rate. Currently, this type of contract is exclusive to buildings requiring 2.3 kV or more, implying that—for the category chosen—it is also embedded in the energy charge rate.	<i>Embedded in D</i>
<b>C</b>	As well as the previous items, it is embedded in the energy charge rate. However, when the consumer opts for participating in the free market, it is billed by the concessionaire due to the use of the distribution system. It is charged in monetary units per energy delivered (\$/kWh), and in cases where a power demand is contracted, there is a component of this rate that is billed in \$/kW.	<i>Embedded in D</i>
<b>D</b>	It is computed and billed by the concessionaire and, for the category chosen, it embraces rates A, B, and C. Moreover, it is composed by three different rates according to the type of day (business or non-business) and the period of consumption (on-peak, intermediate, and off-peak). On-peak rate ( <i>onp</i> ) applies to business days between 18:30 and 21:30, intermediate rate ( <i>int</i> ) applies during the hour before (between 17:30 and 18:30) and during the hour after the on-peak period, and off-peak rate ( <i>ofp</i> ) applies to the rest of the time. Additionally, there is the option of getting a flat ( <i>flt</i> ) rate, that does not discriminate rates by period of consumption.	<i>\$/kWh</i> <i>onp</i> : 0.24927 <i>int</i> : 0.16229 <i>ofp</i> : 0.12027 <i>flt</i> : 0.13346

\*Published in Brazilian Reais (BRL). Exchange rate: 3.8 BRL per USD.



Electricity price structure—*continued.*

Rate	Features	Value*
<b>E</b>	Tributes charged to consumer includes federal and state taxes. They are referred by its acronyms in Portuguese as <i>PIS</i> , <i>COFINS</i> which are federal, and <i>ICMS</i> that is imposed by the state of Santa Catarina. They apply directly on energy charge rate (D) plus surcharges (F) as follows:	<i>PIS</i> : 0.84% <i>COFINS</i> : 3.89% <i>ICMS</i> : 25%
	$\text{Price} = \frac{D + F}{1 - (PIS + COFINS + ICMS)}$	
<b>F</b>	Surcharges apply depending on the electricity production conditions. Since most of the energy production in the country is based on hydro, surcharges are included when, due to climatic conditions or other circumstances, it becomes necessary to increase the share of electricity produced by thermoelectric power plant, which is more expensive. There are four charging levels: <i>green</i> , <i>yellow</i> , <i>red1</i> , and <i>red2</i> .	\$/kWh <i>green</i> : 0.000 <i>yellow</i> : 0.015 <i>red1</i> : 0.040 <i>red2</i> : 0.060
<b>G</b>	There are not differentiated rates for applications were cogeneration plants are installed.	

\*Published in Brazilian Reais (BRL). Exchange rate: 3.8 BRL per USD.

On the other hand, the natural gas commercialization market is currently in a transition; until not long ago, the price to distributors was fixed by the National Petroleum Agency (ANP) and the tariff to concessionaires was regulated by the state regulation agency (ARESC). However, by July 2019, a set of measures was approved by the national government aiming to break the state monopoly on the market allowing the free competition among suppliers, thus favoring the reduction of natural gas tariffs (LIS, 2019). Despite of this, the tariff considered in this work corresponds to that regulated before these measures, since their implementation is still incipient. The tariff is formed by two components: the base rate—including the supply, transportation, and an adjusting addend—which is charged by federal and state taxes, and a distribution margin. Table 3 summarizes the natural gas tariff used henceforth.

These values have been taken from ARES (2019), where a 'reference' heating value of 39330 kJ/kg (9400 kcal/m<sup>3</sup>) is reported. Thus, the natural gas tariff in \$/kWh is

Table 3 – Components of the natural gas tariff (ARESC, 2019).

Base* \$/m <sup>3</sup>	Margin* \$/m <sup>3</sup>	PIS	COFINS	ICMS
0.29021	0.04097	1.65%	7.6%	12%

\*Published in Brazilian Reais (BRL). Exchange rate: 3.8 BRL per USD.

calculated according to Eqn. 2.5

$$\text{Tariff} = 0.09153 \cdot \left[ \frac{\text{Base}}{1 - (\text{PIS} + \text{COFINS} + \text{ICMS})} + \text{Margin} \right] \quad (2.5)$$

## 2.4 REGULATIONS

Depending on the electricity commercialization market, implementation of CCHP entails different means of economic remuneration. While in the regulated market there is a compensation through the acquisition of 'energy credits', in the free market, the plant owner (designated autoproducer) is allowed to sell the electricity surplus (if any). Regulations applicable for the electricity compensation mechanism can be consulted in the normative resolution 482 (ANEEL, 2012), and the decree 5163 (Brazilian Parliament, 2004) collects the main regulations proper to autoproducers and the free commercialization market.

Independently of the commercialization of electricity, CCHP is qualified according to the criteria compiled in the normative resolution 235 (ANEEL, 2006), which establish the definitions and minimum qualifying requirements for cogeneration plants<sup>8</sup>. Particularly, for those based on natural gas and with a capacity smaller than 5 MW, the following relations should be fulfilled:

$$\frac{E_{th}}{E_f} \geq 15\% \quad (2.6)$$

$$\frac{E_{th}}{E_f} \cdot \frac{1}{2.14} + \frac{E_{el}}{E_f} \geq 41\% \quad (2.7)$$

Using the same terms of the normative,  $E_{th}$ ,  $E_{el}$ , and  $E_f$  correspond respectively to the energy of the heat utility, the energy of the electro-mechanic utility, and the energy of the energy source, all expressed as kWh delivered per hour by/to the plant at its

<sup>8</sup> CCHP plant (or system) understood as the specific facility where the cogeneration is operated for producing mechanic energy and heat utilities in combination from *one* primary source; namely it excludes auxiliary boilers and electric chillers.

'mean operation regime'. Note that this normative does not include any mention to the production of cooling utilities. For this reason, in this work, it is considered that the term  $E_{th}$  should include necessarily the heat used for activating the absorption chillers whenever CCHP is implemented.

Once the qualification is certified, other specific technical, safety and contractual requisites should be fulfilled as indicated in the standard (ANEEL, 2016). However, these requisites are part of further engineering stages and are not part of the scope of this work.

## 2.5 PREMISES COMMONLY CONSIDERED IN CCHP DESIGN

Omitting environmental aspects, only the above-mentioned features already impart a great complexity to the CCHP design given:

- The fluctuation inherent to the energy demands in buildings.
- The multiple technologies that are suitable for CCHP and the great number of feasible combinations among them for supplying electricity, cold and heat to a building.
- The wide range of sizes, prices and technical features available in the market for each technology.
- The decisions involved in the definition of the CCHP operation strategy.
- The availability of multiple prices for energy sources, as well as different market conditions and compliance with current applicable regulations.

In spite of that, supply systems implementing CCHP have been installed straightforward for decades, and technologies involved have a high level of maturity. Consequently, in practice, the engineering of these projects is well-defined and specialists in this field are capable of dealing with these issues, supported on their expertise and knowledge, as noted by Matelli (2008). However, still there is room for improvement in this field, given some features identified through the development of a computational tool<sup>9</sup>, created for quick calculation of feasible CCHP projects, which demanded a high level of interaction with experts in this field. It made possible to understand what is commonly done when specialists start a new CCHP project and to collect their requirements (as users) that

<sup>9</sup> The application is named *CogeCalc 2* and currently there is a consultation with Petrobras for registering it to the Instituto Nacional da Propriedade Intelectual (INPI), see appendix B.

should be addressed by the tool. Consulted specialists are from three Brazilian gas distributors (from states of Bahia, São Paulo and Santa Catarina), a company specialized in the engineering and installation of air conditioning systems (ER engenharia), a supplier of absorption chillers (Thermax do Brasil), and a supplier of engine-based generators sets (Stemac). Some common requirements and practices are summarized in the following paragraphs.

Once the specialists get available information about the type and magnitude of utilities required, as well as existing installations of their potential clients, they proceed to characterize their demand profiles using available information (e.g. electricity and fuel bills, hydrometers readings, data from supervisory systems, etc.). It is important to identify with enough detail the seasonality present on the profiles and make the distinction of the amount of utilities charged with different rates (see 2.3). Information is input in pre-designed spreadsheets, which often are modified in accordance with the client particularities. Some technical data can be assumed because are considered typical, other come from equipment catalogs, and other need to be estimated. Commonly, each specialist has its own set of spreadsheets; it was evidenced that formulation is rather basic and use of thermodynamic properties is seldom.

The main purpose of these calculations is to demonstrate to the client whether the implementation of CCHP is economically feasible or not. Once the technical and economical parameters shows the CHP alternative as feasible, and more convenient than the conventional production, the information is addressed to a more detailed analyses, many times conducted by equipment suppliers or by an engineering company; it is usual that the purchase of main equipment is started with the information computed in this preliminary design.

In view of this manner of executing CHP projects by the cited companies, and the potential risk of further stages modify the preliminary results obtained by using spreadsheets, it was required a program to obtaining quicker and more reliable solutions, based on process simulations. The key requirements transmitted by the consulted specialists and some insights of the program are organized in the appendix B.

## 2.6 PRELIMINARY ASSESSMENT OF CCHP PROJECTS

Depending on the size of the utilities' supply facilities, their placement can be executed following the typical stages of an engineering project, *e.g.* determination of CCHP application potential, initial feasibility study, detailed engineering, review of financing options, procurement, energy services contract, construction, and turnkey (FLIN, 2010). As the depth-level of analyses increases, larger capacity for information processing is required. In this way, some computational tools frequently used for assisting the CCHP projects are listed as follows:

1. Spreadsheets with formulation based on order-of-magnitude relations and some related heuristics. They are commonly adapted as required for quick respond.
2. Spreadsheets and other general-purpose programs with pre-defined templates and general formulation.
3. Process simulation programs enabling steady-state mass and energy balances and more detailed equipment specification.
4. Process simulation programs enabling the modeling of the dynamic behavior of the plant along variable operation periods.
5. Computational tools capable of performing optimization procedures.

Mass and energy balances (item 3 in the list) together with energy-based metrics and economic parameters are extensively used for addressing the requirements of CCHP projects (*e.g.* see the works of Badami et al. (2014) and Shnaiderman and Keren (2014)), constituting the standard in the engineering practice. One of the most important advantages of this approach, is that once the simulation model is formulated, diverse scenarios can be solved, according to the supply requirements of a given building. Normally, the designer is looking for the best economic performance of the CCHP project. The most basic and understood metric is the simple payback period (PBP), which by itself does not bring enough information for take a 'go or no go' decision, but an investment with a shorter PBP is considered to have lower risk than those with a longer PBP; additionally, it is easily recognized by clients and is extensively used by the specialists consulted. Additionally, the preliminary feasibility appraisal of CCHP projects against conventional

supply systems considers the additional investment of adopting CCHP and the annual avoided costs with respect to the conventional production. In this way, the formulation of the costs balances is presented as follows:

$$PBP = \frac{INV_{cchp} - INV_{conv}}{TOK_{conv} - TOK_{cchp}} ; \quad INV = 1.15 \cdot EK \quad (2.8)$$

$$EK = \sum_{e=1}^{NE} UK_e \cdot CAP_e \quad (2.9)$$

$$TOK = MOK + IK + \sum_{h=1}^{H_{op}} OK_h ; \quad MOK = 0.07 \cdot EK \quad (2.10)$$

$$IK = af \cdot EK \quad (2.11)$$

Here, the total investment (INV) is the sum of equipment purchasing costs (EK) and indirect costs, which account for engineering, supervision, and legal expenses, as well as contractor's fees and contingencies (BEJAN; TSATSARONIS; MORAN, 1996). In this work, it is assumed that indirect costs are equal to 15% of EK. Moreover, the cost of each equipment  $e$  is estimated as its capacity ( $CAP_e$ ) multiplied by a unitary equipment cost ( $UK_e$ ), which should consider installation costs. On the other hand, total operation cost (TOK) is the sum of the maintenance and operation cost (MOK), which is assumed equal to 7% of EK, the investment (capital) cost (IK)—estimated through an annuity factor ( $af$ )—and the sum of hourly operating cost ( $OK_h$ ) along the operating hours  $H_{op}$ . Particularly,  $OK_h$  is the expenditure caused by the purchase of utilities minus the incomes obtained by the sales of them, expressed in the following equation:

$$OK_h = \sum_{u=1}^{NU} (UK_{u,h} \cdot PUR_{u,h} - SP_{u,h} \cdot SAL_{u,h}) \quad (2.12)$$

$UK_{u,h}$  corresponds to the unitary cost (in \$ per kWh),  $PUR_{u,h}$  is the amount purchased (in kWh),  $SP_{u,h}$  is the sale price (in \$ per kWh), and  $SAL_{u,h}$  is the amount sold (in kWh) of the utility  $u$  during the hour  $h$ . The annuity factor (or capital recovery factor) is determined for an interest rate of 12%, and a project lifetime of 20 years, values judged adequate by the consulted specialists, resulting in  $af = 0.134$ .

Now, the usefulness of the simulation modeling is illustrated through a simple example with the aim of introducing some aspects that will be considered in the following chapters. Suppose that the CCHP layout proposed in Fig. 10 needs to be assessed for a

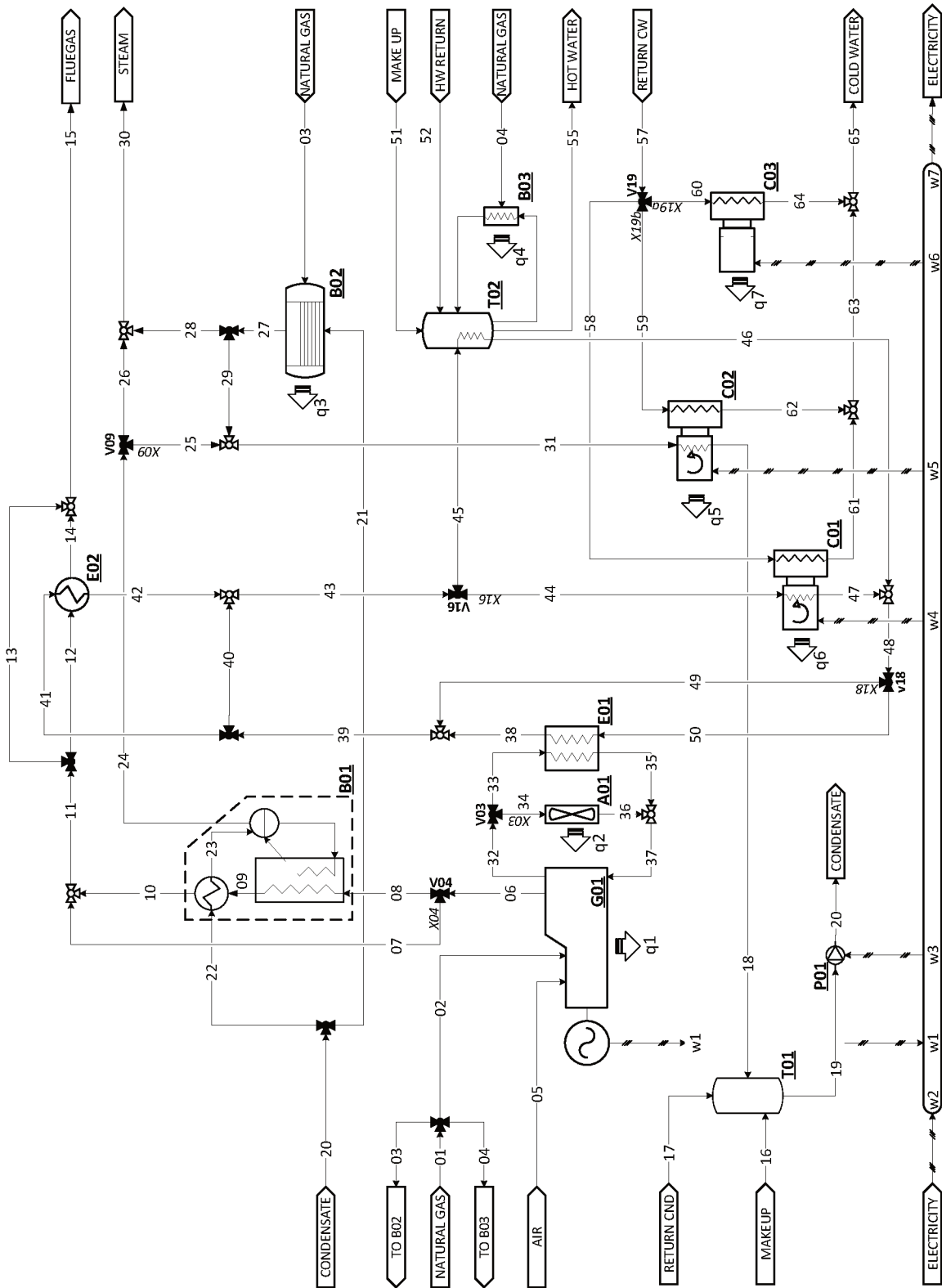


Figure 10 – Example of a CCHP layout for production of electricity, steam, hot water, and cold water.

given application, and that is based on a generator set with nominal capacity of 1035 kW. Heat from the exhaust gases can be recovered through a HRSG (B01) and a gas/liquid heat exchanger (E02), while the heat from the coolant circuit can be recovered through the heat exchanger E01. Heat excess from this circuit can be rejected to the atmosphere through the radiator A01. This layout is capable to deliver—besides electricity—steam, hot water, and cold water for air conditioning. The later can be produced by a hot-water-driven chiller (C01), by a steam-driven chiller (C02), or by the combination of both. Auxiliary equipment for complementing the CCHP production is also included: B02 corresponds to a conventional steam boiler, B03 to a hot water boiler—both fed by natural gas—and C03 is an electric chiller; technical features of the equipment are presented in the appendix A.

Note that through the manipulation of certain valves in the model, it is possible to alter (even cut down) the CCHP production of each utility. For example, if it is required to produce hot water as much as possible (by CCHP), the valve V04 should drive the flow of hot gases through the stream 07 (bypassing B01) for increasing the heat transferred in E02 to the internal water circuit, and the valve 16 should drive the flow of that water through the stream 45 (bypassing C01) for increasing the production of hot water in the coiled tank T02. In this case, steam and cold water would be produced entirely by auxiliary (conventional) equipment. For ease, one path is indicated for each valve by a flow ratio (letter  $X$  followed by the number of the valve), which varies from 0 to 1. In this example,  $X04 = 1$  and  $X16 = 0$ .

The simulation model consists basically in the formulation of mass and energy balances proper of the layout. It was done using the software *Engineering Equation Solver* (EES), taking into account the following premises:

1. Generator set operating at nominal conditions.
2. Electric efficiency of G01 : 31.05%, exhaust gases temperature: 474°C, minimum exhaust gases temperature: 120°C.
3. Maximum engine cooling water temperature: 95°C (stream 32). Minimum engine cooling water temperature: 85°C.
4. LHV of Natural gas: 49650 kJ/kg.



5. The sale of electricity is not enabled. Electric demand is equal to the capacity of the generator set (1035 kW) .
6. Electricity is purchased (for conventional production) at the flat rate (see Tab 2).
7. Minimum temperature difference of 10°C for water/water heat exchangers and 20°C for heat exchanger E02.
8. Pinch point HRSG: 20°C, approach point: 5°C.
9. Water circulating pressure: 150 kPa, pressure drop across piping and devices is neglected.
10. COP of C01: 0.80, COP of C02: 1.51, and COP of C03: 3.6.
11. Unitary costs of equipment considered are presented in Table 4. Each value was corrected to the year 2019 through a plant cost index (CEP, 2019).

Table 4 – Equipment unitary costs for CCHP layout of Fig. 10, installation included.

Tag	UK <sub>e</sub> , \$/kW	Reference	Comments
G01	2366	(DOE, 2016)	Includes E01, E02, and installation.
B01	70	(CAIN, 2013)	
B02	96	(PEERLESS, 2018)	Installation factor: 1.53 (GARRET, 1989)
B03	54	(HEVAC, 2019)	
C01	564	(DOE, 2017)	
C02	853	(DOE, 2017)	
C03	512	(FPL, 2012)	

Firstly, the maximum amount of each utility produced by CCHP, operating G01 at nominal conditions, is determined by altering the flow ratios of some valves in the layout, as described previously. Table 5 presents the supply conditions for each utility, the ratios altered, and their maximum production by CCHP.

These results show that the lower the temperature level, the greater the heat recovered and transformed in energy utilities, consequently reporting better performance, here expressed using the metric PER. However, since metrics used commonly in the CCHP design are based on the first law of thermodynamics, they do not necessarily express

Table 5 – Maximum supply of thermal utilities by CCHP layout.

Utility	Conditions	F. Ratios	Max., kW	PER
Steam	800 kPa, saturated	$X04 = 0$ $X09 = 0$	640.9	50.4%
Hot water	supply: 60°C	$X03 = 0$ $X04 = 1$ $X16 = 0$	1673	81.5%
Cold water, C01 only	supply: 7°C return: 12°C	$X04 = 1$ $X16 = 1$ $X18 = 0$	1201	67.1%
Cold water, C02 only	supply: 7°C return: 12°C	$X04 = 0$ $X09 = 1$	922.7	58.7%

the quality of the energy utilities as it would be the case of an exergy analysis, as that presented previously by Barrera and Bazzo (2018). Note that for producing hot water at 60°C, it is not necessary an excessive temperature in the internal water circuit (stream 38)—e.g. 80°C—allowing the complete recovery of the heat from the engine block cooling circuit (streams 32 to 37). However, by including C01 into the layout, it is imposed that the internal circuit temperature is at least 95°C, since this it is required for activating the chiller at its nominal conditions. Evidently, this temperature can not be reached in E01, given the minimum temperature difference guaranteed in this equipment, thus an additional heat transfer is required at higher thermal level at E02, which is constrained by the minimum temperature allowed for hot gases. Thus, for the proposed layout, the flow rate of the internal water circuit at temperatures greater than 85°C (the maximum attainable in E01) is restrained by the heat balance of E02, and if it is lesser than the minimum flow rate that guarantee the minimum temperature difference of E01, it is necessary to dissipate heat trough A01. For this reason, for the maximum production of cold water, using only C01,  $X18$  is set to 0, letting the model to calculate the value of  $X03$ .

Now, limiting the utilities' production to these maximum values, it is possible to perceive the solution space of the model, i.e. the set of possible outputs obtainable by the model, through Figs. 11a (C01 only) and 11b (C02 only). Here, each line corresponds to the amount of cold water utility produced by CCHP, varying with the production of hot water (in MW) at a given steam production (by B01), expressed as a percentage of

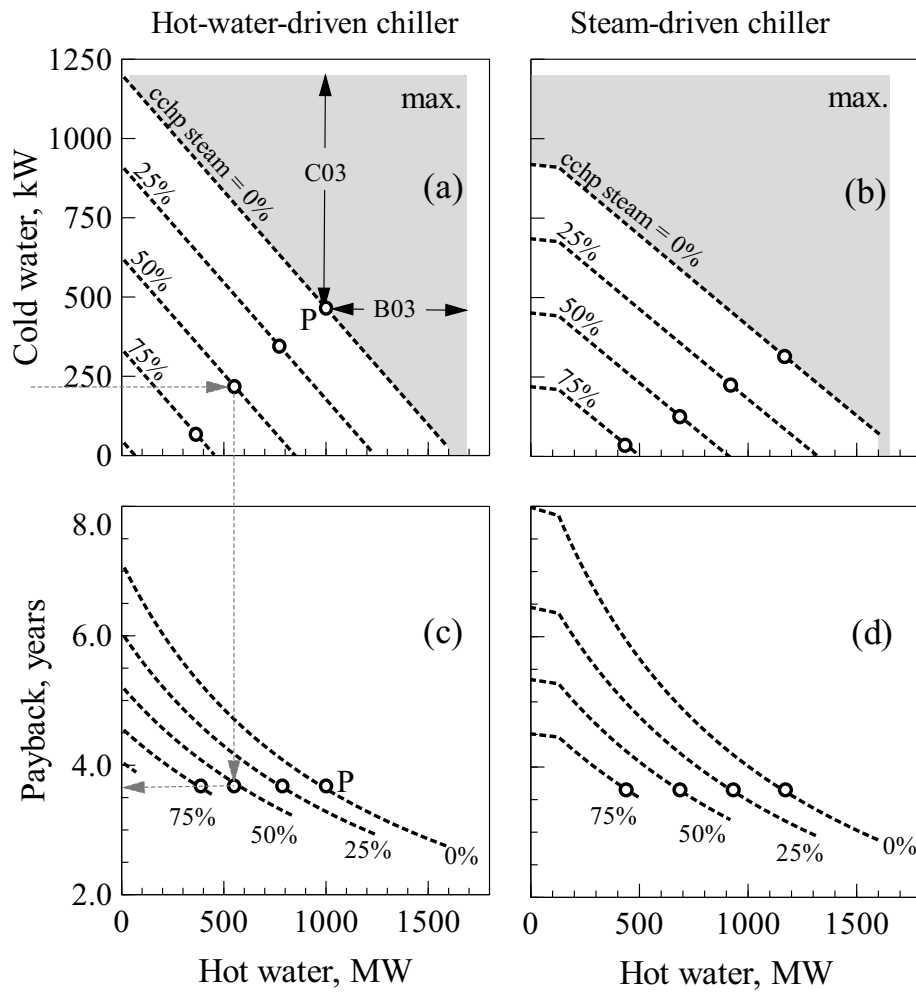


Figure 11 – Solution space of the simulation model of the proposed layout, limited at maximum production of utilities by CCHP.

the maximum. For a given solution  $P$ , the distance to the vertical line of maximum hot water is the production required to be supplied by the auxiliary hot water boiler B03. Analogously, the vertical distance to the maximum cold water line is the production to be supplied by the auxiliary chiller C03. Steam production of auxiliary steam boiler B02 is proportional to the distance of the line crossing  $P$  to the origin.

The lower part of Fig. 11 exhibits the PBP for each line depicted in the upper part, e.g. the point  $P$  in Fig. 11c corresponds to the production values depicted in Fig. 11a. If, for example, only projects reporting a PBP lesser than 3.6 years (indicated by circles) would be considered feasible, it follows that the production of cold water by CCHP should be limited to 465 kW (39% of maximum), in the case of using C01, and to 315 kW (26% of maximum) for the case of using C02. Another way to understand Fig. 11 is that, for

a given pair of cold and hot water production (e.g. 240 kW and 560 kW, respectively), it corresponds a steam supply, limited to 50% of maximum, and a payback of 3.6 years. Moreover, for the conditions given in the example, results of the simulation model favor the conventional production of steam and cold water together with the production of hot water by CCHP.

These results illustrate the usefulness of the simulation model for obtaining helpful information for the decision-making involved in the CCHP implementation. However, any structural change, for example the inclusion of a new device or configuration requires the elaboration of a new model and assessment of new scenarios. Moreover, this example assumes constant demands and no modulation of the flow ratios presented in Fig. 10, which does not represent any actual situation and omits a great number of operation strategies that could be assessed. Thus, despite the apparent usefulness of this approach, it is evident the convenience of more robust models that, among others, are capable of:

1. Assessing the performance of supply systems considering fluctuations on utilities' demands and prices.
2. Consider multiple CCHP technologies and configurations simultaneously.
3. Dealing with different operation strategies and apportioning of utilities produced by CCHP.
4. Include the heat transfer constraints imposed by the temperature levels of the streams of the plant.

The first issue is approached in the Chapter 3, where the modeling of the utilities' demand profiles is presented and some building applications are introduced. On the other hand, considering the other issues, this thesis adopts the linear programming modeling approach, which have been profusely used for the synthesis of CCHP systems (RONG; SU, 2017). Particularly, the inclusion of binary variables into these models, proper to the mixed-integer linear programming (MILP), eases the selection of the most convenient CCHP technologies from a given set of candidates. The development of this model is described in the Chapter 4.

## Chapter 3

---

# MODELING OF UTILITIES LOAD PROFILES

Data on the utilities' load profiles are key to the design of any supply plant based on CCHP; in fact, the modeling of the energy use in buildings constitutes by itself a whole research area. In this chapter, data from two different modeling approaches are presented and the methodology for processing them is described. Firstly, as an illustration of the *data-driven* modeling approach, hourly electricity demand obtained from the local utility, together with the operation conditions of the supply system of an existing hospital, are used to infer its demand profiles. As in many other cases, since there are not separate measurements of the electricity used by the current electric chillers nor air conditioning devices, the application of a suitable methodology for distinguishing their electric demand from the total was necessary. In this way, the Princeton scorekeeping method (FELS, 1984) is adopted, given its widespread use and reliability. Moreover—in this work—the foundation of the method is applied to timescales smaller than a day for assessing its performance and the consistency of the obtained profiles; as far as it is known, no previous works have extended the use of this method for estimating hour-of-the-day loads.

On the other hand, for illustration of the *forward* modeling approach, profiles of some reference commercial buildings across United States (EERE, 2018) were processed for further analysis. These profiles are result of external Energy-Plus models (Building Technologies Office, 2019) using typical climatic data for each location and can be found in OPENEI (2018). The intention of processing these hourly-profiles is to set the cases for the synthesis model described in following chapter.

### 3.1 DATA-DRIVEN MODELING

Also known as *inverse* modeling, it is based on actual measurements of the on-site energy use and is commonly applied in projects aiming to the retrofitting or revamping of the supply facilities of existing buildings. Its primary objective is to determine a mathematical description of the building (the system) and to estimate its energy-use parameters (ASHRAE, 2013). Particularly in this work, that objective is restricted to the characteriza-

tion of the utilities' demand profiles of an existing hospital located at Florianópolis, Brazil. It is supposed that its supply system would be replaced by a new one, but addressing its current energy requirements.

The hospital supply facility corresponds to a conventional system (see Ch. 2) formed by a pair of boilers—one electric and another fueled by diesel—and three electric chillers for centralized air-conditioning, which are complemented by about 290 conventional air conditioners located among the hospital rooms. Hot water is also supplied by using part of the steam produced by the boilers in a coiled tank. The electric boiler is used only when the diesel-fueled is out of service and during some non-business days with low consumption of heat utilities. Table 6 summarizes the general operation conditions and features of these devices.

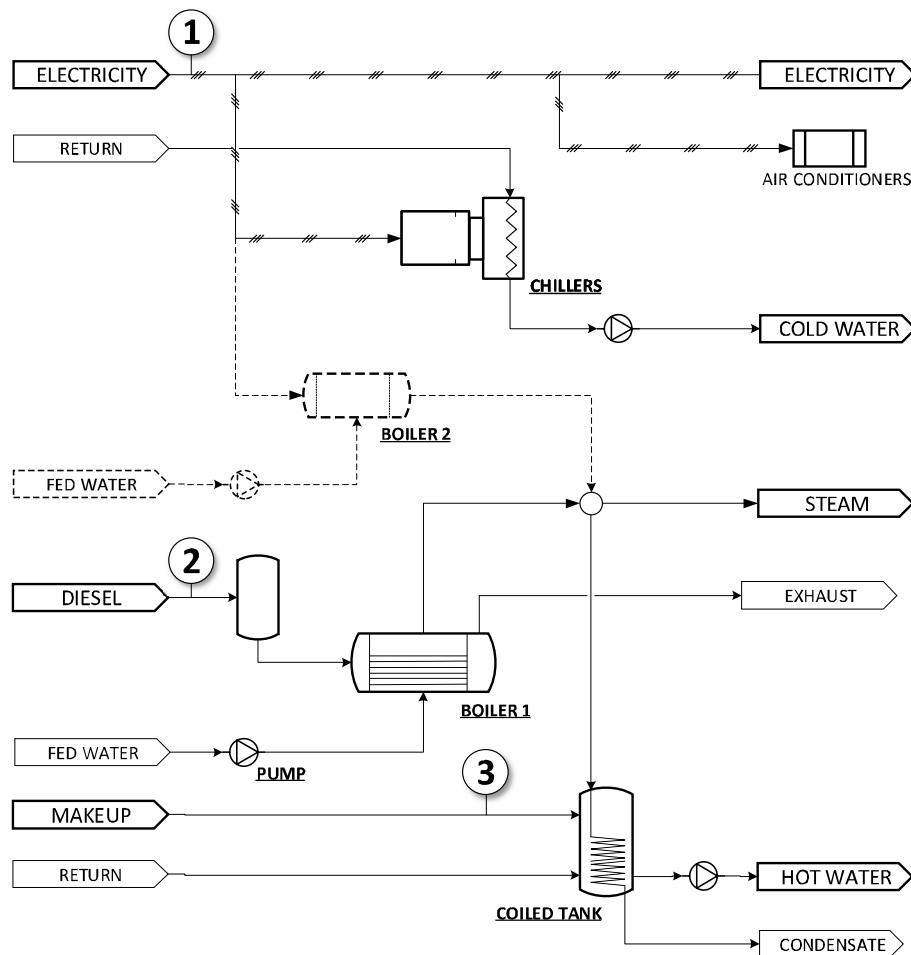


Figure 12 – Scheme of the current hospital supply facilities.

On the other hand, Fig. 12 depicts the current supply facility with indication of

Table 6 – Features of the current supply system of the hospital.

Device	Features	Operation
<i>Saturated steam</i>		
Boiler 1	Fuel: diesel	10 hours per day.
	Capacity: 2000 kg/h	Three operation states: low-fire, high-fire, and off.
	Pressure: 8 barg	
	Efficiency: 0.87*	
Boiler 2	Fuel: electricity	Used for backup and during some non-business days
	Capacity: 1000 kg/h	
<i>Hot water</i>		
Coiled tank	Capacity: 300 l	Temperature is set down to 45°C during hot days.
	Supply temp.: 60°C	
	Supply flow rate: 11.2 m <sup>3</sup> /h	Temperature is maintained overnight through electric resistances.
<i>Cold water</i>		
Chillers	COP(nom.): 3.22	An average COP (chillers + air conditioners) is estimated in 3.6, given that the increase on the electricity demand between the coldest and the hottest day of the year corresponds to about 1 kW per TR installed.
	Capacity : 2 x 80 TR	
	1 x 150 TR	
Air Conditioners	COP: multiple	
	Quantity: about 290	
	Total capacity: 400 TR	

\* Parameter calculated, see Sec. 3.1.3

the measured parameters: (i) hourly electric demand, (ii) hourly diesel makeup, and (iii) hourly hot water makeup. It is important to mention that this facility—as many others—does not have a supervisory system capable of recording these and other operational parameters, thus the choice of these measurement points was restricted to the available instrumentation. The following sections describe the procedure for obtaining each demand profile.

### 3.1.1 Electric Base Load and Cold Water Demand Profile

Data of hourly electricity demand of the hospital from August 2016 through August 2018 were supplied by the local utility. However, these records correspond to the total

demand of the hospital without any indication of its use. Consequently, records of the electricity used for air conditioning devices are not distinguished from other uses, which cause difficulties for the determination of the cooling demand profile and, for this reason, the distinction of this demand from that of non-air-conditioning devices becomes necessary. The simplest way is assuming that the demand of electricity during the coldest periods does not include air conditioning devices and that it remains constant along the entire profile (the baseline); although these premises are adopted by some authors (e.g. Reichmuth (2008)), it is specially sensitive to electricity outages and demonstrates a great uncertainty for values close to that baseline. On the other hand, the methodology adopted in this work, namely the Princeton scorekeeping method (FELS, 1984), is based on the strong correlation that can be evinced between the mean dry bulb temperature and the electric consumption of a building, as well as on the existence of certain base temperature  $\tau$  in whose proximity the operation of air conditioning devices starts to drive the increase of total electric consumption. Its application can be visualized in Fig. 13, where  $\tau$  is located at the inflection point of the plot of daily electricity consumption ( $EC_d$ ) vs the mean dry bulb temperature ( $T_d$ )—this graph is referred as the *energy signature* of the building and is considered a feature of its energy use management (DAY, 2006). Ambient temperature records were taken from a meteorological station located in the proximity of the hospital (UFSC, 2019).

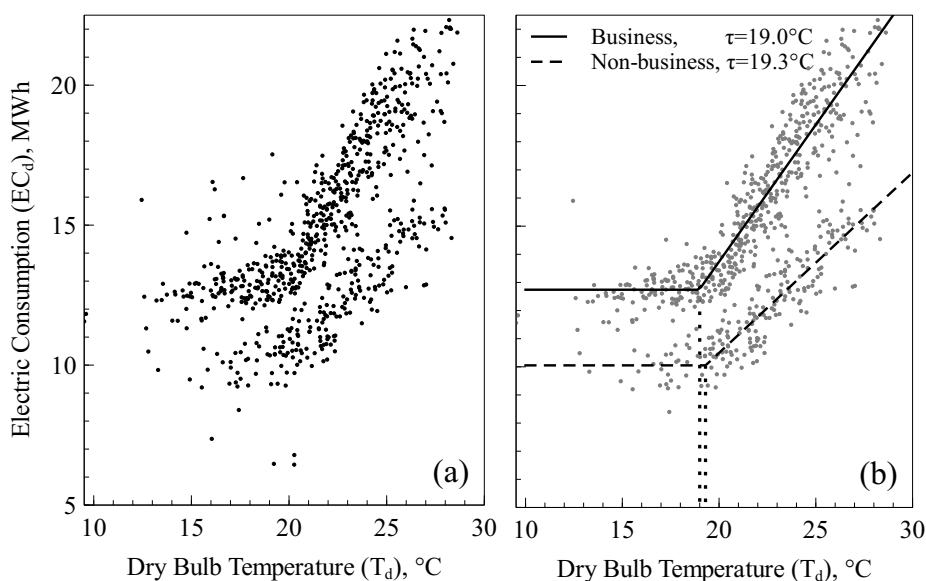


Figure 13 – Energy signature of the hospital: (a) Data records, (b) Distinction between business and non-business days.



The energy signature of the hospital, depicted in Fig. 13a, demonstrates a strong correlation between  $T_d$  and its electricity consumption for values greater than about 20°C. Moreover, two sets are clearly identified, one with higher electric consumption —formed mostly by data of business days, and another formed mostly by data of non-business days; most of the outliers above the higher signature correspond to the operation of the electric boiler and some programmed laboratory tests during non-business days, while outliers below the lower signature correspond to electric outages. Figure 13b illustrates the determination of  $\tau$  for both signatures with the aid of a piecewise regression; resulting values are very close (19.0 and 19.3°C, respectively). Once values of  $\tau$  are determined, the number of cooling degree-days of each day ( $CDD_d$ ) is calculated using Eqn. 3.1, although when hourly values of dry bulb temperatures ( $T_h$ ) were not available,  $CDD_d$  can be simply approximated to the difference  $T_d - \tau$  as long as  $T_d$  is greater than  $\tau$ , otherwise it is equal to zero.

$$CDD_d(\tau) = \frac{\sum_{h=1}^{24} (T_h - \tau)}{24} \quad \forall T_h \mid T_h > \tau \quad (3.1)$$

The values of  $CDD_d$  can be added along periods as weeks, months or seasons, giving the total amount of CDD of that period; however, for avoiding discrepancies when comparing results for periods of different length, it is preferred to express the total CDD as the product of the number of days forming that period ( $ND$ ) and the average CDD *per day* ( $\overline{cdd}$ ), as formulated in Eqn. 3.2.

$$CDD = \sum_{d=1}^{ND} CDD_d(\tau) = \overline{cdd}(\tau) \cdot ND \quad (3.2)$$

The suitability of this methodology relies on the fit of captured data to a linear model of the form  $EC_d = \alpha + \beta \cdot \overline{cdd}$ ; in this way,  $\alpha$  corresponds to the average daily electric base consumption and  $\beta$  to the consumption increment per each additional degree of temperature above  $\tau$ . Fig. 14 illustrates the fitting of the hospital data, showing a good fit for both datasets, given that they report an  $R^2 = 0.88$  for business days and an  $R^2 = 0.83$  for non-business days, with p-values equal to zero for both regressions. Thus, daily base electric consumption are estimated in 12.74 MWh for business days and 10.05 MWh for non-business days. According to the building engineering lingo, this characteristic plot is known as the *performance line* of a building and correlation coefficients of 0.75 or above are considered satisfactory (BIZEE, 2019).

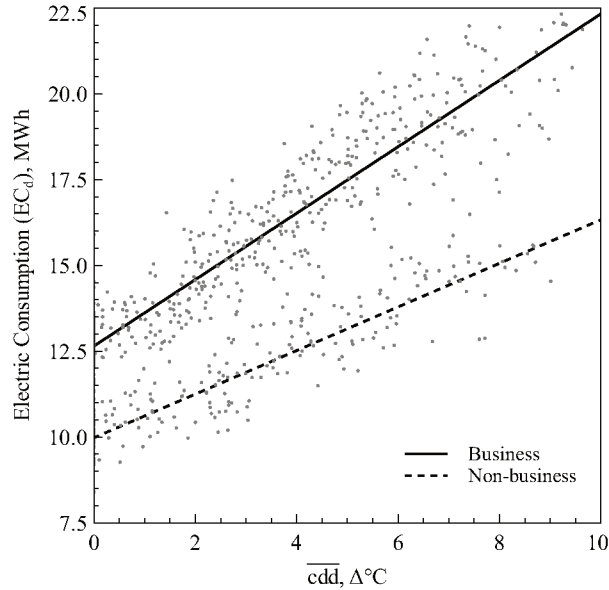


Figure 14 – Energy performance lines of the hospital.

The estimate of the electric consumption of air-conditioning devices is simply obtained (day-by-day) as the difference between the total and the base consumption (as long as the total is greater than the base consumption); the daily cooling load (in MWh of refrigeration) is obtained by multiplying this value by the global COP of the system.

Given the good data availability in this case, and taking into account the great proximity (less than 200 mts) between the place where the ambient temperature is measured and the location of the hospital, the methodology explained above has been adapted for estimating the base electric consumption and cooling load during periods smaller than a day. However, considering that such circumstances are not very common, and that the data sampling can vary from building to building, six timescales are analyzed in the construction of the electric base load and cooling load profiles:

1. Hourly data, e.g. recorded by supervisory systems.
2. Data sampling every three hours, e.g. frequency used in some meteorological stations.
3. Data sampling every 12 hours (at 7:00 and 19:00), e.g. one record for each shift.
4. Daily data.
5. Weekly data.
6. Monthly data, e.g. only information from bills is available.

Hourly records are grouped in such a way that values of  $\tau$  are obtained for the intervals delimited by each timescale e.g. for data sampling every three hours, the value of  $\tau$  for each interval (00:00 to 03:00, 3:00 to 06:00, etc.) is obtained by plotting electric consumption data during that interval (one point per day) against its corresponding mean dry bulb temperature,  $T_i$ . Fig. 15 illustrates the procedure for determining values of  $\tau$  for selected timescales only on business days' data.

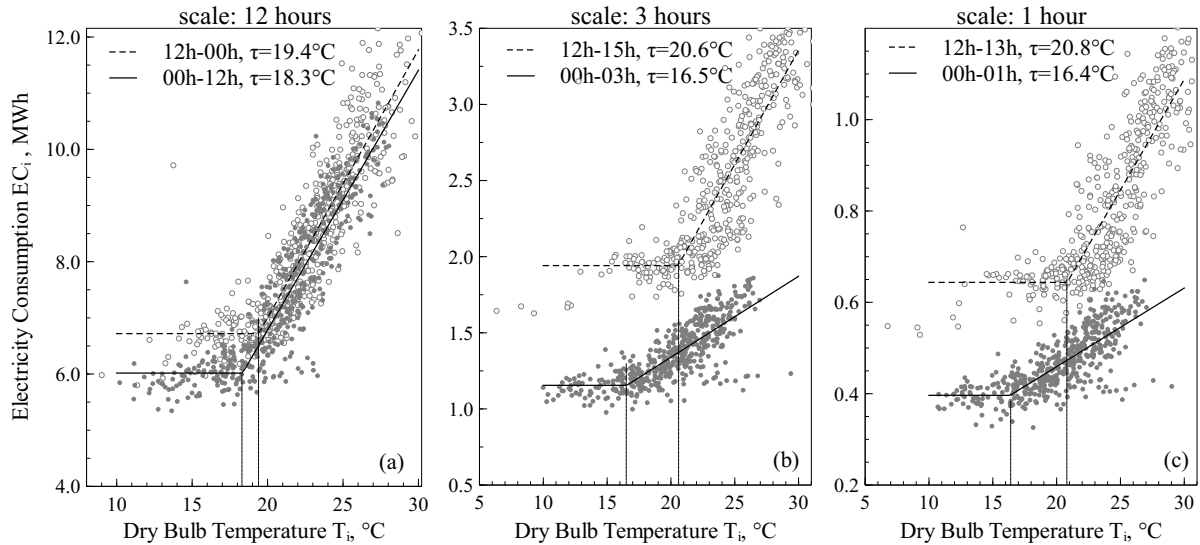


Figure 15 – Selected energy signatures of the hospital using different timescales: (a) 12 hours, (b) three hours, and (c) one hour.

This procedure reveals that values of  $\tau$  vary up to about  $\pm 2^\circ\text{C}$  around the daily value, and that gap does not change markedly between three-hours and one-hour timescales. Evidently, doing the piecewise regression on weekly or monthly data does not give any reasonable result; for these cases and in absence of further information, the estimation of  $\tau$  is commonly done by trial and error, looking for a value that reports a good fit in the building performance line (DAY, 2006). Particularly, the value of  $\tau$  for the hospital was set at  $19^\circ\text{C}$  for daily, weekly, and monthly timescales based on the previous results; Fig. 16 presents the values of  $\tau$  for the hospital using the proposed timescales.

Values of  $\tau$  exhibit certain pattern, showing for example that air conditioning devices are—on average—switched-on at higher temperatures during daylight than overnight; one plausible conjecture is that such a pattern is caused by the building thermal inertia, considering the foundations exposed by Verbeke and Audenaert (2018). However, data shown on Fig. 16 is just indicative and the explanation of any trend should consider

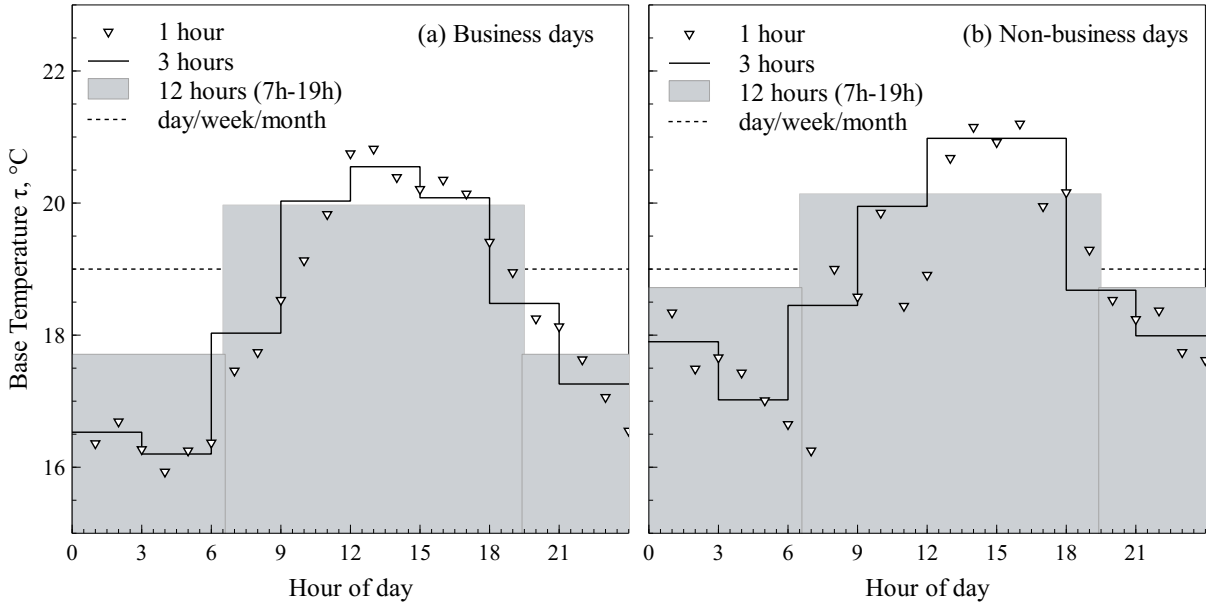


Figure 16 – Base temperatures for different timescales: (a) Business days, (b) Non-business days.

multiple aspects as occupancy, temperature set points, solar radiation gains, wind, etc., which are out of the scope of this work.

Adapting the same procedure used for CDD calculation, the number of cooling degree intervals of each interval ( $CDI_i$ ) is defined as the difference  $T_i - \tau_i$ , as long it is positive (otherwise it is equal to zero);  $T_i$  refers to the mean dry bulb temperature of the interval  $i$  and  $\tau_i$  to the corresponding base temperature. In addition, the total CDI of a period is expressed in the Eqn. 3.3 as:

$$CDI = \sum_{i=1}^{NI} CDI_i(\tau_i) = \overline{cdi} \cdot NI \quad (3.3)$$

where  $NI$  is the number of intervals forming the period and  $\overline{cdi}$  the average CDI per interval. In this way, the base consumption per interval can be estimated as the intercept  $\alpha_i$  of the linear regression model of the form  $EC_i = \alpha_i + \beta_i \cdot \overline{cdi}$ , where  $EC_i$  is the electric consumption per interval, and  $\beta_i$  is the incremental electric consumption per additional degree of temperature above  $\tau$ . Figure 17 illustrates the application of the method for selected timescales (a) one hour (from 9h to 10h), (b) three hours (from 9h to 12h) and (c) weekly.

On the other hand, Tab. 7 presents electric base loads obtained for each interval considered in each timescale; the features of the linear models<sup>1</sup> show that the smaller the

<sup>1</sup> data fit features are organized in Appendix C.

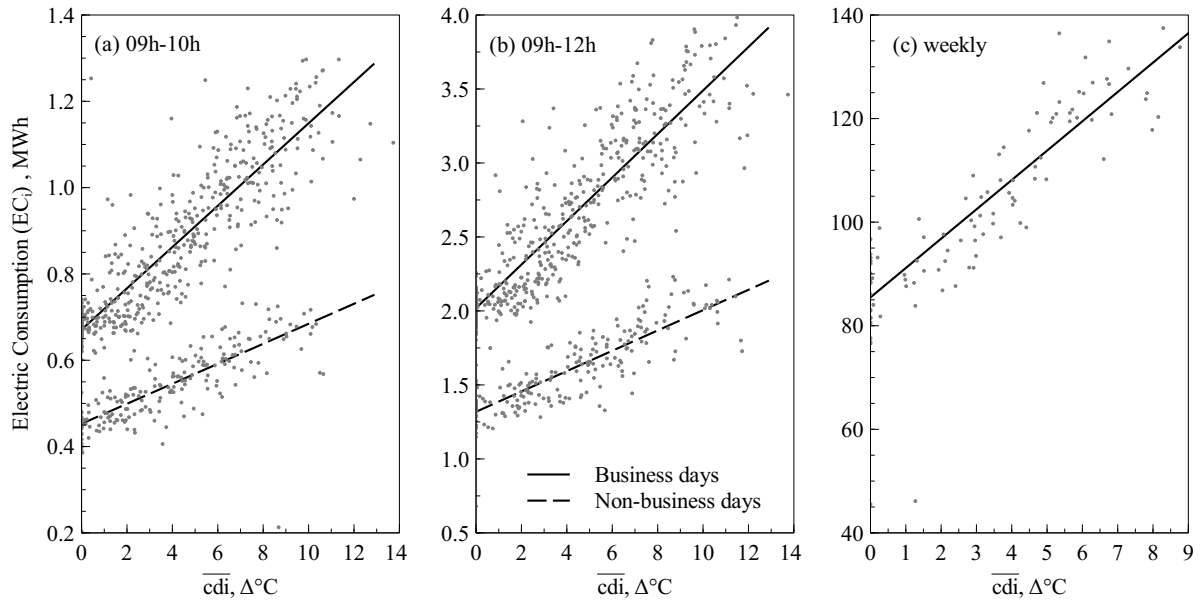


Figure 17 – Selected performance lines for different timescales: a) one hour (9h-10h), b) three hours (9h-12h), c) one week.

timescale the worse the data fit to the model, reporting correlation coefficients as low as 0.58. However, it is expected because data of shorter periods are likely to vary more than the total of longer periods, since they capture the electric load variations due to shorter random events. Results can be contrasted with some aspects of the hospital operation, which serves for checking their consistency, e.g. the base load and the difference of its value between business and non-business days are greater during working hours than overnight periods, as well as the fact that there is a certain proportionality among the results, i.e. the base load of the three-hour timescale is approximately three times the value of the one-hour timescale, and so on. Moreover, the slopes  $\beta_i$ , namely the rate of electricity consumption per  $^{\circ}\text{C}$  increment, are greater for working hours than for overnight periods, which is in alignment with results presented by Day (2005) regarding the relationship between  $\beta$  and the performance of the cooling systems in a building.

The electric load of air-conditioning devices for each period is equal to its total electricity consumption minus the corresponding base load (as long as it is positive, otherwise it is zero). On the other hand, the average electricity demand (kW) for each load is the ratio between the corresponding consumption and the duration the interval; the cooling load demand is obtained by multiplying the corresponding electricity demand by the global COP (3.6).

Table 7 – Electric base loads for the periods of each timescale.

Interval			Interval		
$\alpha_i$ , kWh			$\alpha_i$ , kWh		
<i>1 hour</i>	<i>Bus.</i>	<i>Non-bus</i>	<i>1 hour</i>	<i>Bus.</i>	<i>Non-bus</i>
1	395 ± 6	408 ± 7	21	483 ± 5	426 ± 7
2	382 ± 6	385 ± 8	22	457 ± 5	429 ± 7
3	370 ± 6	381 ± 8	23	433 ± 6	409 ± 8
4	360 ± 6	374 ± 8	24	411 ± 6	398 ± 8
5	364 ± 6	372 ± 9	<i>3 hours</i>		
6	378 ± 8	381 ± 11	1	1147 ± 17	1174 ± 23
7	470 ± 11	411 ± 11	2	1102 ± 18	1125 ± 26
8	585 ± 9	452 ± 10	3	1706 ± 23	1330 ± 27
9	647 ± 9	439 ± 10	4	2019 ± 33	1318 ± 30
10	672 ± 11	453 ± 10	5	1927 ± 38	1284 ± 37
11	676 ± 12	418 ± 12	6	1900 ± 33	1275 ± 34
12	665 ± 12	415 ± 11	7	1564 ± 22	1272 ± 21
13	644 ± 13	419 ± 12	8	1306 ± 16	1234 ± 23
14	624 ± 14	423 ± 13	<i>12 hours</i>		
15	665 ± 14	433 ± 13	1	6019 ± 109	4968 ± 110
16	678 ± 13	447 ± 13	2	6695 ± 61	5162 ± 92
17	632 ± 11	412 ± 13	<i>Day</i>		
18	590 ± 8	415 ± 8		12741 ± 134	10052 ± 163
19	506 ± 11	424 ± 9	<i>Week</i>		
20	505 ± 7	425 ± 7		85477 ± 2026	
			<i>Month</i>		
				368734 ± 19869	

Figure 18 shows the cooling demand and electricity base load profiles (one-year) obtained for the hospital building, using the greatest timescales, namely daily, weekly and monthly data.

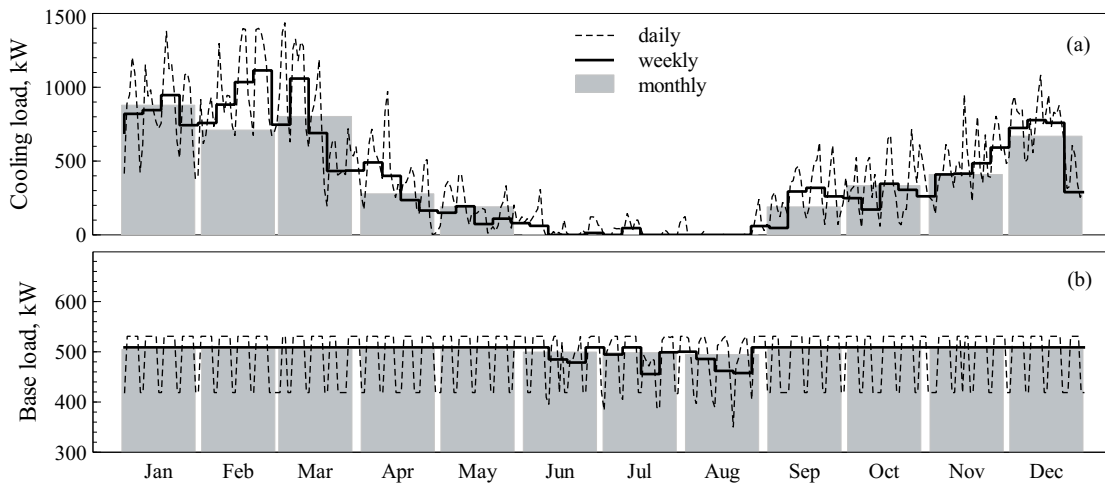


Figure 18 – One-year demand profiles for the hospital case using the greatest timescales: (a) Cooling load profile, (b) Base load profile.

The comparison with smaller timescales is easier through duration curves, as those presented in Fig. 19. Here, the base load demand for business and non-business days and their duration are clearly distinguished (indicated by 'b.' and 'n.b.' on Fig. 19a), while the weekly timescale is almost constant. Regarding the air-conditioning, Fig. 19a show that most part of the time there is simultaneous electricity and cooling load demand, given that only 15% of the time no cooling would be required. In both curves the effect of averaging data for getting profiles with greater timescales is evident, it vanishes the peaks and sinks on the profiles and extends the duration of averaged demands.

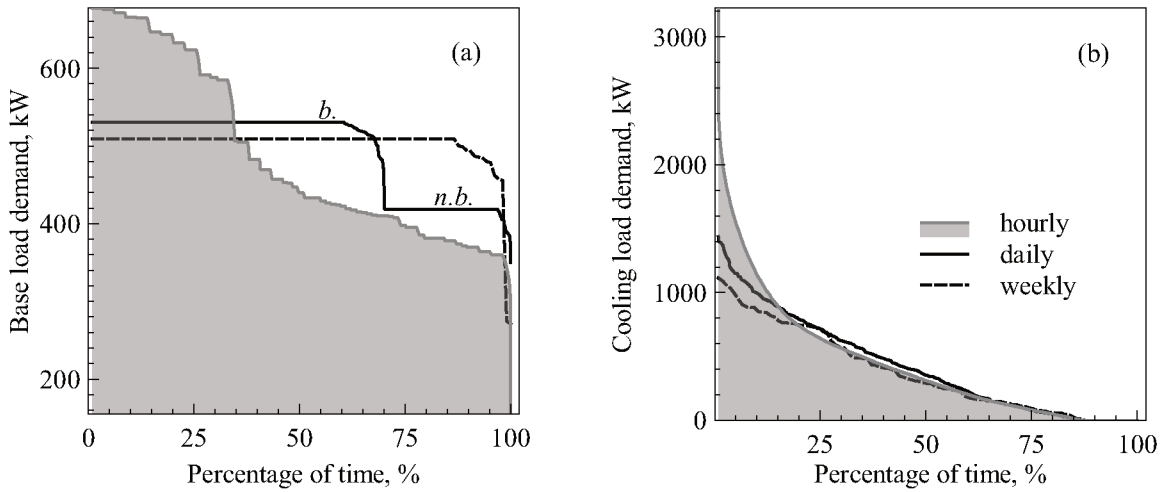


Figure 19 – Duration curves for hospital base load and cooling demand: (a) Base load demand, (b) Cooling load demand.

### 3.1.2 Hot Water Demand Profile

The hot water utility demand is calculated through the energy balance on the coiled tank. Assuming that there are not leakages, it follows that consumption rate equals the makeup rate (in mass basis). Moreover, since the water supply flow rate is practically constant (see Tab. 6), the utility demand, in kW, is calculated using the Eqn. 3.4:

$$DEM = \dot{m}_{sup} \cdot h_{sup} - [\dot{m}_{mkp} \cdot h_{mkp} + (\dot{m}_{sup} - \dot{m}_{mkp}) \cdot h_{ret}] \quad (3.4)$$

The hot water supply pressure is approximately constant and equal to 250 kPa, while the hot water supply temperature is adjusted according to the predominant weather conditions, the tank temperature control is manually set at between 45°C (hotter days)

and 60°C (colder days). Makeup conditions are considered constant (150 kPa and 25°C), as well as the pressure drop across the distribution system (100 kPa), while the hot water temperature drop varies between 3°C (hotter days) and 5°C (colder days). Measurements of the makeup volume flow were taken every half hour during several days in each season, Fig. 20 shows the hot water demands obtained from collected data, grouped by the hour of the day at which points were taken. Note that there is not any classification on these data yet, it will be done later to obtain typical daily profiles.

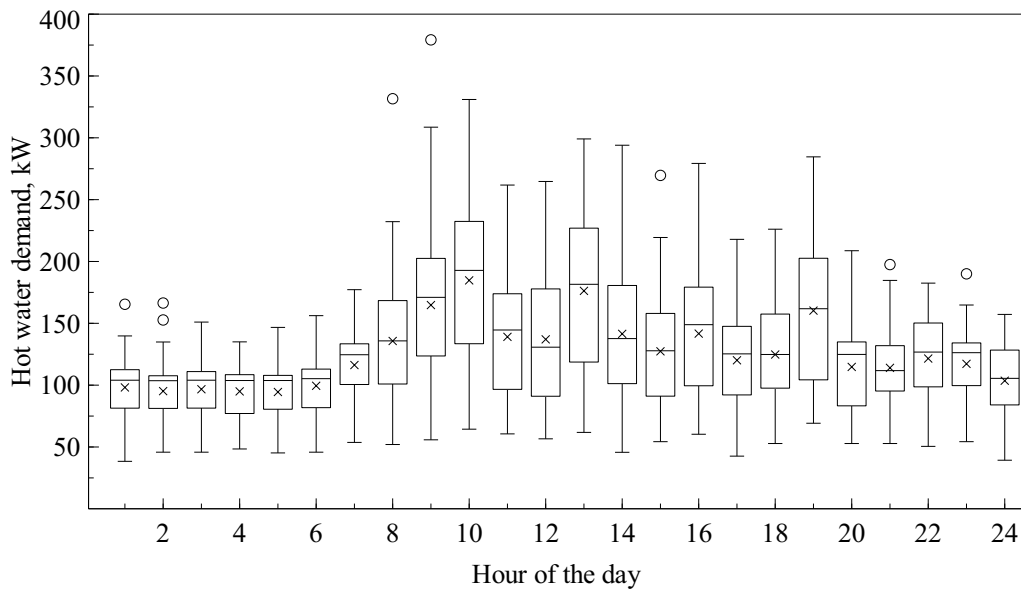


Figure 20 – Hot water demand calculated using collected data.

### 3.1.3 Steam Production Profile

The characterization of the steam demand of the hospital is based only on the operation of the diesel-fueled boiler, given the low utilization of the electric one. Specifically, measurements of the diesel makeup rate are used to calculate the hourly steam production assuming a characteristic thermal efficiency (constant). The determination of this value is done adopting the indirect method exposed by Bazzo (1995), whose key inputs are the elemental composition of the fuel, the temperature of the exhaust gases stream, and the molar percentage of oxygen in it. The hospital diesel stock is formed, on average, by 84.6% of carbon and 15.4% of hydrogen; fractions of other elements are negligible. Measurements of the exhaust gases temperature and the molar fraction of oxygen were taken simultaneously at various intervals during different days, in such a way that the boiler



efficiency can be determined for each sample; results are summarized in Tab. 8.

Table 8 – Results for the thermal efficiency of the boiler.

Range	Mean	Frequency, %
$\eta_{th} < 0.870$	0.862	66.96
$0.870 \leq \eta_{th} < 0.885$	0.880	0.89
$0.885 \leq \eta_{th} < 0.900$	0.892	25.89
$0.900 \leq \eta_{th}$	0.911	6.25

Computation of data obtained results in a weighted thermal efficiency of 87.3% ( $\pm 1.1\%$ ); in this way, the instantaneous steam utility production (in kW) is estimated as the product of this value and the energy input rate of the boiler. The diesel used in the hospital has a lower heating value (LHV) of 42287 kJ/kg, and an average specific gravity of 0.848, values previously measured and reported by Nieto et al. (2015). Figure 21 shows the steam production (in kW) obtained from the diesel makeup rate measurements.

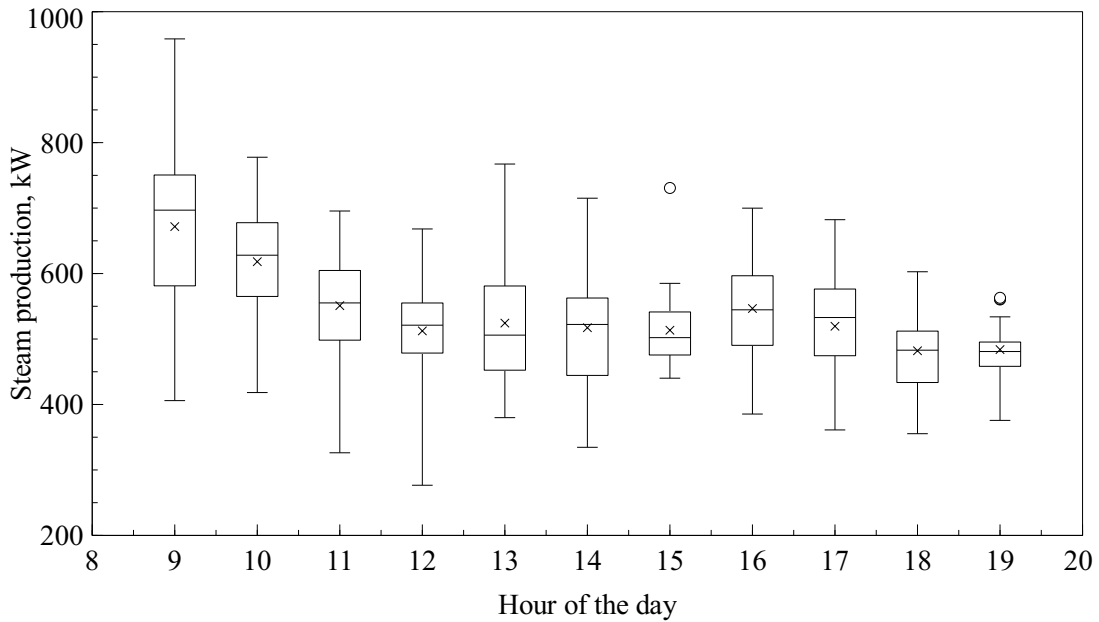


Figure 21 – Steam production calculated using collected data.

Analogously to the Fig. 20, there is not any classification on these data, and they correspond to the *production* of the utility. The steam demand is obtained once the hot water demand is discounted from them (hour-by-hour).

### 3.2 FORWARD MODELING

As previously mentioned, these hourly demand profiles have been modeled according to current standards and can be obtained directly in OPENEI (2018). Additionally, information regarding the climatic data and parameters used in each model can be accessed in EERE (2018). They were calculated through forward modeling, whose main characteristic is that the building is modeled as a physical system—or a set of physical subsystems—exchanging mass and energy with their surroundings (ASHRAE, 2013). Since the outputs of this type of models are unknown (thus, calculated) it follows that electricity demand of air-conditioning and non-air-conditioning devices can be reported separately. For illustration, Fig. 22 presents the duration curves of the utilities demanded at a reference office building using typical meteorological information of Los Angeles, California.

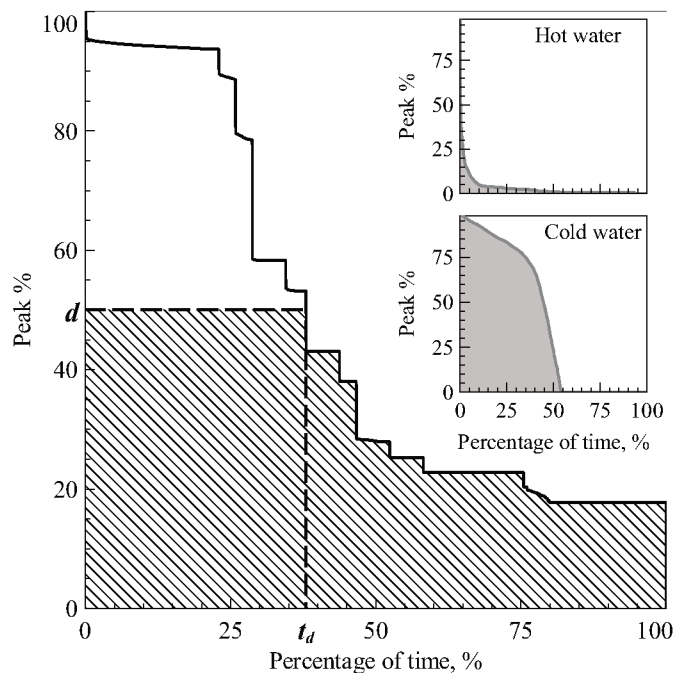


Figure 22 – Duration curves of utilities required at a large office building, modeled using meteorological data of Los Angeles California. Data extracted from OPENEI (2018).

Note that the scale on vertical axis is now relative to the peak demand of each utility for enabling the comparison with other building applications; values of these peaks can be found in Tab. 9. Compared with the Fig. 19, there is a lesser minimum base load demand, associated to unoccupied periods in the building. Moreover, during almost 50% of the time there is not any cooling requirement, fact also attributable to typical occupancy and

weather parameters included into the model.

Table 9 – Peak, annual consumption and duration time of utilities for various applications.

<b>Application—City / utility</b>	<b>Peak demand kW</b>	<b>Consumption MWh</b>	<b>Duration h</b>
<i>Hospital—Florianópolis*</i>			
Electricity	678	4071	8760
Steam	580	1660	3650
Hot water	224	950	8760
Cold water	3227	3668	7216
<i>Office Building—Los Angeles</i>			
Electricity	985	4036	8760
Hot water	355	88	8760
Cold water	2179	7528	4771
<i>Secondary School—Baltimore</i>			
Electricity	472	1878	8760
Hot water	2755	1307	8760
Cold water	4461	7538	4326
<i>Hotel—Chicago</i>			
Electricity	246	1254	8760
Hot water	1050	2120	8760
Cold water	875	4458	8738

\* Data-driven model, see Sec. 3.1

In order to outline the demand profiles of diverse applications, two features are depicted in Fig. 22 for a given demand  $d$ : (i) the duration  $t_d$ , expressed as % of time, which corresponds to the amount of periods reporting a demand greater than or equal to  $d$  and (ii) the utility consumption required at values lesser than or equal to  $d$ , expressed as % of total consumption (hatched area). Table 10 presents these features at three demands for three different building applications. Observe that values of  $d$  for hot water are lower than the others, given that most of the hot water consumption is required at demands much lesser than its peak.

### 3.3 TYPICAL DAYS PROFILES

Conventionally, the design of utilities' supply systems, including those implementing CCHP, is conducted assuming that the building future energy demands—without accounting for eventual changes—will be of similar magnitude and behavior of recent records. Consequently, a utility demand profile is commonly modeled as representative time profiles formed by a set of typical days (day types), whose sub-profiles are repeated several

Table 10 – Features of utilities’ demand profiles for three building applications

Application		Sec. school		Hotel		Hospital		Office Bld.	
Utility	%Peak	$t_d$	%area	$t_d$	%area	$t_d$	%area	$t_d$	%area
Electricity	25%	44	49	100	43	100	35	58	49
	50%	38	72	73	79	99	69	38	73
	75%	23	91	21	95	34	91	29	89
Hot Water	10%	16	41	89	42	100	20	5.5	77
	20%	11	65	45	70	100	41	2.2	89
	30%	6.7	81	26	85	87	60	1.1	95
Cold Water	25%	53	43	88	41	19	82	91	33
	50%	39	73	58	72	4.1	98	82	63
	75%	23	94	39	93	0.1	100	64	89

times a year (e.g. approach used by Kavvadias and Maroulis (2010)), or even through typical duration curves, as the approach used by Martínez-Lera and Ballester (2010). Particularly, one key advantage of the typical days approach is that it reduces the number of iterations—thus the run time—of optimization algorithms involving time cumulative quantities (e.g. annual operation cost, annual CO<sub>2</sub> emissions, annual fuel savings, etc.) given that results of a typical day are replayed the number of times it repeats along the year. However, these sub-profiles should be defined thoroughly, since a poor choice may conduct to misleading results. The most common criteria for categorizing the typical days are the weather season and the schedule of the building (e.g. business or non-business days), and, as mentioned by Frost et al. (2017), there are two distinct methods of constructing their profiles: by aggregating data (averages) or by choosing (sometimes randomly) a daily sub-profile belonging to each category. More recently, the incorporation of classification algorithms, like the  $k$ -means method included into the *Scikit-learn* package (PEDREGOSA et al., 2011), has enabled a better classification since the data is grouped (clustered) based on their ‘similarity’. As explained by Kotzur et al. (2018a),  $k$ -means algorithm creates the clusters in order to minimize the squared error between the empirical mean of a cluster and all data (candidates) in it. For instance, if the algorithm had been applied on the data of the electricity base load of the hospital (see Sec. 3.1) for classifying them in two groups, it had labeled each data as belonging to cluster  $0$  or to cluster  $1$ , which correspond respectively to business and non-business days.

In this work, the construction of the typical days profiles is performed by aggregating data, clustered according to the daily mean temperature and the electricity base

load, justified as follows. Keeping the same hypothesis inherent to the Princeton score-keeping method, i.e. that the energy destined to air conditioning is strongly correlated to the prevailing ambient temperature, the daily mean temperature serves as criterion for separating the days according to their cooling (or heating) load demand. Clearly, values of daily mean temperatures can not be clustered adequately, since they vary more or less homogeneously between the historical minimum and maximum. Thus, this parameter is used simply for dividing the whole time series into three levels: *cold*, *warm*, and *hot* temperatures with the same number of data points (i.e. tertiles). This is convenient given that these tertiles can be obtained with good reliability from historical records (even from typical meteorological information), which are usually available. Additionally, the fact that the obtained groups are not necessarily ordered chronologically brought a practical advantage, since measurements taken in the hospital facilities during 'transition' seasons with highly variable conditions contributed information to the three groups. The same premise was applied to the datasets of the building models presented in the previous section. Table 11 presents the daily mean temperatures that divide each dataset in three parts with the same size.

Table 11 – Ambient temperature tertiles and number of base-load levels for classification.

<b>Building</b>	<b>Tertile 1</b>	<b>Tertile 2</b>	<b>Base Load Levels</b>
Hospital	20.5°C	23.4°C	<i>hot</i> : 2, <i>warm</i> : 2, <i>cold</i> : 2
Office Building	15.4°C	18.3°C	<i>hot</i> : 3, <i>warm</i> : 3, <i>cold</i> : 3
Secondary School	7.0°C	19.2°C	<i>hot</i> : 2, <i>warm</i> : 2, <i>cold</i> : 3
Large Hotel*	3.5°C	17.0°C	<i>hot</i> : 1, <i>warm</i> : 1, <i>cold</i> : 1

\*Base load is practically constant.

On the other hand, the electricity base load is commonly influenced by the level of activity in the building, most of the time associated directly with its occupancy. In the case of the hospital, two different operation regimes were already identified through the signature of the building (see Fig. 13). For the other buildings, without any indication of the premises used for simulating their occupancy, it was necessary to establish the proper number of clusters in each case. It was done applying the *k*-means algorithm several times, varying the number of clusters, and computing the within-cluster sum of squares (WSS) in each run. The inflection point (if any) on the plot of the WSS vs the number of clusters indicates the most adequate number of clusters for making the classification. This method is known as the 'elbow' method that, in spite of being the simplest, was adequate

for analyzed cases; details about this and other methods of estimating the number of clusters can be consulted in (TIBSHIRANI; WALTHER; HASTIE, 2001). Last column of Tab. 11 presents the number of clusters found in each case.

In any case, it is necessary to differentiate the tariff periods, hence each day was labeled as a business day (B), or as a non-business day (NB). The number of day types in each case is determined by the number of label combinations applied according to the chosen parameters; in this way, Tab. 12 summarizes the classification for aggregating data on each building.

Table 12 – Typical days classification for aggregating data.

Day type	Temp. Level	Base L. Level	B/NB	N°of Days	Day type	Temp. Level	Base L. Level	B/NB	N°of Days
<i>Hospital</i>					<i>Secondary School</i>				
1	cold	L1	NB	65	1	cold	L1	B	21
2	cold	L2	B	164	2	cold	L1	NB	16
3	warm	L1	NB	67	3	cold	L2	B	68
4	warm	L2	B	161	4	cold	L2	NB	16
5	hot	L1	NB	78	5	warm	L1	B	21
6	hot	L2	B	158	6	warm	L1	NB	18
<hr/>					7	warm	L2	B	63
<i>Office Building</i>					8	warm	L2	NB	18
1	cold	L1	B	22	9	hot	L1	B	20
2	cold	L2	NB	15	10	hot	L1	NB	18
3	cold	L3	B	66	11	hot	L2	B	34
4	cold	L3	NB	18	12	hot	L2	NB	9
5	warm	L1	B	21	13	hot	L3	B	34
6	warm	L2	NB	18	14	hot	L3	NB	9
7	warm	L3	B	66	<hr/>				
8	warm	L3	NB	15	<i>Large Hotel</i>				
9	hot	L1	B	19	1	cold	L1	B	85
10	hot	L2	NB	18	2	cold	L1	NB	36
11	hot	L3	B	68	3	warm	L1	B	84
12	hot	L3	NB	19	4	warm	L1	NB	36
					5	hot	L1	B	92
					6	hot	L1	NB	32

Particularly for the hospital, the hot water daily profiles show notorious differences among the temperatures levels, but not among business and non-business days. Conversely, once the hot water demand is subtracted from the steam production, the daily steam demand profile is reasonably homogeneous, independently of the temperature level and the electricity base load. Figure 23 presents the the steam and the hot water profiles obtained for the hospital.

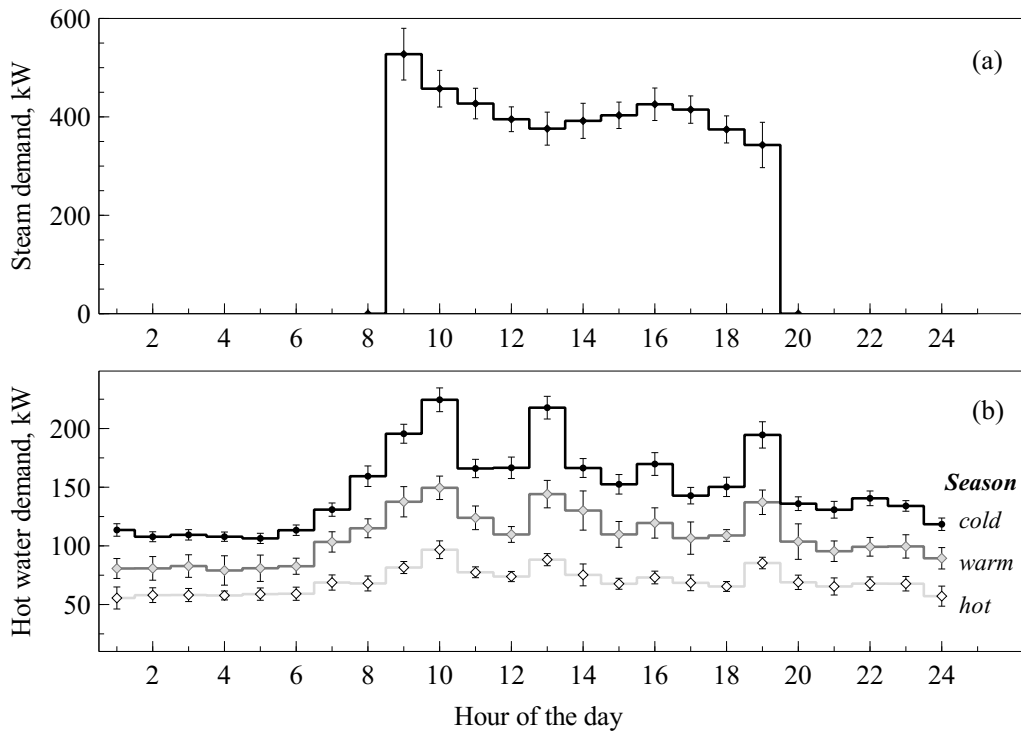


Figure 23 – Daily profiles for the hospital: (a) steam, (b) hot water.

The behavior of these curves was contrasted with the normal routine of the hospital, showing a great agreement. For example, peaks (at 9<sup>th</sup> and 16<sup>th</sup> hours) on the steam demand profile, which is driven mainly by the laundry, correspond to the washing (during the morning) and to the drying (during the afternoon), respectively. On the other hand, hot water demand is greatly influenced by the in-patients and the kitchen activity. In this way, the first ramp in the morning corresponds to the morning showers and breakfast cooking, the peaks shortly before and shortly after noon correspond respectively to the lunch cooking and dishwashing, and the last peak, closing the day, corresponds to showers and dinner cooking. Information regarding the estimation of the uncertainty on these profiles is presented in the appendix C.

Table 13 presents the typical profiles of the hospital, which will be input of the synthesis procedure described later in Ch. 4. Additionally, there is a column reporting the peak demands of each utility. The inclusion of this typical day into the profile is important because, as already noted by Li, Shi and Huang (2008), it avoids the underestimation in the size of the equipment caused by the effect of averaging the data. Although the typical profiles of the remaining buildings are not presented explicitly, they also were processed to be input in the synthesis of their utilities' supply plants.

Table 13 – Typical days profiles for the hospital building

Hour	Steam		Hot Water				Cold Water						
	<i>all types</i>	<i>peak</i>	<i>cold</i>	<i>warm</i>	<i>hot</i>	<i>peak</i>	<i>1</i>	<i>2</i>	<i>3</i>	<i>4</i>	<i>5</i>	<i>6</i>	<i>peak</i>
1	–	–	114± 5	81± 8	56± 9	119	45± 17	74± 13	179± 33	253± 23	426± 36	500± 29	529
2	–	–	108± 4	81± 10	58± 6	112	61± 19	64± 13	205± 33	241± 22	462± 36	494± 26	520
3	–	–	109± 4	83± 10	58± 6	114	53± 18	66± 12	188± 32	254± 22	443± 36	508± 26	534
4	–	–	108± 4	79± 13	58± 4	112	57± 20	74± 12	203± 32	267± 21	454± 33	523± 26	548
5	–	–	106± 4	81± 11	59± 5	111	56± 18	54± 11	214± 34	264± 23	470± 34	530± 26	556
6	–	–	113± 4	83± 7	59± 6	118	59± 22	59± 15	254± 43	361± 37	498± 36	682± 36	718
7	–	–	131± 6	103± 9	69± 6	137	102± 41	68± 22	266± 44	449± 58	515± 46	950± 80	1030
8	527± 53	572	159± 9	115± 8	68± 6	168	158± 95	86± 23	177± 36	541± 54	465± 41	1162± 61	1223
9	457± 37	490	196± 8	138± 13	82± 5	204	143± 57	84± 29	272± 40	575± 50	603± 47	1322± 58	1381
10	427± 31	455	225± 10	149± 10	97± 8	235	112± 71	96± 31	231± 39	590± 52	594± 46	1388± 65	1454
11	395± 25	418	166± 8	124± 10	77± 5	174	164± 48	97± 23	320± 38	610± 56	729± 50	1446± 69	1515
12	376± 34	406	167± 9	110± 7	74± 4	176	100± 24	69± 17	337± 44	598± 53	765± 51	1470± 67	1537
13	392± 36	424	218± 10	144± 12	88± 5	227	85± 23	89± 18	316± 49	632± 53	797± 74	1528± 65	1593
14	403± 27	428	166± 8	130± 17	75± 9	174	86± 58	126± 29	324± 54	781± 55	834± 78	1713± 59	1771
15	426± 33	455	152± 8	110± 11	68± 5	161	80± 21	119± 32	360± 64	758± 52	870± 79	1631± 58	1689
16	415± 28	440	170± 10	120± 13	73± 5	179	105± 60	99± 30	298± 63	637± 53	798± 89	1422± 64	1486
17	374± 28	398	143± 7	107± 14	68± 7	150	167± 92	86± 29	329± 46	567± 48	811± 72	1286± 66	1352
18	343± 46	376	150± 8	109± 5	65± 4	158	85± 48	81± 29	269± 44	441± 41	699± 50	1056± 62	1118
19	–	–	195± 11	137± 10	85± 5	206	57± 17	50± 12	238± 38	276± 33	587± 46	706± 53	759
20	–	–	136± 6	104± 15	69± 6	142	74± 18	63± 13	263± 32	282± 27	579± 35	566± 36	614
21	–	–	131± 7	95± 9	65± 7	138	78± 19	60± 13	266± 32	266± 24	574± 32	566± 28	606
22	–	–	141± 6	99± 8	68± 6	147	66± 16	63± 12	232± 30	268± 23	532± 31	556± 25	581
23	–	–	134± 5	100± 10	68± 6	139	78± 18	63± 12	250± 29	275± 22	544± 33	559± 25	584
24	–	–	118± 5	89± 9	57± 9	124	74± 16	68± 12	235± 27	281± 21	527± 33	560± 25	585



### 3.4 CLOSING REMARKS

In this chapter, the utilities' demand profiles of four different building applications were prepared for performing the synthesis of the corresponding utilities' supply plants. These applications were chosen intentionally for reflecting different demand patterns and scales. Initially, the data processing using six different timescales will enable a sensitivity analysis oriented to check the detail level required for specifying the technologies forming the supply facilities and verify if the inclusion of TES into the system diminish that requirement. Although already was evidenced that the averaging inherent to larger timescales alters the synthesis results for residential sector Hawkes and Leach (2005), as far as it is known, the effect of TES systems have not been analyzed yet.

Another aspect explored in this chapter was the adaptation of a procedure normally applied using daily data to be applied with smaller timescales. Although Day (2006) warns about estimates made for periods smaller than a day due to their higher unpredictability, their processing reveals important patterns, otherwise ignored when greater timescales are used. Evidently, there is a compromise between the timescale used in the profiles and the quality of the synthesis results, since beforehand, it is presupposed that the smaller the timescale, the more rigorous the model, but also greater the uncertainty present, thus lesser the change of design parameters be reproduced.

The information collected is enough for elaborating hourly profiles during at least one year; however, in order to enable a greater complexity of the synthesis model, and avoid excessive execution time, profiles were modeled as a set of typical daily profiles, whose aggregation was based on logical premises to avoid losing details. Particularly, the approach proposed, based on the separation of the time series in daily mean temperature tertiles—although simple—have shown an advantage that can be exploited in actual CCHP projects, since measurements taken during highly variable seasons (few months) can be useful for characterizing all the year round.

Finally, incorporation of the uncertainty on profiles allows the development of robust synthesis and operation models, e.g. Li et al. (2010), Carpaneto et al. (2011), that consider energy demands and the performance of CCHP devices as continuous random variables with a probability density function characterized from available data (MAVROMATIDIS; OREHOUNIG; CARMELIET, 2018a). There are indications that, in spite

of possible divergences concerning annual operation cost obtained without considering uncertainties, these divergences are caused mainly by deviation on tariffs and operation schedules (YANG; ZHANG; XIAO, 2017) and that the optimal selection of the system components are less sensitive and shows a good agreement (MAVROMATIDIS; OREHOUNIG; CARMELIET, 2018c).

## Chapter 4

---

### THE CCHP SYNTHESIS

As previously introduced in Ch. 2, the CCHP design can be conceived as formed by three interrelated tasks, namely the synthesis, the sizing and the definition of operation strategy, which can be approached sequentially or simultaneously, according to the methodology adopted. So far, the simulation-based design, in which the selection of CCHP devices is performed a priori, has proven to be a useful method for analyzing a small set of alternatives, but insufficient when the multiple choices and parameters involved in the CCHP design open a considerable number of options. In order to overcome this limitation, the synthesis of utilities' supply systems—implementing CCHP or not—is carried out adopting one of the approaches most used in this area. It consists in the formulation of an MILP optimization model, whose objective is to minimize the annual costs of the plant, subject to a series of constraints related to:

- A. The costs balance and application of current tariffs.
- B. The capacity and operation of devices forming the system.
- C. The storage of utilities.
- D. The supply and demand of utilities.
- E. Fulfillment of current regulations.
- F. Incorporation of synthesis, sizing and operational criteria.

Particularly, one important aspect that is not common to all the models based on this approach—and already evidenced in the example presented in Ch. 2—is the inclusion of constraints related to the feasible heat transfers between heat-supplying and heat-demanding streams. For this reason, the present work adapts the thermal integration model developed by Ramos (2012), which was used for determining the production of intermediate utilities' by engine-based generator sets. Specifically, it was extended to small turbine-based and microturbine-based generator sets, and reformulated in order to introduce exhaust-gases-driven chillers into the synthesis model.

In general, the synthesis model can be described as a set of candidate technologies, modeled as transformation processes<sup>1</sup>, interlinked in a reducible *superstructure* that contains all the admissible combinations capable of producing the required utilities. Each technology is characterized through one or more *technical factors* that correspond to the energy supply (or demand) destined (or required) to produce a utility, expressed per unit of main technology output<sup>2</sup>. As it will be explained, this model returns, among other features, the subset of technologies included into the optimal structure, as well as their required (total) capacity.

The superstructure conceived in this work includes, instead of various generator sets, cogeneration modules based on them, supplying—in addition to electricity—thermal energy for the production of up to three of the following thermal utilities: (i) hot gases (HG), (ii) saturated steam (ST), (iii) hot water (HW) at 95°C, and (iv) warm water (WW) at 60°C. Utilities produced can be used directly (e.g. ST for laundry) or transformed (e.g. ST activating absorption chillers). The set of technical factors for each module corresponds to the maximum energy supply destined to one of the first three above-mentioned utilities—per kW of electricity supplied. Production of WW occurs as long as there is still available heat, given that it has the lowest temperature level. The following section describes the procedure used for calculation of these factors.

#### 4.1 CHARACTERIZATION OF COGENERATION MODULES

It is clear that the CCHP performance is limited by the amount of heat recoverable from the prime movers, but also by the energy demand capable of use it. In that sense, the thesis of Ramos (2012) assessed the heat supply of large turbocharged natural gas engines (>5 MW) and developed a method for designing CCHP systems with the maximum heat recovery from them. It is based on the *pinch analysis* (LINNHOFF; BOLAND, 1982), which is used for determining the maximum amount of recoverable heat in an exchange network, prior to its design. In this work, that approach was adapted for covering small turbines ( $\approx 1200$  kW), microturbines (between 200 kW and 1000 kW), and smaller engines

---

<sup>1</sup> Each process transforms one or more energy inputs into one or more energy outputs, see Ch. 2.

<sup>2</sup> This *main* output (in kW) is related to the main purpose of each technology, e.g. electricity production for generator sets or steam production for boilers, and is that commonly used for reporting its capacity.

(between 150 kW and 1000 kW). Additionally, it was reformulated for taking into account the hot gases supply, eventually used in hot-gases-driven chillers<sup>3</sup>.

Firstly, the purpose of this method is to determine the maximum energy supply for producing a chosen thermal utility, achieved through an unspecific heat recovery exchange network established among a *given* set of heat-supplying streams (linked to the prime mover, e.g. exhaust gases or engine cooling water), and a set of heat-demanding streams (linked to the end uses or transformation devices, e.g. steam for laundry or hot water for activating absorption chillers). In other words, through this method, it is possible to calculate, for a given prime mover, the mass flow of heat-demanding streams maximizing the energy transfer to the chosen utility production. Subsequent stages are required for determining the heat exchanges forming the network, and further specification of corresponding devices. Heat-demanding streams incorporated to the heat recovery exchange network are presented in Tab. 14, together with their temperature limits. Note that these limits are the nominal temperatures of the heat sources of chosen absorption chillers, or correspond to the supply and return temperatures of the heat utilities used directly in the building applications introduced in the previous chapter.

Table 14 – Heat-demanding streams included in heat recovery exchange network.

Stream	Fluid	Temperatures, °C		Description
		Lower ( $T_l$ )	Upper ( $T_{up}$ )	
C01	Water WW	25	60	Warm water for sanitary use or space heating.
C02	Steam ST	60	170	Saturated steam for hospital laundry, Makeup: 50%.
C03	Water HW	72	95	Hot water activating absorption chiller. See catalog LG (2015).
C04	Steam ST	95	170	Saturated steam for absorption chiller, Press: 8 bar. See catalog Broad (2004).

Following subsections present the heat-supplying streams of each prime mover considered, and describe the procedure for characterizing their cogeneration modules, which is based on a linear programming (LP) model formulated for maximizing the energy supply to a given thermal utility.

<sup>3</sup> As mentioned previously, hot (exhaust) gases can be considered as an intermediate utility, in this case for activating an absorption chiller producing cold water.

### 4.1.1 Turbocharged natural gas engines

Given the high temperatures reached in the engine cylinders' block (over 2000°C), it is necessary to dissipate heat efficiently in order to maintain its components at a safe temperature range and avoid overheating or lubricating problems, but at the same time, guarantying a good operation performance (BASSHUYSEN; SCHAFFER, 2002). On the other hand, supercharged engines are characterized by the increase of the charge density of the working medium (air or air-fuel mixture) before it enters the cylinder, involving a pre-compression and further cooling of the working fluid, given that a marked raise in its temperature would impair the performance of the work cycle (HIERETH, 2003). In this way, for the proper operation of a conventional supercharged engine, its cooling system embraces the heat dissipation from three sources: (i) the engine (cylinders) block, (ii) the lube oil, and (iii) the compressed fluid entering the manifold. Particularly, the characterization of the gas engines presented in this work is based on the turbocharged<sup>4</sup> engine specified in Caterpillar (2000), with a nominal capacity of 1035 kW and whose cooling circuits are depicted in Fig. 24.

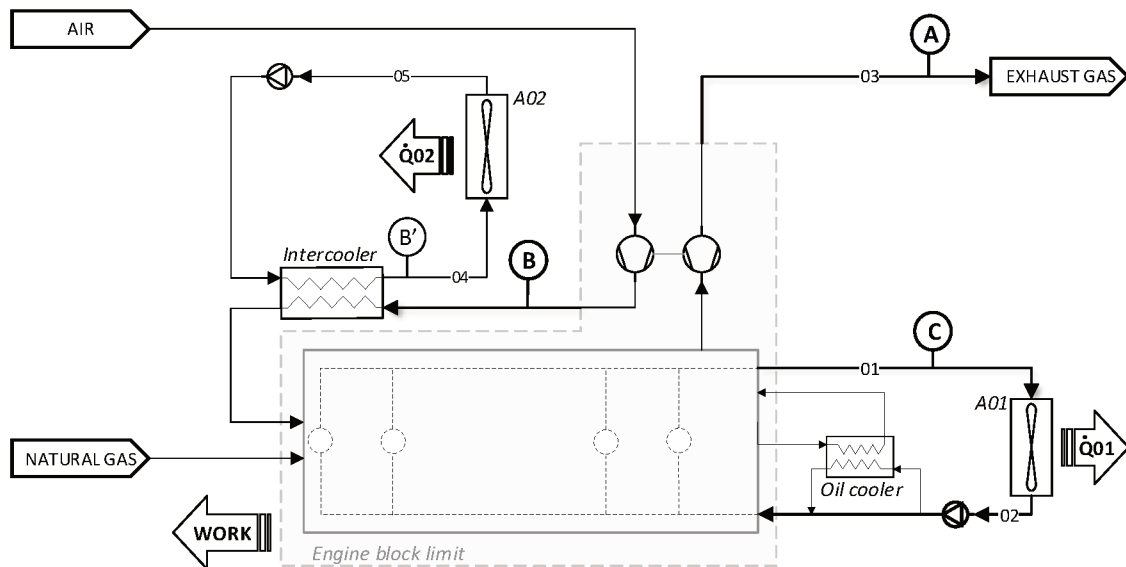


Figure 24 – Heat-supplying streams of natural gas engine Caterpillar model G3516 LE:  
A. Exhaust gases, B. Compressed air, and C. Engine block water.

It is worth noting that this is not the unique possible scheme for the cooling system,

<sup>4</sup> Turbocharged engines provide the supercharging by means of a turbocompressor activated by the exhaust gases stream coming from the cylinders' block.

since it varies according to the size of the equipment and the options given by each manufacturer. For instance, application handbooks (CATERPILLAR, 2016; CUMMINS, 2015) present some variations as follows:

- Use of cooling towers for heat rejection. Figure 24 depicts a heat rejection through air-cooled heat exchangers (i.e. radiators *A01/A02*).
- Two-stage cooling for compressed air, i.e. use of a low-temperature (LT) intercooler together with a second, high-temperature (HT), intercooler<sup>5</sup>. The selected model counts with only one cooling stage (*Intercooler* in Fig. 24).
- Lube oil cooling (*Oil cooler* in Fig. 24) attached to the compressed air cooling circuit. In this case it is attached in the block cooling circuit.
- Independent cooling circuit for lube oil. It is quite common in large engines.
- Combined-circuit cooling, i.e. use of a unique water loop for cooling the engine block, the compressed air and the lube oil. It is frequent in smaller engines.
- Pressurized water circuit for the block cooling system. This enables a higher water temperature, making it suitable for applications involving heat recovery and/or production of low-pressure steam.

In any case, the heat supply of a natural gas engine are divided among four—as they were already introduced—heat-supplying streams: (i) exhaust gases (EG), (ii) compressed—hot—air (HA), (iii) engine block water (EW), and (iv) lube oil. Information given in the catalog of the selected engine does not report the heat supply of the last one, because it is already included into the EW cooling circuit. In this regard, it is important to mention that not all the catalogs include the same information and that it is more common to find the conditions of the water circulating through the intercooler(s)—point *B'* in Fig. 24—e.g. Waukesha (2013), Guascor (2011); even sometimes the conditions (specially the temperature) of the heat-supplying streams are not reported.

Sankey diagram of Fig. 25 illustrates the inclusion of a heat exchange (HEX) network into the cogeneration module and the consideration of a hot-gases-driven absorption chiller using part of the exhaust gases energy for dissipating heat from the ambient (i.e. through

<sup>5</sup> In some catalogs, these devices are also referred as *Aftercoolers*.

the production of the *cold water* utility). As mentioned above, the cogeneration module is able to supply, besides electricity (EE), warm water, hot water, steam, and hot gases utilities. The last one is provided as a stream at high temperature (about 500°C) fed into the chiller, but the internal absorption cycle typical to this type of equipment only allows to cool the hot gases down to about 180°C (DENG; WANG; HAN, 2011; THERMAX, 2014). Thus, it is still possible to take some advantage from the gas stream coming out from the chiller, which can provide heat in the range between about 180 and 120°C to the network<sup>6</sup>.

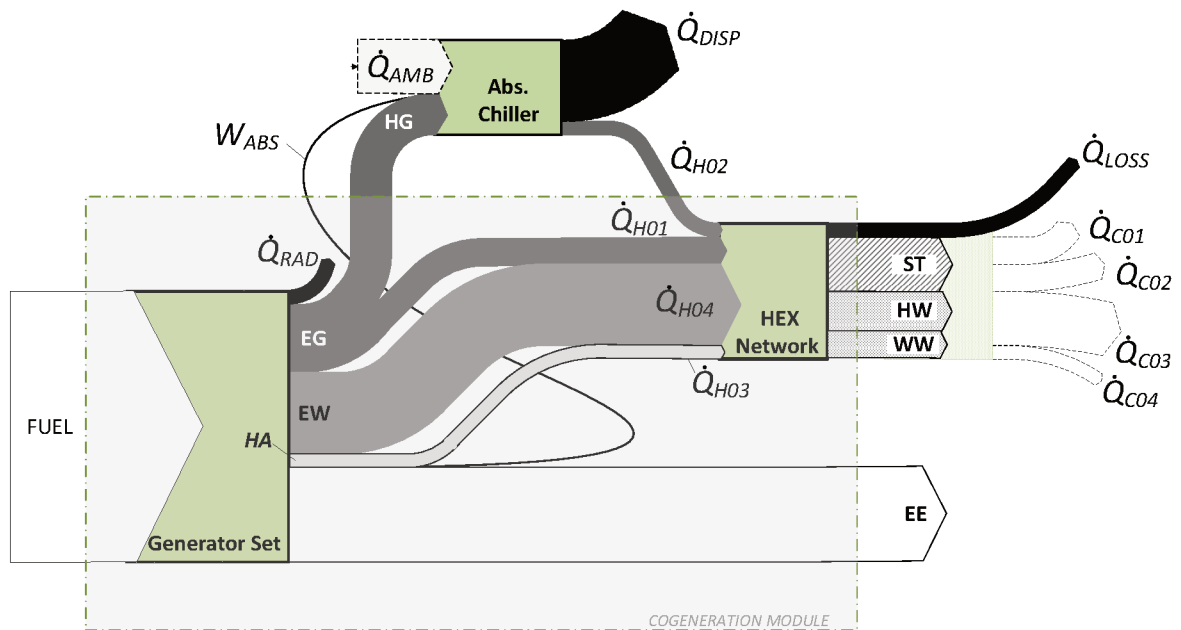


Figure 25 – Sankey diagram for cogeneration module based on natural gas engines. EE: Electricity, EG: Exhaust gases, EW: Engine block water, HA: Hot air, HG: Hot gases, HW: Hot water, ST: Steam.

Note that the incorporation of the chiller is optional, and that all the heat supplied by exhaust gases can be directed to the HEX network (HG production would be 0). Moreover, not all the heat provided by heat-supplying streams ( $\dot{Q}_{H01}$ ,  $\dot{Q}_{H02}$ , ...) is effectively transferred to the heat-demanding streams, given the constraints imposed by the temperature levels at which the heat transfers occur; thus, there could be heat losses (i.e. heat not transferred, i.e. dissipated— $\dot{Q}_{LOSS}$ ). On the other hand, the proportion

<sup>6</sup> 120°C is considered safe for avoiding condensation of the water formed by combustion at the exhaust outlet, given that it would induce corrosion. Most catalogs report the heat recoverable from exhaust gases considering this value, or close to this value.



among utilities ST, HW, and WW is variable, given that the amount of heat required by heat-demanding streams ( $\dot{Q}_{C01}$ ,  $\dot{Q}_{C02}$ , ...) is dictated by the utility demands, directly or through transformation devices, rather than by the module production. Consequently, there are several options for conforming a cogeneration module based on a given engine (or prime mover), and a reasonable way to cover them—taking full advantage from the heat supplied by the engine—is to maximize the energy supply to the utilities produced by the module, considering the constraints imposed in the HEX network (thus, minimizing  $\dot{Q}_{LOSS}$ ). In this way, three modules are conceived: (i) ECM01 prioritizing HG, (ii) ECM02 prioritizing ST, and (iii) ECM03 prioritizing HW. As mentioned previously, HW and WW are also produced using the remaining heat recoverable from the heat-supplying streams. Between these utilities, HW production is prioritized since it has a higher temperature level. Table 15 shows the features of heat-supplying streams considered in the heat recovery exchange network for the cogeneration modules based on the selected model.

Table 15 – Heat-supplying streams considered for cogeneration modules based on generator set Caterpillar model G3516LE.

Tag	Fluid	Temps., °C		Flow, kg/s	Description
		$T_{up}^*$	$T_l^*$		
H01	Exhaust gases EG	474	120	$\leq 1.771$	Hot gases coming from engine.
H02	Exhaust gases EG	180	120	$\leq 1.771$	Hot gases coming from absorption chiller.
H03	Hot air HA	152	59	1.702	Compressed hot air, before intercooler.
<i>H04</i>	Engine water EW	99	89	24.93	Engine block water.

\*  $T_{up}$ : upper temperature limit,  $T_l$ : lower temperature limit.

On the other hand, according to the manufacturer's guideline (CATERPILLAR, 2016), temperatures reported for *H04* (EW) fulfills the following cooling requirements (see Fig. 24):

- Maximum water temperature ( $T_{01}$ ) of 99°C.
- Maximum temperature drop ( $T_{01} - T_{02}$ ) of 11.1°C.
- Water flow between 1325 and 1700 liters per minute. The mass flow reported in Tab. 15 corresponds to 1500 liters per minute.

As mentioned previously, except for the inclusion of the hot gases stream at 180°C, this maximization problem already was formulated by Ramos (2012) as an LP model (thermal integration in the HEX network), where the heat balance among coincident heat-supplying and heat-demanding streams is done on temperature intervals defined by the table problem algorithm proper of the pinch analysis. Details can be consulted in technical references as Kemp (2007). Figure 26 presents the temperature scale obtained for the selected engine as well as the energy balance of each interval, delimited by an upper temperature  $UT_j$  and a lower temperature  $LT_j$ .

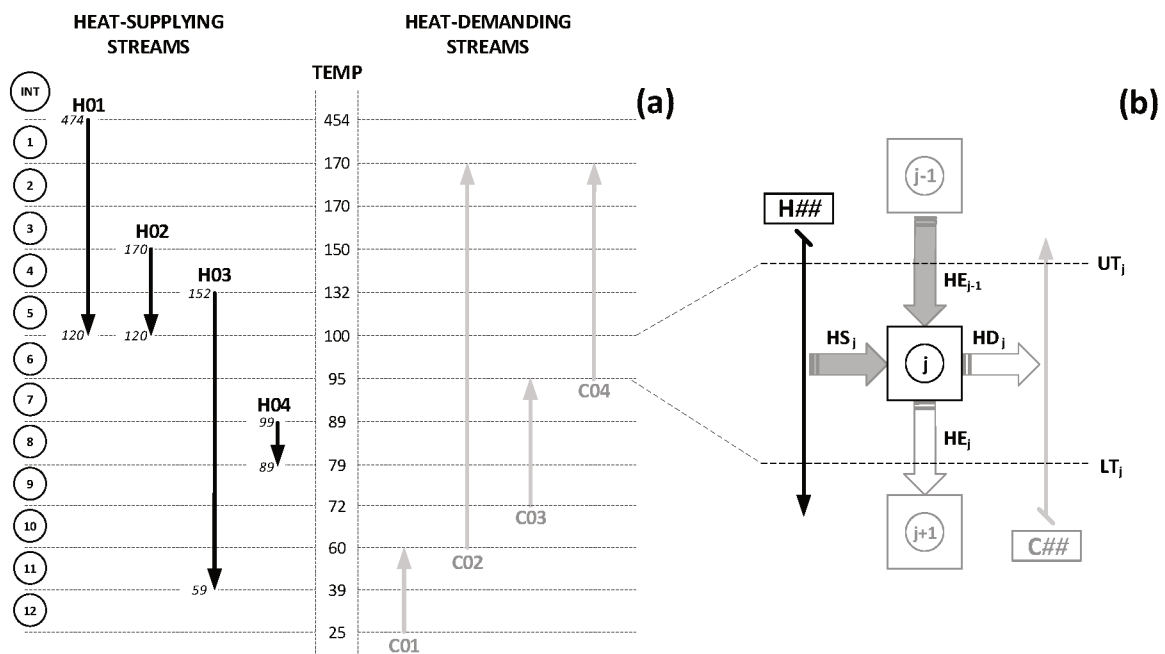


Figure 26 – Thermal integration: (a) Temperature scale, (b) Energy balance on interval  $j$ .

Note that the scale was made by shifting the temperatures of the heat-supplying streams in such a way that a certain minimum temperature difference (*pinch*) is guaranteed for the heat exchanges forming the network. Values for this *pinch* were set at 20°C for exchanges involving gaseous streams and at 10°C for exchanges between liquid streams<sup>7</sup>; original temperatures are indicated on the left side of the heat-supplying streams.

<sup>7</sup> These values are typical for the streams considered and use of conventional heat exchangers (shell and tube).

The energy balance on intervals is expressed as

$$HE_j = HS_j - HD_j \quad \forall j = 1 \quad (4.1)$$

$$HE_j = HS_j - HD_j + HE_{j-1} \quad \forall j \neq 1 \quad (4.2)$$

$$HS_j = \sum^H HS_{h,j} \quad \forall h \quad | \quad T_{l,h} \geq UT_j \quad \wedge \quad T_{up,h} \leq LT_j \quad h \in \{H01, H02, \dots\} \quad (4.3)$$

$$HD_j = \sum^C HD_{c,j} \quad \forall c \quad | \quad T_{l,c} \geq LT_j \quad \wedge \quad T_{up,c} \leq UT_j \quad c \in \{C01, C02, \dots\} \quad (4.4)$$

where  $HE_j$ ,  $HS_j$ , and  $HD_j$  are the heat excess, the heat supply and the heat demand in the interval  $j$ , respectively.  $HS_{h,j}$  is the heat supply by stream  $h$  and  $HD_{c,j}$  the heat demand by the stream  $c$ , both at interval  $j$ . These quantities are calculated according to the following expressions:

$$HS_{h,j} = MF_h \cdot UHS_{h,j} \quad (4.5)$$

$$HD_{c,j} = MF_c \cdot UHD_{c,j} \quad (4.6)$$

where  $MF_h$  and  $MF_c$  are the mass flows of streams  $h$  and  $c$ , respectively.  $UHS_{h,j}$  is the unitary heat supply of stream  $h$  in the interval  $j$ , while  $UHD_{c,j}$  is the unitary demand of the stream  $c$  in the interval  $j$ , which are divided in two addends, according to the following relationships:

$$UHS_{h,j} = \overline{C}_{P,h} \cdot \overbrace{(UT_j - LT_j)}^{\text{Sensible}} + \overbrace{\Delta h_{v,h}}^{\text{Latent}} \quad (4.7)$$

$$UHD_{c,j} = \overline{C}_{P,c} \cdot (UT_j - LT_j) + \Delta h_{v,c} \quad (4.8)$$

here,  $\overline{C}_{P,h}$  and  $\overline{C}_{P,c}$  are the average specific heat capacities of streams  $h$  and  $c$ , respectively; they are considered constants. On the other hand,  $\Delta h_{v,h}$  and  $\Delta h_{v,c}$  are the specific heat of vaporization of streams  $h$  and  $c$ , respectively; these addends are omitted for intervals where no latent heat is transferred (i.e. they are counted only for the interval 2 in Fig. 26).

The objective of the optimization model is maximizing the total energy supply ( $SUP$ ) for producing the utilities addressable by the module, which is expressed as the sum of the individual contributions ( $SUP_u$ ) multiplied by a factor  $UK_u$  that can be adjusted for favoring the energy supply to one utility over the others. Formulation of the problem is presented in the following equations:

$$\text{Maximize } SUP = \sum^U UK_u \cdot SUP_u \quad \forall u \in \{HG, ST, HW\} \quad (4.9)$$

$$SUP_u = UP_{u,c} \cdot MF_c \quad \forall u \mid u \in \{ST, HW, WW\} \quad (4.10)$$

$$SUP_u = UP_{u,h} \cdot MF_h \quad \forall u \mid u \in \{HG\} \quad (4.11)$$

where  $UP_{u,c}$  and  $UP_{u,h}$  are the energy supply to the utility  $u$  per unit of mass flow of streams  $c$  and  $h$ , respectively; Tab. 16 presents the formulation of these parameters. Note in the last row that the HG utility is supplied to the absorption chiller at the temperature range from 474 to 180°C, and it would be proportional to the mass flow of H02.

Table 16 – Supply of utilities per unitary mass flow of streams.

Stream	Utility	Formula	Value, kJ/kg
C01	WW	$UP_{u,c} = \bar{C}_{P,C01} (T_{up,C01} - T_{l,C01})$	146.4
C02	ST	$UP_{u,c} = \bar{C}_{P,C02} (T_{up,C02} - T_{l,C02}) + \Delta h_{v,C02}$	2515
C03	HW	$UP_{u,c} = \bar{C}_{P,C03} (T_{up,C03} - T_{l,C03})$	96.55
C04	ST	$UP_{u,c} = \bar{C}_{P,C04} (T_{up,C04} - T_{l,C04}) + \Delta h_{v,C04}$	2368
H01 / H02	HG	$UP_{u,h} = \bar{C}_{P,H01} (T_{up,H01} - T_{up,H02})$	328.4

The problem can be briefly described as the maximization of  $SUP$  formulated in Eqn. 4.11, constrained by the energy balances on temperature intervals and the thermal cascade formed by them (i.e. the heat excess  $HE$  of an interval  $j$  is transferred to the next  $j+1$  of lower temperature level), formulated in Eqns. 4.1 through 4.8. Additionally, Tab. 17 presents the model inputs not presented so far.

In general, specific heat capacities used in the model are assumed constant over the temperature interval at which each heat transfer takes place. Their values correspond to the average specific heat capacity  $\bar{C}_P$ , formulated directly in the EES environment as shown in Eqn. 4.12.

$$\bar{C}_P = \frac{h_{out} - h_{in}}{T_{out} - T_{in}} \quad (4.12)$$

where  $h_{in}$  and  $h_{out}$  are the fluid' specific enthalpy at its inlet and outlet temperatures ( $T_{in}$  and  $T_{out}$ ) in a given heat transfer, respectively. Particularly, the value of the  $\bar{C}_P$  for hot gases, which is a mixture were taken from the manufacturer guideline (CATERPILLAR, 2016).

Table 17 – Values of the remaining inputs of the thermal integration LP model.

General		Specific				
Input	Value, kJ/kg-K	Module*	Input	Value	Input	Value
$\bar{C}_{P,H01}$	1.0802	EMC01	$UK_{HG}$	2.00	$MF_{H01}$	0.000 kg/s
$\bar{C}_{P,H02}$	1.0802		$UK_{ST}$	0.00	$MF_{H02}$	1.771 kg/s
$\bar{C}_{P,H03}$	1.0111		$UK_{HW}$	1.00		
$\bar{C}_{P,H04}$	4.2091		$UK_{WW}$	0.50		
$\bar{C}_{P,C01}$	4.1820	EMC02	$UK_{HG}$	0.00	$MF_{H01}$	1.771 kg/s
$\bar{C}_{P,C02}$	4.2502		$UK_{ST}$	2.00	$MF_{H02}$	0.000 kg/s
$\bar{C}_{P,C03}$	4.2502		$UK_{HW}$	1.00		
$\bar{C}_{P,C04}$	4.1981		$UK_{WW}$	0.50		
$\Delta h_{v,C02}$	2047.0 kJ/kg	EMC03	$UK_{HG}$	0.00	$MF_{H01}$	1.771 kg/s
$\Delta h_{v,C04}$	2047.0 kJ/kg		$UK_{ST}$	0.00	$MF_{H02}$	0.000 kg/s
			$UK_{HW}$	1.00		
			$UK_{WW}$	0.50		

\*EMC: Engine-based Cogeneration Sets.

Note that for maximum production of HG, all the exhaust gases are directed to the absorption chiller ( $MF_{H01}=0$ ), while for the other utilities, this stream is directed completely to the HEX network. Additionally, the values of  $UK$  are different for each module, to favor the production of one over the others (taking into account that it is a maximization). The model formulated together with its inputs were processed using the software *LINGO* (LINDO SYSTEMS, 2017), obtaining—among others—the results of interest presented in Tab. 18. Since only the hospital uses steam for laundry, the maximum energy supply to ST production—corresponding to ECM02—is slightly higher than the rest of applications, given the portion of heat transferred in the range between 60 and 95°C; this small effect (about 5%), caused by the absence of the stream C02 (steam for the hospital laundry), is considered later in the synthesis model.

Table 18 – Supply of utilities by cogeneration modules based on a 1035 kW generator set.

Module	Heat supply, kW			
	HG	ST	HW	WW
ECM01	581.7	0.0	650.3	654.8
ECM02	0.0	667.6	446.7	772.6
ECM02*	0.0	628.6	470.6	787.7
ECM03	0.0	0.0	1829.8	56.8

\*Apply for applications other than hospital.

Technical factors for each module are obtained simply dividing these results by the nominal electricity output of the generator set (1035 kW). On the other hand, the temperature level of the heat-demanding streams associated with the utility WW is low enough for enabling the recovery of most of the heat supplied by the engine ( $Q_{LOSS} = 0$ ). According to the energy balance reported by the manufacturer, the sum of the (available) heat from EG, EW and HA is 1910 kW, while the value obtained is slightly lower (1887 kW for the three modules).

Analogously to that it was done in the Fig. 11, but without setting the HEX network beforehand, it is possible to determine the maximum energy supply to a *given* utility constrained by the supply to another (i.e. by pairs), as shown in Figs. 27a to 27c. Hatched regions correspond to operating loads below of 50% of the nominal capacity, which is not recommended by the manufacturer. Additionally, in order to visualize the solution space

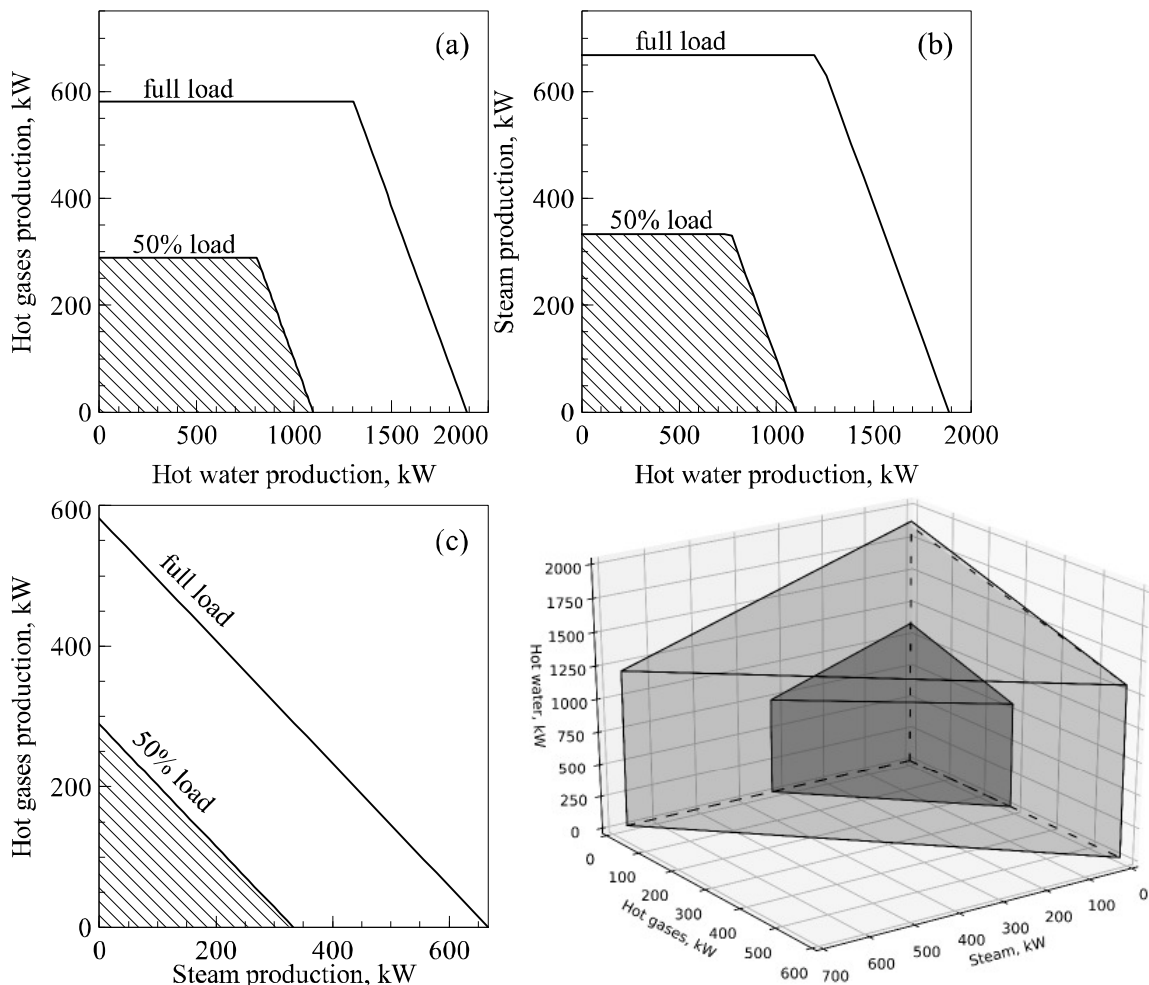


Figure 27 – Supply regions for cogeneration modules based on selected natural gas engine: (a) HW vs HG, (b) HW vs ST, (c) ST vs HG, and (d) Supply surface.

of the modules—since there are four utilities—the energy supply for producing HW and WW were grouped to elaborate Fig. 27d, which shows the thermal energy supply region of the engine considered. It is clear that any point on the external surface correspond to an optimum, where the energy supply to the production of utilities has been maximized; points inside the intermediate region correspond to feasible (suboptimal) supply of energy to utilities, while points outside this region—even those under the surface of 50% load—are unfeasible. Comparing the results of Tab. 18 with those previously reported in Tab. 5, there is a production improvement of 26 kW for ST and 214 kW for HW + WW, which shows the layout proposed in Fig.10 as a suboptimal but reasonable choice, at least considering only the supply of these utilities.

#### 4.1.2 Natural Gas Turbines and Microturbines

Differing from the natural gas engines, the heat supply of turbines and microturbines is just through the exhaust gases. Particularly, the latter count with a recuperator—generally incorporated into their body—whose purpose is to increase the energy of the compressed air leaving the combustor for increasing the equipment performance, as shown in Fig. 28. While microturbines are available with sizes ranging from about 20 to 200 kWe, gas turbines commonly are available at sizes greater than 3 MWe, with few options for smaller sizes. According to the review presented by Kolanowski (2011), the microturbines' technology is relatively recent (beginning by 1988) and its market is dominated by the brand Capstone, successor to the first manufacturer of this type of equipment. Particularly, as far as it is known, it is the only one offering a model of 1 MW, which, according to its technical manual, corresponds to an engineered bundle of five modules of 200 kW each

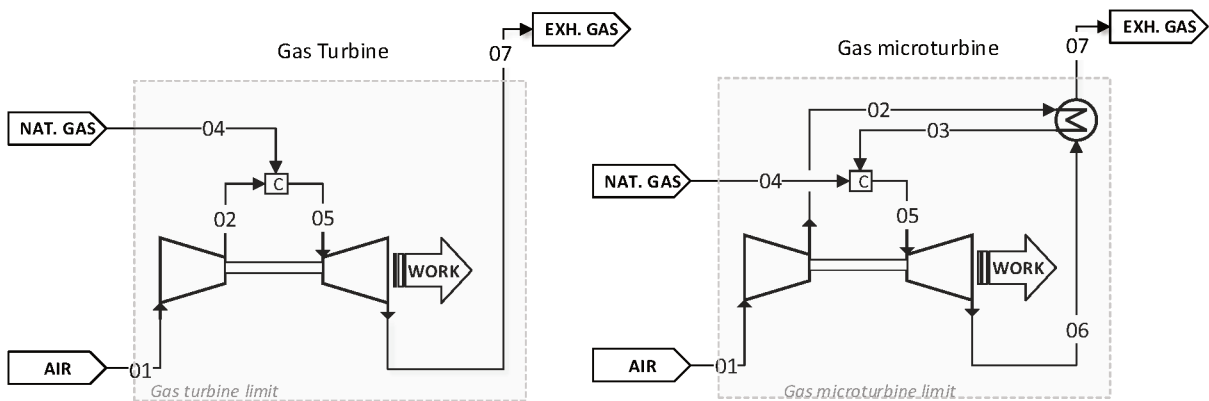


Figure 28 – Typical schemes for natural gas turbines and microturbines.

(CAPSTONE, 2005); analogously, the model considered in this work for characterizing the small turbines has a nominal capacity of 1.2 MWe (SOLAR, 2014). The key difference between these technologies, for specifying the cogeneration modules based on them, is the outlet temperature of the exhaust gases ( $T_{07}$  in Fig. 28). While exhaust temperature of conventional gas turbines can be as high as  $530^{\circ}\text{C}$ , a microturbine exhaust gases usually are at between  $220$  and  $320^{\circ}\text{C}$ . In this way, taking into account the same premises used in the previous section for defining the modules, the following six turbine-based modules are conceived:

1. TCM01 Turbine-based module delivering, besides electricity, HG and HW.
2. TCM02 Turbine-based module delivering, besides electricity, ST and HW.
3. TCM03 Turbine-based module delivering, besides electricity, HW (only).
4. MCM01 Microturbine-based module delivering, besides electricity, HG (only).
5. MCM02 Microturbine-based module delivering, besides electricity, ST and HW.
6. MCM03 Microturbine-based module delivering, besides electricity, HW (only).

Since there is only one heat-supplying stream, calculation of the thermal energy supply to each utility is simpler than in the engine-based cogeneration modules. In fact, it is easily verified that the LP optimization model formulated for the engine-based modules is not required because the exhaust gas stream would provide energy entirely to the HEX network *or* to the HG utility, as shown in Fig. 29. Additionally, for both turbine

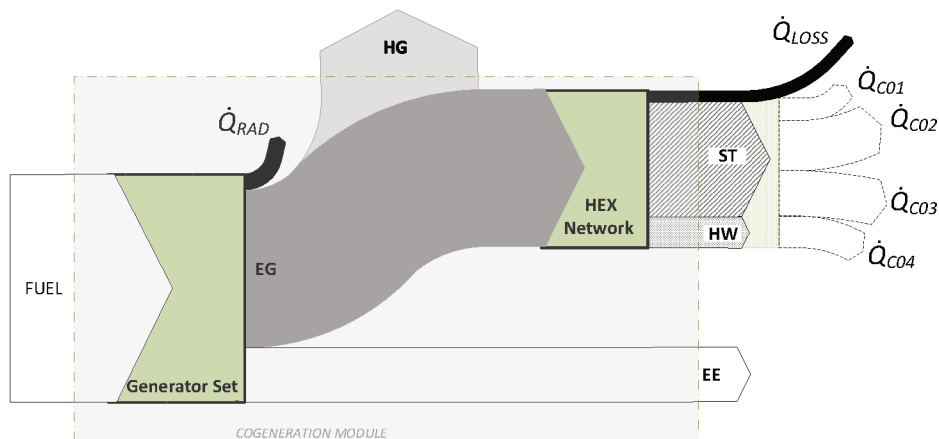


Figure 29 – Typical Sankey diagram for gas turbines and microturbines-based modules.



technologies, the exhaust gases stream has a temperature high enough for supplying energy to ST and further HW production (omitting WW production). Finally, it is important to remark that the hot-gases-driven absorption chillers transforming the HG utility provided by microturbines have technical features different from those taking HG from turbines and engines. They can be activated at temperatures as low as  $260^{\circ}\text{C}$  and rejects the exhaust gases at  $130^{\circ}\text{C}$ , which are not considered useful; for this reason MCM01 produces only hot gases HG.

Despite the energy balance on gas turbines and microturbines is simpler, the performance of these devices is more sensible to the air inlet temperature than engines. Particularly, this feature is caused by to the greater air flow required per kW delivered (ÇENGEL; BOLES, 2006). Consequently, it is necessary to consider this feature for determining the technical factors of the cogeneration modules based on this technology. Figure 30 shows the performance parameters of the chosen models as function of the inlet temperature (adopting  $T_{01}$  as equal to ambient temperature  $T_0$ ).

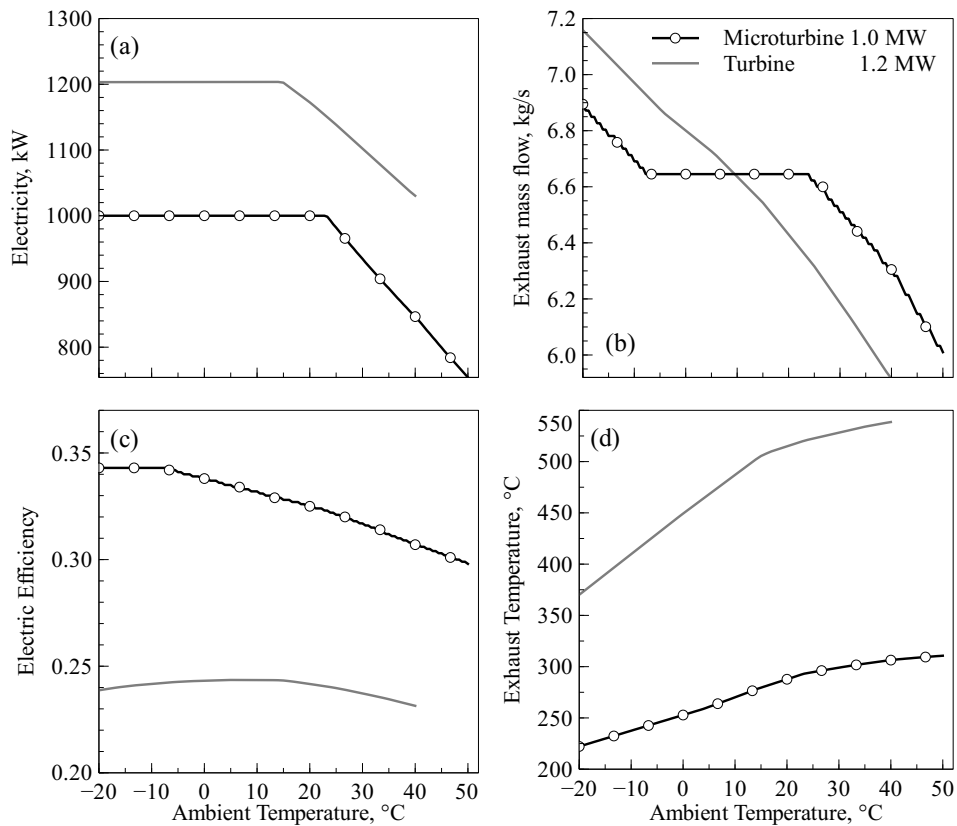


Figure 30 – Performance parameters of gas turbines and microturbines as function of the ambient temperature: (a) electricity, (b) exhaust mass flow, (c) efficiency, and (d) exhaust gas temperature. Data from (CAPSTONE, 2005; SOLAR, 2014).

The thermal energy supply of these devices to each utility can be determined as a function of the ambient temperature ( $T_0$ ), using the available information, according to the following equations:

$$HG_{max}(T_0) = m_{07}(T_0) \cdot 1.123 \cdot (T_{07}(T_0) - 170) \quad \text{for turbines} \quad (4.13)$$

$$HG_{max}(T_0) = m_{07}(T_0) \cdot 1.123 \cdot (T_{07}(T_0) - 130) \quad \text{for microturbines} \quad (4.14)$$

$$HW_{max}(T_0) = \dot{Q}_{EG}(T_0) = m_{07}(T_0) \cdot 1.123 \cdot (T_{07}(T_0) - 120) \quad (4.15)$$

$$ST_{max}(T_0) = \dot{Q}_{VAP} + \dot{Q}_{ECN} \quad (4.16)$$

$$\begin{cases} \dot{Q}_{VAP} = m_{07}(T_0) \cdot 1.123 \cdot (T_{07}(T_0) - 190) = 2047 \cdot m_{ST} \\ \dot{Q}_{ECN} = m_{07}(T_0) \cdot 1.123 \cdot (190 - T_{07}^*) = m_{ST} \cdot 4.25 \cdot (170 - T_{RET}) \end{cases} \quad (4.17)$$

$$HW_{HG}(T_0) = \dot{Q}_{EG}(T_0) - HG_{max}(T_0) \quad (4.18)$$

$$HW_{ST}(T_0) = \dot{Q}_{EG}(T_0) - ST_{max}(T_0) \quad (4.19)$$

here, the average specific heat capacity of exhaust gases (1.123 kJ/kg-K) is that used by the manufacturer of microturbines for reporting their energy balance, and was also used for gas turbines. On the other hand, similar to the natural gas engines, the heat supply to the HG utility considers the hot gases temperature leaving the corresponding absorption chiller, 170 and 130°C for turbines and microturbines, respectively (Eqns. 4.13 and 4.14). As mentioned previously, the temperature level of exhaust gases enables the heat transfer to the HW utility completely down to a minimum outlet temperature of 120°C. Therefore, any excess of heat supply to HG or ST utilities can be recovered as HW (see Eqn. 4.18 and 4.19). Finally, the heat supply to ST is determined considering a saturation temperature of 170°C, a *pinch* of 20°C, a specific heat capacity of 4.25 kJ/kg-K, and a specific heat of vaporization of 2047 kJ/kg. An *approach* is not considered, since most of HRSG at these sizes have the economizer (or an equivalent stage) embedded into their body. Thus, the selection of its value would be part of the device design. Note that the hot gases temperature leaving the economizer  $T_{07}^*$  is not of interest, given the further heat recovery to produce HW. Figure 31 shows the energy supply by gas turbine-based modules to HG, ST, and HW production as function of  $T_0$ .

Technical factors for these modules are obtained dividing, for a given  $T_0$ , each energy supply by the corresponding electricity output (see Fig. 30). Evidently, it means that technical factors can be expressed as function of  $T_0$ . Figure 32 demonstrates that such functions can be approximated by linear relationships, which is convenient for the synthesis model. Table 19 presents the results of linear regressions performed for each factor.

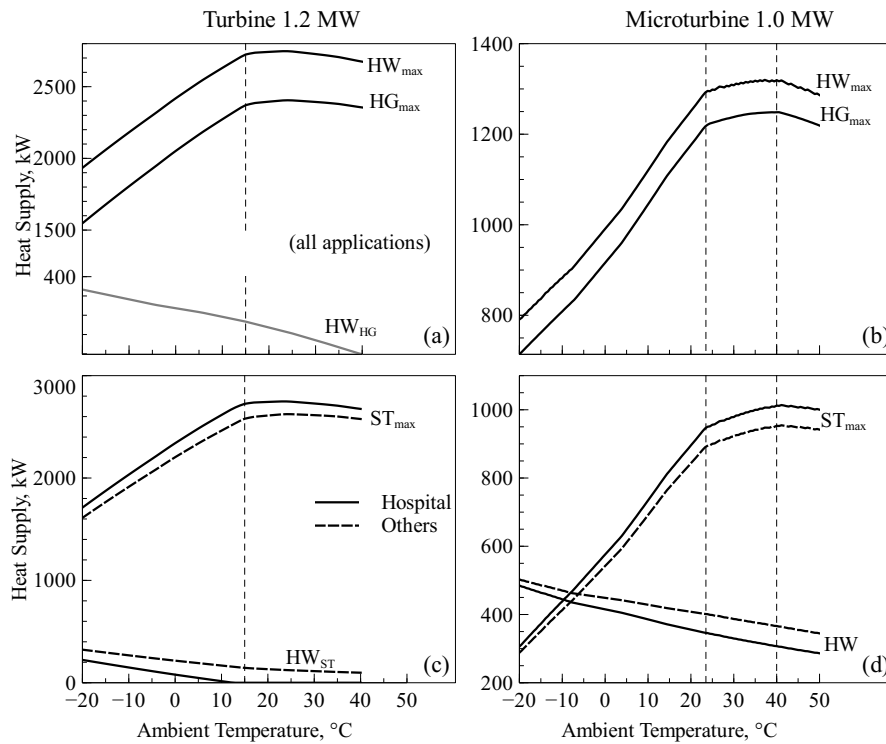


Figure 31 – Heat supply of devices to the production of thermal utilities: (a) turbine/HW and HG, (b) microturbine/HG and HW, (c) turbine/ST, (d) microturbine/ST.

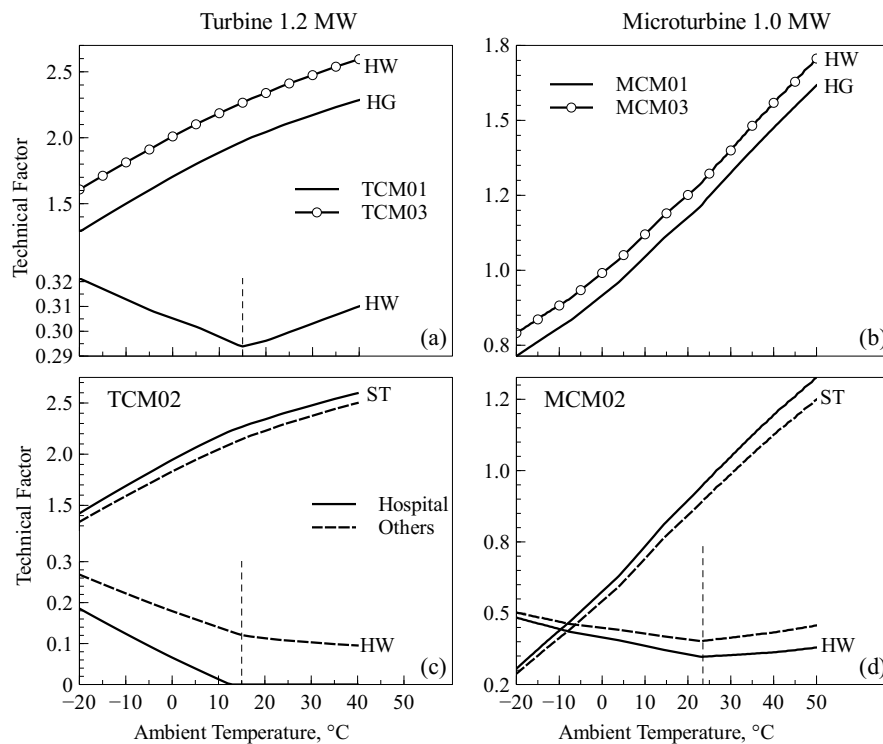


Figure 32 – Technical factors of turbine and microturbine-based modules: (a) TCM01 and TCM03, (b) MCM01 and MCM03, (c) TCM02, and (d) MCM02.

Table 19 – Formulation of technical factors (TF) as function of  $T_0$  for turbine and microturbine-based modules.

Module*	App.	Utility	Formula	$R^2$
TCM01	All	HG	$TF = 1.682 + 1.68 \cdot 10^{-2} \cdot T_0$	0.988
		HW	$TF = 0.305 - 7.72 \cdot 10^{-4} \cdot T_0 ; T_0 < 15^\circ C$	0.999
			$TF = 0.283 + 6.69 \cdot 10^{-4} \cdot T_0 ; T_0 > 15^\circ C$	0.997
TCM02	Hosp.	ST	$TF = 1.910 + 1.97 \cdot 10^{-2} \cdot T_0$	0.978
		HW	$TF = 0.068 - 5.72 \cdot 10^{-3} \cdot T_0 ; T_0 < 15^\circ C$	0.999
			$TF = 0 ; T_0 > 15^\circ C$	0.997
TCM02	Others	ST	$TF = 1.804 + 1.95 \cdot 10^{-2} \cdot T_0$	0.986
		HW	$TF = 0.181 - 4.22 \cdot 10^{-3} \cdot T_0 ; T_0 < 15^\circ C$	0.999
			$TF = 0.133 + 9.78 \cdot 10^{-4} \cdot T_0 ; T_0 > 15^\circ C$	0.983
TCM03	All	HW	$TF = 1.990 + 1.65 \cdot 10^{-2} \cdot T_0$	0.992
MCM01	All	HG	$TF = 0.932 + 1.32 \cdot 10^{-2} \cdot T_0$	0.995
MCM02	Hosp.	ST	$TF = 0.589 + 1.50 \cdot 10^{-2} \cdot T_0$	0.999
		HW	$TF = 0.416 - 3.08 \cdot 10^{-3} \cdot T_0 ; T_0 < 24^\circ C$	0.996
			$TF = 0.317 + 1.19 \cdot 10^{-3} \cdot T_0 ; T_0 > 24^\circ C$	0.976
MCM02	Others	ST	$TF = 0.555 + 1.42 \cdot 10^{-2} \cdot T_0$	0.999
		HW	$TF = 0.451 - 2.21 \cdot 10^{-3} \cdot T_0 ; T_0 < 24^\circ C$	0.991
			$TF = 0.354 + 2.01 \cdot 10^{-3} \cdot T_0 ; T_0 > 24^\circ C$	0.993
MCM03	All	HW	$TF = 1.007 + 1.34 \cdot 10^{-2} \cdot T_0$	0.994

TCM: Turbine-based Cogeneration Module, MCM: Microturbine-based Cogeneration Module.

### 4.1.3 Heat Recovery Network of Cogeneration Modules

The production of utilities—characterized by the technical factors presented in the previous section—corresponds to a heat exchange network proper to each CHP module, which is formed by a set of heat exchangers with different transfer area and thus costs. Taking into account this fact, it becomes necessary to determine the heat transfer area for each module in order to establish a reasonable basis for differentiating its investment costs from the others. The methodology adopted in this work is described in detail in Kemp (2007), which is based on the division of the heat transfer problem in two zones, divided by the pinch point<sup>8</sup>(PP), and the fulfillment of two feasibility criteria:

- Since the temperature driving force at the other side of heat exchangers located immediately to the pinch point must be above the *pinch*, it implies that

<sup>8</sup> Pinch point refers to the temperature at which the temperature difference between two (composite) streams exchanging heat equals the value of the *pinch* (minimum temperature difference).

$MF_h \cdot \bar{C}_{P,h} \leq MF_c \cdot \bar{C}_{P,c}$  immediately above the pinch point, and

$MF_h \cdot \bar{C}_{P,h} \geq MF_c \cdot \bar{C}_{P,c}$  immediately below the pinch point.

- Since all the heat-supplying streams above the pinch point and all the heat-demanding streams below the pinch point must be brought to it only through heat exchanges among them, i.e. without using external cold utility above the pinch point nor external hot utility below it, it follows that: (i) above the pinch point, the number of heat-supplying streams must be *lesser or equal* than the number of heat-demanding streams, and (ii) below the pinch point, the number of heat-supplying streams must be *greater or equal* than heat-demanding streams.

The fulfillment of the latter imply that, in order to match adequately the heat-supplying and heat demanding-streams, a stream may be split into multiple fractions. The steps involved in the heat exchange network design are illustrated in Fig. 33. Here,  $N_H$  and  $N_C$  are the number of heat-supplying and heat-demanding streams, respectively, while  $CP_H$  and  $CP_C$  corresponds to their heat capacity rates ( $MF \cdot \bar{C}_p$ ).

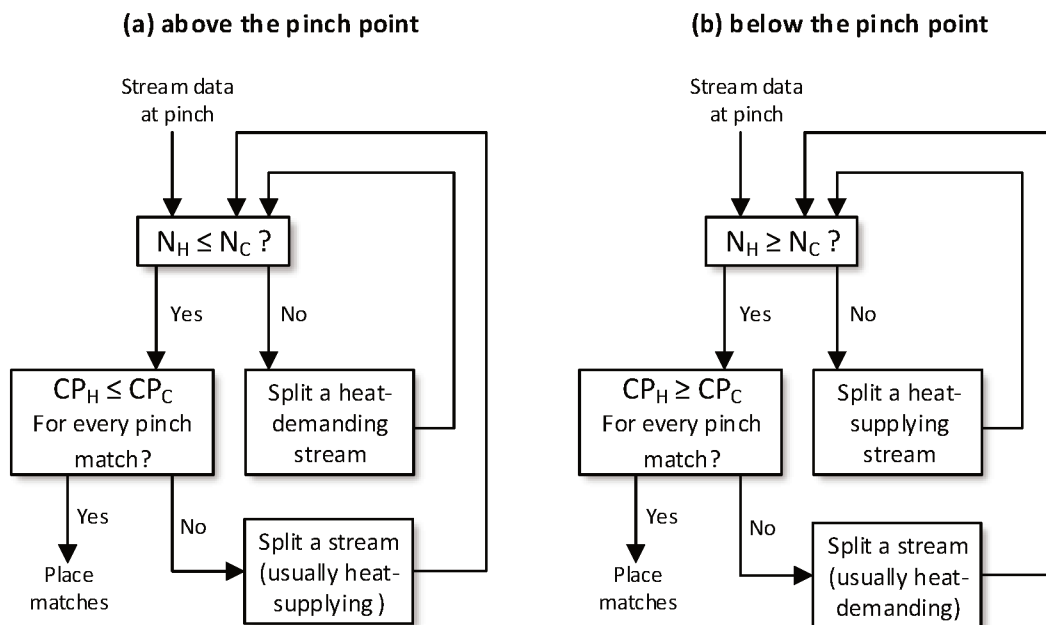


Figure 33 – Procedure for matching heat-supplying and heat-demanding streams into the heat exchange network: (a) design above the pinch point, (b) design below the pinch point. Figure adapted from Kemp (2007).

Evidently, each match corresponds to a heat exchange unit, whose duty is adjusted until the maximum heat recovery goal, established in the previous section, is met. Note that there can be other types of goals, different from the maximum energy recovery, like the minimum heat transfer area, minimum pressure drop, or the minimum number of heat exchangers (CHHABRA, 2018). However, targeting these goals introduces additional decision criteria, particular to each case, that are out of the scope of the present work. Figure 34 illustrates the matching procedure for the cogeneration module ECM01, which produces the maximum amount of hot gases utility (HG), together with hot water (HW) and warm water (WW).

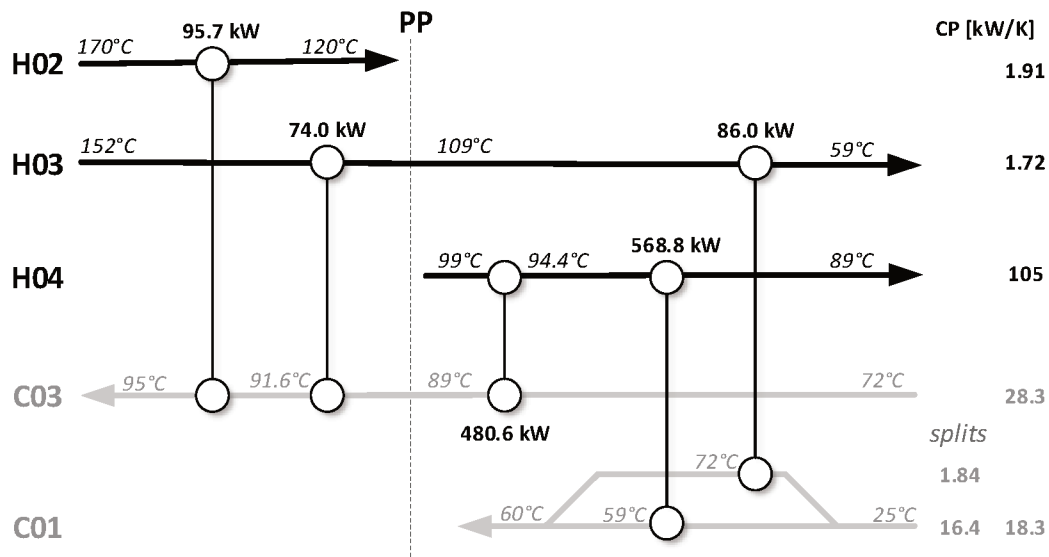


Figure 34 – Matching of heat-supplying and heat-demanding streams in the heat exchange network of the cogeneration module EMC01.

On the left side of the figure are the streams tags that correspond, according to Tab. 15, to the exhaust gases coming from absorption chiller (H02), the hot air stream (H03), the engine cooling water stream (H04); hot gases stream from the generator set (H01) is not present in the network, since it would activate an absorption chiller. Analogously, heat demanding streams are the hot water stream at 95°C (C03) and the warm water at 60°C (C01). On the right side of the figure, there are the specific heat rates of the streams, including for the split done on the stream C01. The network is formed by five exchange units, whose duties are indicated together with the inlet and outlet temperatu-

res of each stream. Note that the sums of these duties on each heat-demanding stream are equal to the values presented previously in Tab. 18.

Once the network is configured, its total heat transfer area is calculated adopting the NTU-effectiveness method (BERGMAN et al., 2011), in which the effectiveness ( $\epsilon$ ) of each heat transfer unit is the ratio between its duty  $\dot{Q}$  and the maximum feasible transfer rate  $\dot{Q}_{max}$ , according to the following relationships:

$$CP_{min} = \min(CP_H, CP_C) \quad (4.20)$$

$$\dot{Q}_{max} = CP_{min} \cdot (T_{H,in} - T_{C,in}) \quad (4.21)$$

$$A = \frac{CP_{min} \cdot NTU}{U} \quad (4.22)$$

$$NTU = f(typ, \epsilon, CP_H, CP_C) \quad (4.23)$$

according to Eqn. 4.21,  $\dot{Q}_{max}$  is the product of the minimum heat capacity rate  $CP_{min}$  and the maximum temperature driving force across each unit. Additionally, the number of transfer units (NTU) is a function of the type of heat exchange selected for each unit (*typ*), its effectiveness and the heat capacity rates of the streams matched (Eqn. 4.23). The calculation of the area was done for each exchange unit in the network of each cogeneration module considered. The type of heat exchanger selected is the same for all the units and corresponds to shell-and-tubes type. Typical values for the overall heat transfer coefficient ( $U$ ) were selected depending on the pairs of fluids exchanging heat in each unit (TOWLER; SINNOTT, 2013); these values are: 0.07 kW/m<sup>2</sup>-K for hot gases—water and 1.20 kW/m<sup>2</sup>-K for water—water exchangers. In this regard, Hewitt and Pugh (2007) mentions that, at first sight, the tradition of ascribing these 'standard values' seems somewhat illogical, but from the point of view of approximate design, it is legitimate to take these values, since in process specifications, the available pressure drop (which affects directly the  $U$  value) normally lie within a restricted range. Computation was done with the aid of the software EES (KLEIN, 1993), Tab. 20 shows the results for the cogeneration modules considered. Particularly, the area of the HEX networks for turbines and microturbines-based modules is determined at the maximum duty of each HEX unit along the ambient temperature profile.

It is important to mention that, considering the sizes of the modules and the fact that the area density of this type of exchangers is greater than 100 m<sup>2</sup> per m<sup>3</sup> (SHAH;

Table 20 – Number of units and total area for the heat exchange networks of modules.

Module	Number of units	Total area, $m^2$
ECM01	5	154.4
ECM02	9	298.4
ECM02*	7	296.0
ECM03	4	215.7
TCM01	1	83.1
TCM02	3	785.1
TCM02*	3	672.7
TCM03	1	230.6
MCM02	3	503.1
MCM02*	3	495.9
MCM03	1	176.8

\* For applications other than hospital.

SECULIC, 2003), the sizes obtained are reasonable. Moreover, taking into account the relationship  $1 - \epsilon = \Delta T_{min} / (T_{H,in} - T_{C,in})$ , which indicates that specifying  $\Delta T_{min}$  for a series of heat exchangers fixes the thermodynamic imperfection of the configuration (HEGGS, 1989), it follows that decreasing this value (20°C for gas-liquid and 10°C for liquid-liquid exchangers) would improve the effectiveness value, but at the expense of an increased transfer area.

## 4.2 TECHNOLOGY SELECTION

### 4.2.1 The Superstructure

As mentioned above, the technology selection problem can be visualized as a set of technologies forming a reducible superstructure, capable of producing a set of required utilities. These technologies are interlinked through energy streams associated with their supply (or demand) of utilities. Figure 35 shows the superstructure modeled in this work; here, the balance of each utility is presented as a gross line where utility streams (arrows) are delivered or received, while each technology is symbolized as a square that receives one or more utility streams, transforms them and delivers to the corresponding balance line. The superstructure is formed by 10 utilities tagged by two capital letters (e.g. NG for natural gas, HW for hot water, etc.) and by 22 technologies tagged using three capital letters followed by two digits (e.g. ECM01 for engine-based cogeneration module, BST01 for *steam* boiler, etc. —see Tab. 21). Note that thermal utilities are ordered from the highest specific exergy (NG) down to the lowest (chilled water–CW).



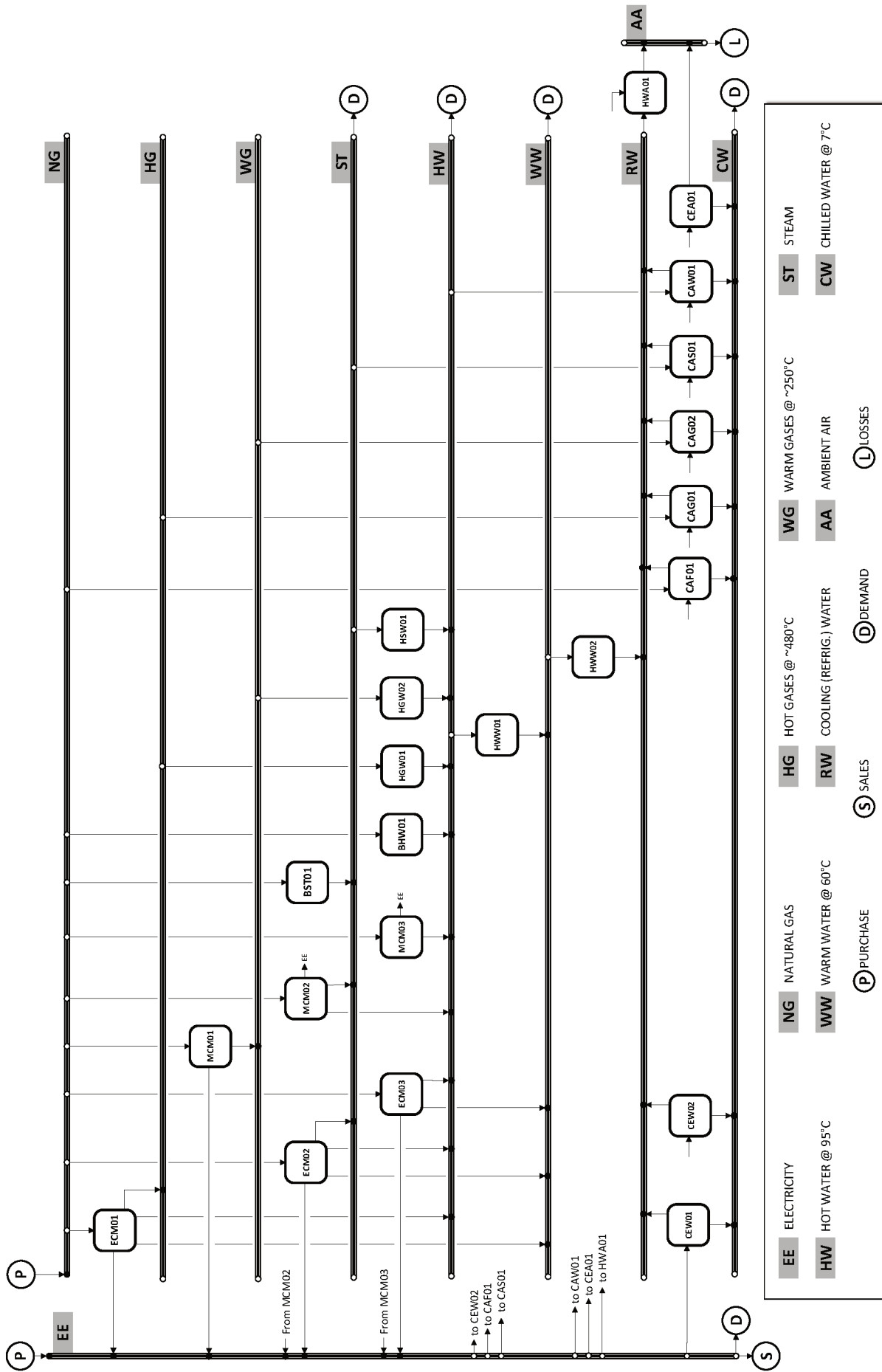


Figure 35 – Superstructure considered for the MILP model.

Additionally, the balance of each utility includes, when applicable, its demand, its exportation (sales), its importation (purchase), and its losses. Considering the goal of the mathematical model, the main inputs related to the utilities are its unitary cost and its sales price. Evidently, these attributes apply only for NG and EE, according to Ch. 2. On the other hand, the magnitude of the utility streams is determined by the operating level of each technology, which in turn, is characterized through technical factors expressing the amount of energy destined, or required, to produce a utility *per unit* of technology output. Table 22 presents the technical factors ( $TF$ ) correlating the feasible pairs technology/utility.

Table 21 – List of technologies considered in the synthesis model.

<b>TAG</b>	<b>TECHNOLOGY*</b>	BK	UVK	UOK
ECM01	Engine-based cogeneration module	0.0	2.106	0.0228
ECM02	Engine-based cogeneration module	0.0	2.292	0.0228
ECM03	Engine-based cogeneration module	0.0	2.156	0.0228
MCM01	Microturbine-based cogeneration module	0.0	2.371	0.0131
MCM02	Microturbine-based cogeneration module	0.0	2.810	0.0131
MCM03	Microturbine-based cogeneration module	0.0	2.531	0.0131
BST01	Boiler, steam	4.8	0.072	0.0005
BHW01	Boiler, hot water	10.3	0.111	0.0003
CEA01	Chiller, electric, air-cooled	39.0	0.279	0.0007
CEW01	Chiller, electric, water-cooled, screw	78.0	0.157	0.0009
CEW02	Chiller, electric, water-cooled, centrif.	186.9	0.116	0.0007
CAF01	Chiller, absorption, direct fired	575.9	0.490	0.0005
CAG01	Chiller, absorption, HG-driven	576.4	0.448	0.0005
CAG02	Chiller, absorption, WG-driven	162.0	0.718	0.0005
CAS01	Chiller, absorption, ST-driven	539.3	0.426	0.0009
CAW01	Chiller, absorption, HW-driven	564.0	0.333	0.0006
HGW01	Heat exchanger, HG→HW	70.9	0.112	0.0000
HGW02	Heat exchanger, WG→HW	70.9	0.185	0.0000
HSW01	Heat exchanger, ST→HW	70.9	0.008	0.0000
HWW01	Heat exchanger, HW→WW	70.9	0.027	0.0000
HWW02	Heat exchanger, WW→RW	70.9	0.027	0.0000
HWA01	Heat exchanger, RW→AA (c. tower)	37.0	0.079	0.0005
AWW01	Accumulator, WW	0.0	0.008	0.0005
ACW01	Accumulator, CW	0.0	0.008	0.0005

\*Names are altered for resembling the capital letters used in corresponding tags.

Table 22 – Technical factors correlating the technologies with the production/consumption of utilities.

TAG	TECHNOLOGY	UTILITIES									
		NG	EE	HG	WG	ST	HW	WW	RW	AA	CW
ECM01	Engine-based module	-3.0811	1.0000	0.4264			0.3455	0.9218			
ECM02	Engine-based module	-3.0811	1.0000			0.4594	0.2193	1.0151			
ECM03	Engine-based module	-3.0811	1.0000				1.6494	0.0441			
MCM01	Microturbine-based module	f(T <sub>0</sub> )*	1.0000		f(T <sub>0</sub> )*						
MCM02	Microturbine-based module	f(T <sub>0</sub> )*	1.0000			f(T <sub>0</sub> )*	f(T <sub>0</sub> )*				
MCM03	Microturbine-based module	f(T <sub>0</sub> )*	1.0000				f(T <sub>0</sub> )*				
BST01	Steam boiler	-1.0870	-0.0002			1.0000					
BHW01	Hot water boiler	-1.0204	-0.0002				1.0000				
CEA01	Air-cooled electric chiller		-0.3226							1.3226	1.0000
CEW01	Water-cooled, screw chiller		-0.1908						1.1908		1.0000
CEW02	Water-cooled, centrifugal chiller		-0.1658						1.1658		1.0000
CAF01	Direct-fired absorption chiller	-0.6622	-0.0056						1.6622		1.0000
CAG01	Hot-gases-driven chiller		-0.0056	-0.7194					1.7194		1.0000
CAG02	Warm-gases-driven chiller		-0.0056		-1.2820				2.2820		1.0000
CAS01	Steam-driven chiller		-0.0029			-0.7194			1.7194		1.0000
CAW01	Hot-water-driven chiller		-0.0003				-1.2500		2.2500		1.0000
HGW01	Heat exchanger, HG→HW			-1.0000			1.0000				
HGW02	Heat exchanger, WG→HW				-1.0000		1.0000				
HSW01	Heat exchanger, ST→HW					-1.0000	1.0000				
HWW01	Heat exchanger, HW→WW						-1.0000	1.0000			
HWW02	Heat exchanger, WW→RW							-1.0000	1.0000		
HWA01	Cooling tower		-0.0087						-1.0000	1.0000	

\* see Tab. 19

Negative factors refer to consumption while the positive ones refer to production of utilities, e.g. values reported for EMC01 (in italics) means that *for each kW* of EE produced, 3.0811 kW of NG are required, while 0.4264 kW of HG, 0.3455 kW of HW, and 0.9218 kW of WW also are produced. On the other hand, heat exchangers within the superstructure enable the energy transfer from higher exergy utilities down to the lowest level, in such a way that—for example—part of the energy from ST produced in a cogeneration module can be transferred to the production of HW. Additionally, heat from utilities produced but not used anyway, can be transferred through this set of exchangers for being finally dissipated through the cooling tower HWA01.

#### 4.2.2 Mixed Integer Linear Programming

In the same terms used by Dantzig and Thapa (1997), the MILP is a special case of the mathematical programming (or optimization theory) concerned with the maximization or minimization of a linear objective function with many variables, continuous and integer, subject to linear (equality and inequality) constraints. The general MILP formulation is presented in Floudas (1995) as

$$\begin{aligned} \min. \quad & c^T x + d^T y \\ \text{s.t.} \quad & Ax + By \leq b \\ & x \geq 0, \quad x \in X \subseteq \mathbb{R}^n \\ & y \in \{0, 1\}^q \end{aligned}$$

where  $x$  is a vector on  $n$  continuous variables,  
 $y$  is a vector of  $q$  binary variables,  
 $c, d$  are  $(n \times 1)$  and  $(q \times 1)$  vectors of parameters,  
 $A, B$  are matrices of appropriate dimension,  
 $b$  is a vector of  $p$  inequalities.

These problems have a combinatorial nature in the domain of  $y$  variables, i.e. each combination of the  $q$  values is an LP subproblem whose solution can correspond, or not, to the global minimum. Consequently, the number of subproblems to solve following the brute-force approach corresponds to  $2^q$ , which is prohibitive in most practical cases. However, despite the complexity given by this combinatorial nature, several algorithmic approaches have been developed and applied successfully to medium and large application

problems. Theory and application of these approaches can be found in references focused on optimization, e.g. Floudas and Pardalos (2014), Dantzig and Thapa (2003). Particularly, this section shows the formulation of the CCHP design problem developed in the present thesis as an MILP problem. Its solution is obtained by using the commercial software LINGO (LINDO SYSTEMS, 2017), which counts with a large set of solving routines for optimization problems, including mixed-integer linear and mixed-integer non-linear models.

Urbanucci (2018) states that MILP is the state-of-the-art approach to tackle the CCHP design problem; according to him, the guarantee of finding global optimality in linear problems and the effectiveness of available commercial solvers make MILP widely used in optimization of CCHP systems. However, the main drawback of this method lies in the impossibility of incorporating nonlinear effects into the model formulation. The most relevant nonlinearities are the performance of devices at partial loads and the variation of the nominal efficiency and unitary cost in relation to the components' size. In this work, this inconvenient is dealt by formulating the optimization problem not in terms of components' size but in terms of the number of components, specifically for cogeneration modules, boilers, and chillers. This approach allows to set their sizes low enough for keeping their operating loads at ranges in which their efficiency does not differ considerably from its nominal value. On the other hand, it is recognized that unitary costs do not have a linear behavior, especially considering that they can be altered by aspects out of the scope of the model (e.g. financing schemes, incentives, etc.). Nevertheless, data collected in this work show certain linear behavior of costs in relation of components' size when they pertain to the same brand. More details can be consulted in Appendix A.

The approach used in this work is adapted from Lozano and Ramos (2010), where the objective of the model is to minimize the annual total costs ( $TK$ ) of the utilities' supply system. This function is formed by two addends: the equipment investment costs ( $IK$ ) and the operation costs ( $OK$ ), as shown in Eqn. 4.24:

$$\text{minimize} \quad TK = IK + OK \quad (4.24)$$

In general terms, the model inputs are the utilities' demands, the applicable tariffs, investment costs and technical data characterizing the candidate technologies. On the

other hand, the model returns the subset of technologies forming the structure capable of obtain the minimum  $TK$  and the number of units of each technology (with fixed size) together with, for each time interval, the supply of utilities by each technology in the optimal structure, the purchase/sale of electricity, and the accumulation of WW and CW. As introduced at the beginning of this chapter, the objective function presented is subject to a series of constraints, grouped as follows:

### Costs Balances

The investment costs corresponds to the product of the annuity factor  $af$ , already obtained in Ch. 2 ( $af = 0.134$ ), and the total investment cost, that is the sum of the capital investment of each technology  $t$  (Eqn. 4.25). It is the annuity destined to amortize the total investment costs along the lifetime of the plant (20 years). As shown in Eqn. 4.26, the investment of each technology is expressed as a linear function of its installed capacity ( $CAP_t$ ). Here,  $BK_t$  is the base cost of each technology (it is the intercept of the linear regression of investment costs vs capacity of each technology),  $Y_t$  is a binary variable used for indicating the presence ( $Y_t = 1$ ) or not ( $Y_t = 0$ ) of each technology, and  $UVK_t$  is the unitary (variable) costs of each technology (it is the slope of the linear regression of investment costs vs capacity). Values of  $BK_t$  and  $UVK_t$  are listed in Tab. 21.

$$IK = af \cdot \sum^T INV_t \quad t \in \{EMC01, EMC02...\} \quad (4.25)$$

$$INV_t = BK_t \cdot Y_t + UVK_t \cdot CAP_t \quad Y_t \in \{0, 1\} \quad (4.26)$$

On the other hand, the  $OK$  is the sum of the operation costs of each typical day  $OK_d$  multiplied by the quantity of occurrences along the year  $QTY_d$  (Eqn. 4.27). The daily costs correspond to the sum of the hourly (average) operating costs  $HOK_{d,i}$  multiplied by the number of hours of each interval  $NH$  (Eqn. 4.28). The average hourly costs takes into account the purchase and the sale of utilities as well as the operating costs of each technology, which is the product of its operating level  $OPR_{i,t}$ —in kW—and its unitary operation costs  $UOK_t$ —in \$/kWh—(Eqn. 4.29). Values of the latter are listed in Tab. 21.

$$OK = \sum_{d=1}^{ND} OK_d \cdot QTY_d \quad d \in \{1, 2, \dots, ND\} \quad (4.27)$$

$$OK_d = \sum_{i=1}^{NI} HOK_{d,i} \cdot NH \quad i \in \{1, 2, \dots, NI\} \quad (4.28)$$

$$HOK_{d,i} = \sum_u^U UK_u \cdot PUR_{d,i,u} - SP_u \cdot SAL_{d,i,u} \quad u \in \{NG, EE\}$$

$$+ \sum_t^T UOK_t \cdot OPR_{i,t} \quad t \in \{EMC01, EMC02, \dots\} \quad (4.29)$$

here,  $ND$  and  $NI$  refer to the number of typical days and the number of intervals in which each day is divided, respectively.  $UK_u$  and  $SP_u$  are the unitary costs and the sales price of the utility  $u$ , respectively, both expressed in \$/kWh. Note that these tariffs can vary in an hour-of-day basis (see Ch. 2) and that the electricity, together with the natural gas are the utilities that can be purchased, while the electricity is the only one that can be sold.

### Capacity and Operation of Components

Initially, the capacity of each technology, expressed in kW, is considered as a continuous variable, in such way that the model returns, besides the set of technologies forming the optimal structure, their installed capacity (Eqn. 4.30a). However, it is well known that the main CCHP components are available as packages of multiple nominal sizes. For this reason, the model is formulated in terms of the number of components of a fixed capacity (Eqns. 4.30b and 4.30c), established according to the value obtained originally using Eqn. 4.30a.

$$Y_t \cdot MIN_t \leq CAP_t \leq Y_t \cdot MAX_t \quad Y_t \in \{0, 1\} \quad (4.30a)$$

$$CAP_t = N_t \cdot UCAP_t \quad (4.30b)$$

$$N_t \leq Y_t \cdot NMAX_t \quad N_t \in \{1, 2, 3, \dots\} \quad (4.30c)$$

here,  $MIN_t$  and  $MAX_t$  are the minimum and the maximum values that bound the computation of the installed capacity (continuous). Values of these parameters are set in such a way that  $CAP_t$  solution does not reach them easily (i.e.  $MIN_t$  low enough and  $MAX_t$  high enough), but determined by constraints related to the supply and demand of utilities. Analogously,  $N_t$  is the number of components,  $UCAP_t$  is the (unitary) capacity of each component, and  $NMAX_t$  is the maximum number of components allowed for each technology (set to 10 units). Note that heat exchangers and accumulators are tailored for

the process requirements, thus their capacity is determined by Eqn. 4.30a. On the other hand, for every time interval, the following inequality must be satisfied:

$$OPR_{d,i,t} \leq CAP_t \quad (4.31)$$

where  $OPR_{d,i,t}$  is the operating level—in kW—of each technology  $t$  during the interval  $i$  of the typical day  $d$ . Particularly for the accumulators, this operating level is equivalent to the amount of utility stored, expressed in kWh.

### Storage of Utilities

The model conceives the thermal energy storage (TES) of WW and CW utilities, since their discharge operation only addresses the building demands, fact that makes their accumulation scheme simpler and more practical than other utilities. Additionally, the method of accumulation considered is the use of thermally-isolated tanks, which is formulated in Eqn.4.32 as a capacity model with a homogeneously distributed temperature (SCHÜTZ; STREBLOW; MÜLLER, 2015):

$$ACC_{d,i,u} = NH \cdot (SIN_{d,i,u} - SOUT_{d,i,u} - LOS^*) + ACC^* \quad u \in \{WW, CW\} \quad (4.32)$$

$$LOS^* = \begin{cases} LF_u \cdot ACC_{d,NI,u} & i = 1 \\ LF_u \cdot ACC_{d,i-1,u} & i \neq 1 \end{cases} \quad (4.33)$$

$$ACC^* = \begin{cases} ACC_{d,NI,u} & i = 1 \\ ACC_{d,i-1,u} & i \neq 1 \end{cases} \quad (4.34)$$

here,  $ACC_{d,i,u}$ ,  $SIN_{d,i,u}$ , and  $SOUT_{d,i,u}$  are amount accumulated (in kWh), the storage input rate (in kW) and the storage output rate (in kW) of utility  $u$  during the time interval  $i$  of day type  $d$ . The energy losses  $LOS$  of the accumulators are considered proportional to the amount of utility stored at the end of the previous interval, expressed through a loss factor  $LF_u$ , which is assumed 0.01 kW per kWh stored ( $\text{h}^{-1}$ ) for both utilities (WIT, 2007). Additionally, since each day type is assessed independently of the others, the cyclic condition is adopted, formulated through Eqns. 4.33 and 4.34, which establishes that the amount of utility accumulated during the first interval of a day type is equal to the last. More detailed studies concerning the modeling of TES consider aspects as the inclusion of inter-period states (KOTZUR et al., 2018b) and the temperature stratification into the



tanks (SCHÜTZ; STREBLOW; MÜLLER, 2015). However, it is expected that results including this cyclic condition does not deviate considerably from those obtained using more sophisticated methods, given that the day-types classification was done according to the daily mean temperature, which induces certain regularity on the thermal utility profiles. On the other hand, the consideration of temperature stratification is common to models focused on TES control schemes, which is out of the scope of the present research.

### Supply and Demand of Utilities

This constraint depends directly on the technical factors determining the supply and the demand of utilities by the technologies in the superstructure. Firstly, each technical factor  $TF_{d,it,u}$  is determined through Eqn. 4.35. For those technologies with constant factors, the value of  $TF1_{t,u}$  is 0. Values of  $TF0_{t,u}$  for these technologies are presented in Tab. 22, while values for  $TF0_{t,u}$  and  $TF1_{t,u}$  for technologies whose capacity depends on  $DBT_{d,i}$  corresponds to the intercept and the slope of linear regressions shown in Tab. 19, respectively.

$$TF_{d,i,t,u} = TF0_{t,u} + TF1_{t,u} \cdot DBT_{d,i} \quad (4.35)$$

General formulation of the total supply/demand—in kW—of the utility  $u$  on the interval  $i$  of the day-type  $d$  is presented in Eqn 4.36. The supply and the demand of utilities by the technologies during each interval are represented by the variables  $SUP_{d,i,u}$  and  $USE_{d,i,u}$  (name chosen for differentiating it from the building demand), respectively. These quantities are calculated as the sum of the products of the operating level of each technology and the corresponding technical factor (Eqns. 4.37 and 4.38). Note the change of sign done in Eqn. 4.38 for expressing  $USE_{d,i,u}$  as a positive quantity.

$$SUP_{d,i,u} + PUR_{d,i,u} + SOUT_{d,i,u} = USE_{d,i,u} + SAL_{d,i,u} + SIN_{d,i,u} + DEM_{d,i,u} \quad (4.36)$$

$$SUP_{d,i,u} = \sum_{t=1}^T OPR_{d,i,t} \cdot TF_{d,i,t,u} \quad \forall TF_{d,i,t,u} > 0 \quad (4.37)$$

$$USE_{d,i,u} = \sum_{t=1}^T OPR_{d,i,t} \cdot -TF_{d,i,t,u} \quad \forall TF_{d,i,t,u} < 0 \quad (4.38)$$

## Current Regulation

The regulation adopted in this work was already introduced in Ch. 2 and its formulation is presented in Eqns. 4.39 through 4.44. The conditions that must be satisfied are expressed in Eqn. 4.39 and 4.40.  $FCON$ ,  $HPRD$ , and  $EPRD$  are the fuel (NG) annual consumption, the heat annual production, and the electricity annual production by cogeneration modules  $\{ECM01\dots MCM03\}$ , all expressed in MWh. Note that  $HPRD$  is formed by the production of thermal utilities HG, WG, ST, HW, and WW and all the production of these utilities that is ultimately dissipated (wasted production— $WPRD$ ) through the cooling tower, in fact is equivalent to the heat transferred by the heat exchanger HWW02 (WW→RW).  $QTY_d$  refers to the quantity of days (ocurrences) of the day-type  $d$  per year.

$$0.15 \cdot FCON \leq HPRD \quad (4.39)$$

$$0.41 \cdot FCON \leq 0.4673 \cdot HPRD + EPRD \quad (4.40)$$

$$FCON = \sum_{d=1}^{ND} \sum_{i=1}^{NI} \sum_{t \in \{ECM01\dots MCM03\}} QTY_d \cdot NH \cdot USE_{d,i,t,NG} \quad (4.41)$$

$$HPRD = \sum_{d=1}^{ND} \sum_{i=1}^{NI} \sum_{t \in \{ECM01\dots MCM03\}} \sum_{u \in \{HG, WG, ST, HW, WW\}} QTY_d \cdot NH \cdot SUP_{d,i,t,u} - WPRD \quad (4.42)$$

$$WPRD = \sum_{d=1}^{ND} \sum_{i=1}^{NI} QTY_d \cdot NH \cdot OPR_{d,i,HWW02} \quad (4.43)$$

$$EPRD = \sum_{d=1}^{ND} \sum_{i=1}^{NI} \sum_{t \in \{ECM01\dots MCM03\}} QTY_d \cdot NH \cdot SUP_{d,i,t,EE} \quad (4.44)$$

## Additional Criteria

The following constraints correspond to decisions that can be altered prior to the model execution in order to configure different scenarios for comparison. The following criteria are included into the model:

1. *Enable/disable sales of electricity:* By setting the binary parameter  $YSAL$  it is possible to disable or enable the electricity sales up to a maximum  $EEMAX$ , which is set to a value high enough for not limiting the result.

$$SAL_{d,i,EE} < YSAL \cdot EEMAX \quad (4.45)$$

2. *Electricity credits*: The annual sales of electricity  $SAL_{EE}$ , in kWh, can be limited in such a way that it does not overcome the annual electricity purchase  $PUR_{EE}$ . This constraint functions as a credit system, since according to Eqn. 4.36, any kWh delivered (sold) by the plant would be discounted from the amount of electricity imported (purchased).

$$PUR_{EE} = \sum_{d=1}^{ND} \sum_{i=1}^{NI} QTY_d \cdot NH \cdot PUR_{d,i,EE} \quad (4.46)$$

$$SAL_{EE} = \sum_{d=1}^{ND} \sum_{i=1}^{NI} QTY_d \cdot NH \cdot SAL_{d,i,EE} \quad (4.47)$$

$$PUR_{EE} - SAL_{EE} \geq 0 \quad (4.48)$$

3. *Enable/disable cogeneration modules*: For not considering the cogeneration modules, simply the binary parameter  $Y_t$  associated with their presence into the structure is set to 0 prior to solving the model. Its solution would correspond to the optimal conventional production.
4. *Enable/disable thermal storage*: Similarly to the previous item, the capacity of accumulator AWW01 and ACW01 are set to 0 prior to the execution of the model.

### 4.3 CLOSING REMARKS

The main purpose of this chapter is to describe and present the formulation of the synthesis model that will be used to identify the technologies forming the optimal structure of each building application introduced in Ch. 3. Furthermore, the model is capable of returning the installed capacity required for each technology, which will be used for setting the size of the devices to be considered into the superstructure. In this way, the model output would be in terms of number of units of each technology (applicable to cogeneration modules, boilers and chillers). Another aspect that can be inferred from the balance of utilities is the basic operation scheme of the plant, since the model returns, for each time interval, the amount of utilities supplied and used by each technology, as well as their accumulation.

The methodology adopted corresponds to an MILP model, which is regarded as the state-of-the-art for the synthesis of energy supply systems. Its objective is to minimize the annual operating costs, subject to a series of constraints related to aspects as the utilities balance, the performance of the technologies and current regulations. Despite there are—in recent publications—more rigorous approaches incorporating non-linearities and environmental targets into the model, even considering the uncertainty on input data,

the present model is regarded as enough for getting a proper design for the building applications considered.

On the other hand, based on a systematic review, the novelty of the model lie in the incorporation of technologies that, although commercially available, are not commonly considered in academic publications focused on the synthesis of energy systems. It is the case of gas turbines, microturbines, direct-fired absorption chillers, hot-gases-driven chillers (taking into account two activation temperature levels), and steam-driven chillers. Moreover, it was shown that the electricity and heat supply derating, caused by the air intake temperature in turbines and microturbines, can be modeled as piece-wise linear functions, suitable for MILP models. Another important aspect covered by the model, that is scarcely explored in works adopting the superstructure approach, is the thermal integration and the configuration of the heat exchange network proper to the cogeneration modules. Particularly here, it was adapted for smaller sizes and for taking into account the eventual use of hot-gases-activated chillers; feasibility regions were constructed (see Fig. 27) for demonstrating the advantages of this approach over the simulation approach.

Evidently, further refinements can be applied to the model as the inclusion, for example, of the on/off status of devices during each interval, their partial load performance (e.g. via piecewise regression), or the minimum load allowed for each technology. However, for including these criteria, with reasonable runtimes, it would be necessary computational resources considerably higher than the currently available to the author.

As it will be shown in the following chapter, the presented model is used, not only for obtaining the optimal solution for each application, but for making sensitivity analyses covering the variation on natural gas tariffs, the annuity factor and the thermal storage extent in the utilities' supply systems.

## Chapter 5

---

# RESULTS AND SENSITIVITY ANALYSES

The objective of this chapter is to organize the key outputs that the synthesis model formulated in Ch. 4 returned for the building applications introduced in Ch. 3. Additionally, multiple sensitivity analyses are carried out in order to verify the suitability and robustness of their optimal structures. Furthermore, a sensitivity analysis involving a Monte Carlo (MC) simulation is proposed for verifying the main premise of this work, i.e. undersized optimal structures, derived from profiles whose best estimation corresponds to large timescales, can address the energy requirements of an existing building, as long as it is complemented with TES.

Firstly, the synthesis model is run letting the capacities of the candidate technologies as continuous variables, i.e. without limitation concerning the availability of predefined sizes, for determining approximately their required capacity. This assessment is done taking into account four scenarios, depending on whether the sales of electricity and inclusion of TES is enabled or not. The purpose is to determine a capacity range that enables the selection of a suitable (and available) size for each technology. Then, the synthesis model is solved with this information and the outputs of interest are presented: (i) the selection of technologies (optimal structures), (ii) the balance of utilities, and (iii) performance parameters.

Once the model is solved for all the building applications considered, a global sensitivity analysis allowing for the effect of two key aspects, the NG tariffs and the weight of investment costs, is performed for verifying the optimal structures obtained by the model, checking the impact of these parameters on the total annual costs (TK), and checking for the most convenient scenario (considering TES/EE sales or not). Analysis of results presented is focused on the hospital building, although the same was done for each of the other cases, whose results are further summarized. With the optimal structure and scenario defined, the optimal operation strategy is presented for two extreme day types (the coldest and the hottest business days) and some insights are exposed for the hospital case.

In regard specifically to the research hypothesis, undersized optimal structures for five timescales larger than one hour are identified. The values chosen for the timescales were already introduced in Ch. 3 and correspond to two sub-daily scales (3 and 12 hours), and three commonly used in the building energy performance assessment (daily, weekly and monthly). These structures will be subject to a sensitivity analysis, based on the generation of random typical profiles using the information gathered from the hospital utilities' supply system.

The methodology proposed for generating the random profiles takes into account the existent correlation between the demand of utilities and the prevailing ambient temperature. For the hospital case, only the cold water demand is considered, although its formulation is general and can be applied to the rest of utilities. Furthermore, the sensitivity analysis considers the incorporation of TES into the structure, varying its share from zero to a value high enough for not limiting the delivery of utilities. Finally, results of this sensitivity analysis are organized and presented, they are focused on the impact of TES share on the total annual costs and the deficit present (if any) in the supply of utilities.

## 5.1 ESTIMATION OF THE INSTALLED CAPACITY OF TECHNOLOGIES

Firstly, in order to get a good estimation of the installed capacity required for each technology, the synthesis model is solved allowing for its calculation as a continuous variable, (see Eqn. 4.30a), i.e. assuming that all the technologies are available at any size required. As shown in Fig. 36, multiple options were considered for each case: (i) sale of electricity and TES enabled, (ii) sale of electricity enabled but TES disabled, (iii) sale of electricity disabled and TES enabled, and (iv) sale of electricity and TES disabled.

At this stage, technologies are grouped according to their function in four categories as follows: (i) CHP modules, (ii) absorption chillers, (iii) boilers, and (iv) electric chillers. Heat exchangers, storage tanks, and cooling towers are not presented, since they are tailored according to each plant. Note that the right half of Fig. 36 corresponds to CCHP, while the left one to conventional technologies. Additionally, the building applications on the upper half are located at cities notoriously colder than those on the lower one.

Each piecewise line in the figure corresponds to an optimal structure and its intercepts with each vertical axis corresponds to the required capacity for each category; in

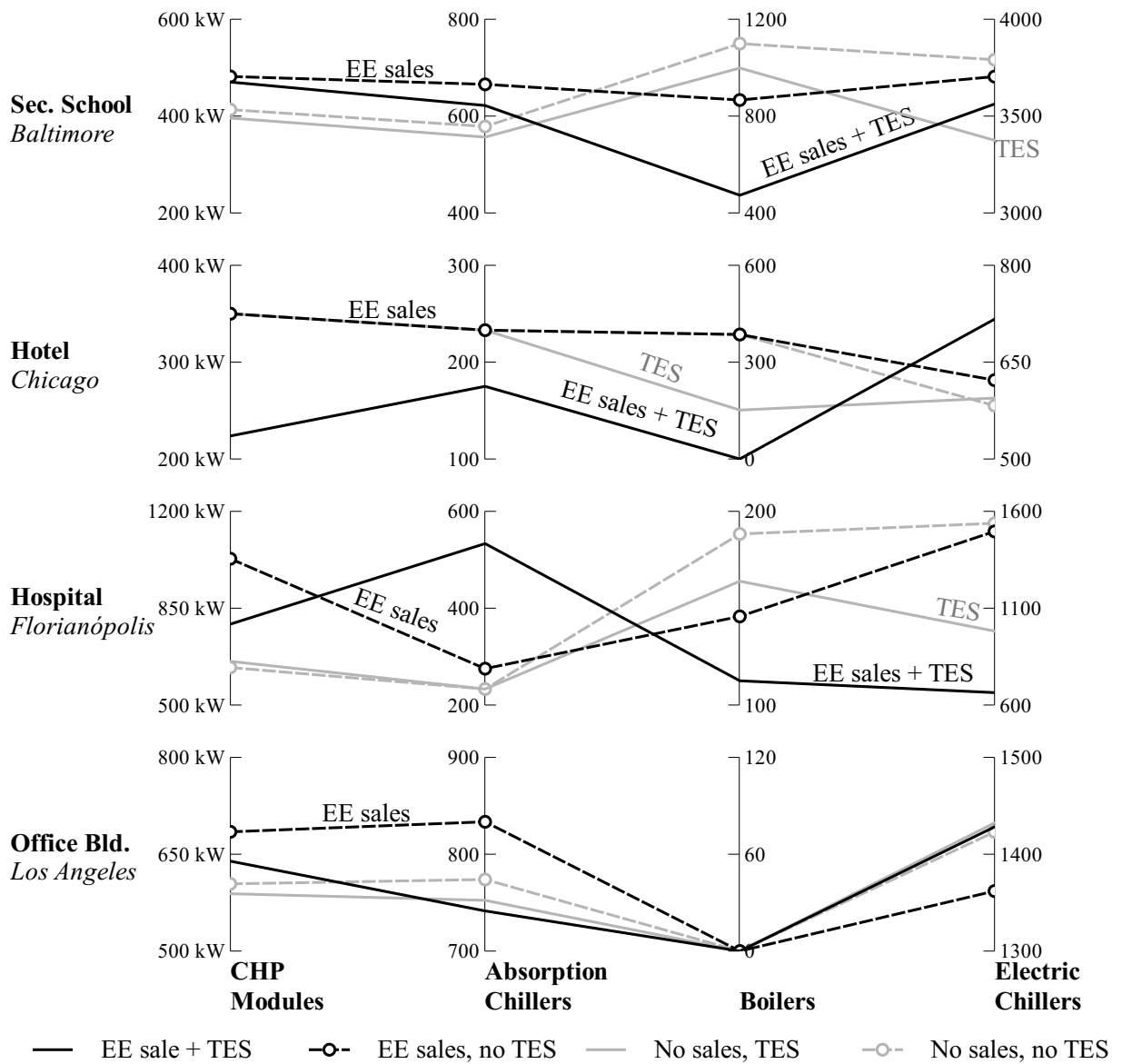


Figure 36 – Installed capacity required for each technology category.

this way, a range of sizes can be identified in each capacity axis. The first observation is that, for all the applications, the implementation of CCHP is considered into the optimal structure. Additionally, there are different features in each building. For example, in the case of the secondary school, it would be clear that the incorporation of TES, independently of enabling the sale of electricity or not, would reduce the size of supplying technologies. However, it would not be the case for the hospital in Florianópolis, where the TES incorporation promotes the increase of absorption chillers' capacity and reduces the size of boilers into the *optimal* structure. Another typical behavior is that the electricity sales promotes the cogeneration share in the supply system. That is evident for all the

applications except for the hotel in Chicago, which has the lowest electricity demand. It is important to remember that, in this work, the sale of electricity is limited to the amount that can be redeemed further (electricity credits scheme).

Based on the capacity range obtained for each category and the sizes commercially available, the unitary capacity  $UCAP$  (see Eqn. 4.30b) of each technology (in each case) is set in such a way that about 2 to 4 units are capable to cover the corresponding capacity range. This approach causes the model to return the number of units—of the chosen size—for each technology forming the optimal structure. The maximum number of units per technology was set at ten, which is high enough to avoid constraining the model solution. Table 23 presents the sizes chosen in each case. Note that sometimes, the unitary capacity was set at the minimum available size of corresponding technology, because of its low requirement. Sizes were chosen considering the information gathered in the appendix A.

Table 23 – Unitary capacity of each technology, for each application.

TAG	Cases Name	Capacity, kW			
		BAL <i>Sec. school</i>	CHI <i>Hotel</i>	FLN <i>Hospital</i>	LAX <i>Office bld.</i>
ECM01	Engine-based module	370	370	370	370
ECM02	Engine-based module	370	370	370	370
ECM03	Engine-based module	370	370	370	370
MCM01	Microturbine-based module	200	200	200	400
MCM02	Microturbine-based module	200	200	200	400
MCM03	Microturbine-based module	200	200	200	400
BST01	Steam boiler	384	142	142	142
BHW01	Hot water boiler	424	111	111	128
CEA01	Air-cooled electric chiller	967	246	545	492
CEW01	Water-cooled, screw chiller	984	280	633	528
CEW02	Water-cooled, centrifugal chiller	950	598	598	598
CAF01	Direct-fired chiller	233	233	233	582
CAG01	Hot-gases-driven chiller	233	233	233	582
CAG02	Warm-gases-driven chiller	233	233	233	582
CAS01	Steam-driven chiller	233	233	233	582
CAW01	Hot-water-driven chiller	352	175	205	512

## 5.2 SYNTHESIS RESULTS

Once the size of each technology unit is defined, the model is solved for determining the number of units of each technology forming the optimal structure. Following sections present the outputs that the model is capable to return. As mentioned previously, the



analysis is focused on the hospital case, since it is the unique configured from actual measurements, and the outputs of rest are presented briefly for comparison purposes. The synthesis considers the four scenarios previously identified in Fig 36.

### 5.2.1 Selection of Technologies

The upper part of Tab. 24 presents the number of units of each technology included into the optimal structure, while the lower part presents the sizes of required heat exchangers (in kW) and accumulators (in kWh). Additionally, the utilization percentage<sup>1</sup> of each technology is presented next to each value.

Table 24 – Technology selection for the hospital case

TAG	Name	EE sale enabled		EE sale not enabled	
		<i>TES</i>	<i>NO TES</i>	<i>TES</i>	<i>NO TES</i>
<i>Number of units</i>					
MCM01	Microturbine module	1 / 82%	1 / 80%	1 / 78%	1 / 74%
MCM02	Microturbine module	2 / 96%	2 / 97%	2 / 85%	2 / 85%
BST01	Steam boiler	2 / 7%	2 / 8%	2 / 7%	2 / 8%
CEW02	Electric chiller	2 / 24%	3 / 16%	2 / 25%	3 / 17%
CAG02	Hot-gases chiller	1 / 67%	1 / 66%	1 / 64%	1 / 61%
<i>Capacity, kW or kWh (accumulators)</i>					
HSW01	Heat exchanger	384 / 47%	384 / 49%	366 / 39%	364 / 40%
HWW01	Heat exchanger	534 / 61%	534 / 63%	510 / 53%	508 / 54%
HWW02	Heat exchanger	428 / 51%	467 / 48%	375 / 43%	439 / 38%
HWA01	Cooling tower	1899 / 48%	2065 / 44%	1807 / 47%	2103 / 40%
AWW01	WW accumulator	267 / 16%	—	267 / 19%	—
ACW01	CW accumulator	1748 / 12%	—	1711 / 16%	—

The optimal structure, for all the scenarios, is formed by microturbine-based CHP modules, including two modules MCM02 producing, besides electricity, the maximum amount of steam, together with one module MCM01 producing hot gases at  $\sim 300^{\circ}\text{C}$  (WG). It is important to mention that, since microturbines are arranged in bundles of various modules of 200 kW (see Appendix A), it can be considered that the supply of two (or more) modules is equivalent to one of 400 kW, with the same features (e.g. technical factors, temperature levels, etc.). Figure 37 depicts the optimal structure found by the model for the hospital case.

<sup>1</sup> The utilization percentage (or factor) is defined as the ratio of the annual utility production—in kWh—and the maximum, at full load all year round.

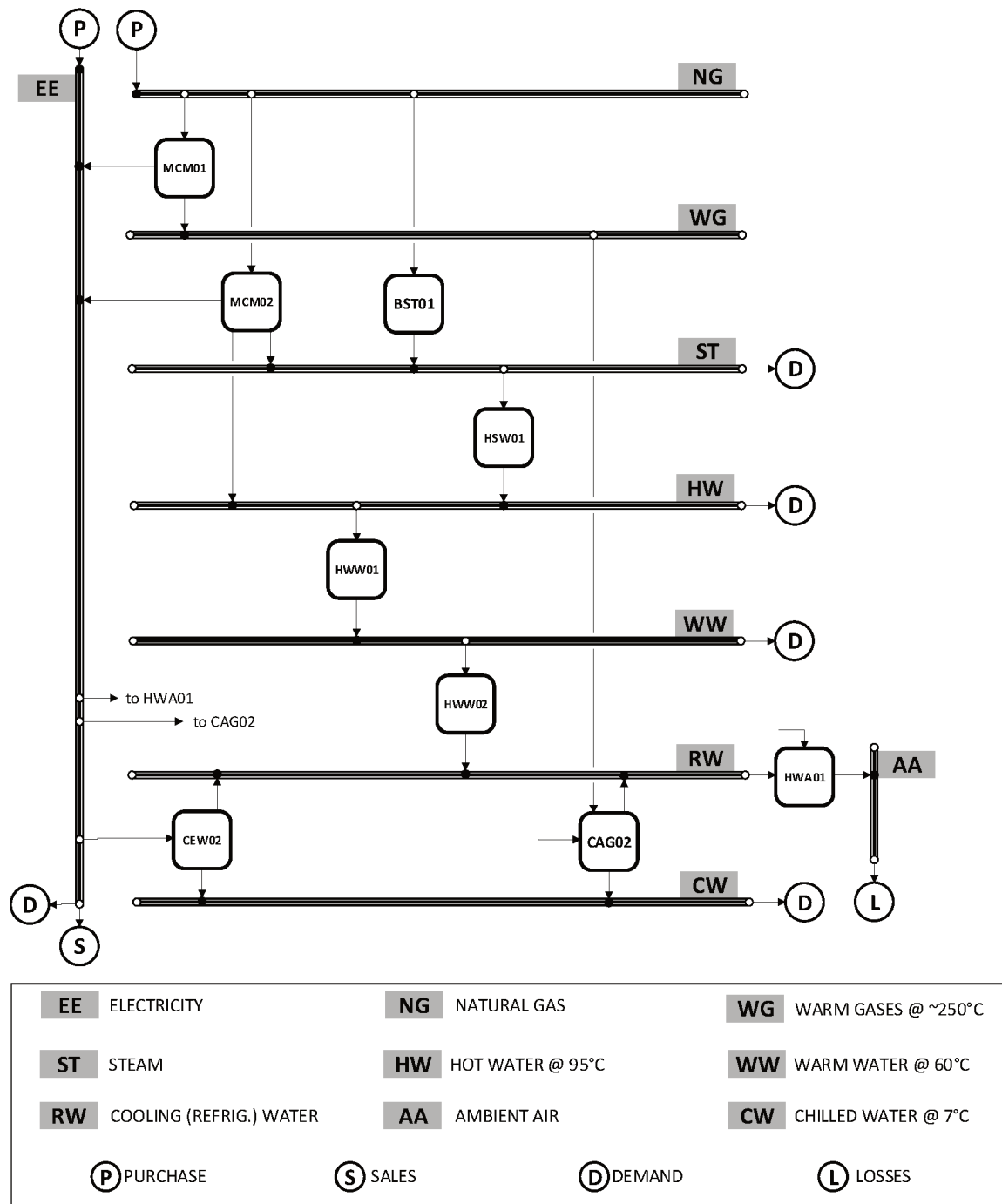


Figure 37 – Optimal structure for the hospital building.

It was found that optimal structures are formed by the same technologies but differing only by the number of electric chillers. When TES is included, there are two electric chillers CEW02 (centrifugal, 598 kW each), but when TES is not included, this number increases by one unit. For all the scenarios, the cogeneration modules are supported by two small boilers (142 kW each) and structures incorporate one absorption chiller CAG02

activated by WG (233 kW each). The presence of the heat exchanger steam-hot water HSW01 indicates that there are moments when part of the steam produced is transformed into hot water, which is used only for producing warm water, since hot-water-driven chillers were not included. On the other hand, water-water heat exchanger HWW02 is used, for all the scenarios, whenever part of the heat recovered from CHP modules must be dissipated, given that the supply of thermal utilities overcomes their demand and the storage is not allowed. Particularly, the latter situation is caused when the amount of utility stored reach the maximum that can be dispatched during the same typical day, due to the *cyclic* constraint (see Ch. 4).

The size required for the thermal storage is greater for cold water, in part because its demand is greater and fluctuates more markedly than the warm water. Looking at the utilization factors, the incorporation of TES favors slightly to the use of the absorption chiller CAG02 (thus, the use of the module MCM01) and reduces the size of heat exchangers on the heat dissipation path (HWW02 and HWA01). Additionally, checking the storage volume ( $V_{tk}$ ) for each tank, using the Eqn. 5.1, tank volumes of about 7 m<sup>3</sup> and 300 m<sup>3</sup> were obtained for warm water and cold water, respectively. These values are considered reasonable for the size of the hospital building.

$$V_{tk} = \frac{3600 \cdot CAP_t}{\bar{\rho} \cdot \Delta h} \quad (5.1)$$

here,  $CAP_t$  is the required capacity of the tank,  $\bar{\rho}$  is the average water density, and  $\Delta h$  is the positive enthalpy difference, both assessed between the supply and return conditions of each utility.

### 5.2.2 Supply System Balances and Performance

Results presented in the previous section serve for identifying which technologies are selected for each optimal structure—recalling that the four configurations obtained are optimal—but defining whether the TES or the sale of electricity are finally considered, or not, requires the comparison of the performance of each configuration. This comparison is based mainly on economic aspects, although the effective use of the resources and the energy efficiency are also relevant. Table 25 presents the parameters of interest used for comparing the scenarios analyzed (basis: one year).

Table 25 – Parameters of interest for the scenarios analyzed in the hospital building application.

TAG	Description	Units	EE sale enabled		EE sale not enabled		Conventional		
			TES	NO TES	TES	NO TES	TES	NO TES	
01	PURNG	Purchased NG	MWh	15079	15118	13660	13508	2764	2764
02	PUREE	Purchased EE	MWh	583	583	465	465	4981	4981
03	SALEE	EE sold	MWh	583	583	0	0	0	0
04	PRDEE	EE produced (net)	MWh	4291	4291	3826	3762	-690	-683
05	NOREC	Heat recovered, not used	MWh	1905	1981	1414	1447	0	0
06	PRDHT	Heat production	MWh	6109	6110	5529	5454	0	0
07	HTCHP	Heat cogenerated (used)	MWh	4204	4130	4115	4007	0	0
08	NGCHP	NG used for cogeneration	MWh	14900	14904	13481	13293	0	0
09	STCNV	Steam produced, conventional	MWh	165	197	165	197	1656	1656
10	HWCNV	Hot water produced, conventional	MWh	0	0	0	0	945	945
11	CWCNV	Cold water produced, conventional	MWh	2524	2535	2600	2631	3917	3882
12	CWABS	Cold water produced, cogenerated	MWh	1376	1346	1306	1251	0	0
13	UTLCW	Heat activating absorption chillers	MWh	1764	1726	1675	1603	0	0
14	$\eta_I$	First-law efficiency		0.590	0.586	0.574	0.570	0.890	0.891
15	$\eta_{th}$	Thermal efficiency		0.282	0.277	0.305	0.301	0.336	0.336
16	ANEEL	ANEEL criteria		0.420	0.417	0.426	0.424	—	—
17	PER	Primary energy rate		0.727	0.723	0.732	0.733	0.752	0.749
18	EEK	Annual EE purchase costs	k\$	-8	0	84	95	943	947
19	NGK	Annual NG purchase costs	k\$	565	567	512	506	104	104
20	OPK	Annual O&M costs	k\$	70	69	64	62	8	6
21	OK	Annual Total operation costs	k\$	627	635	660	663	1054	1056
22	IK	Annual Investment costs	k\$	365	374	364	374	89	104
23	TK	Annual Total costs	k\$	<b>992</b>	<b>1009</b>	<b>1023</b>	<b>1037</b>	<b>1143</b>	<b>1160</b>
24	PBP	Payback period	y	4.5	4.8	4.9	5.1	—	—

Besides the four scenarios already introduced, Tab. 25 is complemented with the conventional (production) scenario, also including the options of incorporating TES or not. The balances of electricity presented in lines 02 through 04 show that the electricity credits scheme enables the annual exportation (and redeem) of about 14% of the total electricity consumed (total: 4291 MWh). Conversely, when this scheme is not adopted, the electricity internal production is restricted and about 11% of the consumption would be purchased. Finally, when the cogeneration is not enabled, it is evident that the purchase of electricity overcomes the building consumption due to the plant feeding (negative figures presented in line 04).

Items 05 through 13 present the balance of thermal utilities taking into account the way they are produced, these values are used for calculating the performance parameters reported later. It should be noted that the incorporation of TES has two main effects on the balance of thermal utilities, independently of the sale of electricity. First, it favors the use of recovered heat in the cogeneration modules, and second, it reduces the share of conventional production of thermal utilities into the supply system. These features also were verified with the results of the other building applications.

Items 14 through 17 presents the energy performance parameters, calculated from the energy balance of the plants. The first-law efficiency and the primary energy rate refer to the whole utilities' supply system, including the production of utilities by auxiliary (conventional) devices. Conversely, the thermal efficiency and the ANEEL criteria refer to the cogeneration of utilities. Although the definition of these parameters was already introduced in Ch. 2, their formulation in the same terms used in Tab. 25 is presented in Eqns. 5.2 through 5.6.

$$\eta_{I,conv} = \frac{SALEE + \overbrace{PUREE + PRDEE}^{\text{NET EE DELIVERED}} + HTCHP + STCNV + HWCNV}{PURNG + PUREE} \quad (5.2)$$

$$\eta_I = \frac{SALEE + PRDEE + HTCHP + STCNV + HWCNV}{PURNG + PUREE} \quad (5.3)$$

$$PER = \frac{SALEE + PRDEE + \overbrace{HTCHP - UTLCW}^{\text{CCHP ST+ HW}} + CWABS}{PURNG + PUREE} + \frac{STCNV + HWCNV + CWCNV}{PURNG + PUREE} \quad (5.4)$$

$$\eta_{th} = \frac{HTCHP}{NGCHP} \quad (5.5)$$

$$ANEEL = \frac{HTCHP}{2.14 \cdot NGCHP} + \frac{PRDEE}{NGCHP} \quad (5.6)$$

As indicated in Eqn. 5.2, the sum  $PUREE + PRDEE$  for the conventional configuration corresponds to the net electricity delivered by the plant, which is equivalent to the building demand. Evidently, it considers that  $PRDEE$  is negative and the electricity purchased covers the hospital and the internal plant consumption, including for electric chillers and auxiliaries. On the other hand, the annual production of ST and HW utilities are not obtained directly, but as the difference between the heat production—effectively used—and the heat destined to the absorption chillers (Eqn. 5.4).

Finally, on the lower part of Tab. 25 there are the main annual costs of the configurations. It should be noted that the negative value of EEK in the first scenario (item 18), when enabling the sale of electricity, correspond to the savings generated by exporting during low-tariff periods and redeeming during high-tariff periods. Considering only the total annual costs, all the structures incorporating CCHP result more interesting than the conventional production of utilities. The lowest operation costs corresponds to the structure obtained from the model enabling the sale of electricity and the inclusion of TES, followed by that enabling the sale of electricity but omitting TES. Evidently, since the optimal structures are very similar, the investment costs does not present significant differences.

The type of information presented in Tab. 25 is useful, for any application project, for the decision-making about the final configuration of the utilities' supply system. Particularly, the simple payback period calculated for the four scenarios, according to the formulation presented in Ch. 2, are between 4.5 and 5.1 years (line 24). Additionally, excluding the conventional production alternative, the margin among the optimal structures is narrow, thus a sensitivity analysis would be helpful for verifying the response of the model to variations on its inputs. The following section introduces the sensitivity analysis, which is focused on the first two scenarios, since these report the least total operation costs, and the fact of disabling the sale of electricity does not seem to have any impact on the optimal structure.

### 5.3 SENSITIVITY ANALYSIS

Basically, the objective of a sensitivity analysis is to determine how the variation on the input information impacts on the model outputs. More specifically, how the change on one of more independent variables alters one of more dependent variables of interest. Through this analysis, it is possible to recognize the divergence of a given output, if the initial model assumptions were different. As mentioned previously, the design of utilities' supply systems involves various quantities subject to important deviations from constant values. Previous publications have been focused on aspects like the fluctuations on utilities' demands (ERNST; BALESTIERI, 2006), the consideration of historical demand peaks (LI; SHI; HUANG, 2008), natural gas and electricity prices (REN; GAO; RUAN, 2008), equipment performance and initial capital costs (YOSHIDA; ITO; YOKOYAMA, 2007), or legal constraints (CARVALHO et al., 2013). Particularly, the sensitivity analysis adopted at this stage of the work is carried out on consideration of the natural gas price and the annuity factor, similarly to the work of Lozano, Ramos and Serra (2010). First, the annuity factor insides directly on the investment costs addend in the model objective function, and by altering this parameter, it is possible to favor (or not) the use of more expensive technologies (CARVALHO, 2011). On the other hand, the natural gas price insides on the operation costs addend, and with a fixed electricity purchase price, varying the natural gas price is equivalent to varying the price relation between electricity and natural gas, which is a key aspect for the adoption of CCHP.

Considering that the purpose of this sensitivity analysis is to check whether the considered structures remain optimal (or close-to-optimal) with the variation of the above-mentioned parameters, the outputs of interest are the structure itself and the annual total costs, i.e. the objective function. The natural purchase price and the annuity factor are modified between -30% and +30% of initial values in increments of 15%, which in combination results in 25 different scenarios, which are solved one-by-one. The results of the sensitivity analysis are exhibited in Fig. 38. The upper part of the figure shows the annual operation costs as a function of the natural gas price variation, each dashed line corresponds to a fixed annuity factor (presented also as a percentage of variation). Additionally, the optimal structures are presented in the lower part of the figure in a convention table.

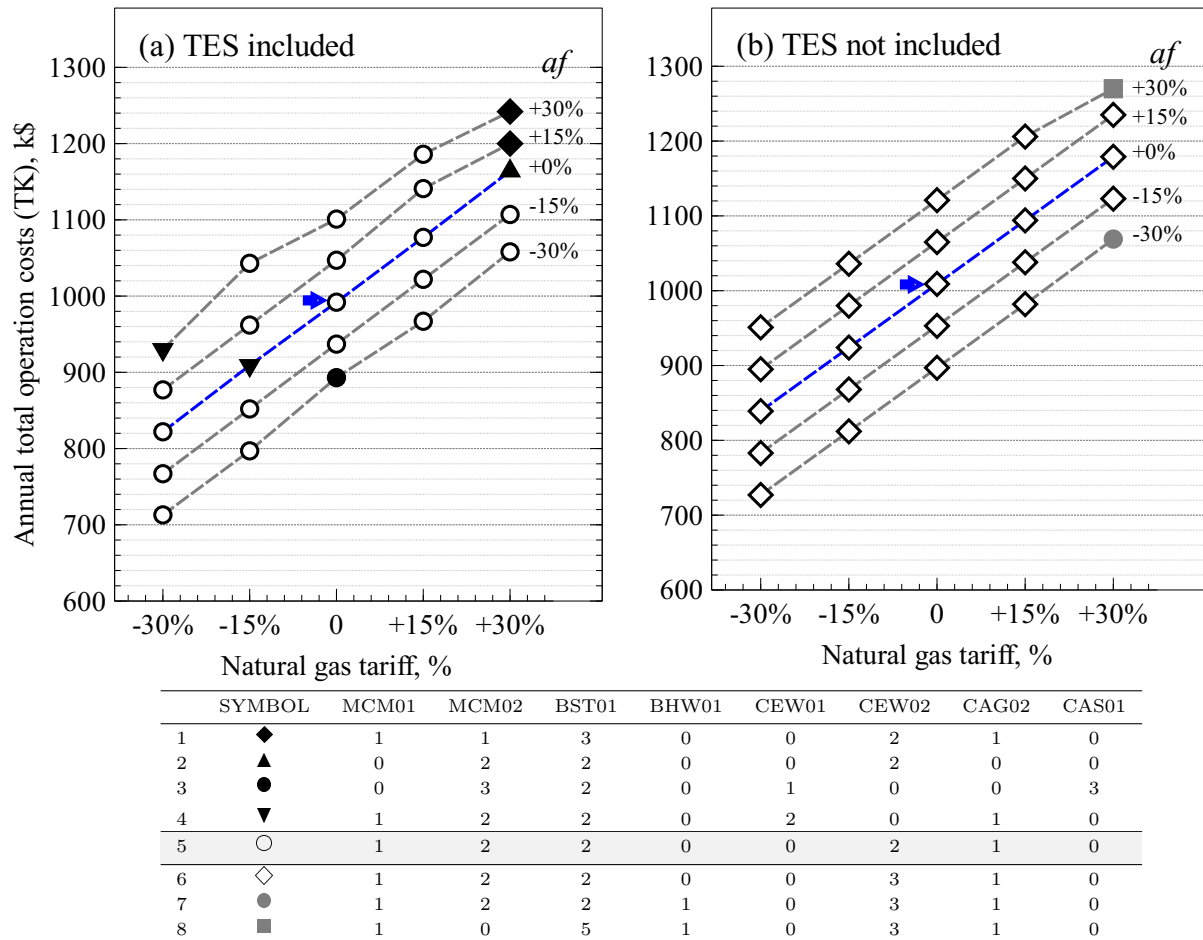


Figure 38 – Results of the sensitivity analysis for the synthesis of the hospital case.

Taking into account both scenarios, there are eight different optimal structures, five enabling TES, shown in Fig. 38a and identified in the upper part of convention table with black symbols, and three disabling TES, appearing in Fig. 38b and identified in the



lower part of convention table with gray symbols. The row remarked corresponds to the structure reporting the lower annual operation costs in Tab. 25.

In general, both optimal structures presented in Fig. 38 (signalized by arrows) remain optimal in most scenarios considered. Moreover, for any given scenario, the annual total operation costs are slightly lower when TES is included into the structure. Except for the extreme scenario of having NG tariffs and an annuity factor 30% greater than those considered originally, and omitting TES (line 8), all the optimal structures obtained favor the use of microturbine-based modules producing the maximum amount of steam. Particularly, just some scenarios with the highest NG tariff (lines 1, 2, 7, and 8) evidence a lesser cogeneration share (given the number of boilers reported in their optimal structures).

When the TES is enabled, there are two scenarios reporting a structure very similar to the original which uses rotary electric chillers CEW01 (633 kW each) instead of centrifugal ones (line 4). Both scenarios correspond to lower NG tariffs, indicating that the lesser operation costs enable the purchase of larger (although less efficient) devices (see Tab. 23). Conversely, on the line of the minimum annuity factor, there is an optimal structure omitting the use of a module MCM01, present in most structures, but including and additional MCM02 module and three steam-driven absorption chillers (line 3). Evidently this option is formed by more expensive technologies than the original.

Finally, according to the analysis done and the information gathered in Tabs. 24–25, the structure judged the most convenient for the hospital corresponds to that remarked in Fig. 38. It was originally obtained for the scenario including TES and electricity exportation. Although it should be mentioned that, excluding TES and including an additional electric chiller would have a low impact on energy and economic performances of the plant. Despite this structure is not robust, it is a highly recommendable alternative.

Similar analyses were carried out for the rest of building cases, whose results are reported in Tab. 26. All the applications include at least one microturbine-based module into their optimal structures, reporting high utilization factors (over 77%), indicating that they operate close to full load during most of the time. As mentioned previously, the small size chosen of these modules (200 kW) favors their implementation, since they fit more easily to the demand profiles and their operation load factors would be higher than for larger sizes.

Table 26 – Technology selection for simulated buildings applications.

<b>TAG</b>		<b>Sec. School</b>	<b>Hotel</b>	<b>Office Bld.</b>
ECM03	Engine module	1 / 44%	—	1 / 60%
MCM02	Microturbine module	—	1 / 99%	—
MCM03	Microturbine module	1 / 82%	—	1 / 77%
BST01	Steam boiler	—	1 / 7%	—
BHW01	Hot water boiler	—	3 / 47%	—
CEW02	Electric chiller	4 / 16%	1 / 51%	2 / 29%
CAS01	Steam-driven chiller	—	1 / 87%	—
CAW01	Hot water chiller	2 / 36%	—	2 / 51%
HWW01	Heat exchanger, kW	887 / 16%	424 / 57%	1098 / 9%
HWW02	Heat exchanger, kW	—	—	1112 / 9%
HWA01	Cooling tower, kW	4474 / 29%	978 / 72%	3331 / 50%
AWW01	WW accumulator, kWh	1767 / 9%	757 / 4%	29 / 25%
ACW01	CW accumulator, kWh	4357 / 14%	983 / 10%	2450 / 21%
$\eta_I$	First-law efficiency	0.696	0.698	0.696
$\eta_{th}$	Thermal efficiency	0.458	0.376	0.396
ANEEL	ANEEL criteria	0.423	0.410	0.461
PER	Primary energy rate	1.19	1.16	0.815
EEK	Electricity costs, k\$	-38	9	-57
NGK	Natural gas costs, k\$	338	252	550
OPK	O&M costs, K\$	66	30	95
OK	Operation costs, k\$	366	290	588
IK	Investment costs, k\$	442	232	477
TK	Total costs, k\$	808	522	1065
PBP	Payback period, y	6.7	6.9	6.3

Particularly for the hospital application, the amount of utilities produced by micro-turbine-based modules would hardly be reproduced only by engine-based modules, since the production of steam per kW of electricity delivered is significantly lesser for the latter. In other words, producing simultaneously the same amounts of steam and cold water (by CCHP) in the optimal structure, would require greater engine sizes, which probably would be limited by the electricity demand and exportation. On the other hand, the selection of only one microturbine module for the hotel building corresponds rather to its low electricity demand, probably choosing an engine-based module would result in a greater investment cost and lesser load factors (thus lesser CCHP efficiency) caused by a greater size.

Conversely, the other two applications, i.e. the secondary school and the office building, present a combination of microturbine-based and engine-based modules, both types producing the maximum amount of hot water. In these cases, the production of hot water

by the optimal structure could be easily obtained adopting modules of only one type of prime mover. However, given the sizes of each technology, the use of a combined scheme fit better than three microturbine-based modules (200 kW each) or two engine-based modules (370 kW each), even though their purchase price is slightly lower than the equivalent microturbine-based modules. On the other hand, the consideration of greater sizes, e.g. modules of 500 kW, probably introduce lower load factors and greater heat waste.

Regarding the energy performance of the structures, only the hotel application appears constrained by the ANEEL criteria (0.41), which indicates that the electricity production is limited in such a way that the amount of heat not recovered (NOREC) remains at the required level; this is reflected in the fact that the acquired credits do not overcome the imported electricity costs (EEK positive). Furthermore, applications with a lower CCHP share report primary energy rates (PER) greater than the unity due mainly to the impact of electric chillers on the second addend of Eqn. 5.4.

#### 5.4 OPERATION STRATEGY

Another key feature of the synthesis model is that it returns the balance of utilities for all the intervals forming each typical day. Since these balances correspond to the minimum annual operation cost, they expose how the utilities' supply system should operate in order to attain it. Nevertheless, it is important to mention that, despite this information is the cornerstone for defining the operation and control philosophies of the plant, there are aspects outside the scope of the model, e.g. startup and shutdown procedures, synchronism between devices supplying the same utility, etc. However, these details correspond to further engineering stages, out from the scope of the present document.

On the other hand, with the amount of utilities delivered for each technology during each interval, it is possible to check diverse aspects as whether there are moments where the load factor is too low, or even whether it is possible to adjust the number of devices. For example, it would possible to replace two small devices reporting high load factors by one with admissible load factors, or conversely, replace one device reporting low load factors by two of smaller size, in such a way that only one device is operated whenever the requirement is too low.

Figure 39 presents the operation profiles for two typical days of the hospital building.

The right side of figure corresponds to a cold business day, while the left side to a hot business day. Here, it is clear the difference on the operation of the plant given the great dissimilarity on the cold water demand and the operation of electric chillers CEW02.

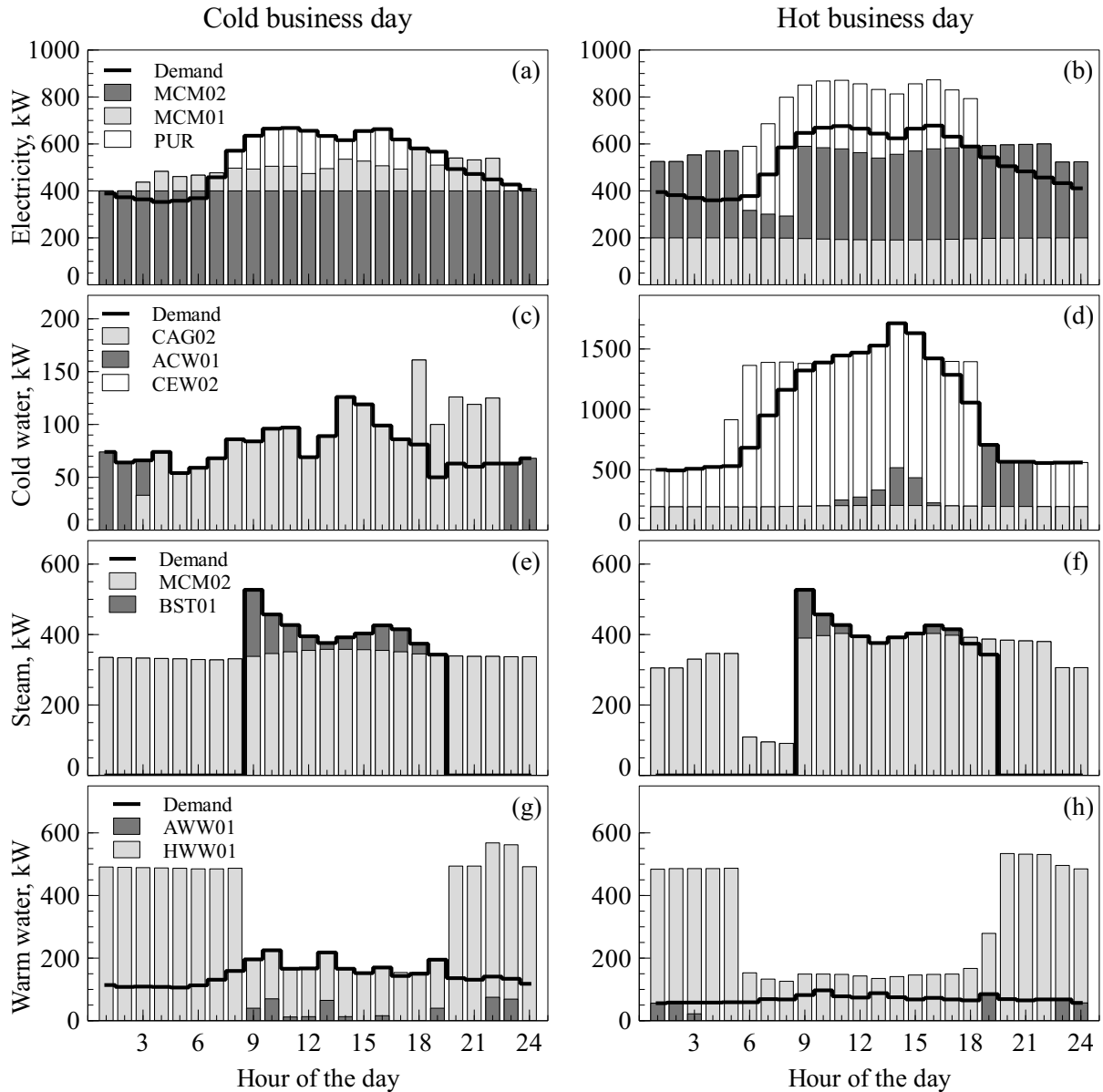


Figure 39 – Supply of utilities for two typical days in the hospital building case.

For the cold day-type, the low cooling requirement makes the electric chillers unnecessary and enables the supply of the electric base load by the modules MCM02 at full load (producing steam) with regulation of the module MCM01 (producing hot gases). Purchase of electricity is necessary during most time between hours 8 and 23 for addressing completely the building demand and the little portion of plant auxiliaries (Fig. 39a). A part of this purchase are credits gained by exporting during off-peak hours, which cor-

respond to the bar portions crossing the demand line. Moreover, regulation of MCM01 is driven mostly by the amount of cold water produced by the absorption chiller CAG02 (Fig. 39b). Looking to this figure, it can be identified that during hours 18 through 22 the chiller CAG02 produces more cold water than that demanded (bar portions exceeding the demand line), which indicates that cold water is being charged into the accumulator ACW01. Conversely, during the lapse between the hour 23 and the second hour of the next day, only cold water from the accumulator ACW01 is consumed (discharged), which causes CAG02—thus MCM01—to shut down.

Regarding the steam production, most of the demand is addressed by steam from the modules MCM02; the rest is provided by steam boilers BST01. All the utility produced overnight is transformed into hot water (HW) through the heat exchanger HSW01 (Fig. 39e). Particularly, the unique use of this utility is producing warm water (WW) through the heat exchanger HWW01, which provides almost all the warm water demand. Note that a small part of the warm water exceeding the demand line would be charged into accumulator AWW01 to be discharged later (Fig. 39g). The rest is transferred to the heat exchanger HWW02 for being further 'degraded' and dissipated through the cooling tower HWA01.

The hot day-type operation is different, specially for electricity and cold water supply. First, absorption chillers CAG02 operates at full load during all the day, which makes the modules MCM01 to operate continuously at their full capacity, now with load regulation on modules MCM02 (contrary to the cold day-type). Moreover, there is a significant increase on the plant internal consumption(chillers and auxiliaries), caused by the operation of electric chillers CEW02 (Fig. 39b). White portions exceeding the demand line are equivalent to the internal consumption of the plant in each interval, while the gray portions crossing the demand line are equivalent to the amount of electricity exported plus the internal consumption, but this time, self-supplied. Clearly, credits gained are then redeemed, which explains the drop on the MCM02 operation during the three hours before the steam demand starts.

On the other hand, during the hours 5 through 9, part of the cold water produced is charged into the accumulator ACW01 for being discharged later (Fig. 39d). Additionally, during the two hours preceding the on-peak tariff (intervals 17 and 18), there is another

charging operation in order to avoid the use of electric chillers (thus the purchase of electricity) during on-peak hours supplying only cold water from the accumulator.

The production of steam and warm water remains almost the same, reflecting the deviations due to the regulation done on modules MCM02 (Fig. 39f). However, given the drop on hot water demand, there are intervals where the discharge of the accumulator displace completely the warm water produced by HWW01, i.e. all the warm water transformed by this device is conducted to HWW02 for being later dissipated (see intervals 19 and 23 through 2 of the next day on Fig. 39h).

## 5.5 OPTIMAL STRUCTURES FOR TIMESCALES LONGER THAN ONE HOUR

One issue already introduced in Ch. 2 is that, for existing buildings, historical energy-use data, specially related to the thermal utilities, are unavailable and when there are records, they are not collected regularly, but for punctual needs (maintenance, operation anomalies, etc.). In that sense, the methodology described in Ch. 3 deals with this issue and was capable to return hourly profiles, in part thanks to the classification of days based on their average temperature and the acceptance of the correlation between hourly electricity consumption and ambient temperature. However, it would not always be the case, in fact it was shown that smaller timescales tends to have poorer correlations, since more random fluctuations are unveiled. For this reason, it is possible that the best approximation obtainable corresponds to longer timescales with reasonable R-squared values. Evidently, this issue does not apply to the forward-modeling approach, since the demand profiles' timestep is defined in the simulation and any fluctuation on a profile can be explained according to the mathematical model. Thus, henceforth only to the hospital case is analyzed, whose profiles were obtained through multiple linear regressions and measurements.

Table 27 presents the synthesis model results considering the timescales presented in Ch. 3. At this point, TES is not included *into the synthesis* model, since it is expected that it would reduce further the size of components and the effect of its inclusion on undersized plants is subject of further analyses. Following the same line of analysis presented so far, the best scenario for all the timescales correspond to that enabling the sale of electricity, although it does not have any impact on the selection of technologies.

Table 27 – Synthesis results using timescales longer than one hour for hospital case.

<b>TAG</b>	<b>Description</b>	<b>3 hours</b>	<b>12 hours</b>	<b>daily</b>	<b>weekly</b>	<b>monthly</b>
MCM01	Microturbine module	1	1	0	0	0
MCM02	Microturbine module	2	1	2	2	2
BST01	Steam boiler	2	2	1	1	1
BHW01	Hot water boiler	0	0	1	1	0
CEW02	electric chiller	3	3	3	2	2
CAG02	Absorption chiller	1	1	0	0	0
$\eta_I$	First-law efficiency	0.597	0.560	0.580	0.582	0.583
$\eta_{th}$	Thermal efficiency	0.309	0.314	0.381	0.381	0.381
ANEEL	ANEEL criteria	0.432	0.426	0.441	0.445	0.446
PER	Primary energy rate	0.759	0.712	0.863	0.842	0.841
EEK	EE purchase costs, k\$	3	226	250	256	254
NGK	NG purchase costs, k\$	572	441	424	423	424
OPK	O&M costs, k\$	69	51	51	50	50
OK	Total operation costs, k\$	645	377	381	383	383
IK	Investment costs, k\$	372	315	251	237	232
TK	Total costs, k\$	1018	692	632	620	615

It is evident that increasing the timescale reduces the number of equipment in the optimal structures, since the apparent requirement of utilities is lesser due to the masking of demand fluctuations. However, except for the optimal structure obtained using the scale of 3 hours, the energy and economic performance parameters do not seem to vary significantly. In other words, there is a leap between values reported for 3-hours-scale and the rest, caused mainly by the disappearance of one cogeneration module from the optimal structure. Clearly, structures other than that obtained from 3-hours-scale, very similar to those presented in Tab. 24, are misleading and it is easily recognized that they correspond to undersized structures.

It is important to mention that the most common issue addressed by works, focused on the timescale used in the synthesis and planning of energy systems, is the increase of the MILP problem dimension when short timescales are considered, e.g. Poncelet et al. (2016), Bahl et al. (2018), Pinto, Serra and Lázaro (2019). Namely, recognizing that the smaller the timescale the greater the number of points forming a profile, it follows that shorter timescales require a larger computational effort. Sometimes, depending on the detail level of the model, it can be excessive, which conduces to what is known as dimension disaster (LI et al., 2010). While the problem of these studies is to reduce a great amount of available data, this work contemplates the possibility of, having a low-

time-resolution data, obtain *foreseen* undersized optimal structures that can be adjusted through further incorporation of TES.

## 5.6 EFFECT OF TES ON UNDERSIZED OPTIMAL STRUCTURES

From the beginning, this thesis suggests the plausibility of designing supply systems using demand profiles estimated through the correlation between electricity consumption and ambient temperature, together with a short-to-medium term measurements of thermal utilities in existing buildings, in which the following premises are met:

1. Historical records of prevailing ambient temperature and electricity consumption are available. Additionally, correlations between time-classified sets are evidenced showing reasonable R-squared values, even if they correspond to timescales larger than one hour.
2. The regularity of the thermal utilities' consumption enables the replication of one-day profiles several times a year, based on the daily average temperature.

Although these conditions are not met necessarily by every building, there may be many cases where they are fulfilled. The problem of this approach relies on the fact that there is a risk of underestimating the utilities' consumption due to low-resolution data, leading to undersized structures. Conversely, use of high-resolution data entails two problems, first—as already mentioned—the high computational requirement in the synthesis models, and second, shorter timescales are more susceptible to randomness, which impairs the data correlation and can lead to high-resolution profiles with a poor demand prediction. Thus, there is a compromise between the detail level used in the prediction of utilities' demands and the effect of randomness on them. On the one hand, the utilities' demand profiles need enough detail for produce structures capable of covering the energy requirements of a building all year round, but on the other hand, the scorekeeping approach (or degree-days method) is considered very approximated and its use is limited to the assessment of the overall energy performance of buildings taking into account daily, weekly, even monthly timescales.

However, in this work it was possible to construct, with a reasonable consistency, a set of hourly profiles using data gathered in a hospital building. They correspond to the



best resolution attainable from the available data, and the most common time resolution used in the literature. Then, an optimal structure is obtained using the MILP synthesis model presented in Ch. 4. However, it is recognized that it may not always be the case, and that the best time resolution attainable could be longer than an hour. In this respect, this thesis assesses the suitability of undersized structures, obtained from low time resolutions, but incorporating TES. Its incorporation is suggested, since it is capable of reducing the operational requirements of utilities-supplying devices.

This assessment is based on the response of the structures, obtained previously for each timescale, to random hourly demand profiles. These profiles were generated from data presented in Ch. 3, taking account their uncertainty and the correlation evidenced with the ambient temperature. Each set of profiles was generated, assuming a normal distribution (GAMOU; YOKOYAMA; ITO, 2002), according to the procedure depicted in Fig. 40 and described in the steps indicated. Note that indexes referring to the day-type ( $d$ ) and utility ( $u$ ) were omitted for simplicity.

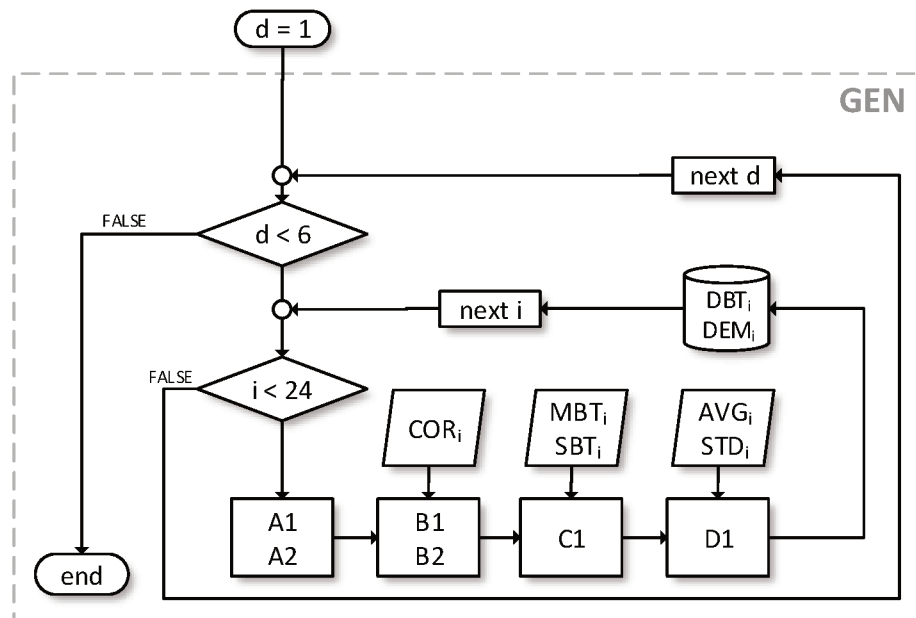


Figure 40 – Flowchart for the generation of random profiles, per utility.

A1. Get a random number  $RND_i$ .  $0 \leq RND_i \leq 1$ .

A2. Get a normal random number  $ZND_i = NORMINV(RND_i)$ .

- B1. Factorize the correlation matrix  $COR_i$  ( $2 \times 2$ ) obtained from the utility demand vs ambient temperature regression. The matrix corresponds to the interval  $i$  of day type  $d$ , see Ch. 3. It is used the Cholesky decomposition method  $L \cdot L^T = COR_i$  (SCIPY, 2015).
- B2. Obtain a normal correlated pair, one element for ambient temperature ( $ZBT_i$ ) and the other for the utility demand ( $ZDEM_i$ ).

$$ZBT_i = ZND \cdot (L_{1,1} + L_{2,1})$$

$$ZDEM_i = ZND \cdot (L_{1,2} + L_{2,2})$$

- C1. Obtain random ambient temperature  $DBT_i = MBT_i + SBT_i \cdot ZBT_i$ , where  $MBT$  is the mean dry bulb temperature of interval  $i$  of day type  $d$ , and  $SBT_i$  is its corresponding standard deviation.
- D1. Obtain random demand  $DEM_i = AVG_i + STD_i \cdot ZDEM_i$ , where  $AVG$  is the utility average demand during the interval  $i$  of day type  $d$ , and  $STD_i$  is its corresponding standard deviation.

On the other hand, for analyzing the impact of TES on each structure, it was set a Monte Carlo (MC) simulation formed by a thousand scenarios, each one corresponding to a random profile. This technique have been already applied in problems of similar nature, specifically the work of Mavrotas, Florios and Vlachou (2010) applied MC simulation combined with a MILP model on the energy planning of a hospital, but on consideration of economic parameters. Resulting optimal structures for the six timescales considered (including that for hourly profile disabling TES) are analyzed. The plant structure is set for each MC simulation, and the model is let to adjust the balances of utilities in each MC scenario, in order to minimize the annual total operation costs (TK). The model itself is based on the model presented in Ch. 4, but disabling the constraints related to the selection of technologies; thus, it corresponds to an LP model. Now, on consideration of TES, the capacity of accumulators is altered from zero to a maximum value, large enough to guarantee the fulfillment of the storage requirements of the plant. Based on previous results, maximum values were set to 1000 and 3000 kWh for WW and CW storage, respectively. The capacities of accumulators are varied simultaneously in steps

of 10% through the relation  $CAP = X \cdot CAP_{max}$ . The scheme for the MC simulations is depicted in Fig. 41, note that the algorithm for the random profile generation, presented in Fig. 40 is embedded into the overall procedure (block GEN).

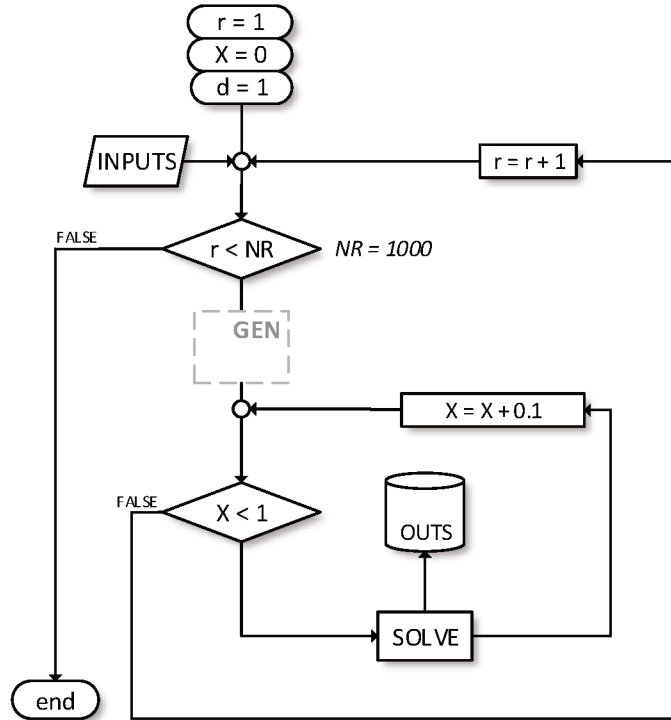


Figure 41 – Flowchart for the Monte Carlo Simulations.

### 5.6.1 Impact on Annual Total Costs

Table 28 presents the results for the sensitivity analysis made on structures obtained using timescales of one and three hours, which were the only ones to get full covering of the hospital requirements in at least one of the MC scenarios. It means that, for timescales greater than three hours none of undersized structures, even with a large TES capacity, was capable to cover the utilities' demand completely in any MC scenario. It is worth mentioning that, despite these structures are formed by the same set of technologies, the heat exchangers and cooling tower of the optimal structure for the timescale of three hours are smaller. The first column correspond to the variation of the TES share into the structures (0-100%), while columns entitled '*% success*' are the percentage of MC scenarios reporting full coverage of demands.

Table 28 – Effect of TES incorporation on the total operation costs.

% TES	1 hour			3 hours		
	%success	TK, k\$	Dev., k\$	%success	TK, k\$	Dev., k\$
<b>0%</b>	<b>10%</b>	<b>1042 ± 25.9</b>	<b>32.83</b>	5%	1097 ± 62.1	88.28
<b>10%</b>	48%	1025 ± 6.9	22.25	35%	1036 ± 11.9	32.96
<b>20%</b>	79%	1024 ± 4.1	22.74	64%	1029 ± 5.6	28.11
<b>30%</b>	93%	1020 ± 1.7	25.26	85%	1023 ± 1.3	27.86
<b>40%</b>	97%	1019 ± 1.5	23.69	94%	1023 ± 2.0	27.97
<b>50%</b>	99%	1019 ± 1.2	27.39	98%	1024 ± 1.6	31.56
<b>60%</b>	100%	1018 ± 1.2	26.25	99%	1022 ± 1.2	29.87
<b>70%</b>	100%	1019 ± 1.1	27.36	100%	1023 ± 1.2	31.22
<b>80%</b>	100%	1019 ± 1.1	26.18	100%	1023 ± 1.2	29.65
<b>90%</b>	100%	1019 ± 1.2	25.67	100%	1022 ± 1.2	28.99
<b>100%</b>	100%	1019 ± 1.1	26.26	100%	1023 ± 1.2	29.65

Note that the first line for the hourly timescale (in bold) corresponds to the same structure presented in Tab. 25 (*NO TES* column) and then analyzed in Fig. 38. Despite it appears as an optimal structure under diverse economic circumstances, the MC sensitivity reveals that in *only 10%* of the MC scenarios, this plant is capable of covering completely the utilities' demands of the hospital. It also becomes evident that, as the TES share increases, the number of fully-covered scenarios also increases up to 100% for both timescales. Moreover, the uncertainty reported on the annual operation costs (TK), diminishes with the increase on the TES share. On the other hand, deviations of the average TK of MC simulations with respect to the optimum obtained by the original model is presented in the column 'Dev.'. Note that, as stated by Mavromatidis, Orehounig and Carmeliet (2018b), results obtained on consideration of uncertainty can differ significantly from those obtained deterministically. In these cases, annual deviations varies between  $\sim 22$  and  $33$  k\$ ( $\sim 2$  and  $3$  k\$ per month) for hourly timescale, and between  $\sim 28$  and  $88$  k\$ ( $\sim 2.5$  and  $7.5$  k\$ per month) for three-hours timescale. Clearly, these deviations are always positive, which means that MC simulations reveal that optimal structures, despite optimal, have a great chance of reporting underestimated results. Apparently, the maximum timescale allowed for obtaining a CCHP design that suffices the energy requirements of the hospital would be three hours, as long as it incorporates TES. However, a closer examination of results can bring insights about the bottlenecks of the design.

### 5.6.2 Deficit in the Thermal Utilities Supply

In spite of the results presented in the previous section, it is possible to check the data obtained from the MC simulations in order to determine the causes of insufficiency for CCHP designs using large timescales. In this regard, Fig. 42 shows the deficit in each thermal utility supply, in terms of its annual consumption (MWh), as function of the TES share in each structure; the heat rejection deficit is also included.

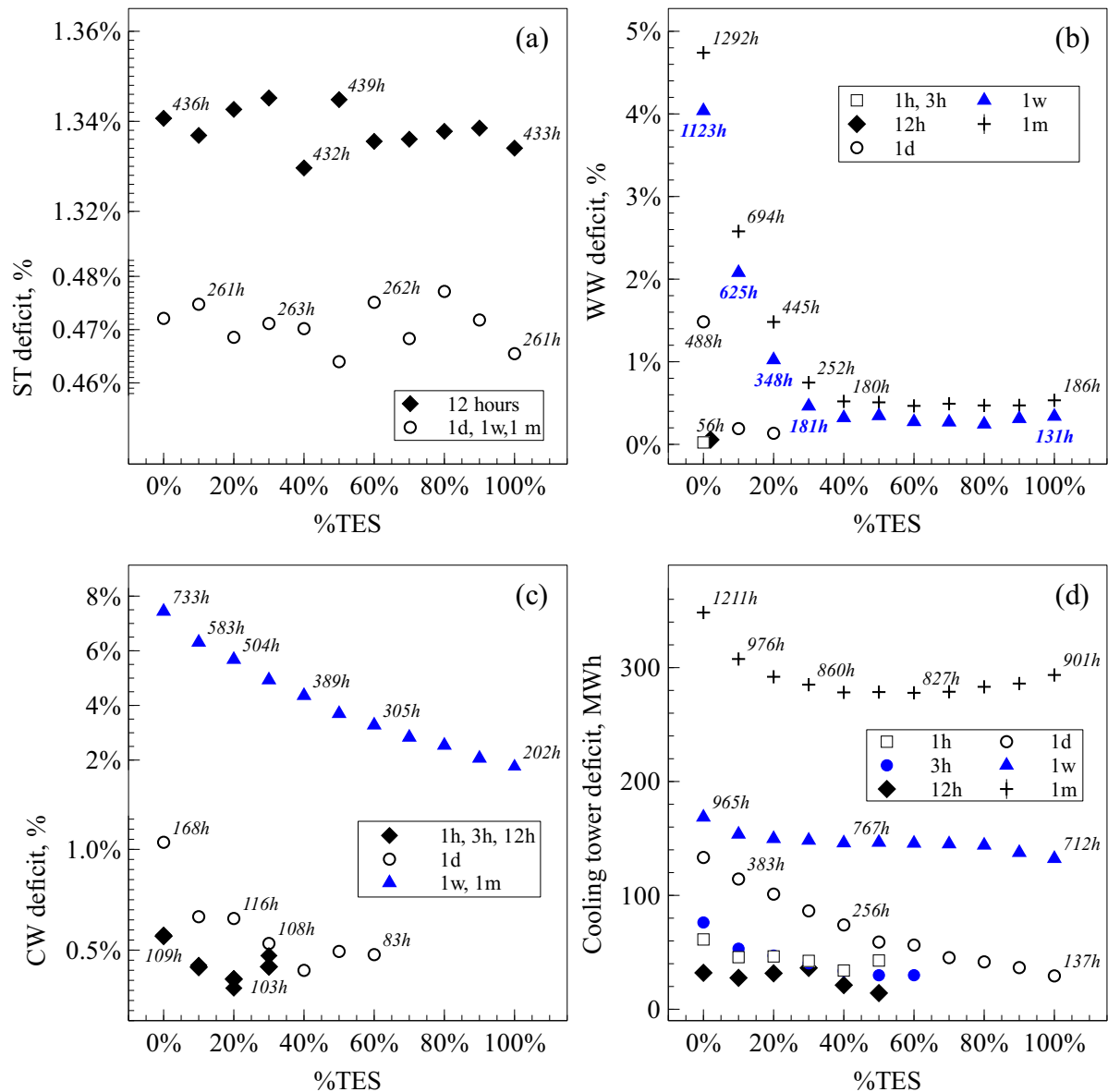


Figure 42 – Deficit in the thermal utilities supply and heat rejection deficit: (a) steam supply, (b) warm water supply, (c) cold water supply, (d) cooling tower capacity.

Each point represents the output of each optimal structure (according to the timescale), with different TES capacity into it. Note that over some points, the average annual

number of hours reporting deficit is displayed. The information presented in Fig. 42 is useful for contrasting the hospital tolerance to work with a reduced supply of each utility. Firstly, all the structures from timescales of 12 hours or superior report a steam deficit for all the MC scenarios, without important variations with respect to the storage of cold and warm water. In any case, the overall deficit does not overcome 1.5% of the steam consumption and  $\sim 440$  hours (about 12% of the working hours). While for the 12-hours timescale the deficit is caused by the reduction of one MCM02 module, for larger scales it is caused by the reduction of one steam boiler, which having a smaller size, makes the deficit lesser (less than 0.5% of consumption during  $\sim 7\%$  of time).

Regarding the warm water (WW), for the two smallest timescales, less than 6% of MC scenarios report a little deficit when no TES is included. On the other hand, a storage capacity over 200 kWh (20% TES) is capable of making the structure obtained with a daily profile to cover the building demand completely. Conversely, although the TES incorporation reduces significantly the chance and the magnitude of WW deficit, reported by structures derived from the two largest timescales, this strategy is insufficient for covering the demand completely. The best results correspond to a deficit of  $\sim 0.5\%$  of total consumption during 131 hours (about 1.5% of total).

The behavior of the cold water (CW) deficit shows something similar although, as it will be shown later, the chance of getting CW deficit is greater. While the three smallest timescales report a maximum CW deficit of  $\sim 1\%$ , the weekly and monthly timescales report CW deficit between 2 and 8%. Furthermore, a storage capacity of 1800 kWh is enough for aiming the optimal structure of the daily timescale to cover the CW requirements completely; the requirement for structures from smaller timescales is about 900 kWh. On the contrary, the best results for larger timescales, with the maximum TES capacity allowed, are a deficit of  $\sim 2\%$  during 202 hours ( $\sim 3\%$  of required time).

Taking into account only the deficit on the utilities' supply, it seems that, except for the steam, the TES incorporation aids to reduce the deficit reported by the undersized structures, even down to sufficiency (only for daily and smaller timescales). Evidently, considering just the supply of utilities, the steam appears as the main cause of insufficiency of the structures, given that its storage is not considered. However, the aspect that is limiting the structures' sufficiency more significantly is the deficit on the heat rejection

capacity. In fact, only a TES share over 60% is capable of guarantee sufficiency in this aspect, and only for timescales of 12 hours or less. In spite that the increase on TES size reduces the heat rejection deficit, this is not enough for attain sufficiency in the structure derived from daily profile. The best result in this case is a deficit of about 32 MWh during 137 hours ( $\sim 1.5\%$  of time); larger timescales are far from sufficiency, reporting deficits of over 150 MWh. Finally, except for the steam, which is not stored, the deficit conditions that have the greatest chances of occurring are the cold water supply and the heat rejection. Figure 43 shows the number of failed MC scenarios (i.e. reporting deficit) taking into account these conditions.

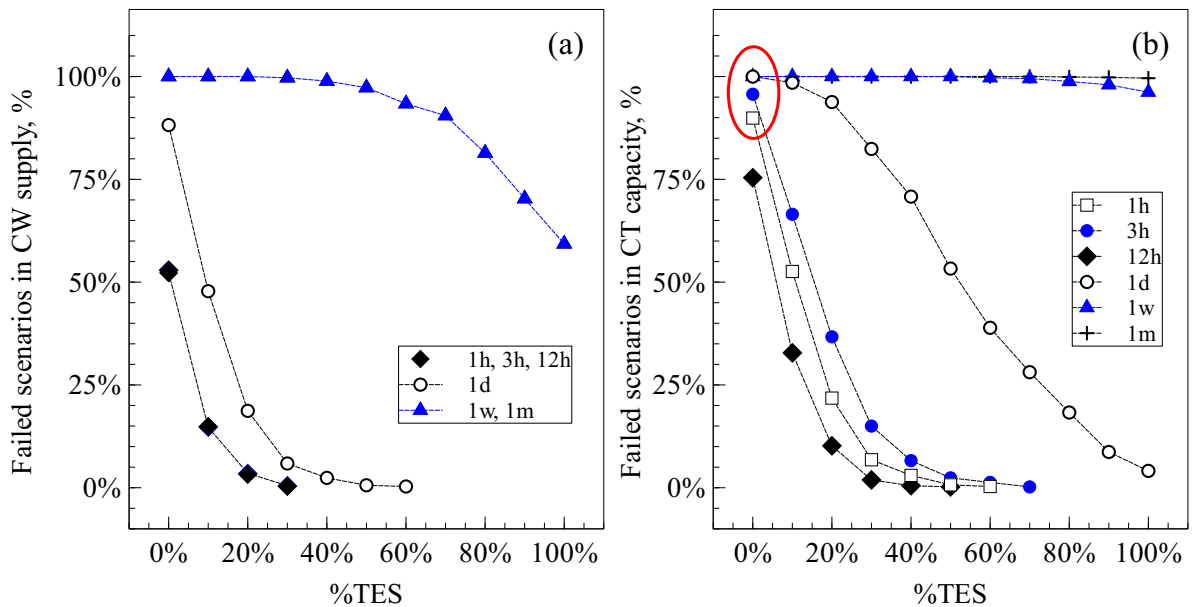


Figure 43 – Number of failed (deficit) scenarios: (a)CW deficit, (b)Heat rejection deficit.

Firstly, the number of failed scenarios in which there is a deficit of CW supply drops significantly with the increase of TES capacity down to zero for daily timescale or lesser. Conversely, the best results achieved for larger timescales is reported for about 50% of the scenarios. On the other hand, the heat rejection deficit is more frequent and, for the daily timescale, it only achieved 0.41% of occurrences with the maximum TES capacity allowed. Furthermore, the heat rejection is the aspect that explains the low percentage of succeeding scenarios in Tab. 28 when TES is not allowed (marked with an oval); curves for hourly and three-hours timescales in Fig. 43 are the complement of '*%success*' column in Tab. 28.

## 5.7 CLOSING REMARKS

This chapter has presented the outputs that the synthesis model is capable of returning according to the utilities' demand profiles introduced in Ch. 3, together with the constraints governing the synthesis problem presented in Ch. 4. It was evidenced that the model is capable of returning different sets of technologies forming the optimal structure in each case. Additionally, a series of steps were conducted for getting a reasonable design. Firstly, except for heat exchangers and accumulators, the size of each piece of equipment is determined accordingly to the capacity required and its market availability, in such a way that the optimal number of pieces can be determined by the model. The inclusion of microturbines was common in all the optimal structures, in part because their small size fits easily to demand profiles, and because their technical factors are higher for individual thermal utilities (i.e. steam and warm gases).

Four design scenarios were contemplated according to the inclusion of TES and the sale of electricity. It was evinced that these both choices aid to reduce the total operation costs, the former reducing the number (thus, the production) of electrical chillers in the optimal structures, and the latter by reducing the purchase of electricity. However, the margin of choice is small, since the energy and economic performance parameters are very close among the scenarios; e.g. payback periods for the hospital building are between 4.5 and 5.1 years.

Optimal structures obtained in each building were subject to sensitivity analyses based on key parameters whose values are uncertain. The natural gas tariffs and the annuity factor are varied  $\pm 30\%$ , showing that for most of the cases, optimal structures are not altered. Based on these results, the set of devices corresponding to the inclusion of TES and electricity sales is presented for each building case. Additionally, for the hospital case, the optimal balance of utilities is presented for illustrating its basic operation schedule; the cold water demand and the utilization of electrical chillers have a strong influence on the way the plant should be operated.

Regarding the hypothesis implied in the method used for obtaining optimal structures using profiles estimated from data correlations, it is recognized that not always the best results correspond to an hourly profile and that larger timescales result in undersized optimal structures. Thus, the suitability of TES for solving the supply limitation of these



structures is assessed through a new sensitivity analysis involving hourly random profiles, generated from the same data used initially for estimating the utilities' load profiles. Evidently, this analysis is focused on the hospital case, which correspond to an actual data-driven model.

Only the hourly and the three-hours timescales, whose resulting structures are practically the same, report full coverage of utilities. Additionally, it was identified a positive deviation from their minimum annual total cost, indicating that, without considering randomness on the demand profiles, their objective function can be underestimated. Unexpectedly, optimal structures without TES report a low probability of coverage (maximum 10%), in spite of the fact that they remain optimal under varying economic conditions (NG tariffs and annuity factor).

Larger timescales reported deficit in the thermal utilities' supply, which is presented as function of TES share for identifying bottlenecks. Firstly, for 12-hours and larger timescales, the first limitation comes from the steam supply, which is not stored. However, the maximum deficit does not overcomes 1.5% of total steam consumption, reported for up to 12% of time. Additional studies can be conducted for determining whether the hospital can tolerate this deficit, or even for reducing its steam consumption. On the other hand, without considering the steam, the storage of cold and warm water reduces significantly the deficit of these utilities, even to attain full coverage for daily or smaller timescales.

In addition to the deficit on thermal utilities demand, there is another key aspect that limits the coverage of the structures that corresponds to their heat dissipation capacity. In fact, this aspect seems, together with the steam deficit, to be the most restricting. Despite TES reduces clearly the heat dissipation requirement of the structure, it is necessary a high TES capacity to reach a full coverage for daily or smaller timescales. In general, optimal structures obtained from weekly and monthly timescales do not report full coverage, even with a high TES capacity.

The deficit on heat dissipation also explains the low probability that the optimal structure without TES has for full coverage, i.e. the greater the TES share the greater the probability of addressing the utilities' demand completely.

## Chapter 6

---

# CONCLUSION

The inclusion of TES into the optimal structures, obtained using timescales larger than one hour, in the definition of the utilities' demand profiles for the hospital building, has demonstrated two key benefits. Firstly, it increases the chance of covering the utilities' demand completely, even for the optimal structure obtained using an hourly profile. Secondly, since it reduces the utilities' supply system requirements, it mitigates the deficit reported by the structure, specially for those utilities that are stored. Particularly, omitting the steam supply—whose storage is not conceived—structures obtained using timescales of 12 hours or less can meet the utilities' demand satisfactorily through the implementation of TES. Otherwise, if the steam supply is considered, only structures derived from three-hours timescale or less can guarantee full coverage. Nevertheless, the optimal structure obtained using daily profiles could report full coverage, but for a small limitation (about 20 MWh a year) on its heat dissipation capacity. Concerning this last issue, the size of the cooling towers appears as the bottleneck for making undersized structures aided with TES to attain full coverage. Finally, structures derived from weekly and monthly profiles does not report sufficiency in spite of the incorporation of TES.

In general, there is no evidence that these results can be replied in other building applications, but they show that—in some extent—the inclusion of TES into a CCHP design beforehand, can reduce the needs of data gathering before its synthesis, without a significant divergence from its optimal outputs. In other words, the consideration of TES can save cost and time destined to activities focused on data collection for a CCHP design project in an existing building. Clearly, as mentioned before, the methodology proposed applies for buildings with high regularity in their thermal utilities' demands and with certain correlation between their electricity consumption and the ambient temperature.

Additionally, the method exposed addresses problems that are common in non-academic CCHP projects, once the CCHP design problem is characterized, the premises adopted in this type of projects are presented, and the limitations of the simulation approach are illustrated in Ch. 2. This diagnosis was supported by the development of a

computational tool—introduced in Appendix B—where the author had the opportunity of interacting with various CCHP specialists. In general, it was found a great gap between the academic literature and the engineering practice.

On the other hand, the adaptation of the Princeton score-keeping method for timescales lesser than a day, resulted suitable for elaborating hourly demand profiles, consistent with the hospital routine. In this way, the full characterization of the energy use of this building was completed through the indirect measurement of the steam and hot water demands during some days along the year. Then, a classification (clustering) algorithm enabled the definition of a set of typical days, based on the average ambient temperature and the electricity consumption level. This procedure was replied to three additional building applications with different consumption patterns and climatic conditions.

Demand profiles created in Ch. 3 are input into a synthesis model whose formulation is described in Ch. 4. This model corresponds to a MILP model, which is the approach most widely used for CCHP synthesis in the academic literature. It is characterized by considering the maximum heat production of cogeneration modules based on internal combustion engines, gas turbines, and microturbines of small-to-medium sizes. Furthermore, it includes the effect of ambient temperature on the supply of the two latter, which could be modeled through linear piecewise functions. Additionally, it takes into account the heat transfer area into the investment cost of the cogeneration modules and incorporates unusual CCHP technologies such as hot-gases-driven and direct-fired absorption chillers into the synthesis superstructure.

The synthesis results have shown that the model is capable of returning different CCHP structures, based mainly on microturbine-based and engine-based modules producing, besides electricity, the maximum amount of steam and hot water. Different scenarios were assessed, indicating that the exportation of electricity and the inclusion of TES aid to reduce the total annual cost of the optimal structures, for all the buildings considered. A Sensitivity analysis varying the annuity factor and the natural gas tariffs  $\pm 30\%$  does not present significant changes in the optimal structures, but except for extreme values. On the other hand, a further sensitivity analysis, now considering different timescales, demonstrates that scales longer than one hour results in undersized but similar CCHP structures.

Finally, a procedure is introduced for generating random demand profiles taking into account the uncertainty present in the data used in Ch. 3 and their correlation with the ambient temperature. This procedure is used to make a new sensitivity analysis, based on a Monte Carlo simulation, which enables the quantification of the chance that these undersized CCHP structures—now complemented with TES—have for covering the hospital utilities’ demands. Moreover, the utilities’ supply deficit also is quantified in order to determine the bottlenecks of these structures. Particularly, through this analysis it was possible to verify a feature already mentioned in the recent literature, that pinpoints the fact that not considering the uncertainty inherent to the utilities’ demand profiles tends to underestimate the total annual cost.

## 6.1 FURTHER WORKS

Evidently, the method used for the synthesis and further sensitivity analyses made for the hospital could be extended to other applications, such as hotels, malls, even residential buildings, in order to corroborate the insights of this thesis. In fact, further studies are necessary for determining/estimating the size of TES that, with limitation on data availability, would guarantee full coverage according to the timescale used for design. Additionally, other intermediate scales can be included, for example two-hours, four-hours, and eight-hours, since here it was found that scales longer than a day, would hardly attain full coverage by implementing TES.

Regarding the synthesis model, it would be interesting to incorporate high temperature storage and electric batteries (or other electricity storage systems). These devices were not considered in the present thesis, since these technologies presents challenges (nonlinearities and delays) for modeling their charge/discharge duration and rates within the MILP model. Another possible improvement, common to this type of models, is to incorporate (i.e. to model) aspects such as the partial load operation of main components, their minimum load factor, or their on/off status, without compromising the runtime of the model.

## BIBLIOGRAPHY

- AL-MOUSSAWI, H.; FARDOUN, F.; LOUAHLIA, H. Review of tri-generation technologies: Design evaluation, optimization, decision-making, and selection approach. *Energy Conversion and Management*, Elsevier Ltd, v. 120, p. 157–196, 2016. ISSN 01968904. Available at: <<http://dx.doi.org/10.1016/j.enconman.2016.04.085>>.
- AL-MOUSSAWI, H.; FARDOUN, F.; LOUAHLIA, H. Selection based on differences between cogeneration and trigeneration in various prime mover technologies. *Renewable and Sustainable Energy Reviews*, Elsevier Ltd, v. 74, n. February, p. 491–511, 2017. ISSN 13640321. Available at: <<http://linkinghub.elsevier.com/retrieve/pii/S1364032117303015>>.
- ANEEL. *Normative 235 10/2006 (in portuguese)*. 2006. 5 p.
- ANEEL. *Normative 414 09/2010 (in portuguese)*. 2010. 205 p.
- ANEEL. *Normative 482 04/2012 (in portuguese)*. 2012. 32 p.
- ANEEL. Module 3: Access to the distribution system. In: *Procedures for the distribution of electricity in the National electric system - PRODIST*. [s.n.], 2016. Available at: <<http://www.aneel.gov.br/>>.
- ANEEL. *The electricity market (in portuguese)*. 2019. Available at: <<http://www.aneel.gov.br/mercado-de-eletricidade>>.
- ARESC. *Current Tariffs (in portuguese)*. DOESC 21046, 2019. 9 p. Available at: <<http://www.scgas.com.br/uploads/editores/20190702104819.pdf>>.
- ASHRAE. *ASHRAE Handbook - Fundamentals*. Si. Atlanta: ASHRAE, 2013. 926 p. ISBN 9781936504466.
- ASHRAE. *ASHRAE Handbook HVAC APPLICATIONS*. Atlanta: ASHRAE, 2015. ISBN 9781936504947.
- ASHRAE. *Combined heat and power design guide*. Atlanta: ASHRAE, 2015. 351 p. ISBN 9781936504879.
- ASHRAE. *ASHRAE Handbook HVAC Systems and Equipment*. Atlanta: ASHRAE, 2016. ISBN 6785392187.
- ATH. *Advanced Thermal Hydraulics Trade Price Book*. 2014.

- Babcock and Wilcox. *Steam its generation and use*. 41. ed. Barberton: [s.n.], 2005. 1–1106 p. ISBN 0963457012.
- BADAMI, M. et al. Energetic and economic assessment of cogeneration plants: A comparative design and experimental condition study. *Energy*, Elsevier Ltd, v. 71, p. 255–262, 2014. ISSN 03605442. Available at: <<http://dx.doi.org/10.1016/j.energy.2014.04.063>>.
- BAHL, B. et al. Typical periods for two-stage synthesis by time-series aggregation with bounded error in objective function. *Frontiers in Energy Research*, v. 5, n. January, p. 1–13, 2018. ISSN 2296598X.
- BALESTIERI, J. A. *Cogeneration: combined generation of electricity and heat (in portuguese)*. Florianópolis: UFSC, 2002. 279 p.
- BARRERA, J. E.; BAZZO, E. Exergy analysis of a multipurpose CCHP layout based on natural gas engines for application in the tertiary sector. In: *17th Brazilian Congress of Thermal Sciences and Engineering*. Águas de Lindóia: ABCM, 2018. p. 6.
- BASSHUYSEN, R. van; SCHAFFER, F. (Ed.). *Internal Combustion Engine Handbook*. Warrendale: SAE International, 2002. 811 p. ISBN 9780768071962.
- BAZZO, E. *Steam Generation (in Portuguese)*. 2. ed. Florianópolis: UFSC, 1995. 216 p.
- BEJAN, A.; TSATSARONIS, G.; MORAN, M. *Thermal design and optimization*. 1. ed. New York: Wiley, 1996. 542 p. ISBN 0471584673.
- BERGMAN, T. L. et al. *Introduction to heat transfer*. 6. ed. Jefferson City: Wiley, 2011. 962 p. ISSN 1098-6596. ISBN 9788578110796.
- BIZEE. *Regression Analysis - Correlate Energy Consumption with Degree Days*. 2019. Available at: <<https://www.degreedays.net/regression-analysis>>.
- Brazilian Parliament. *Decree 5163 July 30 2004 (in Portuguese)*. 2004.
- BROAD. *Catalog of IX absorption chillers*. 2004.
- BROAD. *Model Selection & Design Manual*. 2008.
- Building Technologies Office. *EnergyPlus*. 2019. Available at: <<https://energyplus.net/>>.
- CAIN. *Gas and diesel cogeneration systems*. 2013. 1–16 p. Available at: <<http://www.cainind.com/downloads/Cain-Spiral-Finned-Tubing.pdf>>.
- CALISE, F. et al. A novel tool for thermoeconomic analysis and optimization of trigeneration systems: A case study for a hospital building in Italy. *Energy*, Elsevier Ltd, v. 126, p. 64–87, 2017. ISSN 03605442. Available at: <<http://dx.doi.org/10.1016/j.energy.2017.03.010>>.

- CAPSTONE. *Capstone C1000 Technical reference*. 2005. 1–15 p.
- CARDONA, E.; PIACENTINO, A. A methodology for sizing a trigeneration plant in mediterranean areas. *Applied Thermal Engineering*, v. 23, n. 13, p. 1665–1680, 2003. ISSN 13594311.
- CARPANETO, E. et al. Cogeneration planning under uncertainty. Part I: Multiple time frame approach. *Applied Energy*, Elsevier Ltd, v. 88, n. 4, p. 1059–1067, 2011. ISSN 03062619. Available at: <<http://dx.doi.org/10.1016/j.apenergy.2010.10.014>>.
- CARVALHO, M. *Thermoeconomic and environmental analyses for the synthesis of polygeneration systems in the residential-commercial sector*. 291 p. Phd Thesis (Ph.D.) — University of Zaragoza, 2011.
- CARVALHO, M. et al. Synthesis of trigeneration systems: Sensitivity analyses and resilience. *The Scientific World Journal*, v. 2013, 2013. ISSN 1537744X.
- CATERPILLAR. *CAT G3500 Generator Set Engine Performance*. 2000.
- CATERPILLAR. *CAT Application and Installation Guide—Cooling Systems*. 2016.
- CELESC. *Tariffs (in portuguese)*. 2019. Available at: <<http://www.celesc.com.br/>>.
- ÇENGEL, Y. A.; BOLES, M. A. *Thermodynamics: An engineering approach*. 5. ed. Boston: McGraw Hill, 2006. ISBN 9780072884951.
- CEP. Current business indicators. *Chemical Engineering*, v. 126, n. 3, p. 84, 2019.
- CHHABRA, R. P. (Ed.). *CRC Handbook of Thermal Engineering*. Second. Boca Raton: CRC Press, 2018. 1677 p. ISSN 1098-6596. ISBN 9788578110796.
- CHO, H.; SMITH, A. D.; MAGO, P. Combined cooling, heating and power: A review of performance improvement and optimization. *Applied Energy*, Elsevier Ltd, v. 136, p. 168–185, 2014. ISSN 03062619. Available at: <<http://dx.doi.org/10.1016/j.apenergy.2014.08.107>>.
- COUPER, J. R. et al. *Chemical Process Equipment: Selection and Design*. 2. ed. Burlington, USA: Elsevier, 2010. 832 p. ISBN 0080919723. Available at: <<http://books.google.com/books?id=jlR12Zz2SfoC{&}pgis=1>>.
- CUMMINS. *CUMMINS T-030: Liquid-Cooled Generator Set Application Manual*. 2015.
- DANTZIG, G.; THAPA, M. *Linear Programming: Introduction*. New York: Springer, 1997. ISSN 00222437.
- DANTZIG, G. B.; THAPA, M. N. *Linear Programming : Theory and Extensions*. New York: Springer, 2003. 475 p. ISBN 0387948333.

- DAY, A. R. An improved use of cooling degree-days for analysing chiller energy consumption in buildings. *Building Services Engineering Research and Technology*, v. 26, n. 2, p. 115–127, 2005. ISSN 01436244.
- DAY, T. *Degree-days: theory and application*. London: CIBSE Chartered Institution of Building Services Engineers, 2006. 105 p. Available at: <<https://www.cibse.org/Knowledge/CIBSE-Publications/CIBSE-Technical-Memoranda>>.
- DENG, J.; WANG, R. Z.; HAN, G. Y. A review of thermally activated cooling technologies for combined cooling, heating and power systems. *Progress in Energy and Combustion Science*, Elsevier Ltd, v. 37, n. 2, p. 172–203, 2011. ISSN 03601285. Available at: <<http://dx.doi.org/10.1016/j.pecs.2010.05.003>>.
- DOE. *Fact sheet: Reciprocating Engines*. Washington, DC: DOE, 2016. 4 p.
- DOE. *Fact Sheet Series: Absorption Chillers for CHP Systems*. Washington, DC: DOE, 2017. 1–4 p.
- EERE. *Commercial Reference Buildings*. 2018. Available at: <<https://www.energy.gov/eere/buildings/commercial-reference-buildings>>.
- EPA. *Catalog of CHP Technologies*. 2017.
- ERNST, M. A.; BALESTIERI, J. A. Influences of thermal and electric load fluctuations in the cogeneration attractiveness. *Applied Thermal Engineering*, v. 26, n. 14-15, p. 1500–1505, 2006. ISSN 13594311.
- FELS, M. *The Princeton Scorekeeping Method: an Introduction*. Princeton: The Center for Energy and Environmental Studies, 1984.
- FLIN, D. *Cogeneration A user's guide*. 1. ed. London: The Institution of Engineering and Technology, 2010. 128 p. ISBN 978-1-84919-104-3.
- FLOUDAS, C. A. *Nonlinear and Mixed-Integer Optimization*. Princeton: Oxford University, 1995. ISSN 0007-1250.
- FLOUDAS, C. A.; PARDALOS, P. M. (Ed.). *Encyclopedia of Optimization*. 2nd. ed. New York: Springer, 2014. ISSN 0717-6163. ISBN 9780874216561.
- FPL. *Water-Cooled Chillers*. 2012. 1–4 p. Available at: <<https://www.fpl.com/business/pdf/water-cooled-chillers-primer.pdf>>.
- FPL. *Air-Cooled Chillers*. 2014. 1–4 p.
- FROST, A. E. et al. Patterns and Temporal Resolution in Commercial and Industrial Typical Load Profiles. *Energy Procedia*, Elsevier B.V., v. 105, p. 2684–2689, 2017. ISSN 18766102. Available at: <<http://dx.doi.org/10.1016/j.egypro.2017.03.775>>.



- GABRIELLI, P. et al. Robust and optimal design of multi-energy systems with seasonal storage through uncertainty analysis. *Applied Energy*, Elsevier, v. 238, n. January, p. 1192–1210, 2019. ISSN 03062619. Available at: <<https://doi.org/10.1016/j.apenergy.2019.01.064>>.
- GAMOU, S.; YOKOYAMA, R.; ITO, K. Optimal unit sizing of cogeneration systems in consideration of uncertain energy demands as continuous random variables. *Energy Conversion and Management*, v. 43, n. 9-12, p. 1349–1361, 2002. ISSN 01968904.
- GARRET, D. D. *Chemical Engineering Economics*. New York: Van Nostrand Reinhold, 1989. ISSN 15472701. ISBN 9789401165464.
- GUASCOR. *Gas Engines and Gensets*. 2011.
- HAWKES, A.; LEACH, M. Impacts of temporal precision in optimisation modelling of micro-combined heat and power. *Energy*, v. 30, n. 10, p. 1759–1779, 2005. ISSN 03605442.
- HEGGS, P. J. Minimum temperature difference approach concept in heat exchanger networks. *Heat Recovery Systems and CHP*, v. 9, n. 4, p. 367–375, 1989. ISSN 08904332.
- HEROLD, K. E.; RADEMACHER, R.; SANFORD, A. *Absorbition Chillers and Heat Pumps*. 2nd. ed. Boca Raton: CRC, 2016. 386 p. ISBN 9781498714358.
- HEVAC. *Commercial and Industrial Heating*. 2019.
- HEWITT, G. F.; PUGH, S. J. Approximate design and costing methods for heat exchangers. *Heat Transfer Engineering*, v. 28, n. 2, p. 76–86, 2007. ISSN 01457632.
- HIERETH, H. (Ed.). *Charging the Internal Combustion Engine*. Wien: Springer, 2003. 283 p. ISBN 9783211330333.
- HORLOCK, J. H. Cogeneration–combined heat and power (CHP) : thermodynamics and economics. *Thermodynamics and fluid mechanics series*, 1987.
- IEA. *Linking Heat and Electricity Systems : Co-generation and District Heating and cooling solutions for a cleand energy future*. Paris: IEA, 2014. 58 p.
- IEA. *Energy Technology Perspectives 2017*. New York: IEA, 2017.
- IRENA. *Thermal Energy Storage Technology Brief*. IEA, 2013. 24 p. Available at: <[www.irena.org/Publications](http://www.irena.org/Publications)>.
- JIANG, R. et al. Thermodynamic model development, experimental validation and performance analysis of a MW CCHP system integrated with dehumidification system. *Energy Conversion and Management*, Elsevier, v. 158, n. October 2017, p. 176–185, 2018. ISSN 01968904. Available at: <<https://doi.org/10.1016/j.enconman.2017.12.060>>.

- Joint Committee For Guides In Metrology. *JCGM 100: 2008 Evaluation of measurement data — Guide to the expression of uncertainty in measurement*. Paris: [s.n.], 2008. 134 p. ISSN 00099147. ISBN 9267101889. Available at: <<http://www.bipm.org/en/publications/guides/gum.html>>.
- JONES, E.; OLIPHANT, T. *SciPy: Open Source Scientific Tools for Python*. 2001. Available at: <<http://www.scipy.org/>>.
- KALAISELVAM, S.; PARAMESHWARAN, R. *Thermal Energy Storage Technologies for Sustainability*. London: Academic Press, 2014. 445 p. ISBN 9780124172913.
- KAVVADIAS, K. C.; MAROULIS, Z. B. Multi-objective optimization of a trigeneration plant. *Energy Policy*, Elsevier, v. 38, n. 2, p. 945–954, 2010. ISSN 03014215. Available at: <<http://dx.doi.org/10.1016/j.enpol.2009.10.046>>.
- KEMP, I. C. *Pinch Analysis and Process Integration*. 2nd. ed. Oxford, UK: Butterworth-Heinemann, 2007. 415 p.
- KLEIN, S. A. Development and integration of an equation-solving program for engineering thermodynamics courses. *Computer Applications in Engineering Education*, v. 1, n. 3, p. 265–275, 1993. ISSN 10990542.
- KOLANOWSKI, B. F. *Small-scale cogeneration handbook*. 4. ed. Lilburn,GA: Fairmont, 2011. 244 p. ISBN 9781439876244.
- KOTZUR, L. et al. Impact of different time series aggregation methods on optimal energy system design. *Renewable Energy*, Elsevier Ltd, v. 117, p. 474–487, 2018. ISSN 18790682. Available at: <<https://doi.org/10.1016/j.renene.2017.10.017>>.
- KOTZUR, L. et al. Time series aggregation for energy system design: Modeling seasonal storage. *Applied Energy*, Elsevier, v. 213, n. October 2017, p. 123–135, 2018. ISSN 03062619. Available at: <<https://doi.org/10.1016/j.apenergy.2018.01.023>>.
- LG. *Absorption Chillers*. 2015. 80 p.
- LI, C. Z.; SHI, Y. M.; HUANG, X. H. Sensitivity analysis of energy demands on performance of CCHP system. *Energy Conversion and Management*, Elsevier Ltd, v. 49, n. 12, p. 3491–3497, 2008. ISSN 01968904. Available at: <<http://dx.doi.org/10.1016/j.enconman.2008.08.006>>.
- LI, C. Z. et al. Uncertain programming of building cooling heating and power (BCHP) system based on Monte-Carlo method. *Energy and Buildings*, Elsevier B.V., v. 42, n. 9, p. 1369–1375, 2010. ISSN 03787788. Available at: <<http://dx.doi.org/10.1016/j.enbuild.2010.03.005>>.
- LI, P.-W.; CHAN, C. L. *Thermal Energy Storage Analyses and Designs*. London: Elsevier, 2017. 226 p. ISBN 9781402052880.

- LINDO SYSTEMS. *LINGO: The modeling Language and Optimizer*. Chicago: [s.n.], 2017.
- LINNHOFF, B.; BOLAND, D. *A user guide on process integration for the efficient use of energy*. [S.l.: s.n.], 1982. ISBN 0852951566.
- LIS, L. *Government approves resolution to open the market and attempt to reduce the natural gas price (in portuguese)*. Globo, 2019. Available at: <<https://g1.globo.com/economia/>>.
- LOZANO, M. A. *Thermal process integration in trigeneration plants (in spanish)*. Zaragoza: [s.n.], 2017.
- LOZANO, M. A.; RAMOS, J. Optimal cogeneration technology selection for residential and commercial buildings. *Cogeneration and Distributed Generation Journal*, v. 25, n. 4, p. 8–19, 2010. ISSN 15457575.
- LOZANO, M. A.; RAMOS, J. C.; SERRA, L. M. Cost optimization of the design of CHCP (combined heat, cooling and power) systems under legal constraints. *Energy*, Elsevier Ltd, v. 35, n. 2, p. 794–805, 2010. ISSN 03605442. Available at: <<http://dx.doi.org/10.1016/j.energy.2009.08.022>>.
- MANGOLD, D.; DESCHAIANTRE, L. Large Systems Seasonal thermal energy storage. p. 1–48, 2015. Available at: <[www.solites.de](http://www.solites.de)>.
- MARQUANT, J. F. et al. Comparing different temporal dimension representations in distributed energy system design models. *Energy Procedia*, Elsevier B.V., v. 122, p. 907–912, 2017. ISSN 18766102. Available at: <<https://doi.org/10.1016/j.egypro.2017.07.403>>.
- MARTÍNEZ-LERA, S.; BALLESTER, J. A novel method for the design of CHCP (combined heat, cooling and power) systems for buildings. *Energy*, Elsevier Ltd, v. 35, n. 7, p. 2972–2984, 2010. ISSN 03605442. Available at: <<http://dx.doi.org/10.1016/j.energy.2010.03.032>>.
- MATCHES. *Heat exchanger cost estimate*. 2014. Available at: <<http://www.matche.com/equipcost/Exchanger.html>>.
- MATELLI, J. A. *Sistemas baseado em conhecimento para projeto de plantas de cogeração a gás natural*. 134 p. Phd Thesis (Doctorate) — Federal University of Santa Catarina, Florianópolis, 2008.
- MATELLI, J. A.; BAZZO, E. On the parameters of performance of combined refrigeration and power plants. *International Journal of Refrigeration*, v. 36, n. 8, p. 2169–2175, 2013. ISSN 01407007.
- MATELLI, J. A.; GOEBEL, K. Conceptual design of cogeneration plants under a resilient design perspective: Resilience metrics and case study. *Applied Energy*,

- Elsevier, v. 215, n. February, p. 736–750, 2018. ISSN 03062619. Available at: <https://doi.org/10.1016/j.apenergy.2018.02.081>.
- MAVROMATIDIS, G.; OREHOUNIG, K.; CARMELIET, J. A review of uncertainty characterisation approaches for the optimal design of distributed energy systems. *Renewable and Sustainable Energy Reviews*, Elsevier Ltd, v. 88, n. March, p. 258–277, 2018. ISSN 18790690. Available at: <https://doi.org/10.1016/j.rser.2018.02.021>.
- MAVROMATIDIS, G.; OREHOUNIG, K.; CARMELIET, J. Design of distributed energy systems under uncertainty: A two-stage stochastic programming approach. *Applied Energy*, Elsevier, v. 222, n. April, p. 932–950, 2018. ISSN 03062619. Available at: <https://doi.org/10.1016/j.apenergy.2018.04.019>.
- MAVROMATIDIS, G.; OREHOUNIG, K.; CARMELIET, J. Uncertainty and global sensitivity analysis for the optimal design of distributed energy systems. *Applied Energy*, Elsevier, v. 214, n. February, p. 219–238, 2018. ISSN 03062619. Available at: <https://doi.org/10.1016/j.apenergy.2018.01.062>.
- MAVROTAS, G.; FLORIOS, K.; VLACHOU, D. Energy planning of a hospital using Mathematical Programming and Monte Carlo simulation for dealing with uncertainty in the economic parameters. *Energy Conversion and Management*, Elsevier Ltd, v. 51, n. 4, p. 722–731, 2010. ISSN 01968904. Available at: <http://dx.doi.org/10.1016/j.enconman.2009.10.029>.
- Michigan State Tax Commission. Unit-in-place section. In: *Assesor's Manual - Volume 2: Commercial*. Lansing: Michigan State Tax Commission, 2014. chap. 6.
- NIETO, N. et al. Experimental and thermodynamic analysis of a compression ignition engine operating with straight soybean oil. *Journal of the Brazilian Society of Mechanical Sciences and Engineering*, Springer Berlin Heidelberg, v. 37, n. 5, p. 1467–1478, 2015. ISSN 18063691. Available at: <http://dx.doi.org/10.1007/s40430-014-0287-z>.
- OPENEI. *Commercial and Residential Hourly Load Profiles for all TMY3 Locations in the United States*. 2018. Available at: <https://openei.org/datasets/>.
- ORLANDO, J. A. *Cogeneration Design Guide*. Atlanta: ASHRAE, 1996. 346 p.
- PEDREGOSA, F. et al. Scikit-learn: Machine Learning in Python. *Journal of Machine Learning Research*, v. 12, p. 2825–2830, 2011. Available at: <http://scikit-learn.sourceforge.net.>
- PEERLESS. *Boilers Trade Price List*. 2018.
- PINTO, E. S.; SERRA, L. M.; LÁZARO, A. Evaluation of methods to select representative days for the optimization of polygeneration systems. *Renewable Energy*, 2019. ISSN 09601481.

- PONCELET, K. et al. Impact of the level of temporal and operational detail in energy-system planning models. *Applied Energy*, Elsevier Ltd, v. 162, p. 631–643, 2016. ISSN 03062619. Available at: <http://dx.doi.org/10.1016/j.apenergy.2015.10.100>.
- PROCEL. *Electricity rates handbook (in Portuguese)*. 2011. 16 p.
- RAMOS, J. C. *Design optimization and operation of cogeneration systems for the commercial residential sector (in spanish)*. 202 p. Phd Thesis (PhD) — University of Zaragoza, 2012.
- REICHMUTH, H. A Method for Deriving an Empirical Hourly Base Load Shape from Utility Hourly Total Load Records. In: *ACEE Summer Study on Energy Efficiency in Buildings*. Pacific Grove, CA: ACEEE, 2008. p. 235–247. Available at: [http://aceee.org/files/proceedings/2008/data/papers/5{}\\_256.pdf](http://aceee.org/files/proceedings/2008/data/papers/5{}_256.pdf).
- REN, H.; GAO, W.; RUAN, Y. Optimal sizing for residential CHP system. *Applied Thermal Engineering*, v. 28, n. 5-6, p. 514–523, 2008. ISSN 13594311.
- RONG, A.; SU, Y. Polygeneration systems in buildings: A survey on optimization approaches. *Energy and Buildings*, Elsevier B.V., v. 151, p. 439–454, 2017. ISSN 03787788. Available at: <http://dx.doi.org/10.1016/j.enbuild.2017.06.077>.
- SCHÜTZ, T.; STREBLOW, R.; MÜLLER, D. A comparison of thermal energy storage models for building energy system optimization. *Energy and Buildings*, Elsevier B.V., v. 93, p. 23–31, 2015. ISSN 03787788. Available at: <http://dx.doi.org/10.1016/j.enbuild.2015.02.031>.
- SCIPY. *Carrelated random samples*. 2015. Available at: <https://scipy-cookbook.readthedocs.io/items/CorrelatedRandomSamples.html>.
- SEABOLD, S.; PERKTOLD, J. Statsmodels: Econometric and statistical modeling with python. In: *Proceedings of the 9th Python in Science Conference*. Austin, TX: [s.n.], 2010. Available at: <https://conference.scipy.org/proceedings/scipy2010/>.
- SHAH, R. K.; SECULIC, D. *Fundamentals of Heat Exchanger Design*. first. Hoboken, NJ: Wiley, 2003. 132–133 p. ISSN 0026-0894. ISBN 0471321710.
- SHI, Y.; MINGXI, L.; FANG, F. *Combined Cooling, Heating, and Power systems*. first. Singapore: Wiley, 2017. 161 p. ISBN 9781119283379.
- SHNAIDERMAN, M.; KEREN, N. Cogeneration versus natural gas steam boiler: A techno-economic model. *Applied Energy*, Elsevier Ltd, v. 131, p. 128–138, 2014. ISSN 03062619. Available at: <http://dx.doi.org/10.1016/j.apenergy.2014.06.020>.
- SMITH, A.; LUCK, R.; MAGO, P. J. Analysis of a combined cooling, heating, and power system model under different operating strategies with input and model data

uncertainty. *Energy and Buildings*, Elsevier B.V., v. 42, n. 11, p. 2231–2240, 2010. ISSN 03787788. Available at: <<http://dx.doi.org/10.1016/j.enbuild.2010.07.019>>.

SOLAR. *Saturn 20 Gas Turbine Generator Package*. 2014.

THERMAX. *Exhaust Gas Driven Vapour Absorption Chiller*. 2014.

TIBSHIRANI, R.; WALTHER, G.; HASTIE, T. Estimating the number of clusters in a data set via the gap statistic. *Journal of the Royal Statistic Society*, v. 63, n. 2, p. 411–423, 2001.

TOWLER, G.; SINNOTT, R. *Chemical Engineering Design Principles*. 2. ed. Amsterdam: Elsevier, 2013. ISBN 9780080966595. Available at: <<http://dx.doi.org/10.1016/B978-0-08-096659-5.00022-5>>.

TRANE. *Service Pricelist*. 2012.

TRANE. *Product Catalog Air-Cooled Scroll Chillers Model CGAM 20 to 130 Nominal Tons*. 2017.

TRANE. *Product Catalog Air-cooled Series RTAC Helical-rotary Liquid Chillers 140 -300 Ton*. 2017.

TRANE. *Product Catalog Centravac Water-Cooled Liquid Chillers*. 2017.

TRANE. *Product Catalog Series RTWD Helical Rotary Liquid Chillers 235 - 945 kW*. 2017.

TRANE. *Product Catalog Water-cooled Series RTHD Helical-rotary Liquid Chillers 500 - 1500 kW*. 2017.

UFSC. *Data from UFSC meteorological station*. 2019. Available at: <<http://www.labhidro.ufsc.br/pt/dados-ufsc>>.

URBANUCCI, L. Limits and potentials of Mixed Integer Linear Programming methods for optimization of polygeneration energy systems. *Energy Procedia*, Elsevier B.V., v. 148, p. 1199–1205, 2018. ISSN 18766102. Available at: <<https://doi.org/10.1016/j.egypro.2018.08.021>>.

URBANUCCI, L.; TESTI, D. Optimal integrated sizing and operation of a CHP system with Monte Carlo risk analysis for long-term uncertainty in energy demands. *Energy Conversion and Management*, Elsevier, v. 157, n. December 2017, p. 307–316, 2018. ISSN 01968904. Available at: <<https://doi.org/10.1016/j.enconman.2017.12.008>>.

VERBEKE, S.; AUDENAERT, A. Thermal inertia in buildings: A review of impacts across climate and building use. *Renewable and Sustainable Energy Reviews*, Elsevier Ltd, v. 82, n. September 2017, p. 2300–2318, 2018. ISSN 18790690. Available at: <<https://doi.org/10.1016/j.rser.2017.08.083>>.

VIESSMANN. *Price List 2015-2016*. 2016.

VOORSPOOLS, K. R.; HAESELEER, W. D. Reinventing hot water?: towards optimal sizing and management of cogeneration. *Applied Thermal Engineering*, v. 26, n. 16, p. 1972–1981, 2006. ISSN 13594311.

WAUKESHA. *Gas engine 1104 kWb*. 2013.

WIT, J. de. Heat Storages for CHP Optimisation. *PowerGen Europe 2007*, p. 1–18, 2007.

YANG, Y.; ZHANG, S.; XIAO, Y. Optimal design of distributed energy resource systems based on two-stage stochastic programming. *Applied Thermal Engineering*, Elsevier Ltd, v. 110, p. 1358–1370, 2017. ISSN 13594311. Available at: <<http://dx.doi.org/10.1016/j.applthermaleng.2016.09.049>>.

YOSHIDA, S.; ITO, K.; YOKOYAMA, R. Sensitivity analysis in structure optimization of energy supply systems for a hospital. *Energy Conversion and Management*, v. 48, n. 11, p. 2836–2843, 2007. ISSN 01968904.

YUE, X. et al. A review of approaches to uncertainty assessment in energy system optimization models. *Energy Strategy Reviews*, Elsevier, v. 21, n. June, p. 204–217, 2018. ISSN 2211467X. Available at: <<https://doi.org/10.1016/j.esr.2018.06.003>>.

## Appendix A

### CHARACTERIZATION OF TECHNOLOGIES

This appendix presents the technical and economic features of the technologies, relevant to the development of the MILP model formulated in Ch. 4. Data was obtained from catalogs of commercially-available devices and through consultation with specialists.

#### A.1 TECHNICAL INFORMATION

##### A.1.1 Engine-based Cogeneration Modules

The heat supply of modules ECM01, ECM02 and ECM03 come from the heat recovery performed on natural gas generator sets. The device considered in the simulation approach presented in the Ch. 2 and for the thermal integration algorithm in Ch. 4 corresponds to a Caterpillar model G3516 LE (1035 kW), while data used in the synthesis model corresponds to a model Caterpillar G3508TA (370 kW). Technical data for both models were extracted from the compendium (CATERPILLAR, 2000) and is summarized in Tab. 29, terms and units are presented as the original source.

Table 29 – Technical features of the generator sets considered

Feature	G3516 LE	G3508 TA
Aftercooler inlet temperature, °C	54	54
Jacket water outlet temperature, °C	99	99
Engine power (w/o fan), kW	1090	392
Generator set power (w/o fan), kW	1035	370
Specific fuel consumption, MJ/bkW-hr	11.01	10.48
Air mass flow, kg/bkW-hr	4.35	4.37
Compressor out temperature, °C	152	122
Inlet manifold temperature, °C	59	58
Exhaust gas temperature, °C	474	461
Exhaust gas mass flow, kg/bkW-hr	5.85	4.61
Input energy LHV, kW	3333	1140
Work output, kW	1090	392
Heat rejection to jacket, kW	1027	411
Heat rejection to atmosphere (radiated), kW	120	48
Total heat rejection to exhaust (to 25°C), kW	923	256
Heat rejection to exhaust (LHV to 177°C), kW	710	197
Heat rejection to aftercooler - stage 1, kW	173	33



### Heat Exchange Networks

According to the method exposed in the Ch. 4, a different heat exchange network were obtained for each module. Fig. 44 shows the configurations obtained for each engine-based module. Units are omitted for simplicity, numbers in italics express temperatures in °C, while numbers in bold express heat transfer capacity in kW.

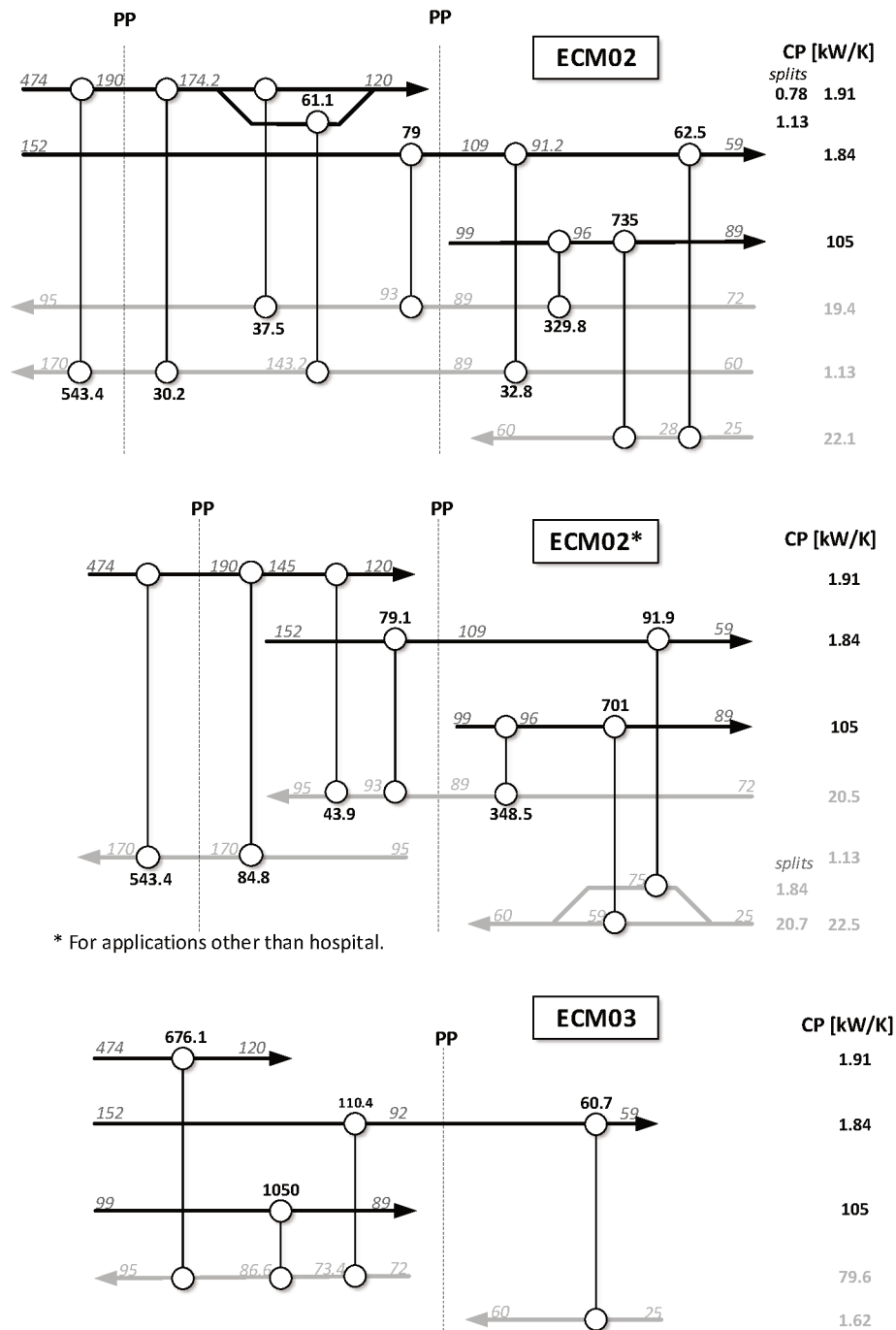


Figure 44 – Configurations of heat exchanger networks for engine-based cogeneration sets.

### A.1.2 Turbine-based Cogeneration Modules

As mentioned in Ch. 2, conventional gas turbines are available at sizes higher than 2 MW with a couple of models close to 1 MW, which limits their incorporation into utilities' supply systems with a lesser electricity demand (like the applications covered in this work). However, the supply of thermal utilities as function of the intake temperature was considered in the formulation of the MILP model. The technical features correspond to the model Solar Saturn 20, with a capacity of 1200 kW (SOLAR, 2014). Technical specifications are shown in Tab. 30, terms and units are presented as the original document. Performance curves are already presented in Ch. 4.

Table 30 – Technical features of the turbine considered

<b>Feature</b>	<b>Solar SATURN 20</b>
Electrical power, MW	1.20
Heat rate, kJ/kWE-hr	14800
Fuel input, MJ/s	4.9
Efficiency, %	24.3
Exhaust mass flow, kg/s	6.5
Exhaust gas temperature, °C	506

### A.1.3 Microturbine-based Cogeneration Modules

Technical characteristics considered for microturbines correspond to the model Capstone C-1000 (CAPSTONE, 2005), which is a bundle of five power modules of 200 kW each. Figure 45 illustrates the physical arrangement of this device, presented in its technical documentation. This fact makes that features like the exhaust gas temperature or the net efficiency are the same that for a single module, while features like the exhaust mass flow, are proportional to the number of modules in the bundle. Basic performance characteristics are presented in Tab. 31. Performance curves are already presented in Ch. 4.

Table 31 – Technical features of the microturbine considered

<b>Feature</b>	<b>Capstone C1000</b>
Net power output, kW	1000
Net efficiency (LHV), %	22
Nominal net heat rate (LHV), kJ/kWh	10900
Nominal generator heat rate, kJ/kWh	10200
Nominal steady state fuel flow (HHV)*, kJ/hr	12000000

\*Ratio HHV/LHV is assumed to be 1.1.

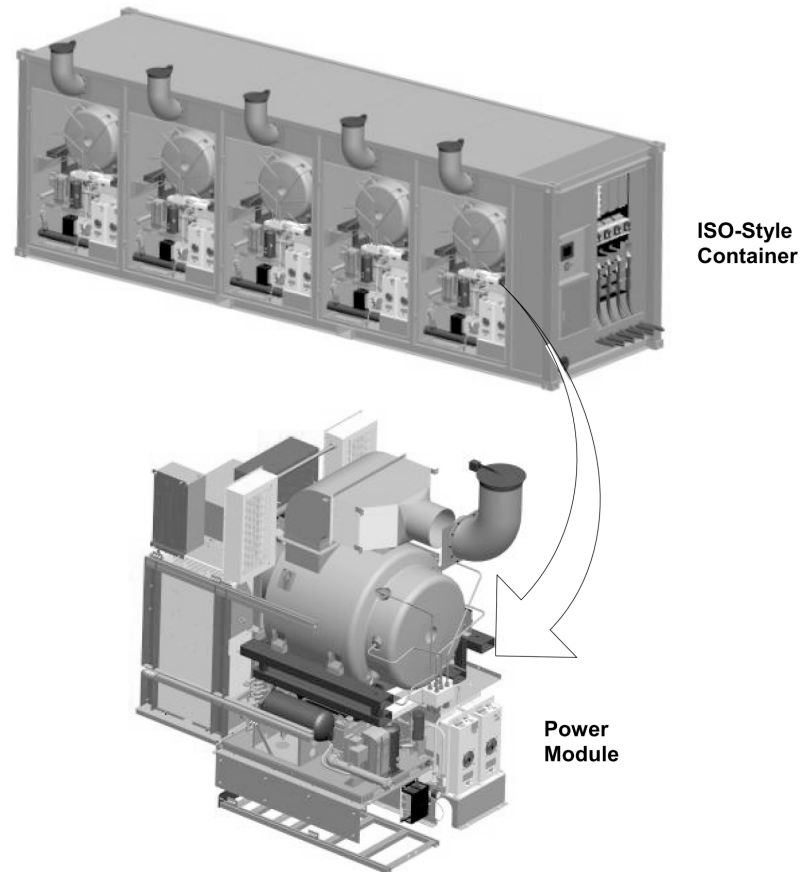


Figure 45 – Configuration of microturbine bundle. Taken from (CAPSTONE, 2005)

#### A.1.4 Steam Boilers and Heaters

The model selected for characterizing the steam boilers corresponds to the series 211A of the brand Peerless (PEERLESS, 2018). According to the catalog, this series includes boilers from 630 MBH to 9450 MBH input. Particularly, it was chosen because of its wide range of sizes. Relevant technical data is presented in Tab. 32 for the sizes considered in the synthesis model. Terms and units are presented as the original document.

Table 32 – Technical features of the steam boilers considered

<b>Feature</b>	<b>211A-04</b>	<b>211A-16</b>
Input, MBH	630	3150
Gross output, MBH	486	2454
Steam, sqft	1521	7938
Steam, MBH	365	1905
Thermal efficiency, %	92	92
Boiler H.P.	14.5	73.3

On the other hand, data for modeling the auxiliary hot-water boilers (or heaters), also correspond to equipment from the brand peerless. They correspond to condensing

boilers of the series *Purefire*. Ratings of the models considered are summarized in Tab.33. Terms and units are presented as the original document.

Table 33 – Technical features of the hot-water boilers considered

<b>Feature</b>	<b>PF-399</b>	<b>PFC-1500</b>
Minimum Input, kW	23.4	43.9
Maximum Input, kW	116.9	439.6
Gross output, kW	111.4	424.3
Thermal efficiency, %	97.2	97.5

### A.1.5 Electric Chillers

Four different types of electric chillers were taken into account in to the synthesis model, depending on the kind of compressor and the fluid used for dissipating heat to the atmosphere. As mentioned in Ch. 2, there are several alternatives not contemplated in this work, including improvements such as the modulation of the rotation speed through a frequency inverter, or the use of magnetic bearings. However, the types considered here are widely used for the air conditioning in buildings. These types are: (i)scroll, air-cooled (up to 130 TR), (ii)screw, air-cooled (140-500 TR), (iii) screw, water-cooled (80-430 TR), and (iv) centrifugal, water-cooled (170-2500 RT). Table 34 summarizes the technical information of the models considered; the brand considered is *Trane*. Values correspond to a chilled water temperature of 7°C and a condenser return temperature of 30 °C.

Table 34 – Technical information of electric chillers.

<b>Tag</b>	<b>Type</b>	<b>Cooling fluid</b>	<b>Capacity tons</b>	<b>COP</b>	<b>Reference</b>
CEA01 <i>COP = 3.10</i>	Scroll	Air	70	3.43	(TRANE, 2017a)
	Screw	Air	140	2.87	(TRANE, 2017b)
	Screw	Air	155	2.87	
	Screw	Air	275	2.87	
CEW01 <i>COP=5.24</i>	Screw	Water	80	5.17	(TRANE, 2017d)
	Screw	Water	150	5.30	
	Screw	Water	180	5.31	
	Screw	Water	280	5.03	(TRANE, 2017e)
CEW02 <i>COP = 6.03</i>	Centrifugal	Water	170	6.03	(TRANE, 2017c)
	Centrifugal	Water	270	6.03	

### A.1.6 Absorption Chillers

This technology also has several options according to the heat source used for activating the refrigeration (absorption) cycle. In this work, four alternatives are considered: (i)direct fired, (ii)hot-gases-driven (at around 480°C and 300°C), (iii)steam-driven (at 8 bar), and (iv)hot-water-driven absorption chillers. Table 35 summarizes the technical features of the absorption chillers considered into the superstructure. These devices are of the brand *Broad* (BROAD, 2004). Terms and units are presented as the original source. Rated conditions for all devices: chilled water 7°C/12°C, condenser water 37°C/30°C.

Table 35 – Technical features of absorption chillers.

Tag	Type	Capacity USRT	COP	Electricity kW
CAF01	Direct fired, two-stage	66	1.51	1.31
	Direct fired, two-stage	165	1.51	3.26
CAG01	Hot gases $\approx$ 500°C, two-stage	66	1.39	1.31
	Hot gases $\approx$ 500°C, two-stage	165	1.39	3.26
CAG02	Hot gases $\approx$ 300°C, single-stage	66	0.68	1.31
	Hot gases $\approx$ 300°C, single-stage	165	0.68	3.26
CAS01	Steam-driven, two-stage	66	1.39	0.676
	Steam-driven, two-stage	165	1.39	1.69
CAW01	Hot-water-driven, single stage	100	0.80	0.106
	Hot-water-driven, single stage	50	0.80	0.052
	Hot-water-driven, single stage	60	0.80	0.062
	Hot-water-driven, single stage	145	0.80	0.154

### A.1.7 Cooling Towers

This equipment is generally tailored for a specific application, according to a required water volume flow at a given temperature range. Additionally, its performance is strongly influenced by the predominant wet bulb temperature. The unique parameter set for this technology was its specific electricity demand that, through consultation with specialists, was assumed 0.0087 kW per kW of heat dissipated.

## A.2 ECONOMIC INFORMATION

This section presents the information concerning the estimation of the capital investment of each technology. Multiple sources were consulted, some of them were compared in order to verify the data consistency. To the best of the author knowledge, the data organized here constitutes a good basis for an order-of-magnitude appraisal. Evidently, real prices are subject to changes depending on issues not covered in the present work (i.e. inflation, taxes, discounts, etc.). Values gathered correspond to purchase prices of equipment, additional expenditures are estimated through applicable factors. Given that the validity of these prices do not coincide for all the equipment, it is necessary to correct them to get the same reference year (2019). It is done through the *Chemical Engineering Plant Cost Index (CEPCI)* (CEP, 2019), which is published regularly. This correction is done using the Eqn. A.1, values of the plant cost index (PCI) for the last 10 years are organized in Tab. 36.

$$INV_{t,2019} \approx INV_{t,y} \cdot \frac{PCI_{2019}}{PCI_y} \quad (\text{A.1})$$

Table 36 – Plant cost index (PCI) for the last 10 years (CEP, 2019).

Year (y)	PCI <sub>y</sub>
2010	550.8
2011	585.7
2012	584.6
2013	567.3
2014	576.1
2015	556.8
2016	541.7
2017	567.5
2018	603.1
2019	617.1

### A.2.1 Cogeneration Modules

The detailed cost breakdown for each cogeneration module is presented in Tab. 37. The main references are the survey published by the U.S. Environmental Protection Agency (EPA, 2017) and the series of fact sheets published by the U.S. Department of Energy (DOE, 2016). Heat recovery is updated according to the results of the thermal integration applied (see Ch. 4).

Table 37 – Investment costs breakdown for cogeneration modules.

TAG	Year	EMC01	EMC02	EMC02*	EMC03	TCM01	TCM02
Ref. Capacity, kWe		370	370	370	370	1150	1150
Min. Capacity, kWe		100	100	100	100	1150	1150
Max. Capacity, kWe		633	633	633	633	5457	5457
<b>Equipment, \$/kW</b>	<b>2019</b>	<b>965</b>	<b>1188</b>	<b>1151</b>	<b>1015</b>	<b>1607</b>	<b>2062</b>
Genset	2013	400	400	400	400	817	817
Heat Recovery	2014	271	480	445	318	67	492
Fuel system	2013	NA	NA	NA	NA	214	214
Electric	2013	140	140	140	140	300	300
Water treatment	2013	74	74	74	74	74	74
<b>Installation, \$/kW</b>	<b>2013</b>	<b>448</b>	<b>448</b>	<b>448</b>	<b>448</b>	<b>628</b>	<b>628</b>
<b>Direct, \$/kW</b>	<b>2019</b>	<b>1452</b>	<b>1676</b>	<b>1638</b>	<b>1502</b>	<b>2290</b>	<b>2745</b>
Construction Man.	2013	269	269	269	269	193	193
Engineering	2013	200	200	200	200	86	86
Contingency	2013	90	90	90	90	114	114
Financing	2013	42	42	42	42	68	68
<b>Indirect, \$/kW</b>	<b>2019</b>	<b>654</b>	<b>654</b>	<b>654</b>	<b>654</b>	<b>501</b>	<b>501</b>
<b>TOTAL \$/kW</b>	<b>2019</b>	<b>2106</b>	<b>2330</b>	<b>2292</b>	<b>2156</b>	<b>2791</b>	<b>3246</b>
O&M Costs, c/kWh	2013	2.1	2.1	2.1	2.1	1.26	1.26
<b>O&amp;M, \$/kWh</b>	<b>2019</b>	<b>0.0228</b>	<b>0.0228</b>	<b>0.0228</b>	<b>0.0228</b>	<b>0.0137</b>	<b>0.0137</b>
TAG	Year	TCM02*	TCM03	MCM01	MCM02	MCM02*	MCM03
Ref. Capacity, kWe		1150	110	333	333	333	333
Min. Capacity, kWe		1150	1150	200	200	200	200
Max. Capacity, kWe		5457	5457	1000	1000	1000	1000
<b>Equipment, \$/kW</b>	<b>2019</b>	<b>1990</b>	<b>1700</b>	<b>1559</b>	<b>1998</b>	<b>1990</b>	<b>1718</b>
Genset	2013	817	817	1189	1189	1189	1189
Heat Recovery	2014	425	154	0	410	403	149
Fuel system	2013	214	214	164	164	164	164
Electric	2013	300	300	0	0	0	0
Water treatment	2013	74	74	74	74	74	74
<b>Installation, \$/kW</b>	<b>2013</b>	<b>628</b>	<b>628</b>	<b>293</b>	<b>293</b>	<b>293</b>	<b>293</b>
<b>Direct, \$/kW</b>	<b>2019</b>	<b>2673</b>	<b>2383</b>	<b>1877</b>	<b>2317</b>	<b>2309</b>	<b>2037</b>
Construction Man.	2013	193	193	195	195	195	195
Engineering	2013	86	86	162	162	162	162
Contingency	2013	114	114	82	82	82	82
Financing	2013	68	68	15	15	15	15
<b>Indirect, \$/kW</b>	<b>2019</b>	<b>501</b>	<b>501</b>	<b>494</b>	<b>494</b>	<b>494</b>	<b>494</b>
<b>TOTAL \$/kW</b>	<b>2019</b>	<b>3175</b>	<b>2884</b>	<b>2371</b>	<b>2810</b>	<b>2803</b>	<b>2531</b>
O&M Costs, c/kWh	2013	1.26	1.26	1.2	1.2	1.2	1.2
<b>O&amp;M, \$/kWh</b>	<b>2019</b>	<b>0.0137</b>	<b>0.0137</b>	<b>0.0131</b>	<b>0.0131</b>	<b>0.0131</b>	<b>0.0131</b>

\*For building applications other than hospital.

Except for the cogeneration modules, the total investment of each technology shows a linear behavior with respect to its capacity. The intercept and the slope of each linear regression correspond to the base cost ( $BK_t$ ) and the unitary variable cost factor ( $UVK_t$ ), respectively. These values are reported in Tab. 21.

### A.2.2 Boilers and Heaters

Prices for the steam boilers were obtained from the catalog (PEERLESS, 2018) and compared with data published by the assessor's manual (Michigan State Tax Commission, 2014). Both data series present a strong linear trend, but presents a difference of about 20 k\$ for a given capacity (see Fig. 46a). On the other hand, prices for heaters were obtained from the commercial catalogs (ATH, 2014; PEERLESS, 2018; VIESSMANN, 2016), showing a great agreement. A bare module factor (BMF) of 1.5 were applied according to the information presented in (COUPER et al., 2010). Operation and maintenance costs are estimated at 0.05 and 0.025 Cents per kWh delivered of steam and hot water, respectively.

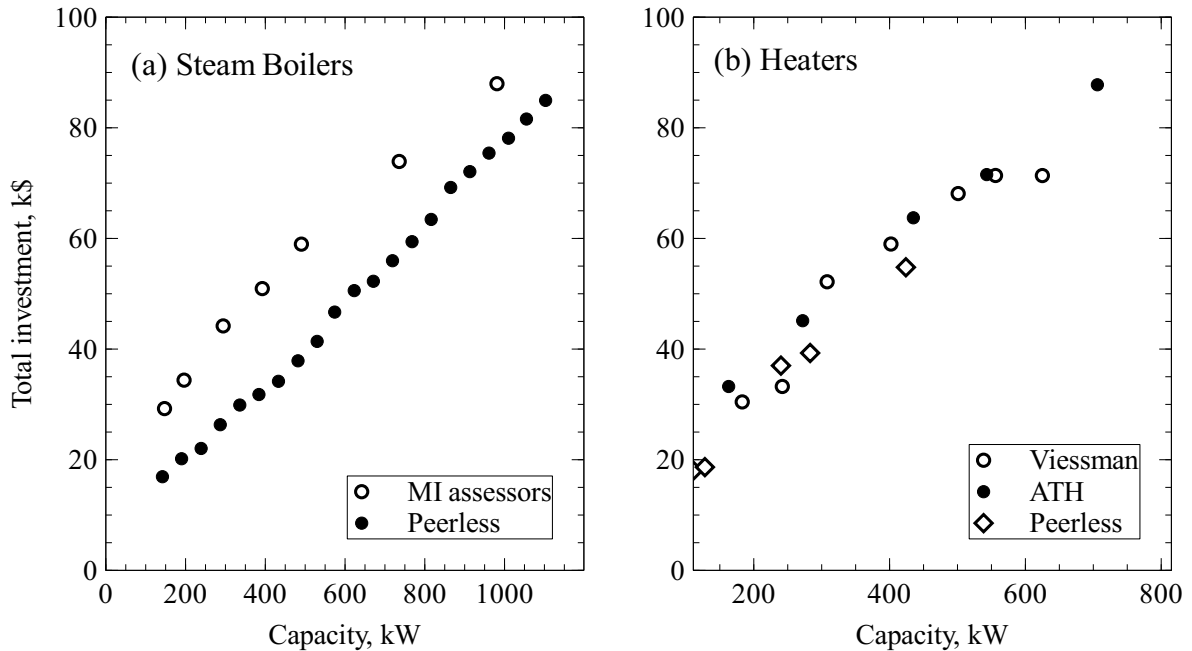


Figure 46 – Investment for steam boilers and heaters, installation included.



### A.2.3 Electric Chillers

Prices for electric chillers were obtained from (TRANE, 2012) and compared with the information of the technical communications (FPL, 2012) and (FPL, 2014), obtaining a good agreement. Additionally, these communications also provided the operation and maintenance costs (see Ch. 4). A bare module factor (BMF) of 1.5 were applied according to the information presented in (COUPER et al., 2010). Additional costs associated to distribution equipment such as pumps, tanks, risers, controls, etc. are assumed as 70% of the equipment purchase price, following the recommendation of specialists. Total investment of these devices are presented in Fig. 47.

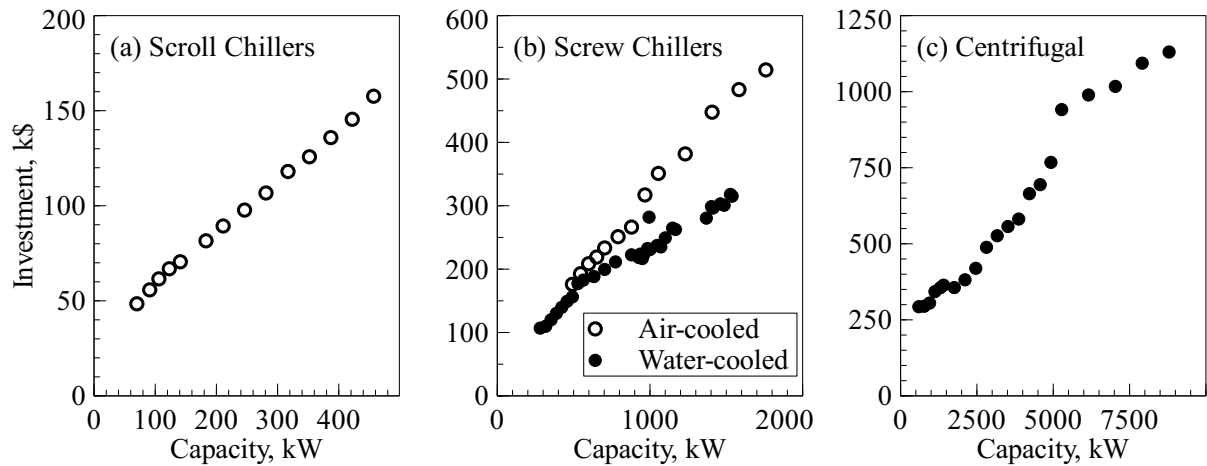


Figure 47 – Investment for electric chillers, installation included.

### A.2.4 Absorption chillers

Purchase price information of these devices were obtained from the design manual from the brand *Broad* (BROAD, 2008) and compared with the information from the fact sheet (DOE, 2017), showing a good agreement. Additionally, data concerning the operation and maintenance costs of these devices also come from this fact-sheet, as well as the BMF, whose value was set at 3. Total investment of these devices are presented in Fig. 48.

### A.2.5 Heat Exchangers

These devices are commonly tailored to specific application requirements, according to the fluids characteristics, their temperatures, flows, etc. although there are manufac-

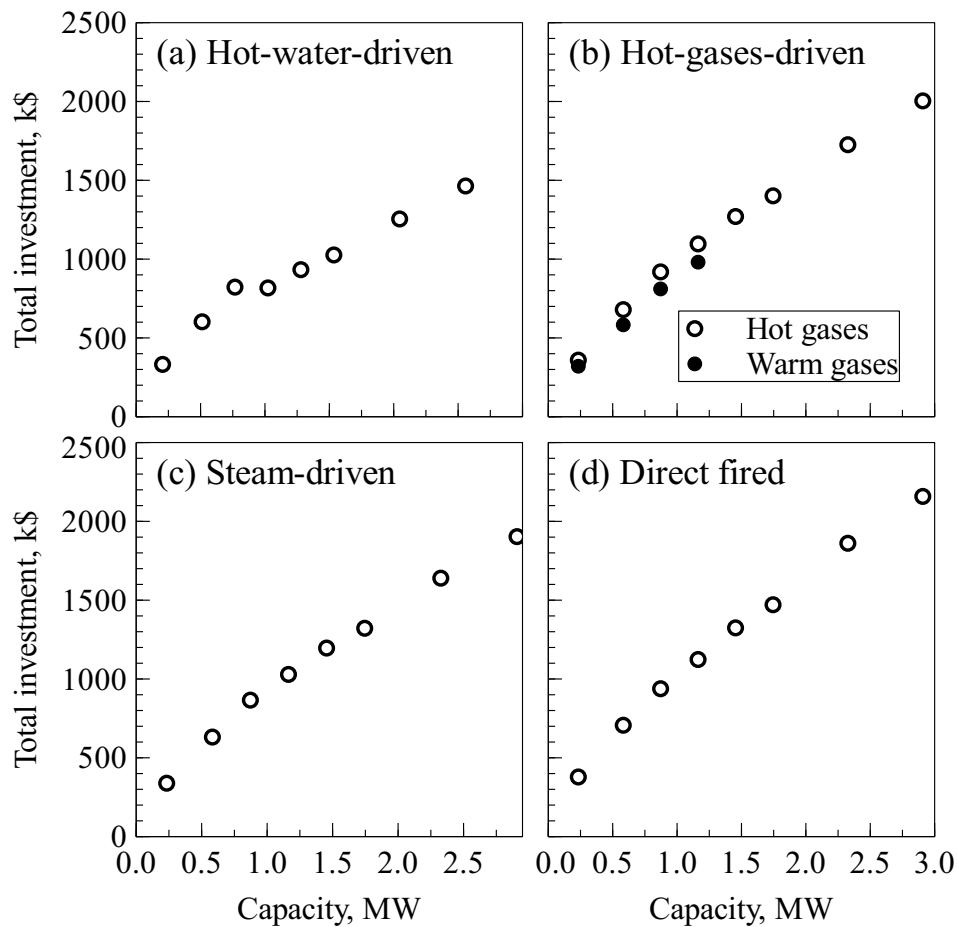


Figure 48 – Investment for absorption chillers, installation included.

tured exchangers involving common fluids, as water or steam, with a nominal exchange capacity at a set of standard conditions. In this work it is assumed that these devices are tailored according to the areas obtained from the thermal integration analysis, and their prices are obtained from the website of the engineering firm *Matches* (MATCHES, 2014). The construction material selected was carbon steel and the rating 150 psi, enough for the pressure levels present in the cogeneration plant. A bare module factor (BMF) of 1.9 were applied according to the information presented in (COUPER et al., 2010). Figure 49 presents the prices of heat exchangers as function of its heat transfer capacity. Operating and maintenance costs were considered negligible.

### A.2.6 Cooling Towers

As well as the heat exchangers, these devices can be tailored to meet a given set of specifications but also can be delivered as modules by demand. In this way, purchase prices

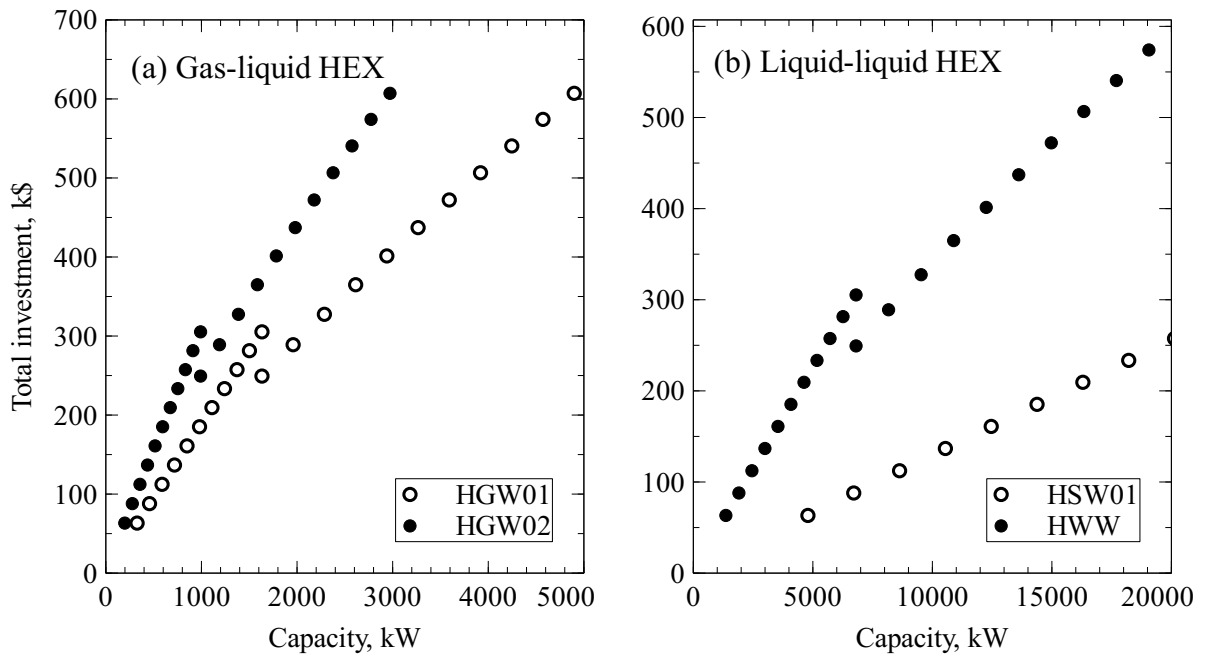


Figure 49 – Investment for heat exchangers, installation included.

for cooling towers were obtained from (TRANE, 2012), assuming that the heta dissipation can be addressed by one or more of these modules. A bare module factor (BMF) of 2.5 were applied according to recommendation from specialists. Total investment are presented in Fig. 50 as function of its capacity.

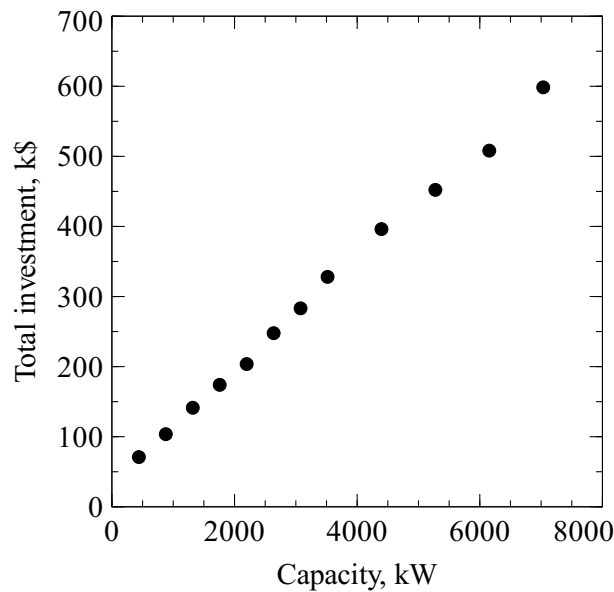


Figure 50 – Investment for cooling towers, installation included.

### **A.2.7 Thermal Storage**

Finally, investment data for the thermal storage based on isolated tanks were derived from the information presented in the report (MANGOLD; DESCHAINTE, 2015), while the operation and maintenance costs were obtained from the technology brief (IRENA, 2013).

## Appendix B

---

### DEVELOPMENT OF A PROGRAM FOR THE FEASIBILITY ASSESSMENT OF CCHP ALTERNATIVES

The purpose of the computational program *CogeCalc 2* is the quick and reliable assessment of the economic feasibility of different CCHP alternatives. It is based on the thermodynamic simulation of different CCHP structures and operational scenarios, oriented by various specialists in the area, which enables the integration of engineering criteria commonly applied in this type of projects and reduce the solution space to those structures that are feasible in practice. The development of the tool can be summarized in the following steps:

1. Creation of multiple CCHP arrangements and selection of the more feasible scenarios together with specialists.
2. Basic process simulation of chosen scenarios and presentation of relevant results to the specialists.
3. Elicitation and discussion of specialists' requirements, aiming the development of a specialized computational tool for assisting the preliminary design of production facilities implementing CCHP. This step has been done by means of periodic meetings whose main purpose is the discussion, verification and validation of the results obtained by the computational tool for its maturing and improvement.
4. Consolidation of a thermodynamic modeling tool of a multipurpose CCHP layout that enables the simulation of multiple production scenarios, taking into account the requirements and constraints considered by specialists and that is capable of assisting the economic feasibility assessment of different CCHP alternatives in the practice.

The computational program used for this task is *Engineering Equation Solver* (EES), which is extensively used in academic publications and is adequate for the level of detailing required in this task. Principal CCHP specialists were convened from different Brazilian natural gas distributors, some others from air conditioning installation companies and

CHP equipment suppliers. It should be remarked that their main interest is to get a useful and reliable tool for quick simulation of the CCHP layout, in such a way that its economic feasibility can be demonstrated to potential clients. For this reason, the development of this tool included the estimation of equipment costs, expenditures, revenues, and other economic feasibility parameters. The key requirements transmitted by the consulted specialist are listed as follows:

- *Utilities:* at the beginning of the program development, an approach focused on each type of application was considered (i.e. a routine for hospitals, another for restaurants, etc.), assuming that each application would present a typical set of utilities. It was changed by a utility-focused approach, where the specialist is enabled to choose any combination among the following utilities: electricity, cold (chilled water), steam, and hot water.
- *Equipment:* specialist is allowed to add technical and cost data of CCHP equipment to a database for further selection in the main graphical user interface of the program. Equipment included in the database are those available as unit (i.e. generator sets, gas turbines and microturbines, absorption chillers, etc.). Key parameters of equipment built according to particular specifications (i.e. heat exchangers, cooling towers, etc.) should be estimated for preliminary budgeting.
- *CCHP layout:* It is required that program presents the CCHP layout visually to the user (specialist) for further presentation to potential clients. Firstly, it was identified seven feasible combinations among the considered utilities, but considering the prime movers currently available for CCHP (gas engines and gas turbines/microturbines), there is a total of fourteen feasible combinations of CCHP utilities/prime movers. For each combination, there are several feasible layouts, in this way, a bunch of pre-selected layouts (about 35) were presented to the specialists for choosing those with more applicability according to their criteria. Initially, Six layouts were chosen, but finally it was agreed that a unique flexible layout, capable of addressing multiple combinations, is a better choice for encourage the utilization of the program.
- *Tariff structure:* Keeping in mind that the program is created as a first attempt to get a good approximation to a proper CCHP implementation, and for maintaining

the familiarity of specialists with their current methods, the program kept the use of three load factors<sup>1</sup>: one for on-peak demand, other for off-peak demand, and another for backup periods.

- *Flexibility of use*: Most of the technical and cost variables should be easily modifiable by the user, sometimes in more than one way according to the availability of information. For example, the user has the possibility of feed the current electricity consumption for each informed price rate, or conversely, informing directly the current annual electricity expenditure.
- *Complementary supply*: When a deficit a given utility supply is detected, the program should enable the user to consider the use of complementary equipment, which can be new or existing. For example, when there is a deficit of chilled water, the program enables the selection of complementary electrical chillers and the indication if they will be purchased or are already installed. Thermal storage is not considered within the CCHP layout; it was considered as part of further analyses.
- *Expected results*: It was requested a more detailed calculation involving thermodynamic properties and formulation. The most relevant results are those related with the quantity of utilities supplied and consumed by the plant and its efficiency. On the other hand, the plant initial investment estimation and annual operation expenditures are presented together with the reference case for demonstrating potential savings and the economic feasibility of the plant to the client. Additionally, results should be organized on screen adequately in spreadsheets, in such a way that users can understand easily the presented data. Two spreadsheets were designed: the first for technical results divided in an overall balance, a breakdown of CHP supplies, and a summary of supplies' consumption; the second spreadsheet is for economic preliminary feasibility data.
- *Comparison with the conventional production*: the comparison of results with conventional production was requested aiming to the promotion of CCHP implementation, since in this way, it is easier to show the eventual advantages of CCHP to the clients.

---

<sup>1</sup> Load factor understood as the ratio between the average demand and the peak demand during each rate period.

- *Explanatory and complementary messages:* Given the number of data presented and some other questions commonly asked by the clients, specialists requested the creation of explanatory and complementary messages according to obtained results. Aspects like electrical/thermal parity, maximum number of equipment activated by the available heat, etc. are covered by these customized messages.
- *Constrained variables / warnings:* It was requested in order to avoid invalid inputs by the users. Each time that the user insert a value out of the valid range (e.g. 0 to 1 for molar fractions), a warning message is activated, indicating possible corrections.

Figure 51 shows the first screen of the program interface (in Portuguese) for the CCHP layout chosen. Here the specialist (the user) inserts the main technical input data. Each input is briefly described according to its number in the screen:

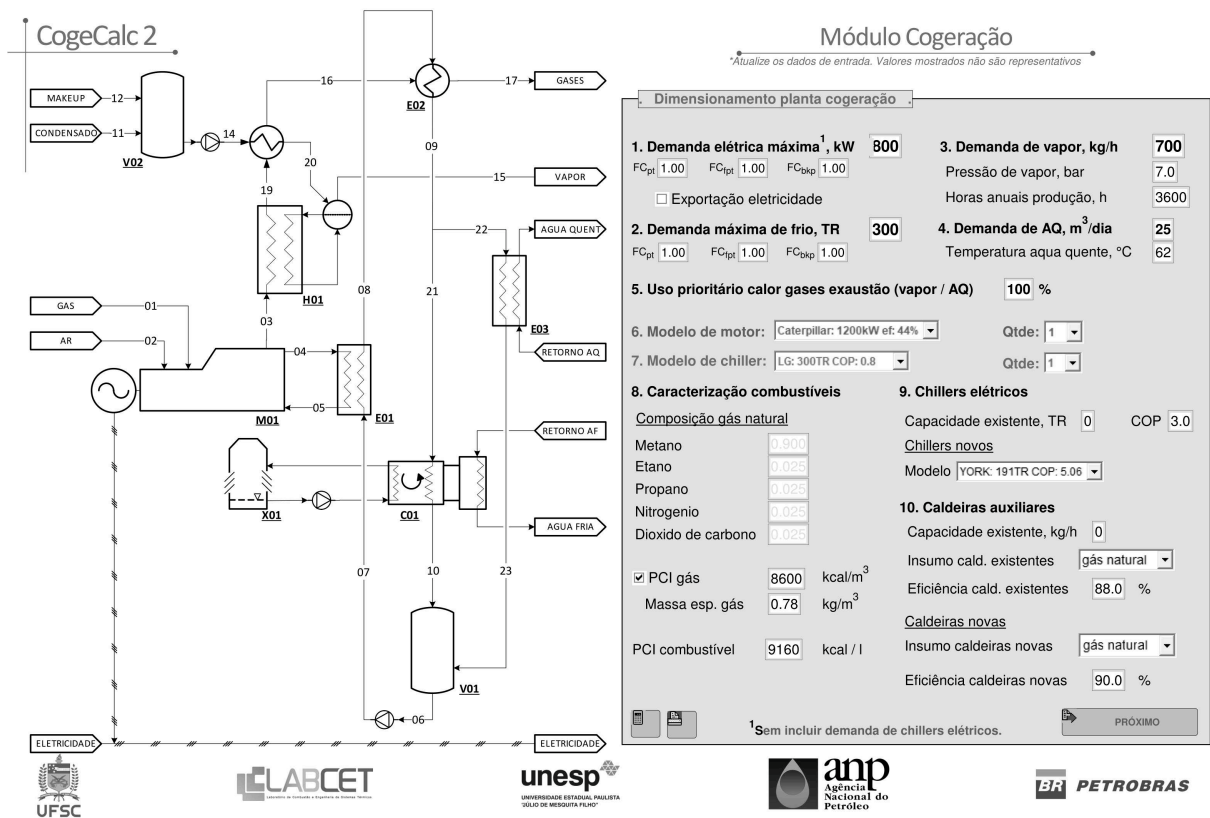


Figure 51 – First screen of *CogeCalc 2* (in portuguese): technical inputs.

1. The maximum electric demand, in kW, can be informed together with three load factors according to current tariffs' scheme, one for off-peak periods, one for on-peak



- periods, and the other for back-up periods. The later, considers the possibility that the price of electricity during programmed shut-downs could be negotiated with the supplier. value informed should exclude air-conditioning devices. Additionally, User informs if exportation of electricity is enabled or not (check box).
2. Cooling demand, in TR, is informed similarly to the previous item, user informs the maximum cooling demand together with the load factors required for distinguishing periods with different electricity tariffs.
  3. The average steam demand, in kg/h, together with its supply pressure, in bar (gauge). The program only considers production of saturated steam. Additionally, the number of steam production hours should be informed, since it can be lesser than the number of operation hours of the generator set.
  4. The average hot water demand, in m<sup>3</sup>/d and its supply temperature in °C.
  5. The priority for using the heat from exhaust gases for producing steam/hot water, expressed in percentage, refers to the apportioning of the heat from exhaust gases between the steam and hot water production, once recognized the compromise between these two thermal utilities, i.e. a lesser steam production enables a greater hot water production and vice-versa.
  6. The engine model can be selected from a drop down list, which is linked to an external database. Technical info (e.g. exhaust gases and cooling circuit temperatures, efficiency, etc.) is automatically updated. Additionally, user can select the number of engines of the same model (five maximum). The list exhibits he brand, the capacity and the efficiency of each engine of the list.
  7. Similarly, the model and number of hot-water-driven chillers can be informed by the user. Technical info is automatically updated from an external database. The list exhibits the brand, the capacity and the COP of each chiller in the list.
  8. The natural gas characterization can be done, according to data availability, informing its molar composition, or through its LHV (PCI in Portuguese), in kcal/m<sup>3</sup> together with its density, in kg/m<sup>3</sup>. Furthermore, the LHV of the fuel used by auxiliary boiler can be input in kcal per liter.

9. The installed capacity (if any) of electric chillers can be informed, together with its characteristic COP. The program takes into account the use of existing devices, as well as the purchase of new devices. Moreover, the model of new complementary (electric) chillers can be informed through a drop down list. Technical information is updated from an external database. The program calculates the number of chillers of the selected model needed for covering the demand informed (if required).
10. The installed capacity (if any) of steam boilers can be informed, together with its characteristic efficiency. User can select the fuel for this equipment. If any value is informed, the calculation assumes that existing equipment will be used. Additionally, the fuel and efficiency of new auxiliary boilers can be informed. Fuels available for selection in the drop down list are natural gas, electricity and a generic 'fuel', whose LHV was informed in the item 8.

Next, the first economic parameters can be input through the second screen of the program, shown in Fig. 52. Description of each item is presented according to its number.

**Dados Econômicos**  
\*Atualize os dados de entrada. Valores mostrados não são representativos

Investimento inicial			
1. Cotação do dólar	3.20	R\$/US\$	
2. Motogerador	600	US\$/kW	<input type="checkbox"/> valor unitário
3. Chiller absorção	800	US\$/TR	<input type="checkbox"/> valor unitário
<b>OUTROS EQUIPAMENTOS</b>			
4. Chiller elétrico	600	US\$/TR	<input type="checkbox"/> valor unitário
5. Torre arrefecimento X01	100	US\$/kW	<input type="checkbox"/> valor total
6. Trocadores água-água E01/E03	232	US\$/m <sup>2</sup>	<input type="checkbox"/> valor total
7. Trocador água - gás E02	280	US\$/m <sup>2</sup>	<input type="checkbox"/> valor total
8. Radiador auxiliar	320	US\$/m <sup>2</sup>	<input type="checkbox"/> valor total
9. Caldeira recuperação H01	70	US\$/kg-h	<input type="checkbox"/> valor total
10. Caldeira auxiliar	50.0	US\$/kg-h	<input type="checkbox"/> valor total
11. Outros investimentos	0		
<b>FATORES DE INVESTIMENTO SOBRE OS EQUIPAMENTOS</b>			
12. Auxiliares elétricos	0.05		
13. Instrumentação e controle	0.05		
14. Auxiliares mecânicos	0.05		
15. Instalação	0.20		
16. Obra civil	0.05		
17. Serviços de engenharia	0.05		

Tarifas serviços / TMA			
	Ref. cliente	Cogeração	
18. Eletricidade (fora de ponta)	0.54	0.54	R\$/kWh
19. Eletricidade (ponta)	1.68	1.68	R\$/kWh
20. Eletricidade (backup)	0.54	0.54	R\$/kWh
21. Gás natural	1.01	1.01	R\$/m <sup>3</sup>
22. Água	10.0	10.0	R\$/m <sup>3</sup>
23. Combustível	2450	2450	R\$/m <sup>3</sup>
24. Venda eletricidade	0.15	0.15	R\$/kWh
25. Taxa mínima atratividade (TMA)	10.0	%	

Figure 52 – Second screen of *CogeCalc 2* (in portuguese): economic inputs.

1. The Dollar exchange rate should be informed, given that the main equipment is usually quoted using this currency. Costs balances are done in Brazilian Reais (BRL).
2. Items 2 through 10: the cost of each equipment can be informed in two ways depending on the information availability, they can be informed through a specific costs in US\$ per characteristic parameter<sup>2</sup>, or informing the cost in US\$ directly (check box must be activated).
11. Other investments can be informed in US\$, if necessary.
12. Items 12 through 17: Indirect costs associated to installation, auxiliary equipment (mechanical and electrical), control and instrumentation, civil construction and engineering services are estimated through cost factors that are applied on total equipment purchase cost.
18. Items 18 through 23: They correspond to electricity, natural gas, water, and fuel rates. Electricity rates are separated by on-peak, off-peak, and back-up periods. User can inform different rates for the reference case (e.g. current rates) on the left column and for the cogeneration case on the right column (e.g. if a discount applies).
24. The sales price of electricity. Similarly, value for reference case (e.g. use of photovoltaic) could be different for the cogeneration case.
25. The minimum attractive rate of return for calculating the economic-performance indicators of the project.

Additional economic information if gathered through the third screen of the program, presented in Fig. 53. They refer to the current expenditures and revenues (informed in thousands of BRL–kR\$) as well as key operation parameters of the plant. Each item is briefly described according to its number.

1. Items 1 through 4: The current expenditures related to electricity, natural gas, water, and fuel can be informed directly. Note that they are optional, since they are calculated from the economic information input on previous screen. It allows the user to input global figures instead of detailed information.

---

<sup>2</sup> Characteristic parameter is the unit used for characterizing the size of the equipment (i.e. kW for gensets, TR for chillers, m<sup>2</sup> for heat exchangers, and kg of steam per hour for boilers).

**CogeCalc 2**

**Dados Econômicos**  
\*Atualize os dados de entrada. Valores mostrados não são representativos

Despesas anuais		
<b>Caso de referência</b>		
<input type="checkbox"/> 1. Despesa eletricidade	0	kR\$
<input type="checkbox"/> 2. Despesa gás natural	0	kR\$
<input type="checkbox"/> 3. Despesa água	0	kR\$
<input checked="" type="checkbox"/> 4. Despesa combustível	150	kR\$
5. Despesa operação e manutenção	0	kR\$
6. Outras despesas	0	kR\$
<b>Cogeração</b>		
7. Despesa operação e manutenção	0	kR\$
8. Outras despesas	0	kR\$

Receitas anuais		
<b>Caso de referência</b>		
9. Receita exportação eletricidade	0	kR\$
10. Outras receitas	0	kR\$
<b>Cogeração</b>		
11. Outras receitas	0	kR\$

Parâmetros de operação		
12. Vida útil da planta	15	anos
13. Disponibilidade	0.95	
14. Horas anuais operação (total)	8760	h
15. Horas anuais operação (ponta)	792	h



Figure 53 – Third screen of *CogeCalc 2* (in portuguese): Economic inputs (2).

5. Current maintenance and operation expenditures.
6. Other expenditures (current). This item can be used for including aspects not considered previously.
7. Maintenance and operation expenditures of the cogeneration plant (estimation).
8. Other expenditures for the cogeneration case can be estimated. This item can be used for including aspects not considered yet.
9. Revenues obtained from electricity sales in the reference case (e.g. photovoltaic).
10. Revenues obtained from other concepts in the reference case (e.g. supply of steam to other users). It can be used for considering aspects not considered previously.
11. Other revenues obtained from other concepts in the cogeneration case.
12. Items 12 through 15: operational parameters of the supply plant are informed for computing the economic performance of the project. The parameters are the lifespan

of the plant, its availability, its annual operational hours, and the annual hours with on-peak electricity tariff.

Once the input information is completed and the program is executed, the first screen of results shows up to the user, as presented in Fig. 54. It corresponds to the summary of the technical features of the plant.

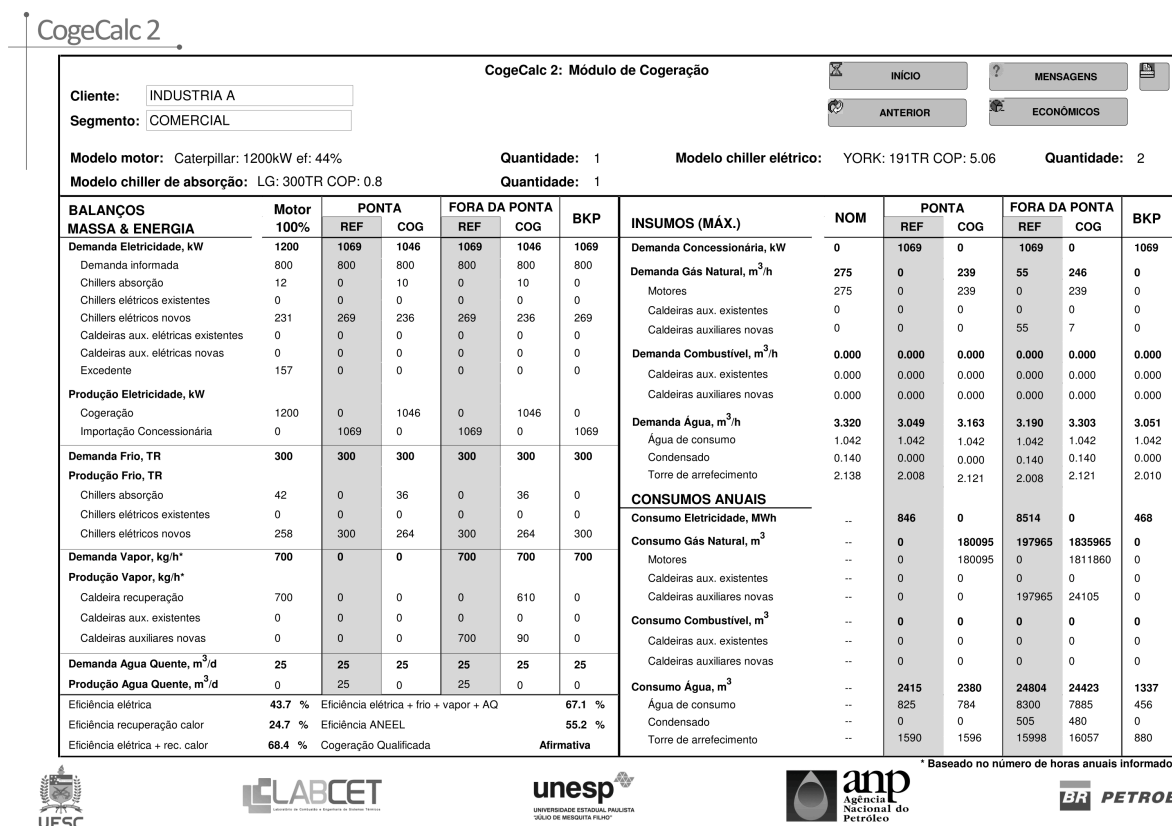


Figure 54 – Technical results reported by CogeCalc 2 (in portuguese).

On the left side of the screen the mass and energy balances are presented. The demand and the production of each utility, discriminated by equipment, are organized in the rows, including the electricity importation from the grid. The first column presents the balances obtained for the generator set operating at full load, while the other columns correspond to the partial balances at periods with different electricity rates, for the reference and for the cogeneration cases. Bold rows are the consolidated balances of each utility. On the lower part, the performance parameters of the plant are presented, including the qualification criteria of the Brazilian electricity agency (ANEEL) and a text field ("Affirmative" or "Negative") indicating whether the project qualifies or not.

On the right side of the screen there is the summary of the resources imported into the plant. The maximum demand of electricity, natural gas, fuel, and water are presented in the upper half of the table, while the annual consumption of these resources are organized on the lower part. Note that these quantities are presented using the units in which they are commercialized. Columns are organized similarly to the left side of the table.

The last screen corresponds to the economic outputs of the program and is presented in Fig. 55. On the upper right part, there is the summary of the different rates of the resources, discriminated by periods, as well as their annual consumption (repeated from previous screen). On the lower part it is the annual operational cost (OPEX)—also discriminated by rate periods—and the annual incomes derived from the sales of utilities. Analogously, on the right side of the screen it is presented the summary of the investment, discriminated by equipment. The column of the reference case is editable, enabling final cost adjustments. The economic performance indicators are presented on the lower part, they are the net present value, the payback period and the internal rate of return.

CogeCalc 2

CogeCalc 2: Módulo de Cogeração										
Cliente: INDUSTRIA A Segmento: COMERCIAL						INICIO ANTERIOR MENSAGENS				
Modelo motor: Caterpillar: 1200kW ef: 44% Modelo chiller de absorção: LG: 300TR COP: 0.8						Quantidade: 1 Quantidade: 1		Modelo chiller elétrico: YORK: 191TR COP: 5.06		Quantidade: 2
TARIFAS	PONTA		FORA DA PONTA		BKP	TOTAL		INVESTIMENTOS	REFERÊNCIA*	COGERAÇÃO
	REF	COG	REF	COG		REF	COG		0	6624
Eletricidade R\$/MWh	1680	1680	540	540	540	--	--	Motor(es), kR\$	0	2304
Gás natural, R\$/m <sup>3</sup>	1.01	1.01	1.01	1.01	1.01	--	--	Chiller(s) de absorção, kR\$	0	768
Combustível, R\$/m <sup>3</sup>	2450	2450	2450	2450	2450	--	--	Chiller(s) elétricos, kR\$	0	733
Água, R\$/m <sup>3</sup>	10.0	10.0	10.0	10.0	10.0	--	--	Trocador(es) água - água, kR\$	0	8
Venda elet. R\$/MWh	150	150	150	150	150	--	--	Trocador(es) água - gás, kR\$	0	10
<b>CONSUMOS ANUAIS</b>								Radiador(es) auxiliar(es), kR\$	0	23
Consumo Elétrico, MWh	846	0	8514	0	468	9360	468	Torre(s) de arrefecimento, kR\$	0	550
Consumo Gás Natural, m <sup>3</sup>	0	180095	197965	1835965	0	197965	2016060	Caldeiras de recuperação, kR\$	0	157
Consumo Combustível, m <sup>3</sup>	0	0	0	0	0	0	0	Caldeiras auxiliares, kR\$	0	14
Consumo Água, m <sup>3</sup>	2415	2380	24804	24423	1337	27725	28139	Auxiliares elétricos, kR\$	0	228
<b>OPEX ANUAL</b>								Auxiliares mecânicos, kR\$	0	228
Eletricidade, kR\$	1422	0	4597	0	253	6019	253	Instrumentação e controle, kR\$	0	228
Gás natural, kR\$	0	181.9	200	1854	0	200	2036	Instalação de equipamentos, kR\$	0	914
Combustível, kR\$	NA	NA	NA	0	0	150	0	Obra civil, kR\$	0	228
Água, kR\$	24	23.8	248	244.2	13.37	277	281	Serviços de engenharia, kR\$	0	228
O&M, kR\$	--	--	--	--	--	0	0	Outros investimentos, kR\$	0	0
Outros, kR\$	--	--	--	--	--	0	0	<b>6. ECONOMIA ANUAL</b>		
<b>VENDA SERVIÇOS</b>								Economia custo operacional, kR\$		4076
Eletricidade, kR\$	0	0	0	0	0	0	0	Venda de serviços, kR\$		0
Outros, kR\$	--	--	--	--	--	0	0	Diferença investimentos, kR\$		6624
									*Editável pelo Usuário	
									VPL, kR\$	24379
									PayBack (anos)	1.6
									TIR	61.5 %



Figure 55 – Economic results reported by CogeCalc 2.

Finally, a set of explanatory messages (in Portuguese) are presented (if required) to the user. They include complementary information and some explanatory notes and change according to the results of the program. Figure 56 shows an example of these messages for an arbitrary application.

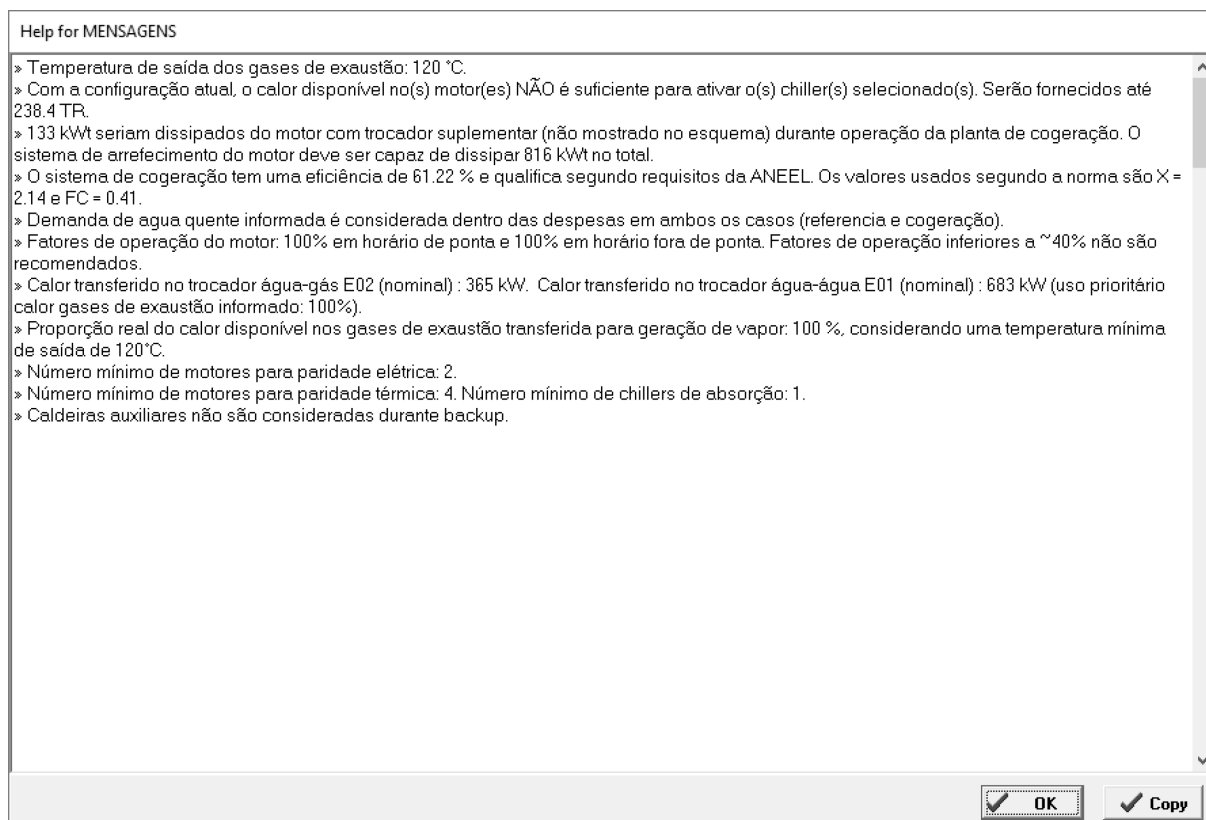


Figure 56 – Example of explanatory messages presented by *CogeCalc 2*.

Aspects covered by these notes are:

- Capacity of auxiliary equipment.
- Exhaust gases outlet temperature.
- Available heat used for activating absorption chillers.
- Heat dissipated at radiators of generator sets.
- Brazilian regulation category fulfillment.
- Consistency of the informed current expenditures (informed vs calculated).
- Partial-load operation of generator sets.

- Heat transferred at each heat exchanger.
- Portion of the available heat destined to steam production.
- Number of generator sets for following-electric-demand (FEL) operation strategy.
- Number of generator sets for following-thermal-demand (FTL) operation strategy.
- Use of auxiliary burners.



## Appendix C

---

### UNCERTAINTY ON THE UTILITIES' LOAD PROFILES

The assessment of the uncertainty on the characterization of the utilities load profiles is carried out according to the guidelines of the Joint Committee For Guides In Metrology (2008). Values reported correspond to the expanded uncertainty  $U_p$ , calculated using the expression  $U_p = k_p \cdot u_c(y)$ , where  $k_p$  is the coverage factor and  $u_c(y)$  is the standard uncertainty of the output estimate  $y$ . Coverage factor adopted is the  $t$ -factor ( $t_p(\nu)$ ) from the  $t$ -distribution for  $\nu$  degrees of freedom, corresponding to a given probability  $p$ . Unless otherwise indicated, the value of  $p$  is 95%. On the other hand, the evaluation of standard uncertainty is of type  $A$  given that the profiles' characterization is based on repeated measurements. The following sections briefly present the considerations taken into account for the uncertainty assessment in each stage described in Chap. 3.

#### C.1 BASE TEMPERATURES FOR COOLING DEGREE-INTERVALS

The estimation of the base temperatures is done with the aid of a piecewise regression model, which is based on the least squares method and is included into the python package *SciPy* (JONES; OLIPHANT, 2001). The slope of the first segment in the fitting function was set to 0. Outputs of the model are the coordinates of the elbow point and the slope of the second segment of the regression. Additionally, it returns the regression covariance matrix, from which it was possible to get the standard deviation of the regression parameters, since its main diagonal corresponds to the values of their variances. In this case, the only parameter of interest is the abscissa of the elbow point (i.e. the base temperature). Results obtained reported uncertainties between 0.01°C and 0.12°C, which are considered insignificant.

#### C.2 PERFORMANCE LINES OF COOLING DEGREE-INTERVALS

Linear regressions were performed using the python package *statsmodels* (SEABOLD; PERKTOLD, 2010), which internally executes the same procedure described at the beginning of this appendix for determining the expanded uncertainty on the estimation

of each regression parameter. Additionally, it enables the discarding of outliers, according to pertinent criteria; in this case, a point is discarded if the  $p$ -value corresponding to the  $t$ -statistic of its residual is equal or greater than the confidence level  $1 - \alpha'/(2 \cdot n)$ , where  $n$  is the sample size (*bonferroni* correction);  $\alpha'$  is equal to 5%. On the other hand, it reports the  $p$ -value of the  $t$ -statistic of each estimation in order to verify its significance. The null hypothesis was rejected for all the regressions. Table 38 presents the coefficient of determination  $R^2$  and the number of outliers found in each regression.

Table 38 – Fitting of linear regressions for performance lines.

<b>Inval</b>		<i>Business</i>		<i>Non-bus</i>		<b>Inval</b>		<i>Business</i>		<i>Non-bus</i>		
<i>1 h</i>	$R^2$	<i>Outs</i>	$R^2$	<i>Outs</i>	<i>1 h</i>	$R^2$	<i>Outs</i>	$R^2$	<i>Outs</i>	$R^2$	<i>Outs</i>	
1	0.615	1	0.683	2	21	0.733	2	0.799	1			
2	0.638	2	0.662	2	22	0.729	1	0.769	1			
3	0.666	3	0.650	2	23	0.706	1	0.748	1			
4	0.683	4	0.651	2	24	0.687	2	0.741	2			
5	0.706	4	0.630	1	<i>3 h</i>							
6	0.666	1	<b>0.580</b>	0	1	0.669	3	0.682	2			
7	0.650	2	0.594	3	2	0.720	3	0.660	2			
8	0.824	3	0.594	5	3	0.846	3	0.665	3			
9	0.842	2	0.731	4	4	0.806	2	0.732	2			
10	0.805	2	0.687	3	5	0.799	2	0.718	2			
11	0.791	3	0.693	2	6	0.765	2	0.741	3			
12	0.788	0	0.750	1	7	0.620	1	0.815	0			
13	0.778	0	0.714	2	8	0.719	0	0.750	0			
14	0.796	2	0.707	2	<i>12 h</i>							
15	0.760	1	0.731	3	1	0.841	1	0.768	1			
16	0.735	1	0.675	4	2	0.745	1	0.770	1			
17	0.750	2	0.722	3	<i>Day</i>	0.880	0	0.831	0			
18	0.823	0	0.808	3	<i>Week</i>	0.829	2					
19	0.758	1	0.731	0	<i>Month</i>	0.817	1					
20	0.656	1	0.801	0								

### C.3 STEAM PRODUCTION

The production of steam is calculated as the product of the fuel input  $E_f$  (kW) and the boiler efficiency  $\eta_{bol}$ . Since both variables were considered uncertain, it follows that standard uncertainty of the steam production  $u_{c,sp}^h$  of a given hour  $h$  of the day is equal to the combined uncertainty according to the relation:

$$u_c^2(y) = \sum_{i=1}^N \left[ \frac{\partial f}{\partial x_i} \right]^2 u^2(x_i) \quad Y = f(X_1, X_2, \dots, X_N)$$

$$\therefore u_{c,sp}^h = \sqrt{\left(E_f^h\right)^2 \cdot (u_{c,\eta_{bol}})^2 + (\eta_{bol})^2 \cdot (u_{c,E_f}^h)^2}$$

where  $E_f^h$  is the mean of the fuel input collected during hour  $h$ ,  $u_{c,\eta_{bol}}$  is the standard uncertainty of the boiler efficiency (this measure is estimated as a weighted mean—see Chap. 3), and  $u_{c,E_f}^h$  is the standard uncertainty of the fuel input readings during hour  $h$  of the day. On the other hand, the effective degrees of freedom,  $\nu_{eff}$ , used for obtaining the coverage factor is calculated according to the following expression:

$$\frac{u_c^4(y)}{\nu_{eff}} = \sum_{i=1}^N \frac{c_i^4 \cdot u_i^4(y)}{\nu_i}; \quad c_i \equiv \frac{\partial f}{\partial x_i}$$

$$\therefore \nu_{eff}^h = \frac{(u_{c,sp}^h)^4}{\frac{(E_f^h \cdot u_{c,\eta_{bol}}^h)^4}{\nu_{\eta_{bol}}} + \frac{(\eta_{bol} \cdot u_{c,E_f}^h)^4}{\nu_{E_f}}}$$

#### C.4 STEAM DEMAND

Steam demand is calculated as the difference between the steam production and the hot water demand. Thus, the standard uncertainty of the steam demand  $U_{c,st}^h$  during a given hour  $h$  of the day is equal to the combined uncertainty expressed in the following equation:

$$u_{c,st}^h = \sqrt{(u_{c,sp}^h)^2 + (u_{c,hw}^h)^2}$$

where  $u_{c,hw}^h$  is the standard uncertainty of the hot water demand during hour  $h$  of the day. Finally, for the calculation of the expanded uncertainty  $U_{p,st}^h$  is calculated using the coverage factor  $k_p$  obtained for the effective degrees of freedom  $\nu_{eff}^h$ , according to the

following expression:

$$\nu_{eff}^h = \frac{(u_{c,st}^h)^4}{\frac{(u_{c,sp}^h)^4}{\nu_{sp}} + \frac{(u_{c,hw}^h)^4}{\nu_{hw}}}$$

where  $\nu_{sp}$  and  $\nu_{hw}$  correspond to the degrees of freedom of the steam production data and hot water demand data, respectively.